THE EFFECT OF UV RADIATION ON FURIN ACTIVITY IN HUMAN KERATINOCYTE CELL LINES

A thesis for the degree of Doctor of Philosophy
By

Rethika Ravi

B.Sc (Microbiology) (S.R.M Arts and Science College -Madras University)
M.Sc (Applied Microbiology and Biotechnology) (RMIT University)

School of Medical Sciences
RMIT University
Melbourne, Australia

July, 2010

Declaration

I the undersigned, author of this thesis, hereby certify that the main text of this thesis is the original work of the author

(a) except where due acknowledgement has been made, the work is that of the candidate alone;

(b) the work has not been submitted previously, in whole or in part, to quantify for any other academic award;

(c) the content of the thesis is the result of work which has been carried out since the official commencement date of the approved research program;

(d) any editorial work, paid or unpaid, carried out by a third party is acknowledged;

(e) ethics procedures and guidelines have been followed.

---------- ----------

School of Medical Sciences Date

RMIT University

Melbourne, Australia

Acknowledgements

It is with heartfelt sincere gratitude that I thank Assoc/Prof Terry Piva, whose exceptional supervision and sensitivity allowed me to develop as a research scientist. His guidance in organizing day to day work and his foresight in directing me to successfully completing along, and at times, difficult, research program has been extraordinary. I wish to thank him for all the scientific discussions that introduced many enriching qualities to this research. I would like to acknowledge his endless encouragement, patience and faith in me during those times when I doubted myself. I would not have been able to complete this project successfully without his periodical assessment of my experimental and theoretical work throughout these three and a half years.

Many thanks to my co-supervisor, Assoc/Prof. Ian Darby for his encouragement all the way through this project.

I thank and acknowledge the generous support of Assoc/Prof. Andrew Wootton for his consideration and acceptance as part of his team.

My deepest thanks to Dr. John Bonacci who patiently taught me the zymography methodology. His guidance has made this project not only worthwhile but fulfilling.

My sincere thanks to my colleague and good friend, Thao Nguyen, who played a pivotal role in designing the qRT-PCR protocol. Her companionship and never-ending confidence in me was extremely motivating.

Many thanks to my colleague and good friend James Musyoka for providing me with the Cell Scratch protocol.

I am indebted to the Biochemistry Technical staff and to the Proteomics Department (School of Applied Sciences) for all their help.

Many thanks to both the past and present members of our close knit team, “The Skin Cancer Research Group” for all the corridor and coffee conversations!!!

I am immensely thankful to the School of Medical Sciences for funding this project. Being the first recipient of the School of Medical Sciences Grant, has not only made me a lot more conscientious but also helped me understand the responsibilities that come along with such an award. I wish to thank the School of Medical Sciences for giving me the opportunity to attend various conferences which have been inspirational (a blessing in disguise!!!).

I shall make use of this golden opportunity to thank my dad, Mr. Ravi Shivram and my mom, Mrs Rajitha Ravi without whom this project would not have been possible. Their blessings, prayers, loving support, cheering cooperation and pride in me and my achievements kept me going through the various phases of this project and made me work towards my ambition. They have been in one way or another, instrumental in the successful completion of this thesis.

A special thanks to my husband, Mr. Kartic Srinivasan for all his help, countless sacrifices, confidence in me and most of all, his belief in my ability to see this project through to completion. He has always been there to listen, assure, advice and applaud.

It has been a challenging, yet wonderful journey and I wish to thank everyone who has helped me reach my destination productively…

Table of contents

List of Figures

Chapter One:

Chapter Two:

Chapter Three:

Chapter Four:

Chapter Five:

Chapter Six:

Appendix:

List of Tables

Chapter One:

Chapter Two:

Chapter Three:

Chapter Four:

Chapter Five:

Appendix:

List of Abbreviations

aa	Amino Acids
APC	Antigen-Presenting Cell
BCC	Basal Cell Carcinoma
BSA	Bovine Serum Albumin
CHS	Contact Hypersensitivity
CMM	Cutaneous Malignant Melanoma
CPD	Cyclobutane Pyrimidine Dimers
Dec-RVKR-cmk	Decanoyl Arg-Val-Lys-Arg- chloromethylketone
CRR	Cysteine-Rich Residue
DTH	Delayed-Type Hypersensitivity
ECM	Extra cellular Matrix
ELISA	Enzyme-Linked Immunosorbant Assay
ER	Endoplasmic Reticulum
FBS	Foetal Bovine Serum
FUR	FES Upstream Region
HBSS	Hank’s Buffered Salt Solution

HEK	Human Epidermal Keratinocytes
ICAM	Intercellular Adhesion Molecule
IHC	Immunohistochemistry
IL	Interleukin
IFN	Interferon
LC	Langerhans Cell
MAPK	Mitogen Activated Protein Kinase
MED	Minimal Erythemal Dose
MMP	Matrix Metalloprotease
NMSC	Non Melanoma Skin Cancer
PACE	Paired Basic Amino Acid Cleaving Enzyme
PBS	Phosphate-Buffered Saline
PGE_2	Prostaglandin
PC	Proprotein Convertases
PMA	Phorbol-12 Myristate-13-Acetate
ROS	Reactive Oxygen Species
RPMI	Rosewell Park Memorial Institute
RT	Room Temperature

SDS	Sodium Dodecyl Sulphate
TACE	Tumour Necrosis Factor α Converting Enzyme
TBS	Tris-Buffered Saline
TBST	Tris-Buffered Saline with 0.025% Triton-X 100
TMB	Tetramethylbenzidine
TNFα	Tumour Necrosis Factor α
Th1	T Helper Cell-1
Th2	T Helper Cell-2
TNF-RI/-RII	TNFα-receptor I/ - receptor II
UCA	Urocanic Acid

Abstract

UV light is acknowledged to be the main carcinogen involved in the formation of skin cancer. It generates a range of biological responses in the skin, which includes adaptive, inflammatory and immunological reactions. In this thesis we exposed cultures of keratinocyte-derived cell lines (HEK cells-primary keratinocytes, HaCaT cells-immortalized keratinocytes and Colo 16 cells-squamous cell carcinoma cell line) to UVA and/or UVB radiation and observed the effect this had on a number of cellular processes. The UV dose used throughout the thesis was equivalent to the UV component observed in one medial erythemal dose which was 40 kJ/m^2 UVA and 2 kJ/m^2 UVB.

In HEK cells, the viability of attached sham-irradiated cultures was 92%. UVA radiation had no effect on cell viability when compared to sham-irradiated controls. In HaCaT and Colo 16 cells, exposure to UVA reduced cell viability by 11% and 7%, respectively. In HEK cells, the attached viable cells were more sensitive to UVB and UVAB radiation as the cell viability was reduced by 46% and 33%, respectively. When HaCaT cells were exposed to UVAB radiation (cell viability was reduced by 32%), the result had characteristics similar to that seen for those cells irradiated by either UVA or UVB where the viability was reduced by 10% and 20%, respectively. In Colo 16 cells, the viability of attached cells in UVB- (49%) and UVAB-irradiated cells (49%) was reduced when compared to the sham-irradiated cultures (90%). The viability of the detached viable cells was low (<5%) for all UV types and doses. The Colo 16 cells were more sensitive to UVR than were HEK or HaCaT cells.

Furin levels in UV-irradiated HEK cells did not change 24 h post-irradiation unlike that seen for HaCaT or Colo 16 cells. Higher furin expression was seen in UVAB-irradiated

HaCaT cells (12x) and UVB-irradiated Colo 16 cells (7.5x) when compared to un-irradiated controls. Furin mRNA levels were shown to be maximal after 24 h in HaCaT cells (91-fold) and 12 h for Colo 16 cells (1.5-fold) exposed to UVB-irradiation. There was a moderate correlation between furin mRNA and protein levels in irradiated HaCaT cells (r^2 = 0.581) compared to that of Colo 16 cells (r^2 = 0.399) 24 h post-irradiation. The turnover of furin protein was longer in Colo 16 cells compared to HaCaT cells ($T_{½}$ = 17.0 h and 5.6 h, respectively). IL-1α had a slightly additive effect on furin expression and activity in HEK cells but a slightly suppressive effect on HaCaT and Colo 16 cells.

The level of MMP-2 and -9 activity in HaCaT cells did not change in the 72 h period following exposure to UVR. Maximal MMP-2 and -9 activity was seen at 12 h (13489.9 and 15392.0 au/mg cell protein, respectively) in UVB-irradiated HEK cells. While high levels of MMP-2 activity was observed at 24 h (1998.1 au/mg cell protein) in UVB-irradiated Colo 16 cells, levels of MMP-9 were highest at 24 and 72 h (6512.8 and 2605.9 au/mg cell protein), respectively in these cells. In HaCaT cells, the expression of proMMP-2 in UVB- (63%) and UVAB-irradiated cells (64%) were similar to that of sham-irradiated controls. Active MMP-2 expression was higher in UVB-irradiated HaCaT cells (41%). In Colo 16 cells the highest induction of pro and active MMP-2 protein was seen in UVA-irradiated cells (139% and 112%, respectively). The level of active MMP-9 protein was only elevated in HaCaT cells exposed to either UVA (80%) or UVAB radiation (121%). This result was not seen in Colo 16 cells. Addition of IL-1α significantly increased MMP-9 activity, protein and mRNA expression in HaCaT and Colo16 cells. The mRNA levels for MMP-2 (73-fold) and -9

(330-fold) were maximal 24 h post UVB-irradiation in HaCaT cells. In Colo 16 cells, maximal mRNA expression was seen at 0 h for MMP-2 and 12 h for MMP-9 (17-fold). There was a strong and positive correlation between furin and MMP mRNA levels in HaCaT cells but not in Colo 16 cells. 1, 10 phe and MMPI significantly decreased the activity of MMP-2 and -9 shed from UV-irradiated cells. When Dec RVKR cmk was added to HaCaT and Colo 16 cells, there was a loss of MMP-9 activity in the media of the UV-irradiated cells. In the presence of these inhibitors migration of the HaCaT and Colo 16 cells were also decreased.

The effect of UVR on the release of TNFα from human keratinocyte-derived cells was also examined. The addition of IL-1α increased the release of TNFα in sham-irradiated HEK (2763.73 ng/mg cell protein), HaCaT cells (935.5 ng/mg cell protein) and Colo 16 cells (81.9 ng/mg cell protein) when compared to untreated controls. UVAB-irradiated cells treated with IL-1α induced the greatest increase in TNFα release in all cell lines (32.9-, 4.2- and 7.7-fold in HEK, HaCaT and Colo 16 cells, respectively) compared to treated sham-irradiated cells. Addition of 1, 10 phe caused an inhibition of ~97% in IL-1α treated UVAB-irradiated HaCaT and Colo 16 cells. 95% in HaCaT cells and 87% in Colo 16 cells The level of TNFα released from Dec RVKR cmk treated UVAB-irradiated cells was significantly reduced by 95% in HaCaT cells and 87% in Colo 16 cells. MMPI also inhibited TNFα release from HaCaT and Colo 16 cells. The maximal mRNA levels post UVB-irradiation for TNFα (59-fold) were at 16 h in HaCaT cells and 8 h (12.1-fold) in Colo 16 cells. The level of TACE mRNA was relatively constant in both these cells for up to 32 h post-irradiation.

The results obtained suggest that UVR up-regulates furin mRNA and protein expression in these keratinocyte-derived cells. Colo 16 cells harbor furin protein for a much longer time which may contribute to increasing their metastatic nature as one of the proteases they process, MMP is known to cleave the ECM, allowing metastasis to occur. The results of this study suggest that (1) the changes in TACE activity are due to the conversion of pTACE to mTACE mediated by furin, and (2) TACE is the main enzyme involved in the release of TNFα but MMPs may also be involved. The three keratinocyte cell lines respond differently when exposed to UVR. The response of HaCaT cells to UVR differs to that of HEK which suggest that these immortalized cell lines may not be a suitable model to study keratinocytes. Colo 16 exhibits a completely different profile to that of both HaCaT and HEK which most likely reflects its carcinogenic nature of these cells which may contribute to their metastatic potential, through changes in MMP and TACE activity.

Chapter One:

Literature Review

1 Literature Review

1.1 The Skin

The skin is the largest organ of the human body, and is a protective barrier that prevents dehydration and invasion by toxic environmental agents (1, 2). It participates in thermoregulation by functioning as an insulator and producing sweat to remove excess heat (1, 3). Skin cells have developed complex communication networks as well as immune and growth regulatory systems which allow them to respond to the external stimuli to which they are constantly exposed (2). The skin is composed of three primary layers; an upper superficial layer (epidermis), a deeper fibroelastic layer (dermis) and the innermost layer (hypodermis) also called as the subcutaneous or basement layer (Figure 1.1).

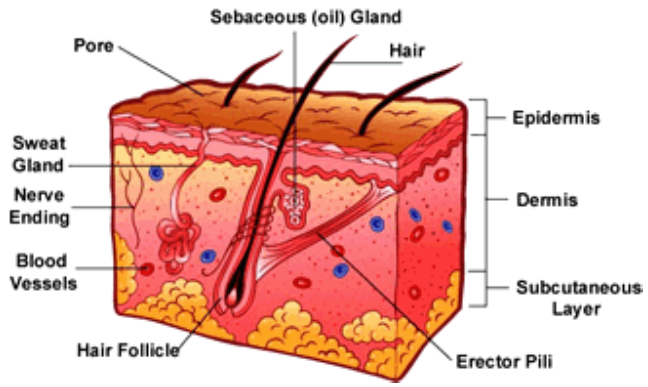

Figure 1.1 The skin consists of three layers: epidermis, dermis and the hypodermis (4).

The epidermis is divided into five layers: stratum basale, stratum spinosum, stratum granulosum, stratum lucidum and stratum corneum as shown in Figure 1.2. The stratum basale is the inner most layer of the epidermis and contains rapidly proliferating and

differentiating keratinocyes, Merkel cells and melanocytes (5, 6). The stratum spinosum layer contains Langerhans cells (LC), which are part of the immune system.

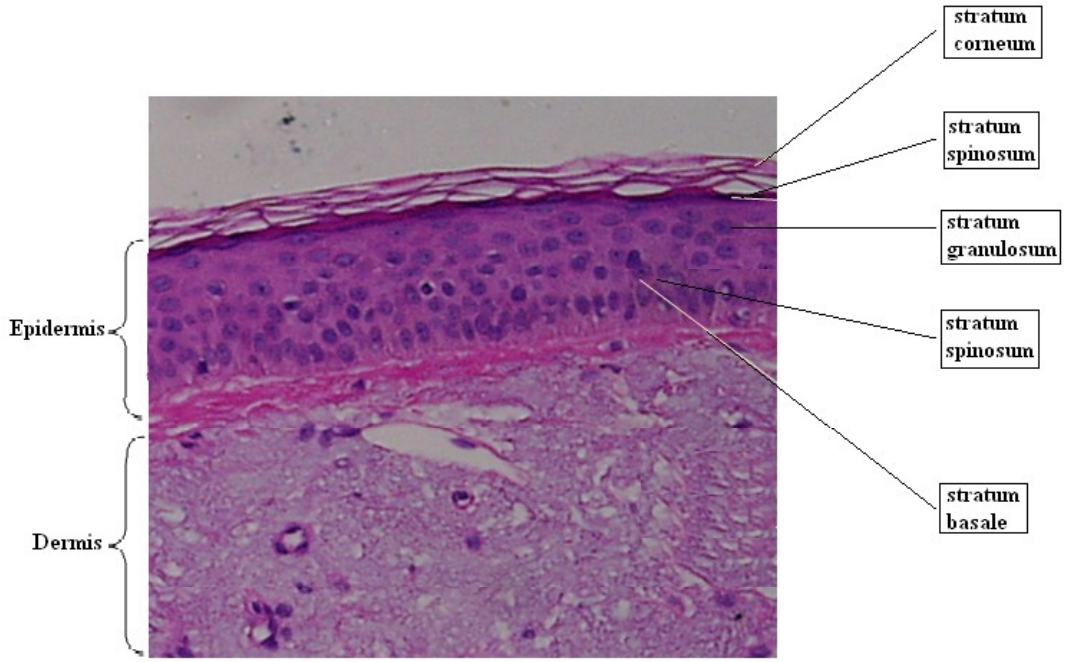

Figure 1.2 The layers of the epidermis.

The dividing keratinocytes are located in the basal layer (1, 3) and move through the layers of the epidermis, from the stratum basale to the stratum corneum undergoing gradual differentiation and producing keratin, a tough protective protein that makes up the majority of the skin structure (3). Melanocytes produce melanin upon stimulation by Ultraviolet (UV) light. The melanin is absorbed by the keratinocytes, giving the skin its pigmentation. UV-induced skin pigmentation occurs in two phases. It commences with immediate pigment darkening followed by delayed formation of new melanin (7). The

presence of melanin in the upper epidermis seems to confer protection against DNA damage caused by UV radiation (UVR) (8). It is thought that melanin has a photoprotective role, as greater the pigmentation of the skin, the greater its resistance to effects of sunlight (9). The dermis is mainly composed of fibroblasts, and LC which are antigen-presenting cells (APC). The subcutaneous layer consists of a network of collagen and fat cells (1, 3).

1.1.1 Skin Types

Human skin can be divided into six types depending on the level of melanin present and their tanning ability (Table 1.1).

Skin Type	Constitutive Skin Colour	Sensitivity to Sunburn	Facultative Tanning Ability	Skin Cancer Risk
I	White	Very High	Virtually Nil	High
II	White	High	Poor	High
III	White	Medium	Good	Medium
IV	Olive	Low	Very Good	Low
V	Brown	Very Low	Very Good	Very Low
VI	Black	Very Low	Very Good	Very Low

Table 1.1 The characteristics of different skin types. Adapted from (9).

The degree of pigmentation in the skin and the ability to tan are important risk factors in skin cancer development (10). Skin types I-IV are mainly lighter skinned people with

varying degrees of tanning ability, while types V and VI are darker skinned people who rarely burn and tan easily (9). People who are fair, sunburn easily and never tan have a higher risk of developing skin cancer compared to those who have darker skin, and tan easily (11).

1.2 Skin Cancer

1.2.1 Incidence

Basal cell carcinoma (BCC), squamous cell carcinoma (SCC) and cutaneous malignant melanoma (CMM) are the three most common types of skin cancer (12, 13). BCC and SCC are together known as non melanoma skin cancer (NMSC) (14). Skin cancer represents a major, and growing, public health problem (15). The incidence of skin cancer is increasing among the general population, as is its mortality rate (16). Most Australians are at risk of skin cancer, but some are more at risk than others. These include people who: are fair-skinned and do not tan but sunburn easily, have freckles or many moles, were exposed to the sun as children, suntan or burn intentionally to make their skin appear browner, have a family history of skin cancer, work indoors, but get a lot of sun exposure every weekend, work outdoors for long periods of time, use sunlamps, sunbeds and solariums (17, 18).

Skin cancer accounts for around 80% of all new cancers diagnosed each year in Australia. In Australia, in 2008, there were 434,000 new cases of NMSC that resulted in 450 deaths and 10,000 new cases of melanoma that resulted in 1,250 deaths (12, 18, 19). Staples *et al*. (20) estimated that 2 in 3 Australians will be diagnosed with skin cancer by the age of 70, and it is estimated that approximately 200 melanomas and 34,000 NMSCs

per year are caused by occupational exposure (21). In Australia, the cost of treating skin cancer is around $300 million annually, which is the highest of all cancers (12, 22).

1.2.2 Types of skin cancer

NMSCs are derived from keratinocytes whereas melanomas are derived from melanocytes. The UV component of sunlight has been implicated to be the main carcinogen involved in the development of skin cancer (7, 23). While genetic and other factors may contribute to skin cancer development, the role UV light plays in the process is well known (17, 24).

1.2.2.1 Basal Cell Carcinoma

BCCs are the most common but least dangerous type of skin cancer. About 75% of the skin cancers in Australia are BCCs (17). They grow slowly over months or years and very rarely spread to other parts of the body. However if they are not treated, they may form an ulcer; as this deepens, it may cause damage to nearby tissues and organs for instance, the eyelids or nose (17).

BCCs occur most often on the head, neck or upper body and can appear on other parts of the body. They usually start as small, round or flattened lumps that are red, pale or pearly in colour, and may have blood vessels on the surface. A BCC may also appear as a small area of red and scaly skin, similar to a patch of eczema (17, 25).

1.2.2.2 Squamous Cell Carcinoma

SCCs are less common than BCCs but are potentially more fatal. They grow more quickly, usually over weeks or months and may spread to nearby lymph nodes or via the bloodstream to other organs (26) of the body if not treated promptly. They occur most often (but not only) on the head, neck, hands and forearms (26). An SCC looks like a red scaly spot, usually thickened, which may bleed easily or ulcerate after some time and may be tender to touch. SCCs rarely occur before 40 years of age, and their incidence is related to the total sun exposure and the risk increases with increased accumulated UV exposure (9, 26).

SCCs are more common in people who have solar keratosis ("sunspots") (17). Solar keratoses themselves are not cancerous, but like skin cancers, are the result of exposure to the sun. SCC varies in size: usually from a 1.2 mm to 2 cm in diameter. They may sometimes be painful or itchy, and may sting when in the sun or if they are scratched (17, 25).

1.2.2.3 Melanoma

Melanoma arise from melanocytes and usually occur on parts of the body that have been sunburnt (17, 27). However, melanomas can be found on the skin or regions of the body that have never been exposed to the sun (28). They can grow quickly and if detected early, most are curable. They are most dangerous of all the skin cancers (26) and are related to intense intermittent sun exposure especially in childhood (29). They are of concern as they can metastasise and develop secondaries in other parts of the body (28).

1.3 Ultraviolet radiation

Sunlight is composed of a continuous spectrum of electromagnetic radiation that can be divided into three main regions: UV light (100 to 400 nm), visible light (400-760 nm) and infrared (760-10^6 nm) (Figure 1.3). UVR itself can be subdivided into three components based on wavelength: UVC (200-280 nm), UVB (280-320 nm) and UVA (320-400 nm). All of the UVC and most of the UVB radiation emitted from the sun is effectively blocked from reaching the Earth's surface by the stratospheric ozone layer. Only high wavelength UVB (>300 nm) and UVA can penetrate the ozone layer and reach the Earth's surface (10, 30). The component of UV light that reaches the Earth's surface consists of 90-95% UVA and 5-10% UVB (7, 30, 31).

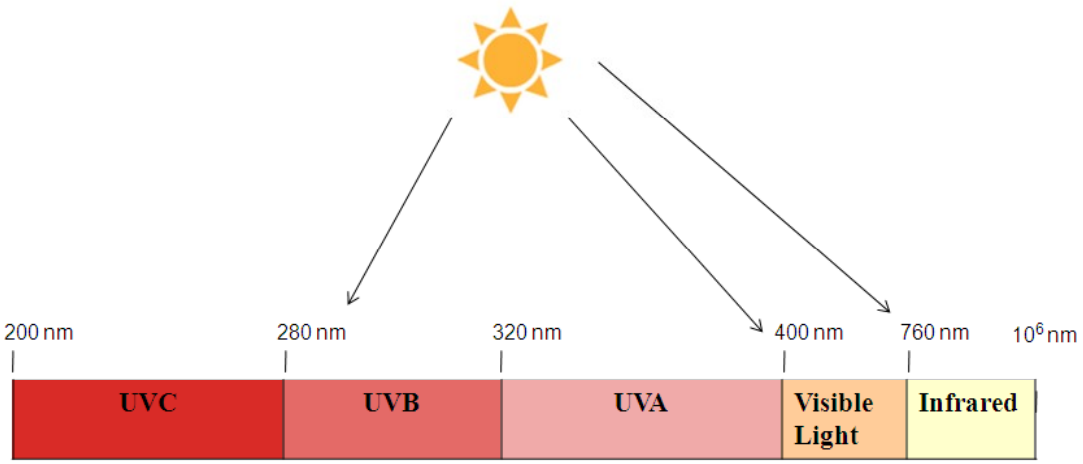

Figure 1.3 The radiation spectrum of sunlight. Adapted from (7).

Ozone depletion, seasonal and weather variations affect the amount of UVR reaching the Earth's surface (15, 32). The time of the day, season of the year, geographical location, and altitude also affect the intensity or dose rate of UV reaching the Earth's surface, with the result that the highest UV intensities occur at noon, in the summer

months, at the equator and at high altitude. In addition UV intensities are affected by local changes in cloud cover or atmospheric pollution (31). The energy carried by each portion of the spectrum is inversely related to its wavelength so UVC > UVB > UVA (30). However, the depth of penetration of UV light into the skin increases with increasing wavelength (Figure 1.4). The penetration of shorter-wavelength UVB radiation is predominantly confined to the superficial epidermis while UVA penetrates deeper into the basal layers and dermis because of its longer wavelength (33).

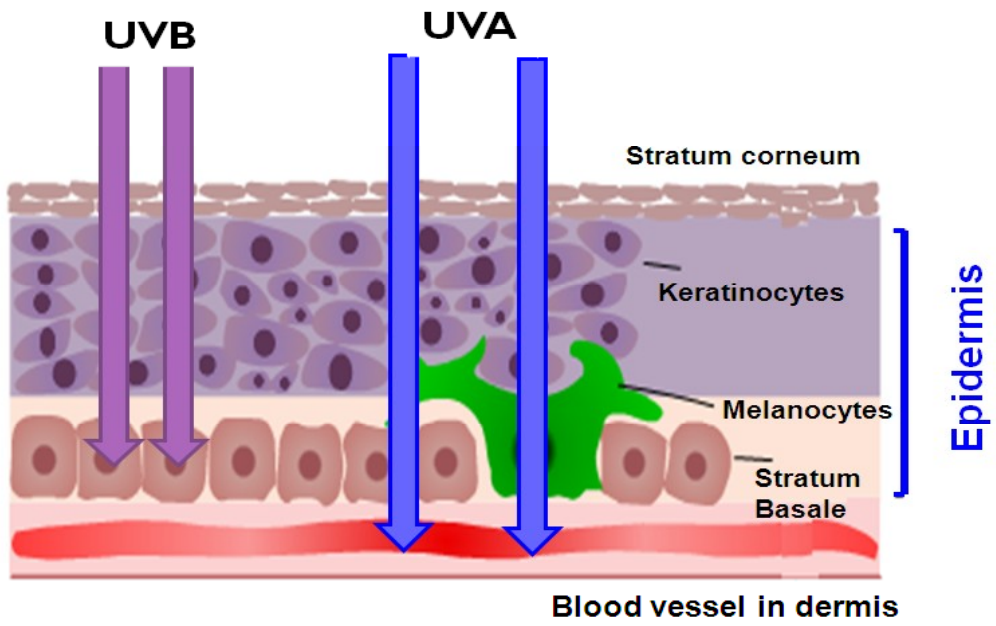

Figure 1.4 The depth of penetration of the skin by UVA and UVB radiation.

UVR generates a range of biological responses in the skin, which includes adaptive, inflammatory and immunological reactions (5). Solar UVR is a major environmental factor that influences the function, survival and proliferation of many cell types (34). UVR causes mutations and increases cellular proliferation; it is therefore able to cause

skin cancer without additional initiators or promoters being present and is thus termed a “complete carcinogen” (30).

UVR augments blood flow and infiltration by macrophages and neutrophils into the skin. These infiltrating cells also produce large amounts of nitric oxide (NO) resulting in peroxynitrite formation and reactive oxygen species (ROS) which can cause damage to tissues (35). Photocarcinogenesis is most commonly thought to be the result of a chain of events that involve formation of DNA damage and subsequent mutations following exposure to UV light as shown in Figure 1.5. These responses are mediated by a tightly controlled network of signalling pathways, many of which involve the tumour suppressor p53 gene (16). UV-induced mutations of p53 with subsequent disruption of cellular damage responses are a hallmark of most sun-induced cutaneous SCCs (16).

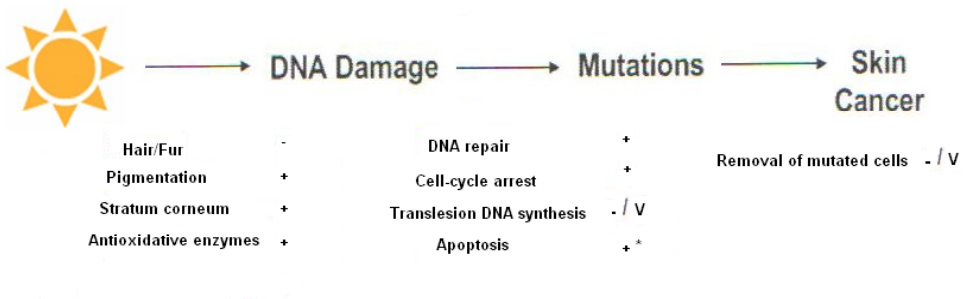

Figure 1.5 The photocarcinogenesis chain of events and intrinsic protective mechanisms for the prevention of skin cancer formation following sun exposure (16). The induction by UVR is represented by -, + and v (variable). * Although UVB readily induces apoptosis, in some instances UVA can inhibit this from (39).

Whereas sunburn exemplifies a proinflammatory effect on the skin, UVR also has an immunosuppressive effect, evidenced by its therapeutic effect against certain inflammatory skin disorders (albeit with carcinogenic risk) (36). UVR also suppresses the normal pathways of immune surveillance responsible for eliminating mutant cells. Kripke and colleagues (37, 38) were the first to show that UV immunosuppression could be transferred by injecting T cells from UV treated mice into naïve recipients It was subsequently established that UV-induced suppression generated a subset of T-suppressor cells that were antigen specific (24, 36). UVR-induced immunosuppression can also affect delayed type hypersensitivity responses (DTH), susceptibility to infections, radiation recall responses, and vaccine immunogenicity (36).

In contrast, UVR in combination with chemicals is used in the therapy of many skin diseases including psoriasis and vitiligo. Although such therapy is beneficial, it is accompanied with undesirable side effects on human skin; Thus UVR is like a two-edged sword, as it has both detrimental and beneficial effects (7).

1.3.1 UVB Radiation

UVB can cause sunburn, inflammation, cataract formation, DNA mutations and membrane damage as well as skin cancer (16, 24, 30, 39). It is known that UVB directly damages DNA and can induce ROS by interactions with chromophores in the skin (40). The DNA damage seen in epidermal cells caused by UVB-irradiation typically results in the formation of cyclobutane pyrimidine dimers and 6-4 photoproducts. Mutations of

this kind are frequently found in p53, p16, PTCH and INK4α/CDKN2A in skin cancer patients (41, 42).

1.3.2 UVA Radiation

UVA on the other hand because of its longer wavelength, can penetrate through the epidermis to the dermis and underlying blood vessels. It can cause premature skin ageing, wrinkle formation, blotching and induces sunburn cell formation in the epidermis, as well as skin cancer (24, 30). Although the main source of UVA exposure is from sunlight, use of UVA emitting lamps in sunbeds for recreational tanning has raised additional concerns about artificial sources of human exposure (24, 43).

UVA affects keratinocytes at a transcriptional level by altering the expression of genes involved in apoptosis, cell cycle, DNA repair, signal transduction, RNA processing and translation, cell structure and metabolism (44). It can cause DNA damage by the generation of ROS (45) that results in a wider range of genomic damage e.g. single-stranded breaks, protein-DNA crosslinks, and oxidative base damage (e.g. 8-oxo-7,8-dihydroxyguanine) (46).

1.3.3 UVA *vs* UVB

For many years UVB was considered to be the main carcinogen involved in skin cancer formation, based largely on the DNA action spectrum of UVR (47, 48), but UVA has more recently been acknowledged as playing an important role in skin carcinogenesis (47, 48). This is in keeping with the growing body of evidence that direct molecular

targets of UV other than DNA are important to carcinogenesis. UVA, although it does not produce an inflammatory response at doses that people would normally be exposed to, produces ROS and so, unsurprisingly, activates many of the same signalling pathways as UVB. Doses of UVB, UVA and solar stimulated UV (ssUV) too low to cause inflammation are able to induce mutations (48). However, this does not exclude a role for ROS from inflammatory cells contributing to skin carcinogenesis, but they may be important for tumour progression (48). Previous research has also demonstrated that UVA has a systematic immunosuppressive effect as it diminishes DTH reactions upon antigen stimulation (49, 50). This has implications for sunscreen design as most protect against UVB only, thus preventing erythema, and oedema.

The ability of sunscreens to prevent UV-induced erythema, a function expressed as a "sun protection factor" (SPF), is well documented. In addition, sunscreens have been shown to prevent photoageing and UV-induced DNA pyrimidine dimer formation (51). The results are still conflicting, however, regarding their ability to protect against UV-induced immunosuppressive effects (51). If UVA does contribute to immunosuppression these narrow spectrums (UVB filter only) sunscreens offer little protection against immunosuppression and problems with absorbance and photostability means protection has often been unsatisfactory (46). This demonstrates a need for broad spectrum (UVA and UVB filter) protection (49, 50). Furthermore, as a result of their widespread misapplication, sunscreens often allow an individual to remain for longer periods in the sun and hence receive greater exposure to UVA at lower dose rates (46).

1.3.4 Effects of Acute UVR

Acute UVR (a single exposure) can cause tanning by enhanced melanogenesis (erythma-more commonly known as sunburn occurring due to the vasodilation of cutaneous blood vessels), oedema, DNA damage at the molecular level, apoptosis and growth arrest as seen in Figure 1.6 (7, 30, 34).

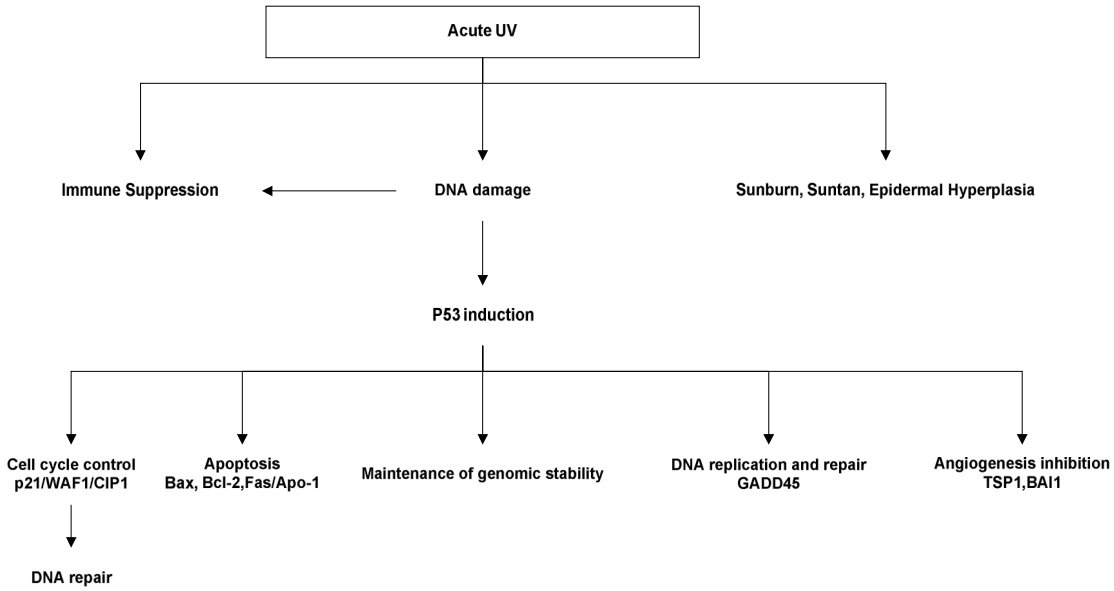

Figure 1.6 Effects of acute UVR on the skin (7).

1.3.5 Effects of Chronic UVR

The long-term effects of UV exposure include photoageing, immunosuppression, tumour promotion and carcinogenesis (7). The reactions caused by chronic UV exposure (Figure 1.7) are believed to be partly caused by multifactorial substances which include cytokines and other proteins (30). Previous studies have demonstrated that chronic

exposure to UVR reduces the antioxidant enzyme levels in both SCC and BCC resulting in a moderate increase in lipid peroxidation markers (33, 52). These findings suggest that an increase in UV exposure induces oxidative stress via an increase in ROS which could potentially lead to cancer (53).

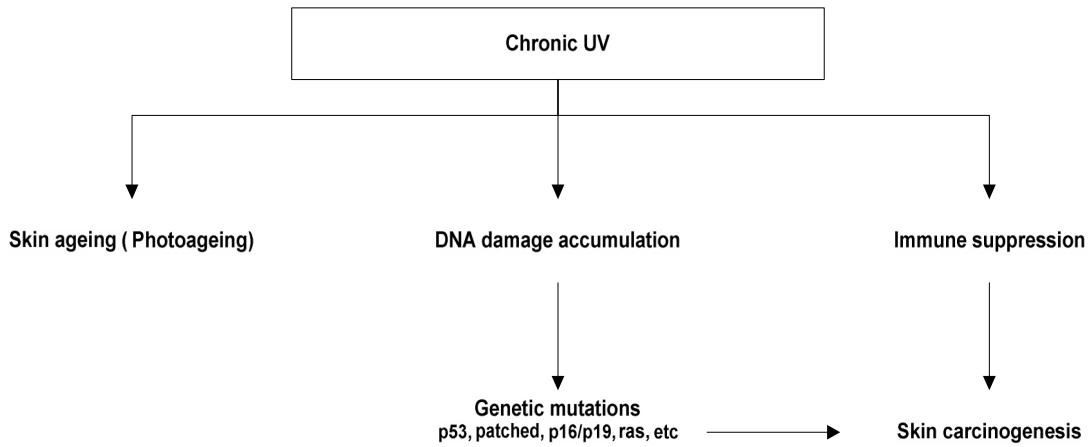

Figure 1.7 Effects of chronic UVR on the skin (7).

1.3.6 UV-Induced inflammation

It has been shown that UV at high doses can induce inflammation which results in the appearance of macrophages and other leukocytes in the skin (54). The infiltrating monocytes and macrophages, which enter the irradiated skin tissue, in turn, secrete mediators that prolong the inflammatory response. As well as these cells, other inflammatory mediators such as prostaglandin (PGE_2) (55), NO (56) and ROS (40, 45, 57), and cytokines such as interleukin (IL)-1α, interferon (IFN)-γ, and tumour necrosis

factor α (TNFα) (48, 58-60) are seen in the skin that has been exposed to UVR (Figure 1.8).

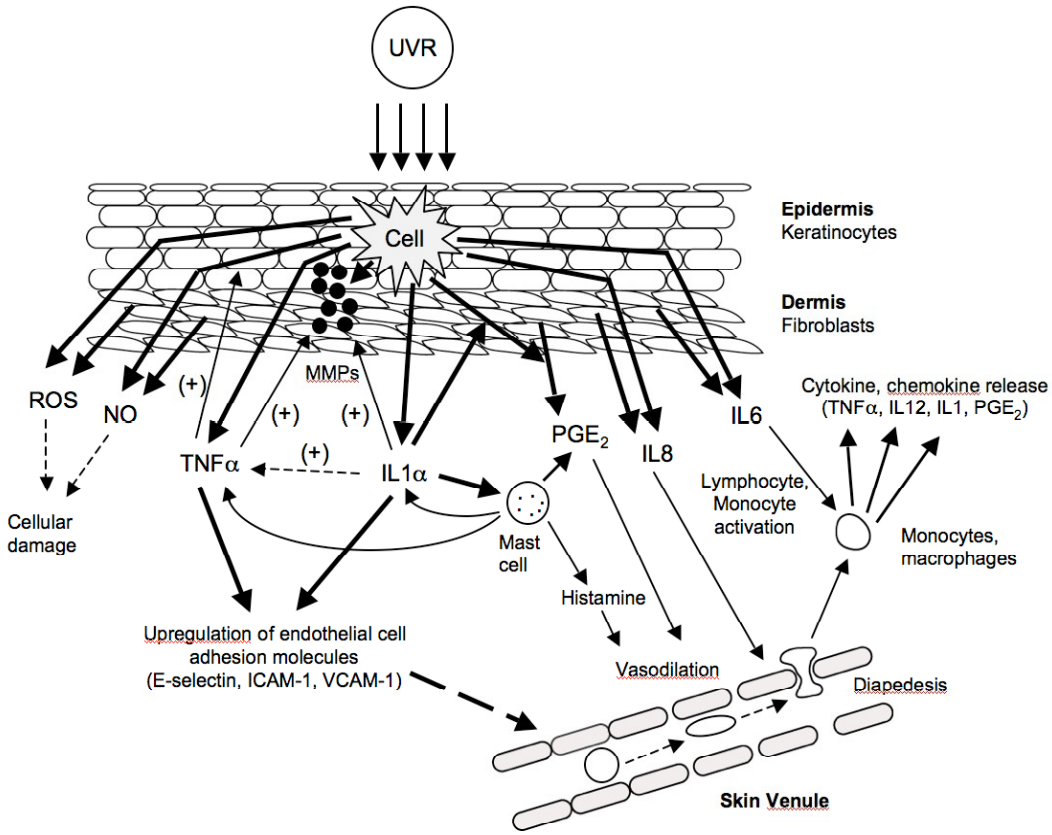

Figure 1.8 The inflammatory response seen in the skin following exposure to UVR, as adapted from (61).

It has been shown that ROS can cause DNA strand breaks as well as lipid peroxidation, membrane and protein damage (35, 40, 45, 46). They can also initiate signal transduction processes leading to rapid synthesis and release of PGE_2 and isoprostanes (57, 62) as well as induction of new gene products such as cytokines, heme oxygenase-1,

cyclo-oxygenase (COX), intercellular adhesion molecules (ICAM) (55, 62) and inflammatory mediators such as TNFα (63, 64). A list of immunomodulatory molecules whose expression is up-regulated by UVR is seen in Table 1.2 (30, 35, 61, 65-69).

Proinflammatory molecules have been shown to have important roles in the pathogenesis of skin cancer, as determined from clinical or experimental animal studies, and the activity or quantities of many of these are affected by UVR (35, 48). It is known that many tumours, even those which have not been caused by UVR, can produce an inflammed environment (59, 72, 73). It is known that inflammatory mediators such as IL-1α, TNFα and IL-6 are involved in melanoma formation (74). Inflammation has also been shown to play a role in NMSC as well (54, 75-77). In a recent study, male mice were shown to be more sensitive to UVB-induced skin carcinogenesis than female mice (78), which is consistent with men having a higher incidence of skin cancer than women (48). In this study, an inflammatory dose of UVB was used to induce the cancers. Damian *et al*. (79) found that while women developed a larger inflammatory response to UVB, men were found to have lower antioxidant protection in the skin resulting in a higher level of oxidative damage to DNA, and are more sensitive to UV-induced immunosuppression than women. This would suggest that UV-induced immunosuppression and DNA damage but not inflammation are associated with the formation of skin cancers in men compared to women (48).

IL-1α and IL-1β are both induced in keratinocytes exposed to UVB radiation (65, 80). IL-1α has also been shown to enhance the expression and release of TNFα from

Mediator	Produced by	Function	References
TNFα	Keratinocytes Mast cells Dermal fibroblasts Langerhans cells	Langerhans cell migration, sunburn cell information, stimulates prostaglandin (PG) synthesis, changes in adhesion molecule expression	(69, 70)
IL-1α	Keratinocytes Langerhans cells	Stimulates PG synthesis, increases TNFα and IL-6, inhibited by IL-1 receptor antagonist	(69)
IL-1β	Keratinocytes Langerhans cells	Langerhans cell migration	(69, 70)
IL-6	Keratinocytes Langerhans cells	Fever Severe sunburn	(30, 69)
IL-10	Keratinocytes (mouse) Macrophages (human) Melanocytes	Blocks cytokine production by T cells, macrophages and NK cells Decreases antigen presentation, Increases IL-1 receptor antagonist	(69) (30, 66, 69)
IL-12p40 (not bioactive)	Keratinocytes, Dendritic cell, Langerhans cells	Decreases Th1 response Decreases antigen presentation	(69)
IFNγ	T cells	Triggers apoptosis T-cell mediated tumour cell destruction	(71)
PGE_2	Keratinocytes, Mast cells	Erythema Decreases antigen presentation Increases IL-4, decreases IL-12	(69)
Histamine	Mast Cells	Increases release of PG Inhibit lymphocyte functions like IL-2 and IFNγ	(30, 69)

Table 1.2 Immunomodulatory mediators in skin cells whose expression is up regulated by UVR.

UVB-irradiated keratinocytes (81-83), while IL-1β enhances the expression of matrix metalloprorease-9 (MMP-9) in these irradiated cells (84). Apart from IL-1β it has been shown that UVB can stimulate MMP-9 expression in human skin via the induction of Activator protein-1 and NFκB activities (85).

Apart from inducing cytokines, UVB radiation has been shown to increase COX-2 expression and activity in keratinocytes (48, 58, 86). High levels of COX-2 activity have been observed in human epithelial skin cancers which are increased in response to UVB radiation (87). The addition of nonsteroidal anti-inflammatory drugs (NSAIDs) has been shown to inhibit COX-2 activity and subsequent PGE formation in the skin, and they have been used in the treatment of actinic keratosis (AK) (88), BCC, SCC and melanoma (89). This suggests that COX-2 plays a role in the formation of these tumours. Recent studies using IL-12-deficient mice, have found that they have higher levels of inflammation and increased incidence of skin cancers compared to wild type controls which suggest that this cytokine may play an important role in modulating the inflammatory response seen in the skin (76).

Up-regulation of TNFα is a key early response by keratinocytes exposed to UVB (30, 83, 90, 91) and represents an important component of the inflammatory cascade in skin. UVB-irradiation induces the expression of TNFα mRNA in both keratinocytes and dermal fibroblasts within a few hours (83, 90). IL-1α stimulates TNFα expression (81) and release particularly in skin where there is substantial preformed amounts of this cytokine (83). Recently, Bashir *et al*. (81) found that TNFα expression and secretion in IL-1α treated keratinocytes was induced by UVB but not by UVA-irradiation. This induction was mediated through increased TNFα gene transcription (81). The IL-1α

formed in the epidermis and dermis can in turn induce mast cells to secrete inflammatory cytokines, such as TNFα and IL-1α, as well as PGE_2 which can enhance the inflammation caused by direct UV exposure on the epidermal cells (48, 61). The histamine released from the mast cells can induce vasodilation of the surrounding blood venules which assists in the leukocytes undergoing diapedesis and entering the region (48, 61).

TNFα secreted from epidermal keratinocytes or dermal fibroblasts has been shown to induce a myriad of pro-inflammatory effects on the skin. There are synergistic interactions between pro-inflammatory cytokines produced in the skin and in synergy with irradiated keratinocytes, leading to later augmentation of TNFα production in UV-irradiated tissue. UVB radiation can induce the synthesis and release of IL-6 and IL-8 from irradiated keratinocytes and fibroblasts (61, 69, 76, 80). IL-8 assists in the homing of leucocytes from surrounding blood venules into the inflamed region, while IL-6 is known to trigger the activation of monocytes and other infiltrating leukocytes to secrete cytokines and chemokines (61).

TNFα has been shown to induce adhesion molecules and chemokines in the surrounding epithelial cells, resulting in the recruitment of inflammatory leukocytes from surrounding blood vessels via diapedesis (48, 61, 92-94). These inflammatory cells secrete additional cytokines that form a positive feedback loop in further up-regulating TNFα and downstream TNFα-induced chemokines, cytokines, and other pro-inflammatory pathways in irradiated skin (30, 81, 95). These effects elicited by the infiltrating inflammatory cells occur some hours after UV-irradiation, and this prolongs the observed inflammation. In addition, UVB radiation also induces inducible nitric

oxide synthase (iNOS) activity in dermal endothelial cells, which play an important role in UVB-induced inflammation observed in skin, This induction of iNOS has been shown to occur via a TNFα-dependent pathway (81, 91, 96).

It can be seen that TNFα plays an important pro-inflammatory role in the skin, both due to (a) the direct effects of UVR and (b) the indirect effects of inflammatory cells that chemotax to the skin. It is clear that UV-and inflammatory cell-derived cytokines further enhance TNFα gene transcription in human skin cells (81, 90), and this can further increase epidermal production of TNFα. However, clustering and internalization of TNF receptors may lessen the response to the TNFα protein over time, and this may account for why persistent TNFα in culture supernatants do not sustain TNFα mRNA upregulation over time (48). For further information on the complex interplay of cytokines, chemokines and other mediators in UV-induced inflammation please read the following reviews (48, 85, 86).

Therefore, inflammation can be induced as a direct result of UV exposure on epidermal cells, or due to the release of secreted molecules, which in turn induce the release of inflammatory mediators from the dermis, as well as attracting inflammatory cells from circulation into this region of the skin.

1.3.7 UV-Induced Immunosuppression

Both UVA and UVB can induce immunosuppression. The local immunosuppression is mainly a result of the functional inhibition of LC in the epidermis (97). Systemic immunosuppression is mainly caused by the UV-induced release of immunosuppressive mediators from keratinocytes that enter circulation (97). Because DNA is one of the

major UV chromophores in the skin, it has been proposed for quite a long time that UV-induced DNA damage may place a crucial role in UV-induced immunosuppression (97, 98).

1.3.7.1 Local Immunosuppression

Local immunosuppression refers to the situation where the hapten is applied directly to UVB-irradiated skin (99). This results in suppressed contact hypersensitivity (CHS) response and alterations in the function of LC occur within site exposed to UVR (30, 100). Suppressing CHS by applying haptens directly to UVB-irradiated skin has been demonstrated in both animals and humans (30, 79, 101). Local immunosuppression is also caused by the reduction of LC in the epidermis following UV exposure (30, 66, 99, 100). LC are killed due to direct exposure to UVR (99) or they migrate to lymph nodes as a result of TNFα secretion from irradiated keratinocytes (69, 105) or mast cells (102). These LC that have been lost are replaced after a short period of time by neutrophils, differentiated macrophages and monocytic APC, which are distinct from those that were present in the epidermis prior to UV exposure (30, 100). The period of immunosuppression seen following UV exposure can persist in the skin for at least 7 days, which would allow cells possessing DNA damage to undergo autocrine and paracrine growth factor driven cell division (30, 100).

1.3.7.2 Systemic Immunosuppression

Systemic immunosuppression results in a suppressed CHS as well as a DTH response (49, 103); and requires immune mediators such as cytokines and *cis*-Urocanic acid

(*cis*-UCA) (42). The process involves LC, Th cells and soluble mediators released from keratinocytes and occurs at draining lymph nodes distal to sites that have been irradiated (30, 100). Recently it has been shown that the numbers of LC in UV-irradiated human skin under *in vivo* conditions were not reduced, which differed from that seen under *ex vivo* or *in vitro* conditions (104). This suggests that changes in antigen presentation by LC in human skin following UV exposure could be due to changes in cytokine levels, and not reduced cell number.

Th1 cells secrete IL-2, IL-12 and IFNγ, which promote the cell-mediated immune response resulting in a downregulation of the proliferation and differentiation of Th2 cells (103). As Th2 cells produce IL-4 and IL-10 they are capable of a further suppression of the cellular immune response (28, 105). The infiltrating macrophages secrete IL-10, which further downregulate the Th1 cellular response while enhancing the Th2 response (30, 63, 106). Although IL-12 enhances cell-mediated immunity and its transcription is upregulated in UVB-irradiated skin cells, the levels produced are insufficient to overcome the immunosuppression induced by IL-10 (70, 103). IL-10 mRNA and protein expression in primary human melanocyte cultures has shown to be upregulated following UV-irradiation but not in keratinocyte cultures (28). In humans, the IL-10 detected in the epidermis following exposure to UV most likely originates from infiltrating macrophages found in the skin (107, 108).

UVB-induced immunosuppression is implicated in the pathogenesis of skin cancers, and is postulated to be mediated in part by *cis*-UCA (109, 110). *trans*-UCA, a deamination product of histidine, is a major chromophore present at a high concentration in the epidermal keratinocytes in the stratum corneum (110). Upon exposure to UVR,

trans-UCA undergoes a photoisomerization to its *cis*-isomer until equilibrium is reached with the two isomers being in approximately equal quantities. In humans, this occurs after 1 minimal erythemal dose (MED) of UVR, which is the lowest dose required to induce a just visibly perceptible erythema (109, 110).

cis-UCA has been shown that it does not exert its immunosuppressive effects through TNFα, but through other factors such as PGE_2 (109). In studies using TNF-R1(-) mutant mice it has been shown that TNFα is not involved in UVB-induced immunosuppression (6, 111). Amerio *et al*. (112) showed that in TNFR1 and TNFR2 (TNFR2; p75) double knockout mice, TNFα was not primarily involved in *cis*-UCA-mediated UVB immunosuppression. Skov *et al*. (113) found that three MED of UVA1 (340-400 nm) radiation caused a decrease in TNFα levels along with an increase in *cis*-UCA levels in suction blisters of human skin. However, in UVB-irradiated skin, high levels of TNFα was detected, suggesting that UVA mediated immunosuppression may occur via *cis*-UCA unlike that seen following UVB exposure (113).

There are many other immunosuppressive molecules (*cis*-UCA, histamine, PGE_2 and granulocyte/macrophage colony stimulating factor and neuropeptides) that may induce immunosuppression in the skin (30, 67, 70, 114). The interplay between these various UV-induced cytokines and bioactive molecules is complex and not completely understood, but it appears that a cytokine cascade is activated that ultimately affects systemic APC function which suppresses the Th1 cell-driven immune reactions (30). While it is now clear that TNFα may not play a major role in UV-induced immunosuppression (112, 115, 116) it does play a significant role in UV-induced

inflammation (48) as well as in other inflammatory diseases such as rheumatoid arthritis, psoriasis or systemic lupus erythematosus (59, 81).

1.4 Tumour Necrosis Factor α

TNFα, which was formerly known as cachexin or cachectin (117), is a member of the TNF ligand superfamily (118-121). It is a type II transmembrane glycoprotein of 234 amino acids which possesses an extracellular carboxy-terminus and a cytoplasmic amino group (118-120). The overall structure of TNFα is described as a "β-jellyroll" in which eight antiparallel β-strands form a sandwich 3D structure (118). It can exist in two forms; a 26 kDa membrane-bound form (mTNFα) and a 17 kDa soluble form (sTNFα).

TNFα is a keystone signalling cytokine and is mainly produced by macrophages and to a lesser extent monocytes, T-cells, mast cells, epithelial cells, dendritic cells, osteoblasts lymphoid cells, keratinocytes, melanocytes, fibroblasts and other cells (30, 83, 118, 120, 122). One of the best known actions of TNFα is in macrophage-mediated cytotoxicity due to its proapoptotic effects (118, 120). TNFα is a key regulator of lipid metabolism in adipose tissue and protein catabolism in muscle as well as in other disease states such as obesity-related insulin resistance (118, 120). It plays a crucial role in the pathogenesis of psoriasis, mainly by inducing the expression of ICAM-1 on keratinocytes and other cell adhesion molecules (e.g. vascular adhesion molecules, E-selectin) on dermal microvascular endothelium (121).

TNFα is also involved in apoptosis, cellular proliferation, differentiation, inflammation, tumorigenesis, apoptosis, viral replication, immune response to extracellular stimuli as well as local and systemic inflammation (103, 118, 123). The dysregulation and in

particular, overproduction of TNFα has been of concern in a variety of human diseases such as lethal shock syndrome and cancer (66, 118-120).

Kock *et al*. (124) found that there was a significant amount of TNFα produced by human keratinocytes following low dose UVB (0.1 kJ/m^2) exposure. Schreiber *et al*. (125) showed that epidermal murine keratinocytes predominantly generated TNFα, which suggests that these cells may be the primary source of TNFα in the epidermis (124-126). TNFα has been shown to maintain the viability of murine-cultured LC, although it does not induce their functional maturation (30, 115, 127, 128). In the dermis, monocyte, macrophages and fibroblasts release varying quantities of TNFα depending on the UV type and dose (103, 129, 130).

Dermal injection of TNFα results in the accumulation of dendritic cells in draining lymph nodes (115, 131), suggesting that this cytokine may serve as a stimulus for the migration of LC from skin to regional lymph nodes (115, 132). Streilein and colleagues (115, 133, 134) suggested that UVB indirectly induces TNFα, which then causes morphologic and functional changes on LC resulting in the impairment of CHS.

Most of the cellular actions described for TNFα correspond to its secreted, soluble form (sTNFα). There is increasing evidence that mTNFα is also biologically active and that it may be responsible for the localized action of this cytokine (118). sTNFα is cleaved from mTNFα between Ala^{76} - Val^{77} by the action of the metalloprotease, tumour necrosis factor α converting enzyme (TACE) (119, 120, 122, 135, 136). Both forms of TNFα can specifically bind to one of two receptors: a 55-kDa (p55 or CD120a receptor) form designated TNF-Rl; and a 75-kDa (p75 or CD120b receptor) form designated

TNF-R2 (115, 122, 137). These two receptors are transmembrane glycoproteins which display a high degree of structural homology and are expressed on most cell types (132).

TNFRI is expressed on all cell types and its signalling mediates cytotoxicity, cell proliferation and antiviral activity (118). TNFRII is expressed on haemopoietic, endothelial cells and LC and plays a role in the proliferation of thymocytes and cytotoxic T lymphocytes (118, 119). Membrane-bound TNFRI and TNFRII can be cleaved by TACE to release the soluble forms of these receptors and this process is activated by IL-10 (117, 118). The soluble forms of TNFR has been postulated to act as (a) an antagonist to the surface receptors by competing for sTNFα or (b) an agonist by stabilizing the TNF trimer; therefore maintaining saturating concentrations in the extracellular fluids (118, 119, 138). UV-induced TNFα is involved in the formation of sunburn cells, suppression of CHS, LC migration from the skin, diminished antigen presentation and loss of immunosurveillance (30, 139, 140)

Studies have shown that when TNFα is bound to the TNFRI receptor it plays a role in UVB-induced apoptosis in keratinocytes (also known as sunburnt cells), which prevents mutated cells from passing on mutations to daughter cells (138, 141). The injection of TNFα antibodies in Balb/c mice after UVB-irradiation showed a reduction but not a complete absence of sunburn cells in skin biopsies (141). Moreover, increasing the dose of TNFα antibodies did not cause any further reduction in the formation of sunburn cells. This suggests that TNFα is involved in sunburn cell formation, but this process is a multifactorial event that probably involves a combination of other cytokines (141).

Transgenic mice deficient for either TNFRI and/or TNFRII have been shown to be less susceptible to UVB-induced skin tumours than are wild type controls (128). Through the use of TNFRI (115, 142, 143) and TNFRII (115, 144) gene-targeted mutant mice, it has been shown that TNFRI plays a decisive role in the host's defence against microorganisms, while TNFα binding to TNFRII plays a role in the induction of tissue necrosis. Using agonist and antagonist antibodies specific for each receptor, it has also been indicated that TNFα binding to TNFRII does not potentiate the cytotoxicity of TNFRI, but instead regulates the rate of TNFα association with TNFRI (115, 145) which suggests that TNFRI is the main mediator of TNFα action in the cell.

While, TNFα is known to be cytotoxic to some tumour cell lines, it can mediate UV-induced tumorigenesis in others (30, 128). The ability of TNFα to suppress immunity following UV exposure could be dependent on several factors like the type and dose of UVR and the influence of other cytokines (5). Overall, the role of TNFα in inflammation and immunologic reaction have been shown to be either beneficial (protective) or deleterious (pathologic), depending on target cells, and magnitude of the inflammatory reaction (115).

Thus, UVR has been shown to be a potent inducer of TNFα and cytokine gene expression, which mediates signalling by human keratinocytes (30, 146, 147). TNFα is released from the surface of the keratinocytes as a mature protein by the action of the metalloproteinase TACE, also known as ADAM-17 (135, 148, 149).

1.5 TACE

TACE is a member of the disintegrin and metalloprotease (ADAM) family of proteases, and is also known as ADAM 17 or CD156q (150-154). ADAM proteases belong to the adamalysin/reprolysin subfamily of the metzincin superfamily, and contain a Zn^{2+}-dependent catalytic domain as shown in Figure 1.9 (152, 153, 155).

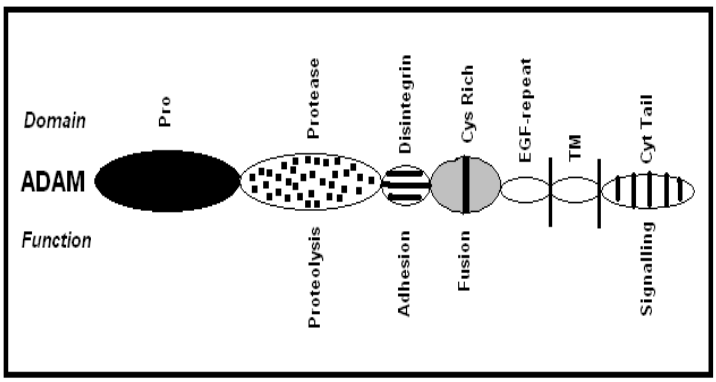

Figure 1.9 Structure of the ADAM proteins. Adapted from (156).

At present, 30 members of the ADAM family have been identified, although many are not fully characterized (152). Table 1.3 highlights some of the biological functions of ADAM family members (157).

Protein	**Function**
ADAM 1 – 7	Spermatogenesis, fertilization
ADAM 8, 28	Immune functions
ADAM 9, 12, 19	Myogenesis, osteogenesis
ADAM 10, 11, 13	Neurogenesis
ADAM 17 (TACE)	Processing of TNFα

Table 1.3 Distinct functions of selected ADAM family members (157).

TACE (ADAM 17) is a multi-domain type I transmembrane protein of 824 amino acids in length which was purified, characterized and cloned in 1997 (136, 157, 158). While the amino acid sequence of TACE (Figure 1.10) shows relatively low homology to other ADAM family members (136, 157), its structure (Figure 1.11) contains all the domain regions which are characteristic for this family of metalloproteases (136, 157, 158). The prodomain of TACE is similar to that of other ADAMs and MMP and, is thought to act as an inhibitor of the protease activity via the cysteine switch mechanism (157, 159). The free cysteine residue from the sequence PKVCGVPD present in the prodomain of the TACE coordinates with the Zn^{2+} in the active site of the protease thus preventing enzymatic activity before maturation (157, 159). Prodomain removal is required for TACE to become biologically active.

The metalloproteinase domain contains the zinc-binding consensus motif HEXGHXXGXXHD involved in coordinating Zn^{2+} with His residues and creating the active site of the enzyme (149, 157). The role of the disintegrin domain in TACE is not known, but it may have an adhesion function since this domain in other ADAM family members has been shown to interact with integrins (157, 160). Analysis of the amino acid sequence sequence of TACE also indicates the presence of an EGF-like domain and a unique crambin-like domain which contains a cysteine switch. However, the roles of which are not fully understood. The cysteine-rich domain may be important for substrate recognition (158) or enzyme maturation (159). The cytoplasmic tail of TACE contains a potential phosphorylation site (157, 161) and an SH3-binding site (157).

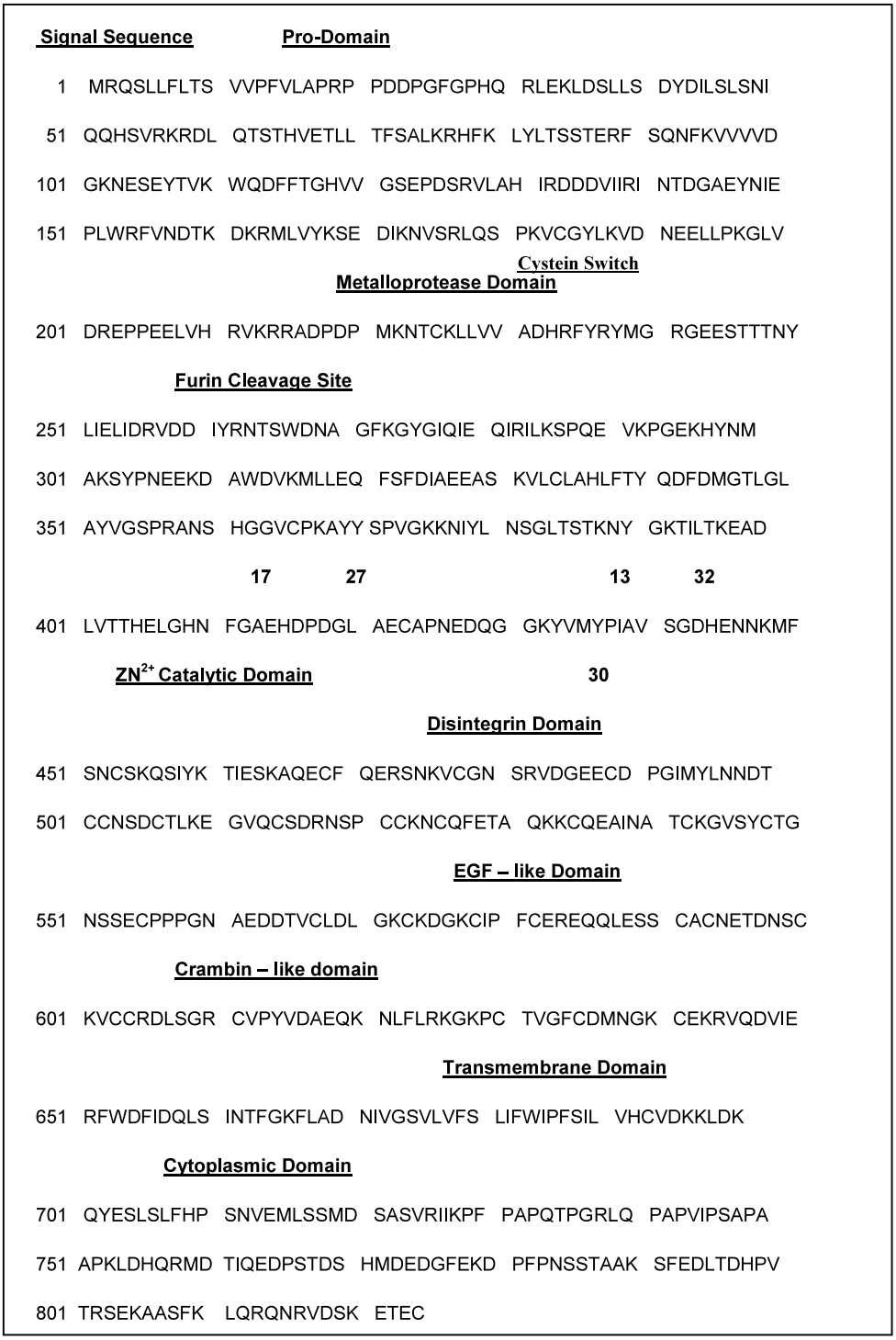

Figure 1.10 The amino acid sequence of TACE: highlighting the cysteine switch, furin cleavage site and Zinc motif. Adapted from (136).

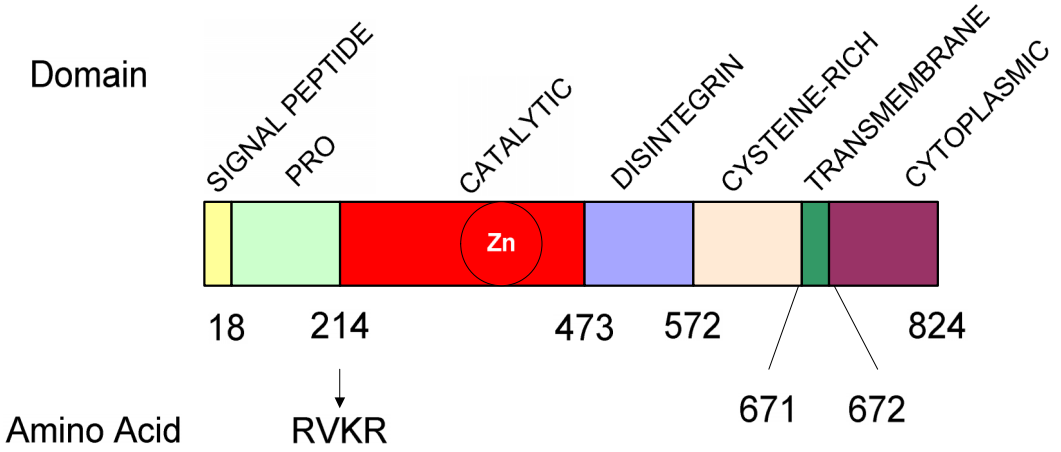

Figure 1.11 The structure of TACE. Adapted from (157).

The expression of TACE mRNA is ubiquitous and is not limited to TNFα-producing cells (136). TACE is synthesized as an inactive zymogen, which is subsequently proteolytically processed to the catalytically active form. In order for TACE to be activated it must first be cleaved from its 120 kDa proform (proTACE) into its 90 kDa mature form by the removal of its prodomain (154, 159, 162). The cleavage of which occurs at the furin cleavage site RVKR (Arg-Val-Lys-Arg) localized between the pro- and the catalytic domain. The removal of the prodomain is due to the action of a furin-type proprotein convertase (160, 162-164) and possibly other intracellular proprotein convertases (PC) such as paired basic amino acid cleaving enzyme (PACE) 4, PC1, PC2, PC5/6 and PC7/8 (157, 162, 165-167).

In mammalian cells, proTACE was shown to be exclusively intracellular, located in the endoplasmic reticulum and the proximal golgi body whereas the mature form is located both intracellularly and on the cell membrane (162, 165, 168). TACE maturation is closely linked to the transport of proTACE through the medial golgi, where upon exit, prodomain removal occurs before the enzyme reaches the cell's surface (160). TACE maturation is negatively influenced by the phorbol-12-myristate-13-acetate, which decreases the amount of mature protein in treated cells (165, 169). The resistance of the mature form of TACE to deglycolysation by Endo H treatment suggests that maturation takes place in the late golgi compartment (160, 169).

TACE has been shown to cleave a wide range of molecules including TNFα, TGFα, amphiregulin, neuregulins, growth hormone receptor, both TNFα receptors, L-selectin (115, 142), amyloid precursor protein and IL-6R (115, 142, 149, 160, 170-172). TACE-knockout mice are less efficient at processing TNFα on the cell membrane compared to wild type controls (136, 157). These mice have elevated levels of mTNFα as well as reduced levels of sTNFα compared to wild-type controls. This suggests that TACE is the main protease responsible for cleaving TNFα on the cell membrane (136). Some MMPs can also cleave TNFα, but the cleaved products are biologically inactive due to hydrolysis occurring at different sites within the molecule (135, 136, 149, 161, 172). The ability of cells to release TNFα despite a variety of mutations around its cleavage site suggests that interactions between regions of pro-TNFα distal to this site along with regions of TACE distal to its catalytic site may be important for recognition and cleavage of TNFα by this protease (156).

While some metalloproteases have been shown to be activated in epidermal cells following UVR (173), it is unknown if TACE is also affected. Whether TACE activity in irradiated skin cells is modulated by changes in the expression and/or activity of furin also remains to be elucidated. Skiba *et al*. (147) reported that UVA- and UVB-irradiation increased TACE mRNA levels in HaCaT cells, with higher induction induced by UVA. The expression patterns for both UVA- and UVB-irradiated cells generally appeared to be constant, although mRNA levels were significantly higher than controls, throughout the 48 h period following exposure (147).

In UV-irradiated HaCaT cells, it has been shown that TACE is responsible for the increased cleavage of EGF family members (174, 175). Inhibition of TACE activity by metalloprotease inhibitors reduced the release of these growth factors, resulting in an increase in apoptotic cell death (174, 175). It appears that TACE mediates an EGF receptor/AKT signalling pathway in these cells that is activated as a result of its cleavage of EGF family members. In HaCaT cells exposed to UVA radiation TACE mediated EGF receptor activation and cell cycle progression, which suggests that UVA, at non lethal doses, has the potential to be a skin cancer promoter (174).

In support of the role TACE may play in skin cancer development, it was shown to be over expressed in a large number of skin cancer cells lines compared to non tumour cells (175). It is also known that members of the EGF family are over expressed in skin cancers (176), and this could be a mechanism by which skin cancer growth is stimulated by autogenic growth factors. The result of these studies suggest that inhibition of the action on TACE following UVR may prevent the stimulation of the surviving irradiated cells, which has the potential in reducing the incidence of skin cancer that may arise

from prolonged sun exposure. What is not clear is that the increase in TACE activity seen in these irradiated skin cells is due to increased levels or a change in its activity. The proprotein convertase furin is known to activate TACE (162, 163) as well as MMPs (155, 167) and may play a role in this process.

1.6 Furin

Furin, also known as PACE, is a 94 kDa, type I transmembrane, Ca^{2+}-dependant serine protease (155, 164, 167, 169). The protein was named furin because it was in the upstream region of an oncogene known as *FES* (155) and the gene was known as *FES* upstream region (FUR) (164). Furin is a mosaic protein consisting of a series of multifunctional domains. At its N-terminal region, a signal peptide directs the translocation of the growing peptide chain to the endoplasmic reticulum and the secretory pathway (155, 163, 177). Next, the pro-region initially folds onto the native protein, thereby keeping the enzyme in a zymogen or inactive state (155). The pro-region is cleaved early in the endoplasmic reticulum by an intramolecular autocatalytic process, where it then associates with the catalytic domain and helps to guide the protein through the endoplasmic reticulum and golgi apparatus for its eventual enzymatic activation (155, 177).

Furin carries structural information within the cysteine-rich region (CRR) that facilitates shedding of its ectodomain (155, 177). The CRR could participate in the shedding process by imparting a conformation to furin facilitating recognition and cleavage by its sheddase (155, 177). The CRR could be considered either as a functional region involved in cell adhesion (171) interacting with specific target proteins or influencing

conformation enabling dimerization or shedding of membrane proteins (155, 177). The CRR is followed by a trans-membrane region that anchors the enzyme in the membrane of the trans golgi network (TGN) or the cell membrane. The cytosolic tail contains the information necessary for furin's sorting to various intracellular compartments (155, 163, 164, 177). In the epidermis, furin can exist either as: (a) a mature 97 kDa membrane bound enzyme or (b) a smaller 75 kDa form that lacks the transmembrane domain and reactivity with the c-FUR antibody specific for the C-terminus (155). This suggests that post-translational cleavage at the C-terminus takes place in the cell (167, 177).

Furin is a ubiquitously expressed member of the PC family. This family is related to the bacterial subtisilin (167) and consists of seven distinct members (PC1-PC7) that vary in regards to their tissue and subcellular distribution as well as enzymatic and biochemical properties (155, 157). Furin and other PC family members process inactive precursor proteins to their functional or mature form. These molecules include growth receptors, growth factors, hormones, plasma proteins, MMP and extracellular matrix (ECM) components (155, 157, 167, 178). The PC family members play a crucial role in a variety of physiological processes and are involved in the pathology of diseases such as cancer and viral infection as shown in Figure 1.12 (179, 180). Furin/PC have been shown to process substrates such as platelet-derived growth factor A and B, insulin growth factor and its receptor, TACE, and TGFβ (178, 181, 182). PCs have also been shown to proteolytically cleave a number of ADAM family members including TACE (178, 180).

Of the PC family members, furin, PACE 4, PC5/6 and PC7/8 are widely expressed in the epidermis whereas PC2 and PC1/3 are limited to neuroendocrine tissues and PC4 to

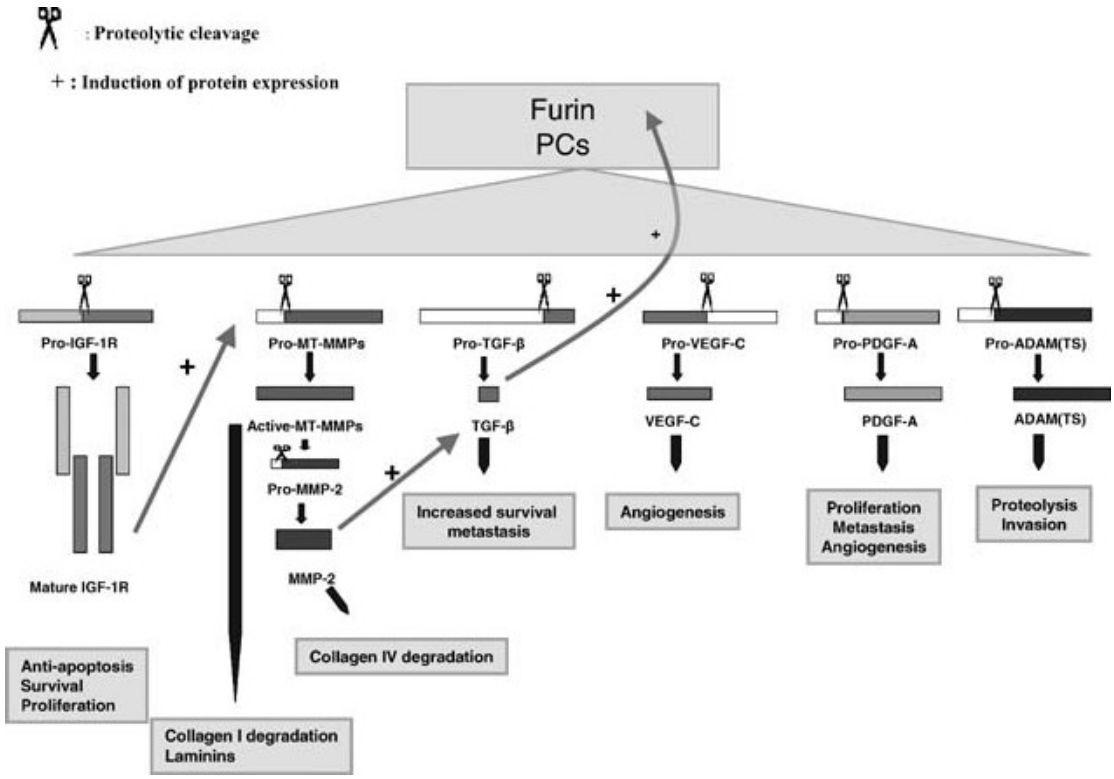

Figure 1.12 Schematic representation of PC processing that results in enhanced tumour progression. Furin has been used as a paradigm of this family of enzymes. The pro-forms of the numerous cancer-associated furin substrates are depicted along with their respective mature forms and their role on the biology of cancer (179).

the testis; suggesting both generalized and tissue-specific patterns of expression and function (167). The PC enzymes recognize basic motifs, cleaving after paired basic

residues (PC2 and PC1/3); or after a canonical Rx (R/K) R (Arg-x-(Arg/Lys)-Arg) motif (furin and PACE4) (155, 167, 177). Both PC7 and furin share an overlapping substrate specificity and therefore the selectivity of substrate proteolysis depends on their cellular localization. As intracellular trafficking is regulated by their cytosolic domains, which contain different sorting motifs, it is likely that the cellular localization of PC7 differs to that for furin (165). Furin/PC expression and processing can increase the incidence and severity of the cancer phenotype (178). Overexpression of PACE4 converts SCC into the more malignant spindle cell carcinoma and is sufficient for malignant conversion of keratinocytes (178, 180, 183).

Furin and PC7 are also involved in the maturation of TACE and experiments have shown that furin cleaves TACE more rapidly and efficiently than does PC7 (162, 165). The maturation of TACE occurs during the transit of the protein through the late golgi compartment suggesting that prodomain removal is performed by a furin-type proprotein convertase (165, 172). TACE contains a putative PC cleavage site, which might play an important role in its activation (158, 165, 181). Furin cycles between the cell surface and TGN through a process regulated by its cytoplasmic domain indicating that it cleaves its substrates mainly in the cytoplasm (154, 177).

Moss *et al*. (158) showed that when insect cells were transfected with baculoviruses containing fragments of TACE sequence with its prodomain, it resulted in the production of recombinant active protein with Arg^{215} at its N-terminus (158, 159, 162). This suggests that proTACE was cleaved at its furin-like cleavage site by a furin-like enzyme. However, in the baculovirus-infected insect cells, the direct involvement of furin and TACE resulted in a decrease in mature TACE rather than a logical increase in

the amount of its mature form (159, 162). A genetic mutation of the FUR gene that encodes for furin resulted in increased proTACE levels in synovial cells due to reduced expression of this gene (169). When the cells were transfected with furin, TACE processing occurred, confirming its role in this process.

Furin over-expression has been shown to inhibit the differentiation of pancreatic islet α and gastric mucosal cells (167). In contrast inhibition of furin in epidermal organotypic cultures leads to premature differentiation of keratinocytes, possibly via its effects on the Notch pathway (167). The cell permeable proprotein convertase inhibitor decanoyl-Arg-Val-Lys-Arg-chloromethylketone (Dec RVKR cmk) and PDX inhibited furin activity, which resulted in reduced levels of mature TACE in both Cos7 cells (162) and keratinocytes (167). These inhibitors prevent the proteolytic activity of PCs by covalently binding at their catalytic site (165). Dec RVKR cmk also inhibited the cleavage of Notch-1, a receptor important in cell fate determination and patterning and integrin signalling (167). Overall it can be seen from these studies that furin cleaves TACE in many different cells including keratinocytes.

Furin mRNA, protein and enzyme activity has been observed in human epidermal keratinocytes (147, 162, 167, 184). Skiba *et al*. (147) found that furin mRNA levels were higher following exposure to UVB compared to UVA (147). The time course for furin mRNA levels in cells irradiated with low dose of UVA and high dose of UVB was similar to that seen for TNFα, while maximal TNFα and furin mRNA induction were detected 8 h post-irradiation (147). Although UV-irradiation does appear to have an effect on furin gene expression, no direct relationship was apparent between TACE and furin mRNA induction. A recent study has shown that in HaCaT cells exposed to UVA

and UVB, furin levels fell with respect to time (185). It is unknown whether this change in furin levels was that of the immature and/or mature enzyme.

1.7 MMPs

Furin/PC processing of substrates has been shown to also contribute to tumour progression, aggressiveness, metastasis, and angiogenesis (178, 179, 181). Tumour invasion and metastasis represent a multistep process that depends on the activity of many proteins (186). Proteolytic degradation of the ECM components is a central event of this process. Several classes of proteinases, including MMPs, serine proteinases and cysteine proteinases have been implicated in the tumour cell invasive process (186).

Among these different proteinases, MMPs which are a family of zinc-dependent endopeptidases are collectively referred to as metzincins (187, 188). The metzincin superfamily is distinguished by a highly conserved motif containing three histidines that bind to zinc at the catalytic site and a conserved methionine that sits beneath the active site (189). The metzincins are subdivided into four multigene families: seralysins, astacins, ADAMs/adamalysins, and MMPs (189). So far to date, 28 members of the MMP family have been identified (147, 190, 191) which are primarily responsible for most of the ECM degradation observed during the invasive processes (152).

The basic structure of MMPs is made up of the following homologous domains: 1) signal peptide which directs MMPs to the secretory or plasma membrane insertion pathway; 2) prodomain that confers latency to the enzymes by occupying the active site zinc, making the catalytic enzyme inaccessible to substrates; 3) Zn^{2+} containing catalytic domain; 4) hemopexin domain which mediates interactions with substrates and confers

specificity of the enzymes; and 5) hinge region which links the catalytic and the hemopexin domain MMP-2 and MMP-9 (referred to as gelatinases based on their substrate preference) contain fibronectin-like domain repeats which aid in substrate binding (192, 193). The domain structure of the gelatinase family of MMPs that are discussed in this thesis is represented in Figure 1.13.

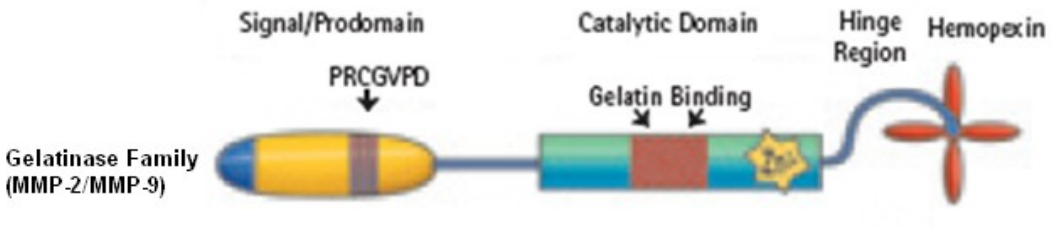

Figure 1.13 Domain structure of gelatinase family of MMPs. Adapted from (188, 194).

Two sequence motifs are highly conserved in the protein structure of MMPs. The consensus motif HExGHxxGxxH, found in the catalytic domain of all MMPs, contains three histidines that coordinate with a Zn^{2+} in the active centre. The PRCGxPD motif is located in the C-terminal portion of the prodomain of MMPs; coordination of the cysteine residue (C) of this locus with the Zn atom of the active centre confers latency to the proenzyme (192, 193).

Recently, it has been recognized that MMPs also cleave peptides and proteins which have a myriad of functions that is independent of proteolytic activity (195). MMPs have distinct but often overlapping substrate specificities, hence leading to the absence of

distinct phenotypes in most genetically-engineered mice with knockdown of specific MMPs (195).

The activity of MMPs under *in vivo* conditions is under tight control at several levels. These enzymes are generally expressed in very low amounts and their transcription is tightly regulated either positively or negatively by cytokines and growth factors such as IL-1, IL-4, IL-6, TGFβ, or TNFα (196, 197). Some of these regulatory molecules can be proteolytically activated or inactivated by MMPs (via a feedback loop). Post-transcrpitionally, MMP activity is restricted by the latency conferred by the propeptide located in the N-terminal end of the newly synthesized proenzymes. Activation of MMPs following secretion from cells depends on disruption of the prodomain interaction with the catalytic site, which may occur by conformational changes or proteolytic removal of the prodomain. MMPs that contain furin-like recognition domains in their propeptides (MT-MMPs) can be activated in the TGN by members of the subtilisin family of serine proteases (196, 197). With the exception of MMP-2, the mechanism for *in vivo* activation of secreted MMPs is not well understood (196, 197).

MMPs can be produced by fibroblasts, keratinocytes, macrophages, endothelial cells and mast cells (187). MMPs can contribute to tumour growth not only by degrading the ECM but by the release of sequestered growth factors or the generation of bioactive fragments VEGF, EGF or TGFβ, the suppression of tumour cell apoptosis and the destruction of immune-modulating chemokine gradients (198-200). These enzymes are also implicated in cell migration, proliferation, and tissue remodeling and thereby may

also play a role in growth and development, angiogenesis, atherosclerosis (182, 201, 202) and destruction of local tissue architecture and basement membranes (187).

At the protein level, the expression of MMP is low in keratinocytes but elevated in BCC and SCC (187, 203). In SCC, MMP proteins (1, 2, 3 and MT1-MMP) are expressed both in tumorous and stromal cells (187, 204-206). MMP proteins (1, 2, 3 and 9) are expressed in BCCs and melanomas (187, 207). This expression correlates with the progression and the metastatic potentials of these tumours (187, 208-210). At the time of writing, mutational analysis of MMPs in skin cancers is still lacking.

MMP-2 (also known as gelatinase A or 72 kDa type IV collagenase) and MMP-9 (also known as gelatinase B or 92 kDa type IV collagenase) has been frequently associated with the invasive and metastatic potential of tumour cells (160). MMP-9 (190, 211, 212), has been reported to play an important role in the pathophysiologies of many skin conditions, including tumour invasion and metastasis (190, 192, 213), wound healing (214, 215), and angiogenesis (212, 216). On the other hand, the expression of MMP-2 is regulated independently of MMP-9 (190, 191, 211, 212, 217, 218). MMP-1, which is produced by both dermal fibroblasts and epidermal keratinocytes, cleaves type I collagen into specific fragments, which can then be further hydrolyzed by MMP-2 and MMP-9 (219, 220). The close correlation observed between MMP-2 activation and metastatic progression in various tumours suggests that it is a “master switch” triggering tumour spread (186).

In normal skin, MMPs are not constitutively expressed but can be induced temporarily in response to exogenous signals such as UVR (187, 221). UVR can participate to the

development of skin cancer by the activation of MMPs. Two molecular mechanisms contribute to the UV-induced MMPs expression. First, the activation of cell-surface receptors with subsequent activation of mitogen activated protein kinase (MAPK) cascade which in turn contributes to the transcriptional up-regulation of MMPs. Second, the expression of pro-inflammatory cytokines, which induce the expression of MMPs (187, 222, 223). The role of UV in the induction of MMPs is supported by two experimental findings. First, UV-irradiation of SCC cell lines results in an increased secretion of MMPs (187). Second, UV-induced phosphorylation of extracellular signal-regulated kinase (ERK) and stress kinases precedes the rapid stimulation of MMPs in SCC cells (187, 224).

Exposure to UVR elevates MMP production in human skin, implicating sunlight as a major factor in photoageing (225). Regulation of MMP activity involves both the control of zymogen activation and the inhibition of the active enzyme by specific inhibitors such as TIMPs (225). MMPs are synthesized as latent proenzymes which are converted into mature, catalytically active forms by proteolytic cleavage of the N-terminal propeptide mediated by serine proteases, such as furin, or by membrane-type MMPs (MT-MMPs) (182, 193, 226).

TNFα has been shown to induce proMMP-2 in human dermal fibroblasts (227), while IL-1α induced proMMP-9 levels in fibroblasts and keratinocytes (228). Recently Sato *et al*. (229) identified MT1-MMP as a potential physiological activator of MMP-2 (186). Activation of proMMP-2 takes place at the cell surface and involves interactions with active MT1-MMP, which is itself activated through rapid trafficking to the cell surface and proteolytic processing (182). MT1-MMP is cleaved at a RXKR

cleavage site of its prodomain sequence by furin (182). Maquoi *et al*. (186) demonstrated that furin-inhibitor reduces the level of mature MT1-MMP, which is paralleled by a decrease in proMMP-2 activation as well as in cell invasiveness.

Some of the skin cells which become cancerous as a result of DNA damage may become metastatic due to increased MMP activity (230). This increase in levels of activated MMPs on the surface of the cell could be due to either increased expression of proMMP protein and/or increased furin activity. The role furin plays in the development of skin cancer suggests that it may play a significant role, and as such the development of specific inhibitors may offer a new therapy to treat these tumours (188, 231).

1.8 Conclusion

While it has been shown that UVA and UVB radiation causes different effects on the immune response this could be related to the activity of cell surface metalloproteases found on the skin cells. Keratinocytes secrete TNFα following exposure to UVB radiation, and this is enhanced if IL-1α is present (126). Although the effect of TNFα in UV-induced inflammation has been well documented, little is known if the changes in TACE activity is due to increased protein levels or a change in enzyme activity. The inflammatory environment, seen in the skin following exposure to UVR, assists in creating an environment allowing for development of mutated cells which possess DNA damage. Apart from increasing the release of TNFα, TACE also cleaves EGF family members, which can stimulate the growth of these mutated cells, which over time may become cancerous. As TNFα is a powerful inflammatory cytokine, considerable research has been under taken to develop inhibitors which inhibit TACE activity (122,

157, 232). These inhibitors may play an important role in preventing the development of UV-induced skin cancers. An increased knowledge of the roles played by metalloproteases in tumour progression, combined with the use of more selective inhibitors, could lead to effective use of these compounds in cancer therapies (233).

Similar to that of TACE, MMPs are also activated by UVR and also play a crucial role in skin tumour cell development and metastasis. Furin and other proprotein convertases have been shown to play an important role in activating both TACE and MMP in skin cells. Whereas the overexpression and activity of furin/PC exacerbate the cancer phenotype, inhibition of its activity decreases or nullifies furin/PC-mediated effects, and thus, inhibition of furin may also be a viable route to cancer therapy (178). Based on this information a model on the role furin plays in the UV-irradiated keratinocyte cells has been hypothesized as shown in Figure 1.14.

UVR has been shown to induce furin mRNA in skin cells, its protein levels do not appear to change with respect to time, which suggests a rapid turnover of the enzyme. Further study is needed on how UVR activates furin, TACE and MMPs in skin cells. These proteases appear to play an important role in the changes observed in these cells following their exposure to UVR. The development of specific furin inhibitors has the potential to reduce the carcinogenic effects of sunlight by preventing the activation of TACE and MMPs and their subsequent downstream effects. Such compounds may have the potential to offer therapies in the treatment of skin cancer and can significantly reduce the incidence of skin cancer among the general population.

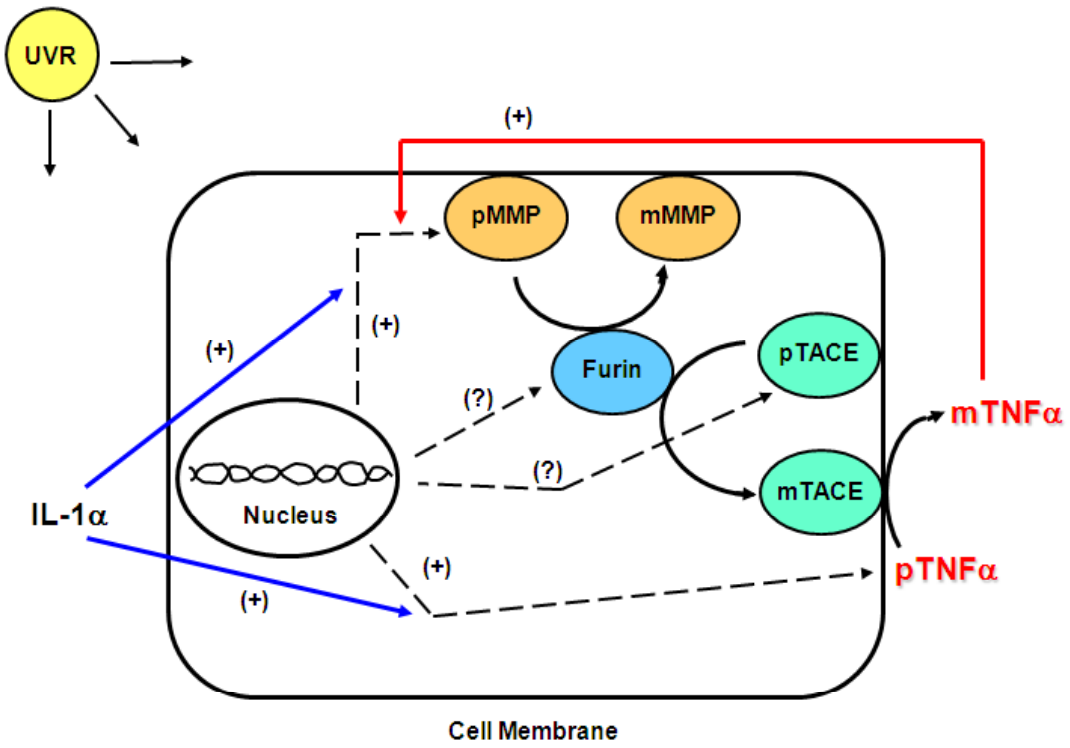

Figure 1.14 The role furin plays in the maturation of TACE and MMPs in skin cells. Furin cleaves and activates TACE, which in turn can process TNFα from its preproform. Keratinocytes secrete TNFα following exposure to UVB radiation, and this is enhanced if IL-1α is present. Furin also cleaves MMPs from their respective proforms, and the expression and activity of these proteases are elevated when the cells have been exposed to UVB radiation, and they are enhanced if either IL-1α (MMP-9) or TNFα (MMP-2) is present. The effect of UVB radiation on the expression of the enzymes and pTNFα in the cell is represented by dashed lines, if it is enhanced it is represented by (+), and if it is unknown (?).

1.9 Outline and Scope of thesis

UVR is acknowledged to be the main carcinogen involved in the formation of skin cancer. It has been shown to be a potent inducer of TNFα and cytokine gene expression in human keratinocytes. TNFα is proteolytically cleaved from its membrane-bound precursor by the action of the metalloprotease, TACE which in turn is cleaved from its preproform by the action of furin. Furin activates many other proteases in the cell including MMP-2 and -9. These gelatinases have been associated with the invasive and metastatic potential of tumour cells. While furin is known to be expressed in skin cells, the effect UVR has on its expression and/or activity and that of the proteases it activates in keratinocytes is not known.

Therefore, to understand the role UV plays on the activity of these enzymes we wish to investigate the following:

1) To investigate the effect of UVR on the expression and/or activity of furin and of the effect this has on TACE and MMPs activity in keratinocyte-derived cells?
2) Does UV type and dose have an effect on the expression and release of TNFα from human keratinocyte-derived cells?
3) Are changes in TACE activity following UV exposure due to
    (a) Changes in furin expression and/or activity?
    (b) Changes in TACE expression and/or activity?
4) Are changes in MMP activity seen in UV-irradiated keratinocyte cells related solely to that of furin?
5) To observe if these pathways are increased as a result of tumourigenesis?

Chapter Two:

Materials and Methods

2 Materials and Methods

2.1 Materials

2.1.1 Cell lines

Human epidermal keratinocytes (HEK) cells were purchased from Invitrogen (Melbourne, Australia). HaCaT (221) and Colo 16 (222) cell lines were kindly donated by Drs Peter Parsons and Glen Boyle from the Queensland Institute of Medical Research (QIMR), Brisbane, Australia.

2.1.2 Tissue culture material

Roswell Park Memorial Institute (RPMI) 1640 medium, penicillin-streptomycin-glutamine, EpiLife medium, 100X human keratinocyte growth supplement (HKGS), Phosphate-Buffered Saline (PBS), Trypsin-EDTA solution and Hank's Buffered Salt Solution (HBSS) were purchased from Invitrogen; 60 mm diameter petri dishes, 6-well plates, 96-well plates, centrifuge tubes (15 and 50 ml), pipette tips and Barrier pipette tips were obtained from Greiner-Bioone (Interpath Services, Melbourne, Australia) and tissue culture flasks (25 cm^2 and 75 cm^2) were purchased from Corning (Melbourne, Australia).

2.1.3 Chemicals and biochemicals

Bicinchoninic acid solution (BCA), Trypan Blue solution, Bromophenol Blue, Coomasie Blue, Ponceau S, Ethidium bromide (EtBr) Orange 6 loading buffer, Tween-20, Ammonium Persulfate, Sodium azide, $ZnCl_2$ and $CaCl_2$ were bought from Sigma (Sydney, Australia); Agarose 1 (Biotechnology grade), 50 bp PCR DNA marker Plus, Lysis buffer, Laemmli's sample buffer (223), glycine, Triton X-100, and Tris were

purchased from Astral Scientific (Sydney, Australia); Gelatin, NaOH, $NaHCO_3$, and CH_3COOH were purchased from BDH Biochemicals (Sydney, Australia). Glycerol, DEPC RNase-free water and SYBR® Green ER™ qPCR Supermix were supplied by Invitrogen; Kaleidoscope Prestained Standards, Acrylamide Bis solution and TEMED were obtained from Bio-Rad (Sydney, Australia). Foetal Bovine Serum (FBS) and Bovine Serum Albumin (BSA) were purchased from Bovogen (Melbourne, Australia). HPLC grade Methanol and Molecular Biology-grade Ethanol were supplied by Merck (Melbourne, Australia) and protease inhibitor was bought from Roche (Melbourne, Australia).

The ADAM 17 antibody was obtained from Abcam (Sydney, Australia); furin convertase (human) was from Alexis biochemicals (Sydney, Australia); Rabbit anti-MMP-2 antibody and mouse monoclonal anti-β-actin antibodies were from Sigma and Rabbit polyclonal MMP-9 antibody was obtained from Sapphire Biosciences (Sydney, Australia). Sheep HRP conjugated anti-rabbit immunoglobin antibody was from Chemicon (Melbourne, Australia).

Decanoyl-Arg-Val-Lys-Arg-chloromethylketone (Dec RVKR cmk) (furin convertase inhibitor) was obtained from Sapphire Bioscienes; 1, 10 phenanthroline (1, 10 phe) (metalloprotease inhibitor) was from Sigma; Cycloheximide (CHX) inhibitor and 2R-2-[(4-Biphenylsulfonyl) amino]-3-phenylpropionic acid (specific MMP-2/-9 inhibitor) (MMPI) were obtained from Merck.

2.1.4 Primers

The primers used in this study were commercially synthesized by GeneWorks (Adelaide, Australia).

2.2 Methods

2.2.1 Cell culture

HEK were grown in EpiLife medium supplemented with 100X HKGS, 0.5 ml of 0.09 M $CaCl_2$, 1% (v/v) Penicillin-Streptomycin-Glutamine (10,000 units/ml penicillin G sodium, 10,000 μg/ml streptomycin sulphate and 2 mM L-glutamine), in a 37°C incubator containing an atmosphere of 5% CO_2. HaCaT and Colo 16 cells were cultured with RPMI medium 1640 supplemented with 5% (v/v) FBS and 1% Penicillin-Streptomycin-Glutamine in 75 cm^2 cell culture flasks which were placed in a 5% CO_2 cell incubator at 37°C. Spent media was removed every three to four days and the cells given fresh pre-warmed EpiLife or RPMI media depending on the cultured cell line. EpiLife media used was pre-warmed by placing the container at RT for 40 min. The RPMI media used in cell culturing was pre-warmed at 37ºC prior to use. Unless mentioned otherwise the temperature of EpiLife media and RPMI used in cell culturing was at RT and 37°C, respectively.

2.2.2 Cell Passaging

2.2.2.1 HEK cells

The HEK cells reached confluency between seven to ten days. Confluence was monitored visually using an inverted microscope (Olympus CK2). The spent culture media was aspirated and the cells washed once with pre-warmed (37ºC) sterile

Trypsin-EDTA solution [0.214 M trypsin (1:250), 0.005 M EDTA•4Na, 0.142 M NaCl made in sterile PBS]. After which, the cells were incubated with 2 ml of sterile Trypsin-EDTA solution for 2-3 min. Cells were dislodged upon gentle tapping of the flask. The cell suspension was added into 4 ml of 1% (v/v) FBS in PBS and centrifuged (200 *g* for 5 min at 20°C) in a Universal 16 R centrifuge (HD scientific, Melbourne, Australia). After centrifugation, the supernatant was discarded and the cell pellet resuspended by repeated pipetting in 1 ml EpiLife media. An aliquot [three to four drops (~ 0.15-0.20 ml)] of the cell suspension was added to a new cell culture flask containing 20 ml of pre-warmed EpiLife media. The flasks were capped and sprayed with 70% ethanol before being placed flat in the 5% CO_2 incubator.

2.2.2.2 HaCaT and Colo 16 cells

The HaCaT and Colo 16 cell cultures usually reached confluency between four to five days. Confluence was monitored visually using an inverted microscope (Olympus CK2). The spent culture media was aspirated and the cells washed thrice with pre-warmed (37ºC) sterile PBS and twice with pre-warmed (37ºC) sterile Trypsin EDTA solution. After which, the cells were incubated in the 5% CO_2 incubator with 2 ml of sterile Trypsin-EDTA solution for 2-3 minutes. Cells were dissociated by gentle tapping of the flask after which, an aliquot of the cell suspension was added to a new cell culture flask containing 20 ml of pre-warmed RPMI media.

2.3 UV-irradiation

2.3.1 UV-irradiation of cells

Cells used in the experiments described in this thesis were either grown in 60 mm diameter petri dishes or 6-well plates. Once the cultures in the 75 cm^2 flask reached confluency (Section 2.2.2), cells were dislodged from their respective flasks using trypsin as described (Section 2.2.2) The trysinized cells were resuspended in their respective media (cells from one flask was suspended in ~ 20 ml tissue culture media), and 2ml of which was added to a 60 mm petri dish and 1 ml in a well of a 6-well plate.

Once the cultures in the petri dishes or 6-well plates reached 70-75% confluency, the spent media was discarded and the cells were gently washed twice with pre-warmed (37ºC) PBS. After which, the PBS was discarded and 1.5 ml of phenol-red free HBSS was added carefully to the side of the petri dish or 1 ml to the side of the well in a 6-well plate. Media was always added to the side of the petri dish or 6-well plate to avoid direct contact with the cells which could cause them to become dislodged. The petri dish or 6-well plate was then placed in the middle of the top shelf in the UV cabinet without their respective lids and were exposed to UVA and/or UVB-irradiation. The cells were exposed to the type and dose of UV radiation as outlined in Table 2.1. In order to ensure that the cells were not exposed to any UVB light emitted by the UVA lamps a sheet of 10 mm thick glass plate was placed over the culture vessels.

Immediately after irradiation, the HBSS was aspirated from the petri dish and 2 ml (petri dishes) or 1 ml (6-well plates) fresh pre-warmed tissue culture media was gently added. This media was added to the irradiated cells as described in the results section. The petri dishes or 6-well plates were returned to the cell incubator for various time

points (0-72 h). Sham-irradiated (control) cells were treated in the same manner, except that they were not exposed to UVR.

2.3.2 Inhibitor studies

In order to inhibit the activation of furin, cells were treated with 100 μM Decanoyl-Arg-Val-Lys-Arg-chloromethylketone (Dec-RVKR-cmk) (furin convertase inhibitor) for the times listed in the results section. Metalloprotease enzyme activity was inhibited by adding 100 μM 1, 10 phenanthroline (1, 10 phe) (metalloprotease inhibitor) for the times listed in the results section. Protein synthesis was inhibited when 100 μM cycloheximide (CHX) was added to the cells. In all cases, the inhibitors used above were added to the cells for 24 h prior to the cells being UV-irradiated. Following irradiation cells were growth in the presence of the inhibitors for the times listed in the results section.

MMP-2 and -9 activity was inhibited by the addition of 5 μM 2R-2-[(4-Biphenylsulfonyl) amino]-3-phenylpropionic acid (for simplicity in this thesis it will be called MMPI) (dissolved in DMSO) for 1 h prior to the cells being irradiated. Following UV-irradiation cells were grown in the presence of 5 μM MMP inhibitor for the times listed in the results section.

Following treatment with the above mentioned inhibitors and UV-irradiation, in some cultures IL-1α was added as it is known to stimulate TNFα release from the cells (77). Thereafter the media with inhibitor was removed and kept aside and replaced with 1.5 ml of HBSS for petri dishes or 1 ml HBSS for 6-well plates after which the petri dishes or 6-well plates were exposed to UV-irradiation as described in section 2.3.1. Following

UV-irradiation HBSS was removed and replaced with the same media containing the specific inhibitors with or without addition of IL-1α (10 ng/ml) and the cultures incubated for up to 24 h as described in the results section. Following the incubation period, the cells in the culture were either used for cell viability determination (Section 2.4) or used to prepare lysates for western blotting (Section 2.5) or for protein determination (Section 2.5.3). At the end of the experiment, a 0.5 ml aliquot of the media was placed in a 1.5 ml microfuge tube and stored at -80°C prior to being assayed for TNFα (Section 2.6).

2.3.3 UV variance

The UV cabinet (Wayne Electronics, Sydney, Australia) housed 6 UV fluorescent lamps: 3 UVA (maximal output 354 nm) (Cosmolux 15504 40W; Cosmedico, Stuttgart, Germany) and 3 UVB lamps (maximal output 312 nm) (Philips Ultraviolet 8 TL 20W/01 RS lamps; Philips, Eindhoven, Holland) (Figure 2.1).

Figure 2.1 UV cabinet.

The variation in the output (W/cm^2) of the UV lamps was measured using the relevant UV filter and detector (UVA or UVB) attached to an International light IL-1400A Traceable Photometer (Newburyport, USA) (Appendix A.2). The output of the UVA and UVB lamps in the middle and the sides of the cabinet on the top shelf were measured, with the highest doses observed in the middle region of this shelf. By knowing this information, the cultures could be placed on the top shelf, where the output of the UV lights were maximal, thereby minimizing the exposure times.

2.3.4 UV type, dose and exposure time

The cells were exposed to either UVA and/or UVB radiation as described in the results section. The outputs of UV lamps were measured (Section 2.3.1) and the following UV doses were calculated (Appendix A.2 and Table 2.1). The UVA and UVB dose used in this thesis represents the respective UVA and UVB component found in one minimal erythemal dose (1 MED) (174, 224). One MED is defined as the level of UVR that causes skin reddening in caucasian skin (types II-III) and has been calculated to be approximately 40 kJ/m^2 UVA and 2 kJ/m^2 UVB (174, 224).

UV Type	UV Dose (kJ/m^2)	Exposure Time (s)
UVA	40	770
UVB	2	185
UVA+B	(40+2)	(770+185)

Table 2.1 UV types, doses and exposure times used in the experiments outlined in this thesis.

2.4 Cell viability

The viability of the cell cultures (control and treated) were determined using the trypan blue exclusion method 24 h post-irradiation. In brief, the media in the petri dish or well of a 6-well plate was removed and placed in a 10 ml centrifuge tube. The cultures were then washed twice with pre-warmed PBS and the washings added to the 10 ml centrifuge tube. The tubes were centrifuged (200 *g* for 5 min at 4°C), after which the supernatant was discarded and the pellet resuspended in 1 ml PBS. A 50 μl aliquot of cell suspension was added to 50 μl of 0.4% (v/v) trypan blue solution in a microfuge tube and mixed well by pipetting. A 50 μl aliquot from the microfuge tube was added to a haemocytometer and the cells were counted using an Olympus BH2 light microscope. This count represented the number of detached cells in the culture.

The attached cells on the petri dish or 6-well plate were washed with ~2 ml pre-warmed Trypsin-EDTA after which the cells were suspended by adding 1 ml of pre-warmed Trypsin-EDTA solution and incubated for 4-5 min. The cells were gently dislodged from the base of the petri dish using a pipette. The suspended cells were transferred to a 10 ml centrifuge tube that contained 4 ml of 5% (v/v) FBS in PBS. The dish was washed twice with 1 ml of PBS to remove any remaining cells and the washings were added to the tube. The tubes were centrifuged (200 *g* for 5 min at 4°C), after which the supernatant was removed and the cell pellet resuspended in 3 ml PBS. A 50 μl aliquot of the cell suspension was added to a microfuge tube containing 50 μl of 0.4% (v/v) trypan blue solution. Following mixing, a 50 μl aliquot was added to a haemocytometer and the cells counted. This count represented the number of attached cells in the culture.

Cell viability was determined as a percentage of the total cell population. The total cell population represented the total number of live and dead cells found in both the attached and detached sub-populations (Appendix A.3).

2.5 Western blotting

2.5.1 Cell lysates preparation

2.5.1.1 Detached cells

At the end of the incubation period, the detached cells present in the tissue culture media in the petri dish or well of a 6-well plate were transferred into a centrifuge tube and centrifuged (200 *g* for 5 min at 4°C). The cell pellet was then resuspended in 100 µl ice-cold (4°C) lysis buffer [20 mM Hepes pH 7.4, 2 mM EGTA, 50 mM β-glycerophosphate, 1 mM Dithiothreitol, 1 mM Na_3VO_4, 1% Triton X-100, 10% (v/v) Glycerol, 0.5 mM PMSF, 0.5 mM NaF, 2% (w/v) protease inhibitor] and transferred into a 1.5 ml microfuge tube that was placed on a rocking platform for 20 min at 4°C. This fraction represented the protein lysates from detached cells. A 5 µl aliquot was used to determine the protein concentration (Section 2.5.2). The supernatant was collected and placed in a microfuge tube on ice. This was treated as described in section 2.5.1.3.

2.5.1.2 Attached cells

The attached cells in the petri dish or well of a 6-well plate were washed twice with ice-cold (4°C) PBS. After which, 100 µl of ice-cold (4°C) lysis buffer was added and the cells were dislodged with a scrapper before the dish was placed on a rocking platform (Ratek Instruments, Australia) for 20 min at 4°C. The cell lysates were

collected in a 1.5 ml microfuge tube and centrifuged (8,500 *g* for 15 min at 4°C). This fraction represented the protein lysates from attached cells. A 5 µl aliquot was used to determine the protein concentration (Section 2.5.2). The supernatant was collected and placed in a microfuge tube on ice. This was treated as described in section 2.5.1.3.

2.5.1.3 Western blot sample preparation

Laemmli's sample buffer [0.5 M Tris, 100 mM Dithiothreitol, 8.2% (w/v) Sodium Dodecyl Sulfate (SDS), 0.1% (v/v) Bromophenol Blue and 40% (v/v) Glycerol] (223) (223) was added to the supernatant from the attached and detached cell fractions (Cell lysate : Laemmli's sample buffer, 4:1) and boiled for 5 min at 95°C. The samples were then stored at -80°C until they were used for SDS PAGE gel electrophoresis (Section 2.5.3).

2.5.2 Protein concentration determination

The level of protein in samples was determined using BCA as per the manufacturer's instructions with BSA as the standard. Briefly, duplicate 10 µl protein standards (0-10 µg) and 5 µl aliquots of the cellular extract were placed in a 96-well flat-bottomed plate. After which 200 µl BCA solution was added to each well. The plate was left to incubate for 1 h at 37°C and read at 560 nm using a Perkin Elmer Victor^3 plate reader (Wallac, Turku, Finland). The level of protein in each sample was calculated from the standards run on the plate.

2.5.3 SDS PAGE gels

The SDS PAGE gels were set in a Mini Protean II Multicasting Chamber (Bio-Rad) and consisted of a 10% running gel [3.35 ml of 30% (v/v) Acrylamide Bis solution, 4 ml H_2O, 2.5 ml 1.5 M Tris (pH 8.8), 0.1 ml 10% (w/v) SDS, 0.1 ml 10% (w/v) Ammonium Persulfate and 0.01 ml TEMED]. Once the running gel had set, the stacking gel [0.43 ml 30% Acrylamide Bis solution, 1.7 ml H_2O, 0.32 ml 1.5 M Tris (pH 8.8), 0.025 ml 10% (w/v) SDS, 0.025 ml 10% (w/v) Ammonium Persulfate and 0.005 ml of TEMED] was overlaid on top. After which the combs were placed within the cast to form 10 wells. Once the stacking gel had set, the sample comb was removed and the gel chamber was immersed in a tank containing Running buffer [25 mM Tris (pH 8.8), 192 mM Glycine and 3.5 mM SDS]. In each gel, 5 μl of Kaleidoscope Prestained Standards was added to the first lane while 50 μg protein lysate extracts were added to each subsequent lane. The gel was run for 1 h at a constant voltage of 120 V.

2.5.4 Immunoblotting

When the gel electrophoresis was completed, the proteins were electro-transferred onto a pre-wet nitrocellulose membrane (Amersham Biosciences, Sydney, Australia), which had been pre-soaked (10 min) in cold transfer buffer (4°C) [25 mM Tris, 192 mM Glycine, 20% (v/v) Methanol], using a semi-dry transfer unit (Bio-Rad), at a constant amperage of 0.06 mA for 90 min for each gel. The efficiency of the semi-dry transfer was determined by visually observing the nitrocellulose membrane which had been soaked in Ponceau S solution [0.1% (w/v) Ponceau S in 0.05% (v/v) acetic acid] for 2 min and that had been rinsed with water.

The nitrocellulose membrane was then placed in a dish containing blotto [5% (w/v) skim milk powder in TBST (20 mM Tris, 138 mM NaCl, 0.05% (v/v) Tween-20, pH 7.6)] and agitated on a rocker for 2 h at RT. After which the membrane was placed in a dish with 10 ml of 5% Blotto containing the relevant primary antibody and placed on a rocker, overnight at 4°C. The next day, the nitrocellulose membrane was washed thrice (10 min per wash) with TBST at RT, after which it was placed in a dish containing 10 ml of 5% blotto containing the relevant secondary antibody for 1 h at RT. After this, the nitrocellulose membrane was washed thrice (10 min per wash) with TBST at RT.

2.5.5 Western blot protein detection

After the final TBST wash (Section 2.5.4), the nitrocellulose membrane was exposed to 2 ml chemiluminescent solution (Chemilucent, Chemicon, Melbourne, Australia) for 3 min. The membrane was then placed in a Chemidox XRS unit and the chemiluminescence detected using a CCD camera connected to the Chemidox XRS unit and a digital image was obtained. The digital image was analysed for densitometry using Quantity One Digital Imaging Software Version 4.5.1 (Bio-Rad). The protein levels in untreated control sample were expressed as 100% while those in UV-irradiated and/or treated samples were expressed as a percentage of this value.

2.6 ELISA

Aliquots of media samples (0.5 ml) from the experiments were placed in 1.5 ml microfuge tubes and stored at -80°C prior to being used for the TNFα ELISA assay (AccuKine, Apollo Cytokine Research, NSW, Australia).

Once the media samples had thawed out, they were first concentrated at 4°C using Microcon YM-10 microconcentrators (10 kDa MW cut-off filters) as per the manufacturer's instructions. These microconcentrated samples were assayed as described below.

Wells of a 96-well plate were first coated with capture antibody (100 µl) per well and washed thrice with wash buffer [0.05% (v/v) Tween-20 in PBS]. The plate was then blocked with 200 µl of assay diluent (10% FBS in PBS) per well for 1 h at RT. Then the wells were washed thrice with wash buffer. After which, 100 µl of TNFα standards (0-500 pg/ml) and duplicate microconcentrated media samples were added to wells and incubated for 2 h at RT. The plate was then washed five times with wash buffer before 100 µl of working detector (detection antibody) was added to each well and the plate incubated for 1 h at RT. After which, the wells were washed seven times with wash buffer for 30 s per wash. Then 100 µl of substrate solution was added to each well and incubated for 30 min at RT in the dark. Once the assay was completed the absorbance was read at 450 nm using the Perkin Elmer Victor^3 plate reader. The level of TNFα in the cultured media of irradiated cells was calculated from the standard curve and was expressed as a function of cell protein level in order to determine the amount of TNFα secreted by the cell.

2.7 Gelatin-Zymography

2.7.1 Treatment of the cells

Cells in 60 mm petri dishes or 6-well plates were pre-treated with the inhibitors as described in section 2.3.2. In the zymogen assays, serum-free media was used (EpiLife

for HEK cells or RPMI 1640 for HaCaT and Colo 16 cells). After which, the petri dishes or 6-well plates were exposed to UV-irradiation as described in section 2.3.3. Following UV-irradiation HBSS was removed and replaced with serum-free media containing inhibitors (see results section 4.2.2) and the cultures incubated for 0-72 h. Sham-irradiated (control) cells were treated in the same manner, except that they were not irradiated. After which, 1 ml aliquot of supernatant was placed in a 1.5 ml microfuge tube and stored at -80°C prior to being used for the Zymogen assay (Section 2.7.3). The attached cells in the petri dish were washed with ice-cold (4°C) PBS after which, 1 ml of 0.1 M NaOH was added to dissolve cell protein. The cells were dislodged with a scrapper before the dish was placed on a rocking platform for 30 min at RT. The cell proteins were collected in a 1.5 ml microfuge tube and centrifuged (8,500 *g* for 15 min at 4°C). A 5 µl aliquot of the supernatant was used to determine the protein concentration (Section 2.5.2).

After incubation, 1 ml of the conditioned media was removed from petri dish or 6-well plate and added to a 1.5 ml microfuge tube and was stored at -20°C prior to being assayed. These media samples were concentrated at 4°C for 30 min using a Microcon YM-10 microconcentrator. Sample buffer [0.5 ml H_2O, 2.5 ml 0.5 M Tris-HCl (pH 6.8), 2.0 ml 40% Glycerol, 4.0 ml 10% SDS, 0.1 mg Bromophenol Blue] was added to the microconcentrated conditioned media (microconcentrated conditioned media : sample buffer, 5:1) and the samples were stored at -20°C until they were used for zymogen gel electrophoresis (Section 2.7.3).

2.7.2 Zymography gel

The SDS PAGE gels were prepared as described in section 2.5.4. Gelatin (0.125%) was added to a 10% running gel (Section 2.5.4) along with 0.05 ml 10% (w/v) Ammonium Persulfate. In the first lane, 10 µl of Kaleidoscope Prestained Standards was added while 50 µl of microconcentrated conditioned media (Section 2.7.1) was added to the other lanes. The gel was run for 40 min at a constant voltage of 200 V.

On completion of electrophoresis, the gel was rinsed using distilled water and incubated (15 min) twice in wash buffer [12.5 ml of 2.5% (v/v) Triton X-100 in 500 ml dH_2O] followed by an incubation between 16-20 h at 37°C in substrate buffer [50 mM Tris (pH 7.0), 5 mM $CaCl_2$ 1 µM $ZnCl_2$, 0.5% (v/v) Triton X-100, 0.01% (v/v) Sodium azide]. At the end of this period, the gel was washed twice with distilled water (5 min between each wash). The gel was then stained with Coomassie brilliant blue stock solution [0.5 g Coomasie Blue, 25% (v/v) methanol, 5% (v/v) Acetic Acid] for 45 min and destained using the destain solution [7% (v/v) acetic acid and 25% (v/v) methanol] for 2-3 h with regular changes of the destain solution every hour to visualise bands of proteolytic activity.

After the final wash, the destained gel was placed in a Gel-Doc image analysis system and a digital image was captured. This image was inverted using the inverted display option and analysed for densitometry using Quantity One Digital Imaging Software Version 4.5.1. The level of activity in non-irradiated control sample was expressed as 100% while those in the treated samples were expressed as a percentage of this value.

2.8 Cell Migration

2.8.1 Cell Passaging and Preparation

When cultures grown in 6-well plates reached ~ 90% confluency (Section 2.2.2), the cell culture media was aspirated and the cells washed thrice with pre-warmed (37°C) sterile PBS. After which, 1 ml of serum-free media was added to the wells and the plates were returned to a 5% CO_2 cell incubator at 37°C for 2 h. After which, the plates were removed from the incubator and the cell monolayer was scraped in a straight line to create a ‘‘scratch’’ using a sterile 10 µl pipette tip. Removal of the debris and edge of the scratch was smoothed by washing the cells with 1 ml pre-warmed PBS. The cultures were either incubated for 24 h at 37°C in the presence or absence of inhibitors (100 µM Dec RVKR cmk or 100 µM 1, 10 phe) or for 1 h at 37°C (5 µM specific MMP inhibitor) in serum-free culture medium.

At the end of this incubation period, the cells were washed twice with pre-warmed sterile PBS and 1 ml HBSS gently added to the cells. The culture was then exposed to UV-irradiation (Section 2.3.3). Following UV-irradiation, HBSS was removed and the cells were grown in same serum-free media containing the specific inhibitors for either 24 or 48 h. At the end of this period, a 0.5 ml aliquot of the tissue culture media was placed in a 1.5 ml microfuge tube and stored at -80°C prior to being used for the zymogen assays (Sections 2.7.2 and 2.7.4). The attached cells were then washed twice with ice-cold PBS before being fixed with 1 ml of ice-cold ethanol. The 6-well plate was then placed on an ice-bath for 10 min after which analysis was done as described below in section 2.8.2.

2.8.2 Cell scratch image analysis

After 10 min, the ethanol was aspirated from the cells and replaced with 1 ml ice-cold PBS. Phase contrast images of the cell cultures in the 6-well plates were obtained using 20X objective of Olympus CK2 microscope and an Olympus DP10 digital camera, a representation of which is shown in Figure 2.2. The images of 10 fields per condition were analyzed.

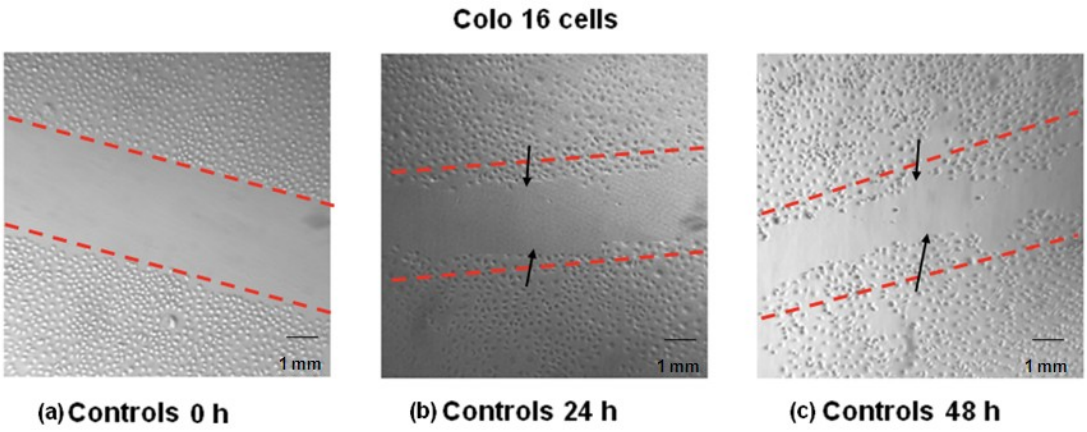

Figure 2.2 Time course of cell migration of Colo 16 cells. The culture was scratched at 0 h (a) and viewed at 24 h (b) and 48 h (c).

In order to obtain the same field during the image acquisition, markings were created which were used as reference points close to the scratch. The reference points were made by etching the plate lightly with a razor blade on the outer bottom of the plate or with an ultrafine tip marker. After the reference points were made, the plate was placed under a phase-contrast microscope; the reference mark was left outside the capture image field but within the eye-piece field of view.

The first image of the scratch was thus acquired. The plate was then placed under a phase-contrast microscope, the reference point was matched, the photographed region acquired in the previous step was aligned and a second image was acquired. This procedure was repeated until 5 images were obtained. Digital prints of the images were made and distance between one side of scratch and the other was measured at defined intervals. Cell migration was quantified by measuring the readings of distance for each sample and each experiment was repeated three times. An average of the readings was calculated and the results were represented as the distance (in mm) the cells migrated compared to that travelled by untreated controls (Appendix A.4).

2.9 Real-Time PCR (qRT-PCR)

2.9.1 Treatment of the cells

Cells were grown in 60 mm diameter petri dishes and UV-irradiated as described in section 2.3.1. After irradiation, the HBSS was removed from the petri dish and 2 ml fresh pre-warmed (37°C) tissue culture media with or without IL-1α (10 ng/ml) was gently added to the cells. The petri dish was returned to the cell incubator for defined time points (0-48 h). At the end of this period, the experiment was terminated, the cells were washed and the RNA was extracted as described in section 2.9.2. Sham-irradiated (control) cells were treated in the same manner, except that they were not exposed to UVR.

2.9.2 RNA Extraction and quantitation

RNA was extracted using a Pure Link RNA mini-kit as per the manufacturer's instructions (Pure Link RNA mini-kit, Invitrogen). A 1:70 dilution of pure RNA was made by adding 2 µl to 138 µl RNase-free H_2O and the absorbance spectroscopically determined at 260 nm (Appendix A.5). The concentration and purity of RNA in each of the samples were determined using matched quartz cuvettes (Bio-Rad). The isolated RNA was stored at -20°C until required for Reverse Transcription (Section 2.9.3).

2.9.3 Reverse Transcription

Each RNA sample was diluted 1:5 with RNase-free water. The diluted RNA was incubated a in a Gene Amp PCR system 2400 (Perkin Elmer) for 2 min at 50°C. The samples were then reverse-transcribed using SuperScript® III First –Strand Synthesis Supermix for qRT-PCR (Invitrogen). A 10 µl reaction contained up to 1 µg of RNA (depending on the quantification of RNA samples), 10 µl of Reaction Mix (includes oligo$(dt)_{20}$ (2.5 µM), randon hexamers (2.5 ng/µl), 10 mM $MgCl_2$ and dNTPs), 2 µl of the RT-Enzyme (Includes SuperScript^{TM} III RT and RNaseOUT^{TM}), which was made up to 20 µl with RNase-free water. The reverse transcription reaction underwent the following conditions using a Perkin Elmer Gene Amp PCR system 2400; 10 min at 25°C, 30 min at 50°C and 5 min at 95°C to stop the reaction. The cDNA samples were then placed on a bed of ice for 1 min and 1 µl of E. *coli* RNase H enzyme added to each one of the reactions after which the subsequent cDNA was stored at -20°C until required for qRT-PCR.

2.9.4 SYBR®Green™ qReal-Time PCR

All primers used in this thesis were as previously described by Skiba *et al*. (136). Primers for MMP-2 were designed using Genbank NCBI database. The primers to the genes described in this thesis (Table 2.2), were reconstituted before use (Appendix A.6). Each cDNA sample was loaded in triplicate wells of a 96-well microtitre plate.

Each reaction (total volume 20 µl) contained 25 ng cDNA, 10 µl SYBR® Green ER™ qPCR Supermix (Invitrogen), 2 µl forward primer, 2 µl reverse primer, 2 µl cDNA sample and 4 µl of RNase-free H_2O. In all reactions, 20 µl of RNase-free H_2O was used as the negative control. PCR amplification was performed using an iCycler iQ Real Time Detection System version 3.021 (iCycler, Bio-Rad). The thermal cycling parameters used were 2 min at 50°C, 8 min at 95°C followed by 55 cycles of: 95ºC for 15 sec and 60ºC for 60 sec. The melting curve analysis was done according the parameters: 95°C for 1 min, 55°C for 1 min and 80 cycles of: 55°C ± 0.5°C/cycle. Standard curve of amplication efficiencies (Appendix A.7) were obtained for both, the gene of interest and the reference genes for each of the cell lines.

The relative expression of the target genes (TNFα, TACE, Furin, MMP-2 and MMP-9) for each sample was calculated using the Pfaffl Correction method (225). β actin was used as the reference gene. Post qRT-PCR samples were stored at -20ºC until they were used for DNA agarose gel electrophoresis (Section 2.10) to verify the integrity of these samples.

Gene	Forward Primer	MW	TM	Reverse Primer	MW	TM
TNFα	CCA GGC AGT CAG ATC ATC TTC TC	6960	57	AGC TTG AGG GTT TGC TAC AAC AT	7079	53
TACE	GAG GCG ATT AAT GCT ACT TGC A	6774	53	TGG AGG CGG GCA CTC A	4947	51
Furin	GGC CTG CTC GTC CAC ACT	5412	55	TCG TCA CGA TCT GCT TCG CAT T	6652	55
MMP-2	GTC CCC ATG AAG CCC TGT TC	6029	56	CGT AGT CCT CAG TGG TGC CG	6125	58
MMP-9	CAC TGT CCA CCC CTC AGA GC	5983	58	GCC ACT TGT CGG CGA TAA GG	6158	56
β actin	GCG AGA AGA TGA CCC AGA TCA TG	7107	57	GTC CAT CAC GAT GCC AGT GGT AC	7025	59

Table 2.2 Primers used in the qRT-PCR study

2.10 DNA agarose gel electrophoresis

2.10.1 Agarose gel preparation

Agarose was prepared as follows: 2.5 g agarose was dissolved into 100 ml of Tris-Acetate EDTA (TAE) buffer [Tris-base 48.4 g (pH: 8.3), glacial acetic acid 10.9 g, EDTA 2.92 g in 1000 ml of dH_2O] in a 250 ml conical flask. The conical flask was placed in the microwave (Sharp, Melbourne, Australia) and the solution microwaved for about 1 min to dissolve the agarose. After 45 seconds, the conical flask was removed and the contents were stirred. Following this, the flask was left on the bench for 5 min to allow the contents to cool to about 60°C. The open ends of the Gel casting trays (Bio-Rad) were closed with tape while the gel was cast, and were removed prior to electrophoresis. Sample combs, were then inserted around which molten agarose was poured to form sample wells in the gel. The gel was left to solidify for about 45min after which, the comb and the tape were removed and the gel slided into the electrophoresis chamber. After this, TAE buffer (running buffer) was poured into the chamber to submerge the gel to 2-5 mm depth.

2.10.2 Sample preparation

DNA samples were mixed with the loading buffer usually at a ratio of about 3:1 Here, 5µl of the 50 bp DNA molecular weight marker was mixed with the 2 µl of the loading buffer (Orange 6, Promega). This was then loaded into the first lane of every gel. Similarly, 5 µl of each post qRT-PCR sample was mixed with 2 µl of the loading buffer which was then transferred to the subsequent lanes in the gel using a pipette. Care was taken to ensure the samples were loaded into each well. The gel tank was then closed, and the gels run at 30 V/cm for 3 h. The progress of the gel was monitored by reference

to the marker dye and was stopped when the Orange 6 loading buffer had run ~ 3/4 the length of the gel.

2.10.3 Ethidium bromide staining

Once the electrophoresis was completed, the gel was removed from the chamber and placed in the ethidium bromide (EtBr) stain [5.25 mg/ml H_2O] box for 10 min. After which, the gel was transferred to a clear tray and dH_2O was run over the gel for ~30 min. The gel was then photographed using a CCD camera connected to the Chemidox XRS unit and a digital image obtained under UV light transmission. Once the digital images of the gels were acquired, presence of the post qRT-PCR products were noted and the size (length of the DNA molecule) of the product was quantified by referencing against the kbp migration of the DNA molecular weight marker.

2.11 Statistical analysis

Statistical analysis of the effects of treatments on different aspects of cell function was performed and included UV wavelength (UVA and/or UVB), treated vs untreated cell cultures and timepoints (0, 6, 12, 24, 48 and 72 h post-irradiation), depending upon the relevant experiments. A control (untreated culture) was included in all experiments. All data points are expressed as the mean ± SEM for 3 replicates. All results were graphed using the Graph Pad Prism® 5 for Windows (GraphPad Software Inc., San Diego, USA) and analyzed using the one-way Anova test. As many comparisons were made a Bonferroni's correction of the p value was calculated. The data were considered significant if $p<0.05$.

Chapter Three:

Effect of UVR on furin activity in human keratinocyte cell lines

3.1 Introduction

Furin is a Ca^{2+}-dependant serine protease (144, 153, 156, 158) and is a member of the proprotein convertase (PC) family (156). In the epidermis, furin can exist either as: (a) a mature 97 kDa membrane bound enzyme or (b) a smaller 75 kDa form that lacks the transmembrane domain and reactivity with the c-FUR antibody specific for the C-terminus (144). It is localized to the constitutive secretory pathway (144, 226). Furin and other PC family members are proteases that play a key role in the maintenance of cell and tissue homeostasis by activating inactive precursor proteins to their functional or mature form via limited proteolysis in a timely and spatial fashion (227). These molecules include growth receptors, growth factors, hormones, plasma proteins, MMPs and ECM components (144, 146, 156, 167).

The role PCs play in the metastatic process is not clear. It is believed that for tumour progression to occur, the finely regulated autocrine/paracrine mechanism of growth factors and growth factor receptors expression and/or activation has to be deregulated. The abnormal production of those factors is a critical step in promoting the growth and malignant behavior of cancerous cells (227). In this context, PCs may be involved in the neoplastic process due to their inherent ability to process and activate these factors and receptors (227). Furin/PC expression and processing can increase the incidence and severity of the cancer phenotype (167).

PCs have also been shown to proteolytically cleave a number of ADAM family members including TACE (167, 169) and its maturation occurs while it transits through the late golgi compartment which that prodomain removal is performed by a furin-type proprotein convertase (154, 161). In contrast, inhibition of furin in epidermal

organotypic cultures leads to premature differentiation of keratinocytes, possibly via its effects on the Notch pathway (156). Inhibition of furin has been shown to reduce levels of mature TACE in both COS-7 cells (151) and keratinocytes (156).

Furin has been detected in keratinocytes and melanocytes (156) but the effect UVR has on its activity and/or expression and that of the proteases it activates in human keratinocyte cell lines is unknown. Furin mRNA, protein and enzyme activity has been observed in human epidermal keratinocytes (136, 151, 156, 173). Skiba *et al*. (136) found that UVA and UVB radiation increased furin mRNA levels immediately following exposure in HaCaT cells. Significant dose-dependent furin mRNA induction was detected 24 h after UVA-irradiation and 4 h post-UVB exposure (136).

Huynh *et al*. (174) showed that furin levels were unchanged in Colo 16 cells post-UVA-irradiation while those in HaCaT cells fell post-UVB-irradiation. Higher levels of furin were seen in Colo 16 cells compared to HaCaT cells. This agrees with that seen in other studies, where furin levels are higher in tumour cells compared to non-tumorous counterparts (144, 174, 227). It is unknown whether this change in furin levels was that of the immature and/or mature enzyme. While furin mRNA expression has been shown to be induced by UVR, its protein expression has not been investigated (136).

3.1.1 Aim and hypothesis

While furin is known to be expressed in skin cells, the effect UVR has on its expression and/or activity in human keratinocyte cell lines is poorly understood. We wish to observe if the cellular expression of furin is associated with its mRNA levels.

Therefore, the aim of this study is to investigate the effect of UVR on protein expression and/or activity of furin and whether UVA and/or UVB radiation induces the same response.

The UVA (40 kJ/m^2) and UVB (2 kJ/m^2) dose used in this thesis represents the respective UVA and UVB component found in one MED (174, 224). Therefore, the effects of singular (UVA or UVB) and concurrent (combination of UVA and UVB mimicking solar light, herein referred to as UVAB for simplicity) exposures of UVR were examined. In order to understand the effects of UVR on different keratinocyte-derived cell lines; primary keratinocytes (HEK), spontaneously immortalized keratinocytes (HaCaT) and SCC-derived (Colo16) cells were examined.

HaCaT cells are often used as a substitute for primary keratinocytes (228, 229) and both cell lines were used to see if furin activity in HaCaT cells was similar to that observed in primary keratinocytes. It is unknown if the activity and expression of this protease is increased as a result of tumorigenesis, and as such Colo 16 (a SCC cell line) was used in comparative studies.

3.2 Results

3.2.1 Effects of UVR on keratinocyte-derived cell viability

The effect of UVA- and/or UVB-irradiation on HEK, HaCaT and Colo 16 cell viability was determined 24 h post-irradiation using the trypan blue exclusion assay (Section 2.4) (Figure 3.1).

In HEK cells, the viability of attached sham-irradiated cultures was 93.3% (Figure 3.1i). UVA radiation had no effect on cell viability when compared to sham-irradiated controls. The attached viable cells were more sensitive to UVB and UVAB radiation as the cell viability was lower at 47% and 61%, respectively. The percentage of attached dead cells was highest in UVB- (49.3%) and UVAB-irradiated cells (38%) compared to sham-irradiated controls (7%). The percentage of the detached viable and dead cells was <5% for all UV types and doses. The results suggest that when HEK cells are exposed to UVAB, the viability profile is similar to that of UVB and not UVA radiation.

In HaCaT cells, the viability of attached sham-irradiated cultures was 92.4% (Figure 3.1ii). UVA radiation caused a slight drop in cell viability (81.1%). However, the number of attached viable cells was lower in UVB- (72%) and UVAB-irradiated cultures (60%) compared to the sham-irradiated controls. A significant ($p<0.05$) number of attached dead cells (~20%) was observed in UVA- and UVAB-irradiated cultures when compared to sham-irradiated cultures (8%). The percentage of detached viable cells was low for all UV types and doses. There were less dead detached cells observed in UVA-irradiated cells compared with those exposed to either UVB- (18%) or UVAB-irradiation (18%). The results suggest that when HaCaT cells were exposed to UVAB radiation, the result had characteristics similar to that seen for those cells irradiated by either UVA or UVB.

In Colo 16 cells, the viability of attached sham-irradiated cultures was 90% (Figure 3.1iii). UVA radiation caused a slight reduction in attached viable cells (83%). The

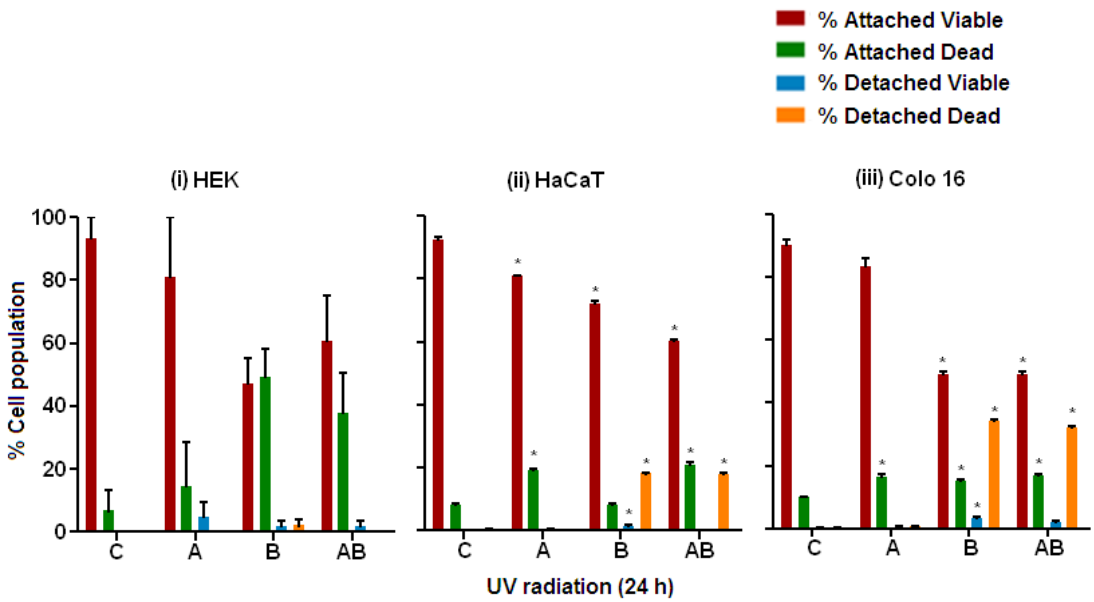

Figure 3.1 Effect of UVR on the viability of keratinocyte-derived cell cultures. HEK (i), HaCaT (ii) and Colo 16 cells (iii) were exposed to sham-irradiation or controls (C), UVA (A), UVB (B) or UVAB (AB) radiation and cell viability was determined 24 h post-irradiation. Results expressed are the mean ± SEM for three separate experiments. Statistical significance of the effect of UVR on the cell groups is represented as $p<0.05$ (*).

viability of attached cells in UVB- (49%) and UVAB-irradiated cells (49%) was significantly ($p<0.05$) reduced when compared to the sham-irradiated cultures. A significant ($p<0.05$) number of attached dead cells (16.4, 15 and 17%) was observed in UVA-, UVB- and UVAB-irradiated cultures when compared to the unexposed controls (9%). The percentage of detached viable cells was low for all UV types and doses. The highest numbers of dead detached cells (35%) were observed in cells exposed to either UVB- or UVAB-irradiation. These results suggest that when Colo16 cells are exposed to UVAB radiation, the viability profile is similar to that of UVB. The effect of UVR on Colo 16 cell viability was different to that seen in HaCaT and HEK cells. The morphology of the irradiated cells appeared to be slightly altered as a response to being exposed to UVR as represented in the phase contrast images seen in Figure 3.2.

3.2.2 Cellular expression of furin protein

The mature form of furin (97 kDa) has been detected in foreskin epidermal extracts and cultured keratinocytes (156) and HNSCCs (173). The purpose of this study was to determine the effect UVR has on the levels of furin in keratinocyte-derived cell lines (HEK, HaCaT and Colo 16 cells).

In order to quantify changes in furin levels in the cells, western blots (Section 2.5) of 50 µg cell lysates were run and probed with a furin convertase antibody. β-actin was used to quantify the level of protein added to each lane. Representative blots of the effect of

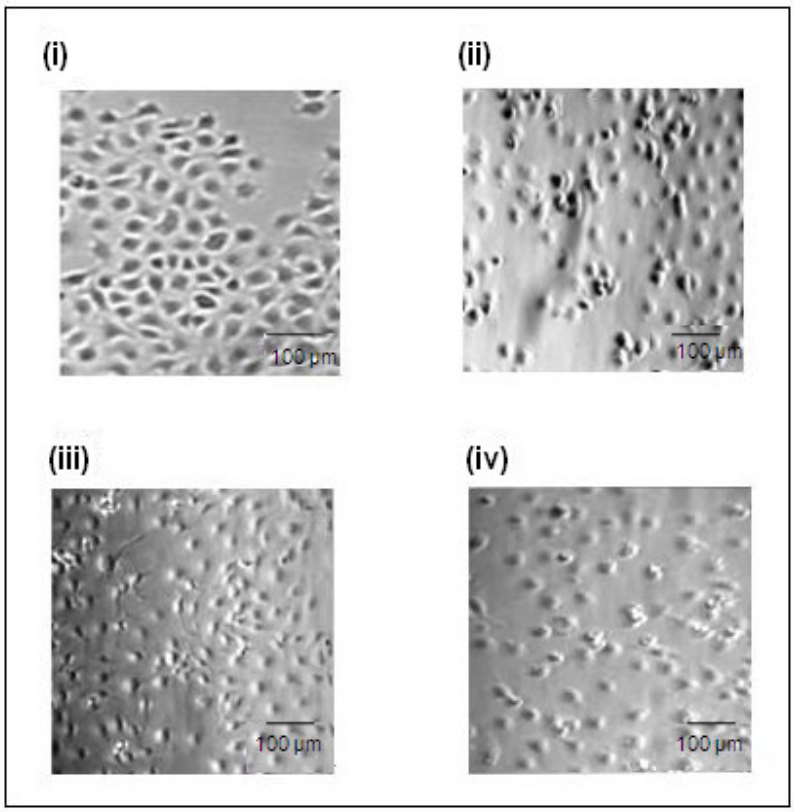

Figure 3.2 Effect of UVR on the morphology of Colo 16 cell cultures. Phase contrast images of Colo 16 cells were observed 24 h after being exposed to no UV-irradiation (sham-irradiated or controls) (i), UVA (40 kJ/m^2) (ii), UVB (2 kJ/m^2) (iii) and UVAB (40 kJ/m^2 UVA + 2 kJ/m^2 UVB) (iv) radiation.

UVR on furin levels in HEK, HaCaT and Colo 16 cells are seen in Figure 3.3. The level of furin in the treated cell was calculated as a ratio to that seen in untreated controls which was assigned a value of one.

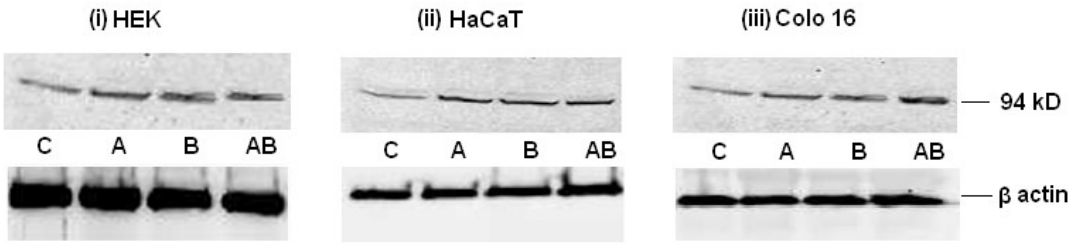

Figure 3.3 Representative western blots to show the effect of UVR on the expression of furin in HEK (i), HaCaT (ii) and Colo 16 cells (iii). The cells were exposed to no irradiation (controls) (C), UVA (A), UVB (B) and UVAB (AB) radiation and after 24 h, 50 µg of cell lysates were run on western blots. β-actin was used as a loading control.

3.2.2.1 Effects of UVR

The level of furin in HEK cells remained unchanged in response to UVR irrespective of the type or dose used (Figure 3.4). Furin levels in HaCaT cells were elevated when the cells were exposed to UVR (Figure 3.4). The levels were 6x higher in UVA-irradiated cells and 12x and 15x in UVB- and UVAB-irradiated cells, respectively when compared to the untreated controls.

In Colo 16 cells, furin was elevated in response to UVR. The levels of furin were 2x, 7.5x and 6.2x times higher in UVA-, UVB- and UVAB-irradiated cells, respectively

when compared to the untreated controls. The greatest increase in furin levels in both HaCaT and Colo 16 cells were seen in these cells which were exposed to either UVB or UVAB radiation.

When the level of furin in sham-irradiated (control) cell lines were compared (Figure 3.5), it can be seen that HaCaT cells expressed the highest amounts followed by Colo 16 cells with HEK having the lowest levels. Compared to HEK cells, furin levels were 10.9x higher in HaCaT cells and 5.7x higher in Colo 16 cells.

3.2.2.2 Effects of CHX

Cycloheximide (CHX) has been used in many studies to inhibit *de novo* protein synthesis (230-232). We used it in this study to determine the half-life of furin protein expression in the keratinocyte-derived cell lines. However, before we could determine the half-life of furin, the effect of CHX on cell viability needed to be determined.

3.2.2.2.1 Cell viability

The effect of CHX on cell viability of UV-irradiated HaCaT and Colo 16 cells was determined 24 h post-irradiation using the trypan blue exclusion assay (Section 2.4) (Figure 3.6).

In HaCaT cells, the viability of attached cells in untreated controls was 92.5%, however, in the presence of CHX, this fell to 77% (Figure 3.6i). The viability of untreated UVAB-irradiated attached cells (60%) fell slightly to 57% in the presence of CHX. The level of attached dead cells was <10% across all treatments and conditions

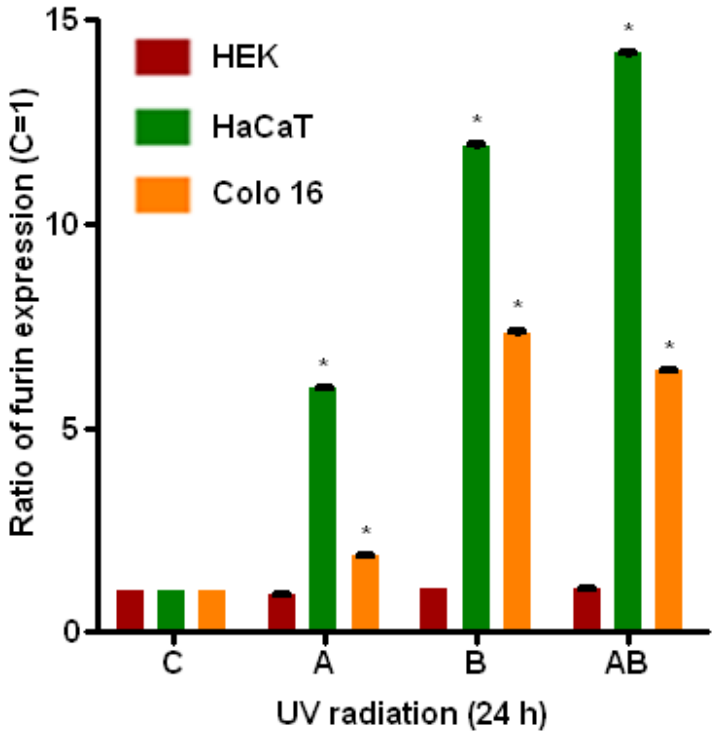

Figure 3.4 Effect of UVR on the expression of furin in HEK, HaCaT and Colo 16 cells. Cells were exposed to no irradiation or controls (C), UVA (A), UVB (B) and UVAB (AB) radiation and furin levels determined 24 h post-irradiation. The level of furin in each cell was expressed as a ratio to that seen in untreated controls which was given the value of 1. Results expressed are the mean ± SEM for three separate experiments. Statistical significance of the effect of UVR on furin levels was shown as $p<0.05$ (*).

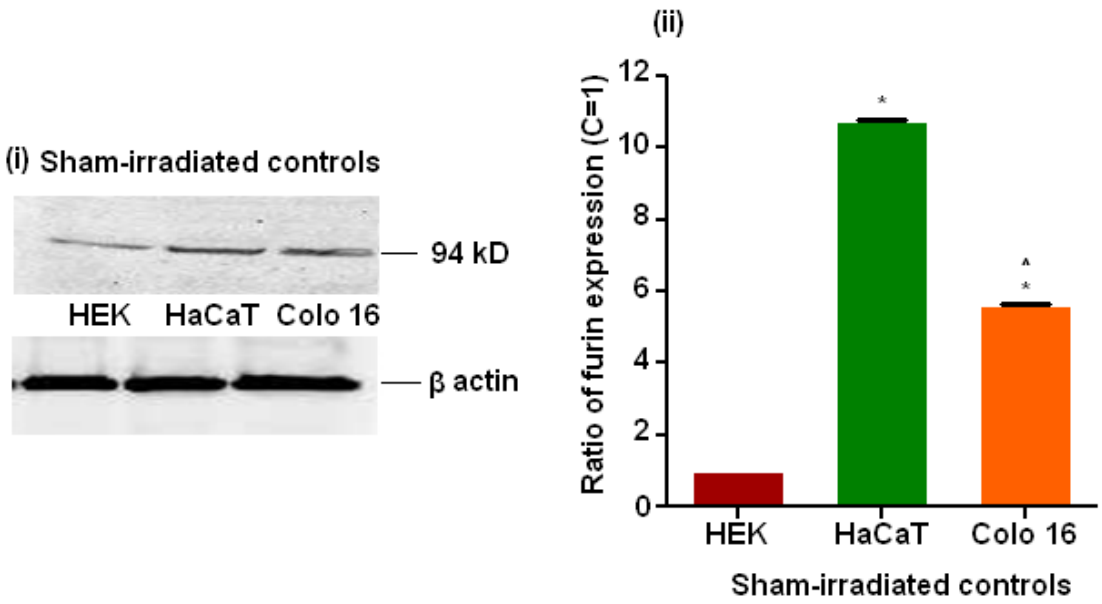

Figure 3.5 Comparison of the expression of furin in untreated cultures of HEK, HaCaT and Colo 16 cells. On a western blot, 50 µg of cell lysates were run and β-actin was used as a loading control (i). Quantification of the level of furin in HEK, HaCaT and Colo 16 cells (ii). Results expressed are the mean ± SEM for three separate experiments. Statistical significance of furin levels in different cell types was shown as $p<0.05$ (* HEK vs other cells) and (^ HaCaT vs Colo 16) (ii).

except for untreated UV-irradiated cells (20%). The number of detached viable cells was <5% in response to the different treatments and does. There were less dead detached cells observed in the untreated controls compared to CHX-treated controls and UV-irradiated cells (20%). The results show that 100 µM CHX did not significantly affect the viability of HaCaT cells.

In Colo 16 cells, the viability of attached cells in the untreated controls was 90% whereas this fell to 80% when CHX was added to these cells (Figure 3.6ii). The viability of untreated UVAB-irradiated attached cells was 50% and in the presence of CHX, it fell slightly to 48.2%. The number of attached dead cells was ~20% under all treatments and conditions except that it was ~30% in the untreated and treated UVAB-irradiated cells. The percentage of detached viable cells was negligible (<5%) in all experimental conditions.

In general, CHX at 100 µM had a minimal effect on cell viability of sham- and UVAB-irradiated HaCaT and Colo 16 cells and therefore, this dose was used to determine the half-life of furin protein expression.

3.2.2.2.2 Time course furin protein expression

A time course (0-24 h) of the level of furin expressed in HaCaT and Colo 16 cells was investigated. In order to investigate the half-life ($T_{1/2}$) of furin protein expression, the cells were either treated with or without CHX in UVAB-irradiated cells (Appendix A.9). The cells were irradiated with UVAB as it stimulated maximal furin expression in

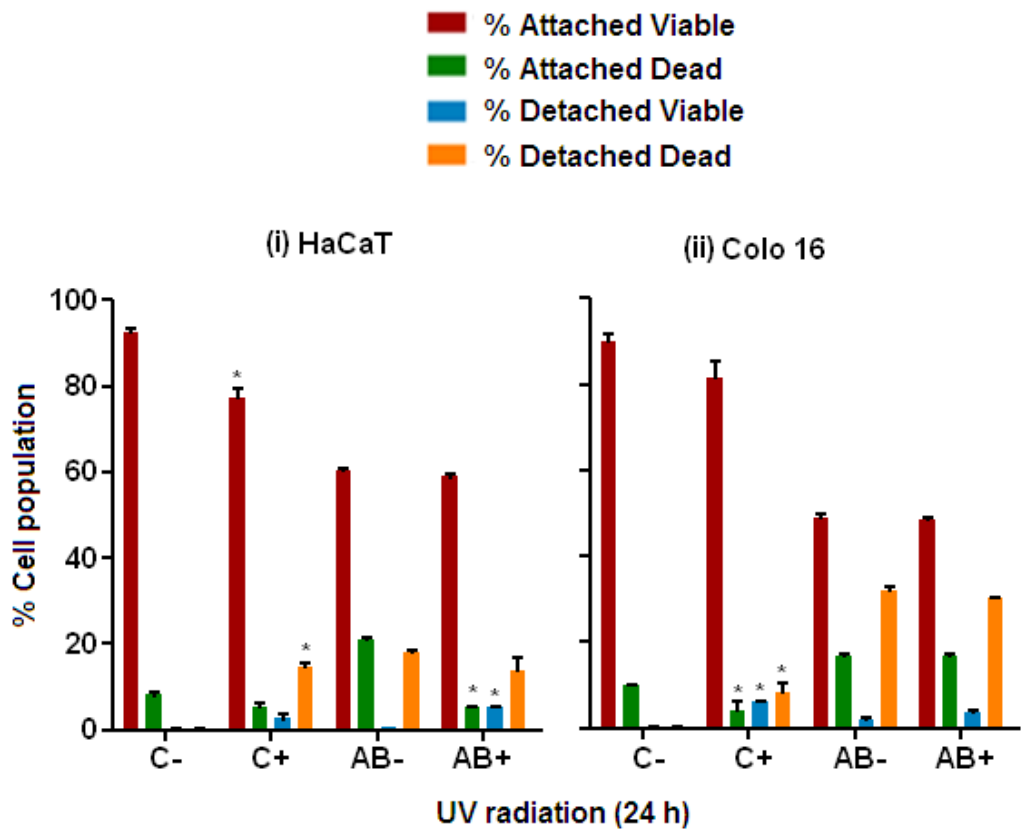

Figure 3.6 Effect of CHX on the viability of UVAB-irradiated HaCaT (i) and Colo 16 cells (ii). Cells were exposed to sham-irradiation or controls (C) or UVAB (AB) radiation in the presence (+) or absence (-) of CHX. Cell viability was determined 24 h post-irradiation. Results expressed are the mean ± SEM for three separate experiments. Statistical significance of the effect of CHX on the cell populations was represented as $p<0.05$ (*).

HaCaT and Colo 16 cells (Figure 3.4). The effect of 100 μM CHX on furin levels in UVAB-irradiated HaCaT and Colo 16 cells was used as it was shown to have a minimal effect on cell viability (Figure 3.6). Western blots of cell lysates from the treated cells were quantified (Section 2.5) and the results are shown in Figures 3.7 (HaCaT cells) and 3.8 (Colo 16 cells).

In HaCaT cells, the expression of furin in the untreated controls was constant over a 24 h period (Figure 3.7). On the other hand, furin protein levels in the corresponding CHX-treated cells decreased over the same period falling from 100% at 0 h to 10% by 24 h. Furin levels in the UVAB-irradiated HaCaT cells steadily increased following exposure reaching a maximal value of 15x that of sham-irradiated controls at 24 h. This was similar to that seen previously (Figure 3.4). However when CHX was added to the UVAB-irradiated cultures the furin levels was lower. There was a steady decline of furin expression in these cells from 100% at 0 h to 55% at 4 h and 5% by 24 h. The calculated half-life of furin in the un-irradiated HaCaT cells was 6.0 h while in the UVAB-irradiated cells, it was 5.6 h (Figure 3.7).

In Colo 16 cells, furin expression in the untreated controls was constant throughout the 24 h period (Figure 3.8). Furin protein levels in the corresponding CHX-treated cells were slightly elevated at 4 h (107%) before it fell to 77% at 8 h and 37% by 24 h. Furin levels in UVAB-irradiated HaCaT cells showed a steady increase with respect to time reaching 6.5x that of the sham-irradiated controls by 24 h. The level of furin in these irradiated cells at 24 h was similar to that seen previously (Figure 3.4). On the other

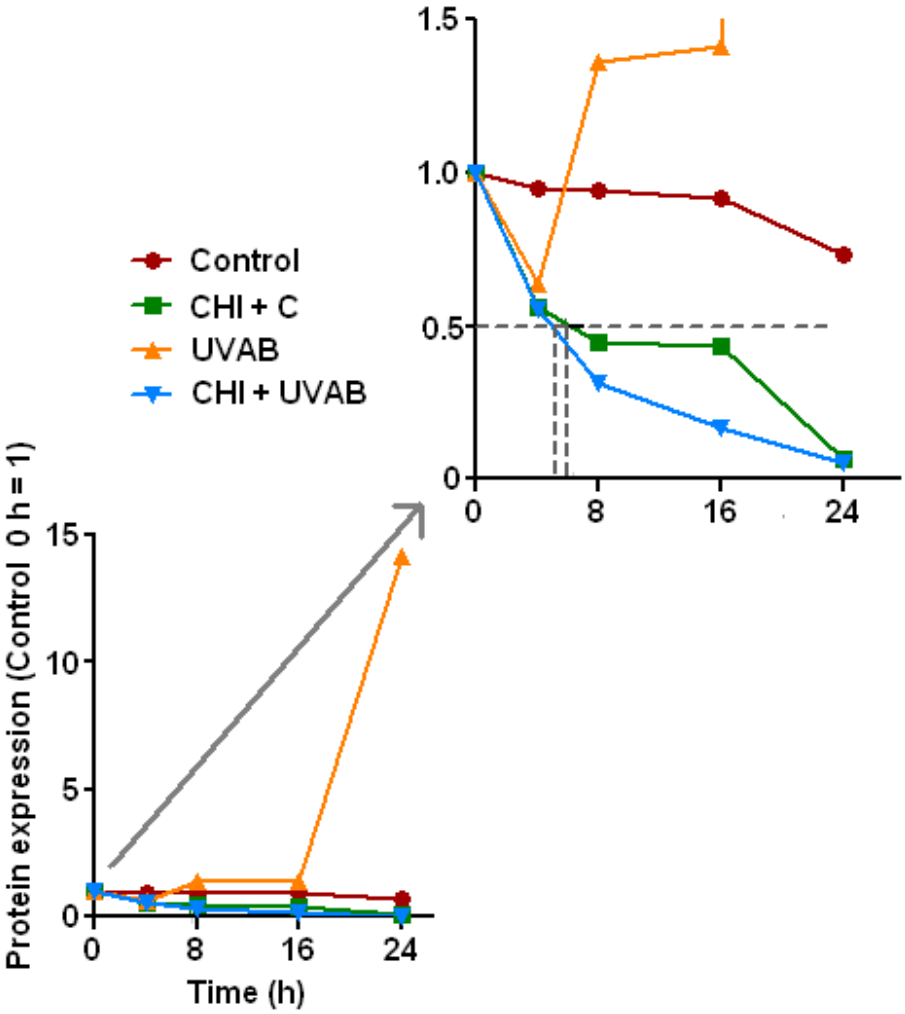

Figure 3.7 The effect of CHX on furin expression in UVAB-irradiated HaCaT cells. Cells were exposed to sham-irradiation or controls (C), or UVAB radiation (UVAB) in the presence (+) or absence (-) of CHX. The level of furin expression was measured up to 24 h post-irradiation. The calculated half-life of furin was represented as dotted lines. The level of protein in sham-irradiated (control) cells was given a value of unity. Results expressed are the mean ± SEM for three separate experiments.

hand, furin levels were much lower in the CHX-treated UVAB-irradiated cultures compared to their untreated counterparts. There was a steady decrease of furin expression over the course of the experiment falling to ~20% by 24 h. The calculated half-life of furin in the un-irradiated Colo 16 cells was 17.0 h while in the UVAB-irradiated cells, it was much shorter at 8.1 h (Figure 3.8).

3.2.2.3 Effects of IL-1α

Exposure to UV light induces many changes to the skin microenvironment, including the production of cytokines (233-235). IL-1α is a major epidermal cytokine that is constitutively synthesized by keratinocytes in response to stimuli like UV-irradiation (236, 237). Several growth factors and cytokines induce IL-1α expression in epidermal keratinocytes, these include TNFα (238, 239), TGFβ (239) and also IL-1α (240).

Bashir *et al*. (77) recently showed that IL-1α stimulates the secretion of TNFα from UVB-irradiated keratinocytes. TNFα is cleaved from its proform by the action of TACE (125, 137, 138). TACE is activated by the action of furin (151, 156, 158). As IL-1α stimulates TNFα release from irradiated cells, I investigated if this cytokine increased TNFα release from the cells by enhancing TACE and/or furin levels (see Chapter 5). As a result, the effect of IL-1α (10 ng/ml) on the expression of furin in cells exposed to UVR was investigated.

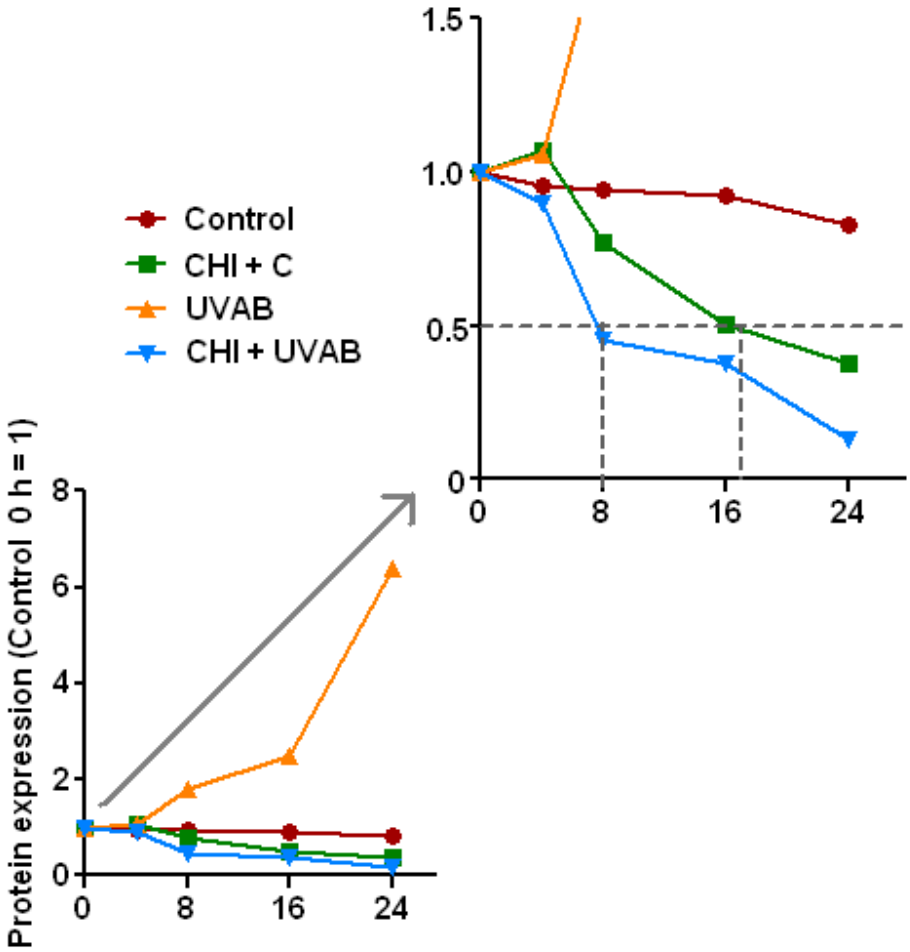

Figure 3.8 The effect of CHX on the expression of furin in UVAB-irradiated Colo 16 cells. Cells were exposed to sham-irradiation or controls (C), or UVAB radiation (UVAB) in the presence (+) or absence (-) of CHX. Furin levels were determined over a period of 24 h post-irradiation. Protein half-life is represented as dotted lines. The level of protein in sham-irradiated (control) cells was given a value of unity. Results expressed are the mean ± SEM for three separate experiments.

3.2.2.3.1 Furin protein expression

The effect of IL-1α on the expression of furin in UV-irradiated cells was determined 24 h post-irradiation using western blots of cell lysates (Section 2.5). In HEK cells, the IL-1α was shown to have no pronounced effects on furin expression in the UV-irradiated cells (Figure 3.9i).

In HaCaT cells, furin expression was elevated 5.9x in UVA-irradiated cells, 10.5x in UVB-irradiated cells and 15x in UVAB-irradiated cells when compared to the sham-irradiated controls (Figure 3.9ii). The addition of IL-1α to these irradiated cells caused a slight reduction in the observed furin levels.

In Colo 16 cells, furin levels were significantly elevated in UVB- and UVAB-irradiated cells compared to sham-irradiated cells (Figure 3.9iii). The increases seen in Colo 16 cells were less than that seen for the same UV dose in HaCaT cells. However, when IL-1α was added to the irradiated cells, there was a slight reduction in the observed levels of furin.

In summary, IL-1α had a slight additive effect in HEK cells but a slight suppressive effect on furin expression in HaCaT and Colo 16 cells.

3.2.2.3.2 Combined effects of CHX and IL-1α

IL-1α has been shown to have a slightly suppressive effect on furin levels in UV-irradiated HaCaT and Colo 16 cells (Figure 3.9). Therefore the effect of CHX and IL-1α on the level of furin expressed in UVAB-irradiated HaCaT and Colo 16 cells was investigated in a time course (0-24 h) experiment. In order to investigate the half-life of

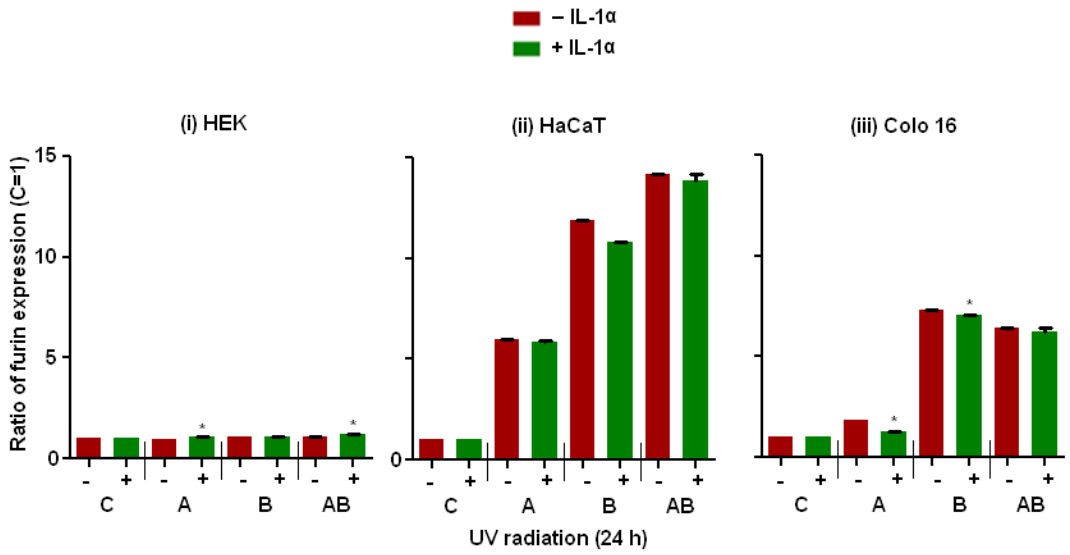

Figure 3.9 Effect of IL-1α on the expression of furin in UV-irradiated HEK (i), HaCaT (ii) and Colo 16 cells (iii). Cells were exposed to sham-irradiation or controls (C), UVA (A), UVB (B) and UVAB (AB) radiation in the presence (+) or absence (-) of IL-1α. Furin levels were determined 24 h post-irradiation. The furin levels were expressed as a ratio to that seen in untreated controls which was given a value of 1. Results expressed are the mean ± SEM for three separate experiments. Statistical significance of the effect of IL-1α on furin levels was shown as $p<0.05$ (*).

furin protein expressed in these cells, the cells were either treated with or without CHX in UVAB-irradiated cells in the presence of IL-1α (Appendix A.9). The cells were irradiated with UVAB as it stimulates maximal furin expression in HaCaT and Colo 16 cells (Figure 3.4). Western blots of cell lysates from the treated cells were quantified (Section 2.5) and the results shown in Figures 3.10 (HaCaT cells) and 3.11 (Colo 16 cells).

In HaCaT cells, the expression of furin in IL-1α treated UV-irradiated cells increased with respect to time and reached 15x that of untreated un-irradiated controls by 24 h (Figure 3.10). This result was similar to that seen previously (Figure 3.7). However, when CHX was added to the UV-irradiated cultures, furin levels fell 50% by 4 h before reaching <5% after 24 h. The calculated half-life of furin in the CHX-treated UV-irradiated HaCaT cells grown in the presence of IL-1α was calculated to be 4.3 h (Figure 3.10). The corresponding half-life of furin in CHX-treated controls was 6.0 h while in UVAB-irradiated cells it was 5.6 h (Figure 3.8).

In Colo 16 cells, the expression of furin in the IL-1α treated UV-irradiated cells increased with respect to time and reached 6.2x that of the untreated un-irradiated cells at 24 h (Figure 3.11). This was similar to that seen previously (Figure 3.8). However, when CHX was added to the IL-1α treated UV-irradiated cultures, furin levels fell to 70% after 4 h before reaching 10% by 24 h. The half-life of furin in the CHX-treated UV-irradiated Colo 16 cells grown in the presence of IL-1α was calculated to be 8.3 h (Figure 3.11). It can be seen that in UV-irradiated Colo 16 cells, the half-life of furin (in the presence or absence of IL-1α was 8.3 and 8.1 h, respectively) which was much less than that seen in un-irradiated cells (17.0 h).

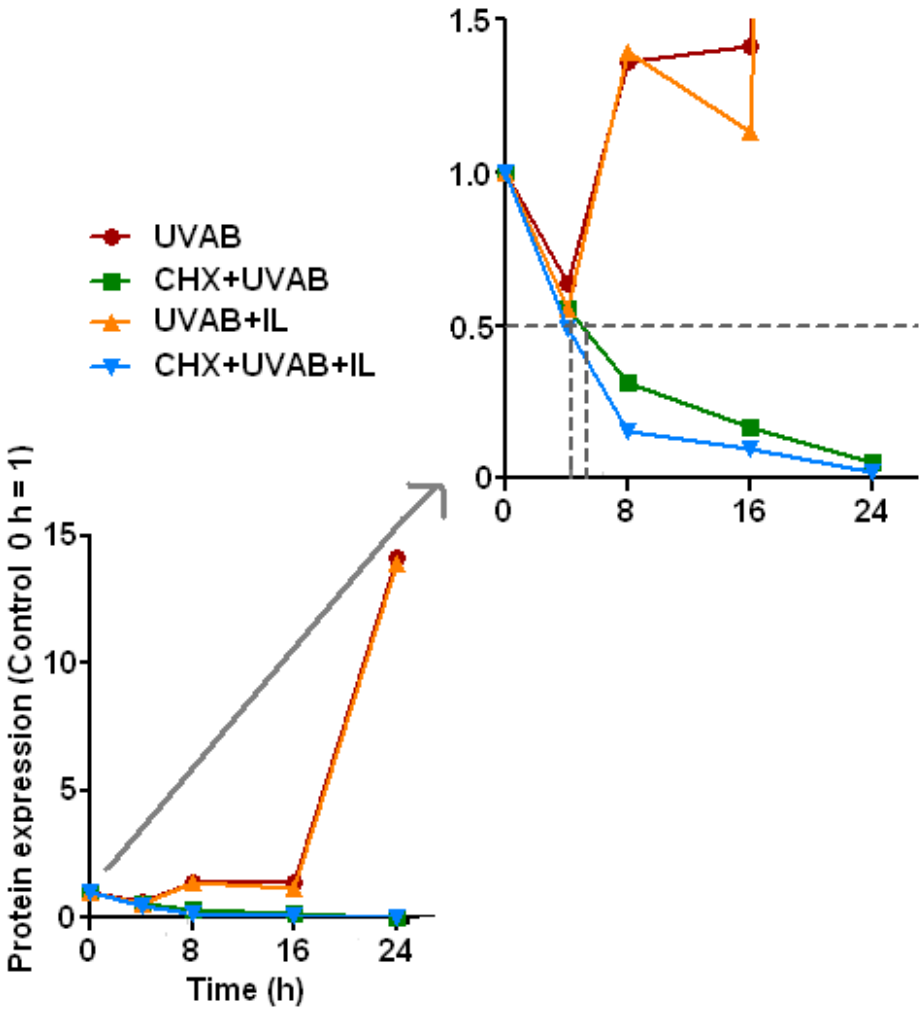

Figure 3.10 The effect of CHX on the expression of furin in IL-1α treated UVAB-irradiated HaCaT cells. Cells were exposed to sham-irradiation or controls (C) or UVAB radiation (UVAB) in the presence of IL-1α (IL) and/or CHX (CHX). Furin levels were determined over a period of 24 h post-irradiation. Protein half-life is represented as dotted lines. The level of protein in sham-irradiated (control) cells was given a value of unity. Results expressed are the mean ± SEM for three separate experiments.

In conclusion, these results show that IL-1α has no significant effect on the half-life of furin in UVAB-irradiated HaCaT or Colo 16 cells compared to that seen in the irradiated cells.

3.2.3 Furin mRNA expression

An investigation of the effect of UVR on furin gene expression was undertaken to see if changes in mRNA levels corresponded to changes in its protein levels. Skiba *et al*. (136) showed that UVA (2 kJ/m^2) and UVB (2 kJ/m^2)-irradiation induced a significant increase in furin mRNA, with higher levels seen in the UVB-irradiated cells.

The aim of this study was to observe the changes in furin mRNA levels in UVB-irradiated HaCaT and Colo 16 cell lines over 32 h. Skiba *et al*. (136) used qRT-PCR to quantitate changes of mRNA levels in cultured HaCaT cells following UV exposure. In order to quantify the gene expression of furin, qRT-PCR was used because of the low levels of mRNA seen in these tissues(136).

3.2.3.1 Time course gene induction

Following exposure to UVB-irradiation, samples were taken at various time points over 32 h from the HaCaT and Colo 16 cells and the mRNA levels measured using qRT-PCR (Section 2.9). While Skiba *et al*. (136) used the TaqMan™ qRT-PCR protocol and $\Delta\Delta C_T$ method for analysis, SYBR®Green ER™ qRT-PCR protocol and Pfaffl correction method was used in this study (Appendix A.8) (225). In this method,

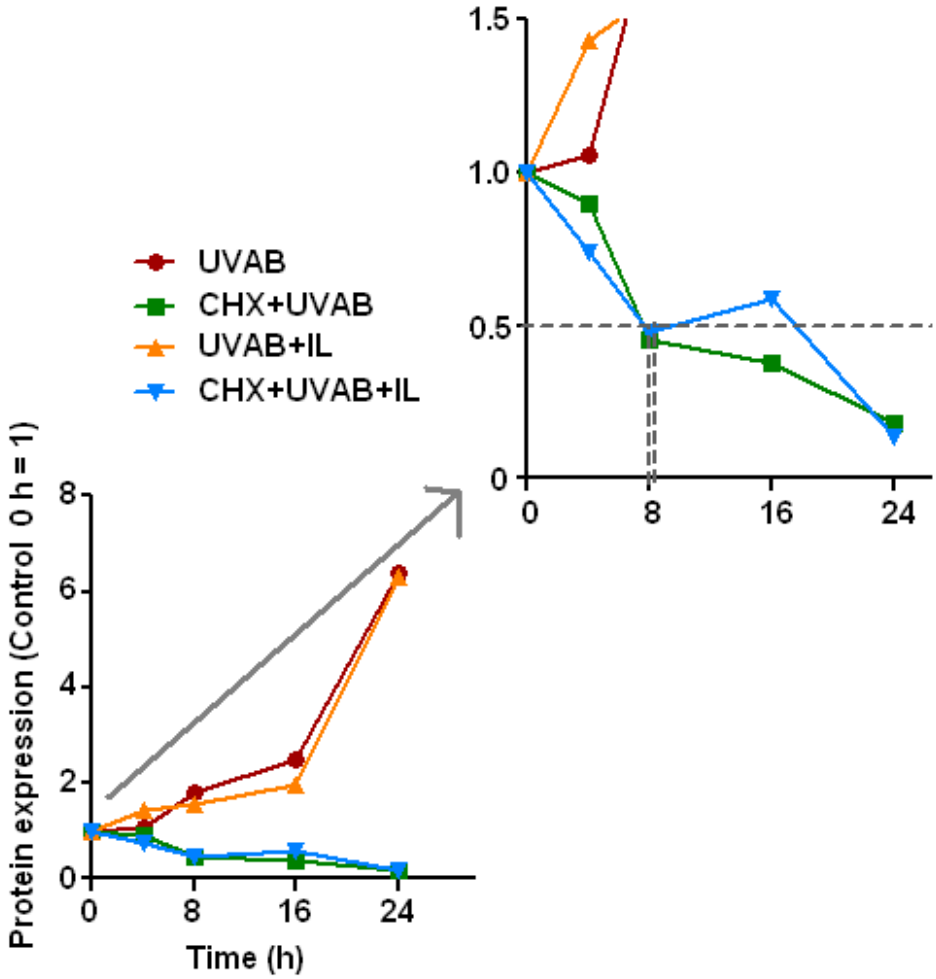

Figure 3.11 The effect of CHX on the expression of furin in UVAB-irradiated Colo 16 cells treated with IL-1α. Cells were exposed to sham-irradiation or controls (C), or UVAB radiation (UVAB) in the presence of IL-1α (IL) and/or CHX (CHX). Furin levels were determined over a period of 24 h post-irradiation. Protein half-life is represented as dotted lines. The level of protein in sham-irradiated (control) cells was given a value of unity. Results expressed are the mean ± SEM for three separate experiments.

the relative expression of the internal control gene (β actin) and target gene (furin) for each UV-irradiated sample was compared against un-irradiated sample. Results from this study shows that in UVB-irradiated HaCaT cells, a significant ($p<0.05$) increase in furin mRNA levels compared to untreated controls was not detected until 8 h (1.5-fold), after which it increased reaching a maximal level at 24 h (91-fold) before it falling to 3.3-fold by 32 h (Figure 3.12).

In Colo 16 cells furin mRNA expression in UVB-irradiated Colo 16 cells remained constant for the first 8 h before it increased to its maximal value (1.5-fold) at 12 h. After this it fell slightly at 16 h (1.2-fold) and remained constant until 24 h before falling to undetectable levels at 32 h. It can be seen from these cells that furin mRNA levels following UVB radiation differs between HaCaT and Colo 16 cells. The Colo 16 cells have an earlier peak but a lower level of furin mRNA expression than do HaCaT cells.

3.2.3.2 Effects of UVR

Furin mRNA was shown to be induced by UVB-irradiation in both HaCaT and Colo 16 cells (Figure 3.12). We extended that study to see if other UV types had an effect on furin mRNA levels in the cell. We chose the time point of 24 h post-irradiation to perform this study.

In HaCaT cells, maximum induction of furin mRNA was observed in UVB-irradiated cells (91-fold) (Figure 3.13). Furin mRNA levels were also increased 40- and 52-fold in the UVA- and UVAB-irradiated HaCaT cells, respectively when compared to that seen

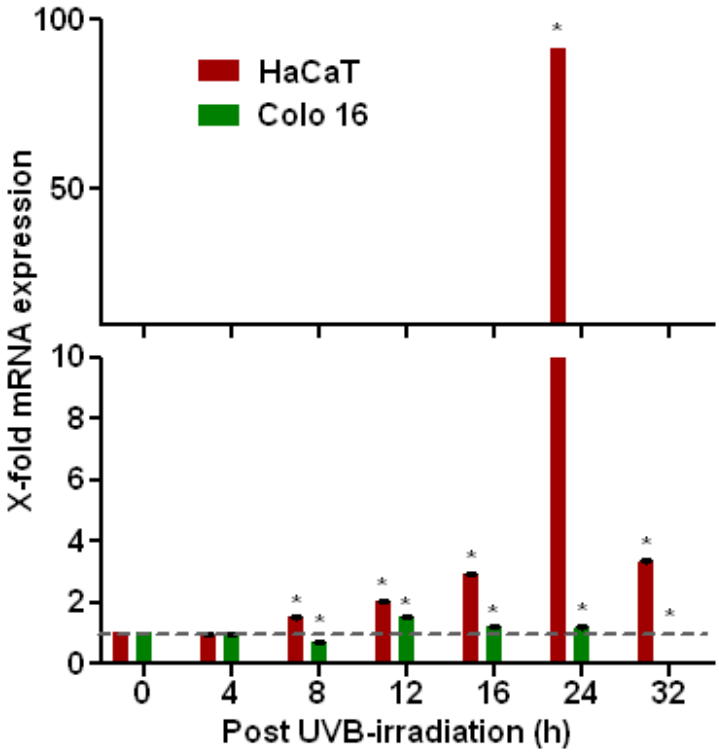

Figure 3.12 Effect of UVB on time course furin mRNA induction/expression in HaCaT and Colo 16 cells. Cells were exposed to UVB-irradiation and mRNA expression determined over a 32 h period. Control mRNA levels found in un-irradiated cells (=1) are represented as dotted lines. Results expressed are the mean ± SEM for three separate experiments. Statistical significance of the effect of UVB on furin mRNA levels against sham-irradiated (control) cells was shown as $p<0.05$ (*).

in the sham-irradiated controls. However, maximal induction of furin mRNA was induced in UVB-irradiated cells which agreed with that seen previously (136).

In Colo 16 cells, furin mRNA expression was relatively constant following UV-irradiation (Figure 3.13). Furin expression was slightly higher in UVB-irradiated cells (~2-fold) compared to the un-irradiated controls. This was similar to that seen previously (Figure 3.12). Furin gene expression was much greater in HaCaT cells compared to that seen in Colo 16 cells, while UVB-irradiation induced the highest levels in both cells.

3.2.3.2.1 Furin mRNA vs protein levels

Correlation studies were performed by comparing the levels of furin mRNA (Figure 3.13) and protein (Figure 3.4) seen in the HaCaT and Colo 16 cells 24 h post-irradiation. The level of mRNA and protein in the un-irradiated controls was given the value of unity.

The values for both mRNA and protein in the irradiated cells are expressed as a ratio of that seen in their respective un-irradiated controls. The results were plotted and a line of best fit was calculated for each UV type (Figure 3.14).

There was a moderate correlation ($r^2 = 0.581$) between furin mRNA and protein levels in the irradiated HaCaT cells. However in Colo 16 cells this correlation was weaker ($r^2 = 0.399$). While there appears to be a correlation between furin mRNA and protein levels at 24 h in these cells, this correlation may be more pronounced at other time points.

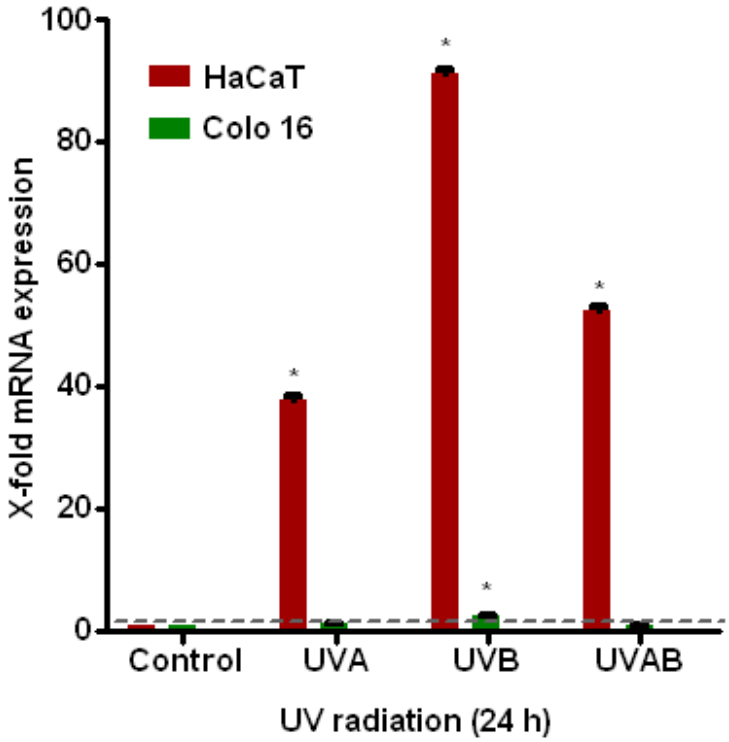

Figure 3.13 Effect of UVR on furin mRNA induction/expression in HaCaT and Colo 16 cells. Cells were exposed to control (no irradiation), UVA, UVB and UVAB radiation and mRNA expression determined 24 h post-irradiation. Control mRNA levels found in un-irradiated cells (=1) are represented as dotted lines. Results expressed are the mean ± SEM for three separate experiments. Statistical significance of the effect of UVR on furin mRNA levels against sham-irradiated (control) cells was shown as $p<0.05$ (*).

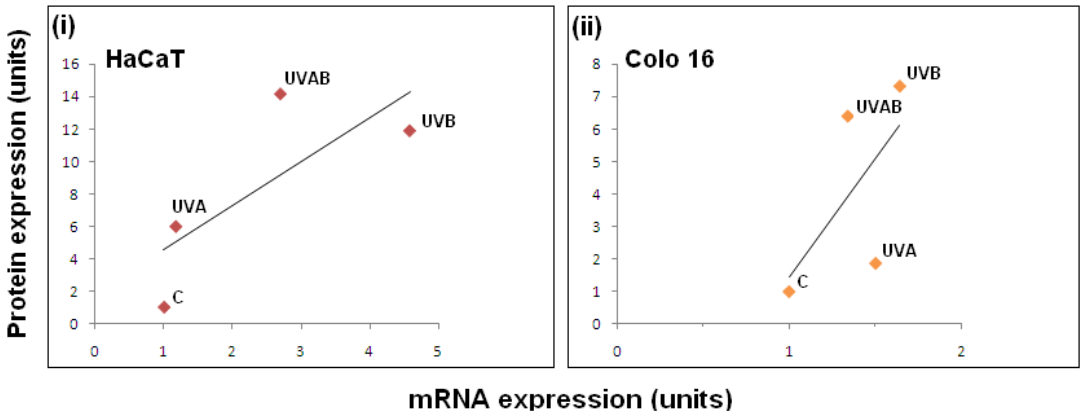

Figure 3.14 Correlation between furin protein and mRNA levels 24 h post-irradiation in HaCaT (i) and Colo 16 cells (ii). Cells were exposed to sham irradiation or controls (C), UVA, UVB and UVAB radiation and the protein levels and mRNA expression of furin in the cell extracts for each UV type were expressed as a ratio to that observed in sham-irradiated cells, which were given the value of unity.

3.2.3.3 Effect of CHX

We have shown earlier that CHX inhibits the synthesis of furin protein in HaCaT (Figure 3.7) and Colo 16 cells (Figure 3.8). In order to look at the effect CHX (100 µm) had on furin mRNA levels. We used UVAB-irradiated HaCaT and Colo 16 cell lines at 0 and 24 h post-UVAB-irradiation.

In HaCaT cells, the furin mRNA expression was similar in sham-irradiated cells or CHX-treated cells 0 and 24 h after the commencement of the experiment. Furin mRNA levels immediately decreased by 50% in both untreated and CHX-treated

UVAB-irradiated cells. However, at 24 h, the furin mRNA levels increased to 52-fold compared to that seen in untreated controls at 0 h. The addition of CHX to these UVAB-irradiated cells had no effect on furin mRNA expression at either time point (Figure 3.15i).

In Colo 16 cells, the furin mRNA levels did not change in either the controls or CHX-treated cells 0 or 24 h after the commencement of the experiment. Furin mRNA levels immediately increased ~2-fold post-irradiation in both untreated and CHX-treated UVAB-irradiated cells. However, at 24 h, the furin mRNA levels had fallen to only 70% of that seen in untreated controls at 0 h (Figure 3.15ii). The addition of CHX to these UVAB-irradiated cells had no effect on furin mRNA expression at either time point.

In both cell lines CHX was shown to have no effect on furin mRNA expression.

3.2.3.4 Effects of IL-1α

Earlier we found the addition of IL-1α to UV-irradiated cells resulted in a reduction of furin protein expression in HaCaT and Colo 16 cells (Figure 3.9). In this experiment, the effect of IL-1α on furin mRNA expression in UVAB-irradiated HaCaT and Colo 16 cells was examined to see if this change might be due to altered mRNA levels.

Immediately following exposure to UVAB-irradiation, IL-1α was added to HaCaT and Colo 16 cells and samples were collected over the next 24 h. The mRNA levels were measured using qRT-PCR (Section 2.9). In this method, the relative expression of the internal control gene (β actin) and target gene (furin) for each UV-irradiated sample

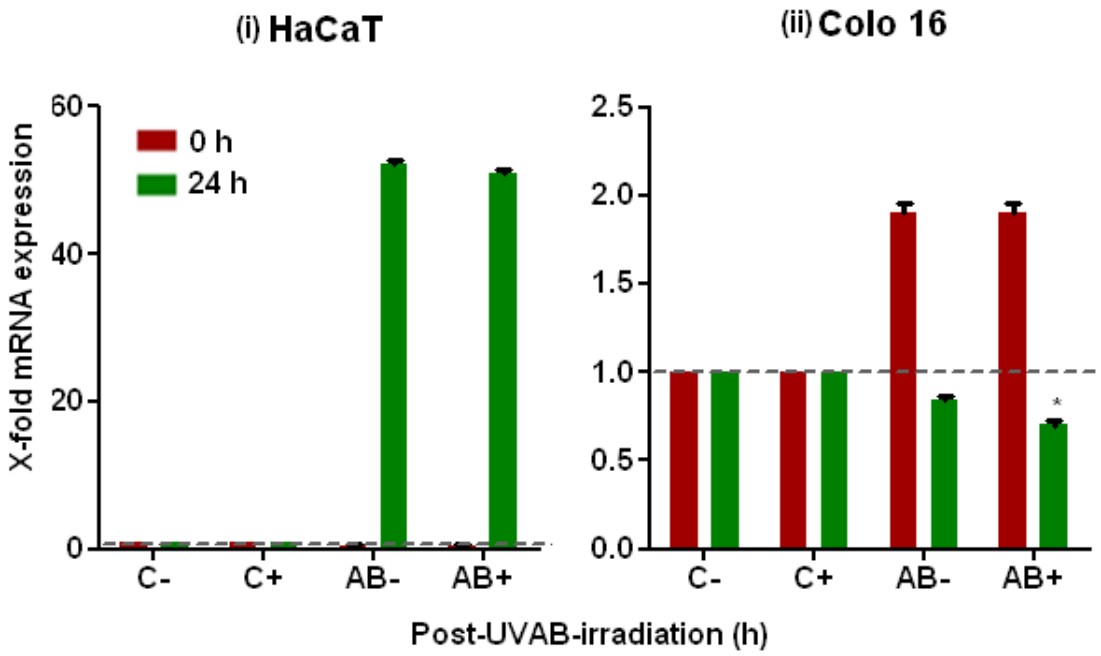

Figure 3.15 Effect of CHX on the mRNA expression of furin in UVAB-irradiated HaCaT and Colo 16 cells. Furin mRNA induction/expression was measured in HaCaT (i) and Colo 16 cells (ii) compared with controls either at 0 or 24 h post-irradiation. Cells were exposed to sham irradiation or controls (C) and UVAB-irradiation (AB) in the presence (+) or absence (-) of CHX. Control mRNA levels found in un-irradiated cells (=1) are represented as dotted lines. Results expressed are the mean ± SEM for three separate experiments. Statistical significance for effect of CHX on furin mRNA levels against sham-irradiated (control) cells was shown as $p<0.05$ (*).

with IL-1α at different time points was compared against the un-irradiated sample with IL-1α at 0 h. This was calculated using the Pfaffl Correction method (Appendix A.8) (225). UVAB-irradiation was shown to induce maximum furin protein levels 24 h post-irradiation in HaCaT cells (15x) (Figure 3.4) and Colo 16 cells (6.2x) when compared to un-irradiated controls. The addition of IL-1α to these irradiated cells caused a slight suppression of furin levels in these cells (Figure 3.9). In this study, we irradiated the cells with UVAB, so the effect of IL-1α on furin mRNA expression could be examined.

In HaCaT cells, the effect of UVAB plus IL-1α on the expression of furin mRNA levels fell post-irradiation reaching a minimal value (60%) at 4 and 8 h before increasing to a peak (5.3x) at 16 h after which it fell back to 4.2x that of the treated un-irradiated controls at 24 h.

In Colo 16 cells, under the same conditions, furin mRNA levels increased immediately at 4 h (2.6-fold) compared to the treated un-irradiated controls after which it remained constant between 8 and 12 h (~similar to controls) before it fell by 70% at 16 and 24 h (Figure 3.16).

In conclusion, over a 24 h time period, addition of IL-1α initially decreased furin mRNA expression over the first 12 h before dramatically increasing over the next 4 h in UVAb-irradiated HaCaT cells. In the Colo 16 cells there was an initial increase in furin mRNA expression peaking at 4 h before it fell steadily.

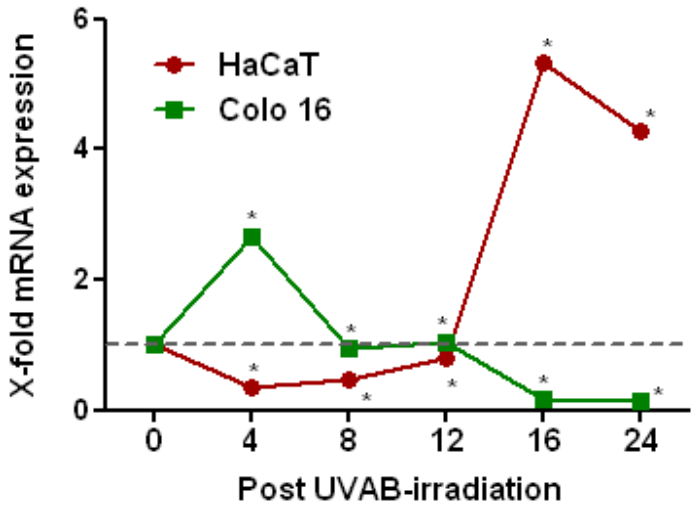

Figure 3.16 Time course of the effect of IL-1α on furin mRNA induction/expression in UVAB-irradiated HaCaT and Colo 16 cells. Cells were exposed to UVA+UVB (UVAB) radiation and mRNA expression was determined at different time points over a 24 h period. Control mRNA levels found in un-irradiated cells (=1) are represented as dotted lines. The relative expression of the furin gene for each IL-1α treated sample was compared against the treated un-irradiated controls and calculated using the Pfaffl Correction method (Appendix A.8). Results expressed are the mean ± SEM for three separate experiments. Statistical significance of the effect of IL-1α on furin mRNA induction/expression was shown as $p<0.05$ (*) for UVAB-irradiated HaCaT cells and (^) for UVAB-irradiated Colo 16 cells.

3.2.4 Summary

In this study, I investigated the effect UVR had on furin activity, protein and mRNA expression in the keratinocyte-derived cell lines (HEK, HaCaT and Colo 16 cells). Cell viability using trypan blue exclusion showed that the cells in general were more sensitive to UVB than UVA radiation (Figure 3.1). UVR increased furin protein expression in both HaCaT and Colo 16 cells but not in HEK cells (Figure 3.4). UVAB-irradiation stimulated the greatest increase of furin levels in HaCaT while in Colo 16 it was due to UVB. The turnover of furin protein was longer in Colo 16 cells compared to HaCaT cells ($T_{½}$ = 17.0 h and 5.6 h, respectively) (Figures 3.7 and 3.8). The addition of IL-1α had a suppressive effect on furin expression when the cells (HaCaT and Colo 16 but not HEK cells) were exposed to UVR (Figure 3.9).

In general, furin mRNA expression was higher in UV-irradiated HaCaT cells compared to Colo 16 cells. Maximal furin mRNA levels were observed at 24 h in HaCaT cells and 12 h in Colo 16 cells following UVB-irradiation (Figure 3.12). There was a weak correlation between furin mRNA and protein levels in Colo 16 cells, but it was stronger in HaCaT cells (Figure 3.14). CHX had no effect on furin mRNA expression in UVAB-irradiated HaCaT and Colo 16 cells (Figure 3.15). The addition of IL-1α in a time course study increased furin mRNA levels in UV-irradiated HaCaT cells but reduced them in Colo 16 cells compared to that in treated un-irradiated controls (Figure 3.16).

In conclusion these results show that UVR up-regulates both furin protein and mRNA expression, although there was not a strong correlation between the two. While addition of IL-1α had a slightly suppressive effect on furin protein expression, it increased furin

mRNA levels in HaCaT cells. On the other hand, in Colo 16 cells, effect of IL-1α caused reduction of both furin protein and mRNA levels.

3.3 Discussion

Furin is a member of the PC family and is expressed at low levels in a wide range of human tissues (173). PCs are proteases that play a key role in the maintenance of cell and tissue homeostasis by activating protein precursors via proteolysis in a timely and spatial fashion (227). While furin is known to be expressed in skin cells, the effect UVR has on its expression and/or activity and that of its substrates in human keratinocyte is unknown.

UV light is intricately linked to the functional status of the cutaneous immune system. In susceptible individuals, UVR can activate pathogenic inflammatory pathways leading to allergy or autoimmunity (241). It is a major environmental factor that affects pigmentation in human skin and can eventually result in various types of UV-induced skin cancers (242). Much emphasis has been placed on the role of UVB in skin carcinogenesis but not on UVA. However, a large body of evidence now points to a role for UVA in skin carcinogenesis (242-246). Unlike UVB, which is absorbed in the epidermis, UVA radiation penetrates into the underlying dermis causing a reduction in the number of superficial dermal fibroblasts (16). Although the magnitude of UVA is less carcinogenic than UVB (247, 248), chronic UVA exposure has been shown to induce photoageing (249) and skin tumours (squamous cell carcinomas) in experimental animals (247, 250, 251).

The predominance of UVA mutations in the basal cell layer of the epidermis reinforces the pivotal role UVA may play in the malignant transformation of human skin cells (252). UVA radiation also induces epidermal lipid peroxidation, which stimulates LC migration from the epidermis, thus contributing to UV-induced immunosuppression (244). Therefore, in this study, UVA and/or UVB were used in all experiments, as they are the components of UV light that reach the Earth's surface (7, 253). As UVC is unable to penetrate the ozone layer (253), it was not used in this study as it was not of physiological relevance (30). In this study some of the cellular changes elicited by UVA and UVB on furin activity and/or expression in cultured keratinocyte-derived cell lines were investigated.

Three keratinocyte cell lines were used in this study; primary human keratinocytes (HEK), immortalized (HaCaT) and SSC-derived (Colo16) cells. HaCaT cell line were chosen as it is a non-tumorigenic, fully differentiated and potentially immortalized model for primary keratinocytes (221). Previous studies comparing the effect of treatments between HaCaT and primary keratinocyte cultures, or human keratinocytes *in vivo*, reported that the results were comparable and a good correlation existed between the two cell lines (228, 229). Therefore, based on such findings, we chose HaCaT cells as a model to study the effects of UV-irradiation in keratinocytes. Where possible, we also repeated the experiments using HEK cells to observe if the results seen in HaCaT cells were similar to that of primary keratinocytes. Colo 16 cells were isolated from a SCC and were used to observe the effects of UVR has on a tumour-derived keratinocyte (222). Hence by using the three cell lines we can evaluate (a) if HaCaT cells are a suitable substitute for HEK to investigate the effect of UVR on

cell function and (b) are these cellular processes affected as a result of carcinogenic transformation.

It is important while examining activity, cellular and mRNA expression in skin cells that the UV doses used do not induce cell death, as it is only the surviving cells *in vivo* that can become carcinogenic (174). Therefore, in this study, the UVA dose (40 kJ/m^2) and the UVB dose (2 kJ/m^2) represented the respective UVA and UVB components found in one minimal erythemal dose (MED) (224). One MED is the amount of UVR that causes perceptible erythemal or edema, generally called sunburn (48). The UVAB used in this study is a combination of the respective UVA and UVB doses in one MED. The doses (Section 2.3.4 and Table 2.1) used in this study was chosen because they represent the dose most people would receive in a single exposure period when they are outdoors (174). While the cumulative daily UV dose some people would receive may be higher, this study was designed to observe the cellular effects elicited from a single exposure, and as such these doses were chosen (174).

For all experiments used in this study, keratinocyte-derived cell cultures were exposed to a bank of UVA and UVB lamps (Section 2.3.3). In order to ensure cultures were not exposed to any UVB emitted by the UVA lamps, a 10 mm thick glass plate was placed over the cultures. The glass blocked penetration by UVB light therefore ensuring the cultures were only exposed to UVA radiation. The effects of both heat and dehydration when the cells were exposed to UVA and/or UVB were minimal in these studies due to short exposure periods. In this study, the confluency of the cultures used in all experiments was ~75%. This was preferred as cell growth was still maximal and the cellular physiological processes were optimal. When the cultures reach confluency,

many cellular processes slow down and if they are used, the results obtained may not correctly reflect what may occur (254).

The purpose of the viability experiment was to show the effect UVR has on cell viability. We observed that cells exposed to UVA had a higher cell viability compared to those irradiated by UVB or UVAB (Figure 3.1). The difference could be due to the fact that UVA radiation is absorbed by chromophores that give rise to the production of reactive oxygen species (ROS) and ROS-dependent DNA lesions are repaired quickly and have low mutagenicity (255). These results agreed to previous studies by Skiba *et al*. (136) who showed that cell survival rates was ~85% in both sham- and UVA (2 and 8 kJ/m^2)-irradiated HaCaT cells. It is likely that the higher doses of UVA used in this study could be more cytotoxic. Budai *et al*. (256) determined that in human fibroblasts, at small UVA doses (<80 kJ/m^2) a smaller level of damage was observed but with increasing dose (150-200 kJ/m^2), higher level of damages were seen where the viability detected was 20%. Thus UVA at higher doses can be strongly mutagenic because of the formation of oxidative DNA damage (257) and thus could play a pivotal role in the malignant transformation of human skin.

Interestingly, when HEK and Colo 16 cells were irradiated with UVAB radiation their viability was similar to that observed in UVB-irradiated cells (Figure 3.1). These results were similar to that seen in studies by Huynh *et al*. (174) who showed that when Colo 16 cells were exposed to UVAB radiation (20 kJ/m^2 and 2 kJ/m^2), the cell viability profile was similar to that of UVB and not UVA. This suggests that UVB has a more profound effect on the cells than does UVA. As UVB radiation is of higher energy level compared to UVA, a high dose can cause more lesions ((6-4)-photoproducts) as well as

a degeneration of inner and outer cellular membranes (258). These lesions are repaired more slowly and may give rise to mutations (255). If DNA damage is severe and the cells are beyond repair, multiple death pathways are activated resulting in the elimination of these compromised cells (42). In general these cell lines were more sensitive to the UVB component of one MED and not the UVA component.

In comparison to HEK and HaCaT cells, Colo 16 cells had less attached viable cells and a slight increase in detached viable cells when exposed to either UVB- or UVAB-radiation (Figure 3.1). Takasawa *et al*. (259) and Huynh *et al*. (174) showed that these detached viable cells (HaCaT and Colo 16 cells, respectively) were unable to re-adhere when they were transferred to fresh media and eventually died in culture. Colo 16 cells had less attached dead cells and a corresponding increase in detached dead cells following UVB- and UVAB-radiation compared to un-irradiated controls. This could also be due to the fact that the Colo 16 cells grow at a faster rate and as such the rate of cell death was also high (259).

Although cell viability determination using trypan blue exclusion is a relatively easy, fast and cost-efficient method, there are limitations to this method. Trypan blue stains dead cells blue as the cells tend to lose their membrane integrity. However, it does not help differentiate between apoptotic and necrotic cells. The trypan blue dye is cytotoxic and can cause cell death if there as a delay in performing viability counts. Similarly, cells in early stage of apoptosis are not stained blue as the plasma membrane is still intact (260). Therefore, this can give rise to inaccurate results.

Armeni *et al*. (261) determined keratinocyte viability 24 h post UVA-irradiation using annexin V-labelled flow cytometry. Other staining methods which could be used in flow cytometry include acridine orange and ethidium bromide (EtBr) (270) or Hoechst 33342 and propidium iodide (260, 262). Liegler *et al*. (260) demonstrated that acridine orange-EtBr stained cells is more sensitive and accurate than that seen using other methods like trypan blue exclusion and DNA fragmentation. Thus use of these methods may help differentiate and quantify the number of viable, apoptotic, late-stage apoptotic and necrotic cells in the UV-irradiated cultures.

UVR is known to induce the activation of stress-inflammation signal transduction pathways (263), and to induce the activity of many proteases in skin cells (174). Though furin is expressed in skin cells (156), it is not known what effect UVR has on its activity. When Bassi *et al*. (173) looked at human SCC cell lines (A 253, Detroit 562, SCC9, SCC 12 and SCC 15), they observed that highest furin expression was seen in the most invasive cell lines. In order to investigate the effect of UVR on furin protein expression, western blots were performed (Figure 3.4). UVR increased furin protein expression in both HaCaT and Colo 16 cells but not in HEK cells. Endogenous furin protein expression was higher in HaCaT cells compared to that of Colo 16 cells (Figure 3.5ii). The greatest increases in furin levels were observed in HaCaT cells irradiated with UVAB (15x) and in Colo 16 exposed to UVB (7.5x). Huynh *et al*. (174) found that in Colo 16 cells, both UVB and UVAB radiation increased furin levels 24 h post-irradiation, but not in HaCaT cells where furin levels fell in response to UVR. The results obtained in this study agree with that seen for Colo 16 cells but were different to that observed for HaCaT cells. These differences may be attributed to the fact that

Huynh *et al*. (174) combined attached and detached cells whereas only attached cells were examined in this study.

The results from this study suggest that furin expression increases in the immortalized (HaCaT) and tumour (Colo 16) cells but not in the primary (HEK) cells. It has been shown by others that furin levels are higher in tumour cells compared to their non-tumorous counterparts (144, 227). While Colo 16 cells has higher furin levels than HEK cells, which agrees with that seen in other studies (144, 227) the reasons for the high levels observed in HaCaT cells are not clear. HaCaT cells are an immortalized cell line but are not metastatic (221, 259, 264) and the high furin levels observed in these cells may have arisen as a result of immortalization. Bassi e*t al*. (173) also showed moderate to high levels of furin expressed in HNSCC cell lines. They showed an association between tumour cell invasiveness and PC levels in these cell lines (173). Higher furin levels observed in tumour cells reflect these cell's metastatic potential as one of the proteases they activate, the MMPs, cleave the ECM, allowing metastasis to occur (265). This increase in furin can subsequently activate other proteases that furin is known to processes, including MMP and TACE, which in turn, when activated, process a wide range of biological molecules crucial for cell function and growth (151, 169, 266, 267).

The results from this study also show that there are differences between the effect of UV types and doses on cell function in the keratinocyte-derived cell lines examined in this study. While, UVAB-irradiation (Figure 3.1) had a stronger effect on HaCaT cells, UVB-irradiation induced maximum furin expression in Colo 16 cells. This was probably due to the fact that when cells were irradiated with UVB (2 kJ/m^2) (alone) or

in combination with UVA, (40 + 2 kJ/m^2), UVB-irradiation appeared to be of predominance, dominating the effect of UVA. This suggests that following UV exposure, the level of furin is elevated as its potential to cleave enzymes such as TACE, MMPs, TGFβ, PDGF and other growth factors thereby increasing inflammation, the ability of the cell to degrade the ECM, tumour cell proliferation, motility, invasiveness and adhesiveness (168, 268).

In order to determine the half-life of furin in the cells, we used CHX. This inhibitor inhibits new protein synthesis and interferes with the translocation step in protein synthesis thus blocking translational elongation (230-232, 269). Thus, by measuring the level of furin in the cells over a period of time, we can calculate its half-life of this protein. Before undertaking these experiments, I investigated the effect CHX had on cell viability (Figure 3.6). The purpose of this was to ensure that the dose (100 μM) used was not cytotoxic to the cells. The cells were exposed to UVAB-irradiation in the presence or absence of CHX. The cells were irradiated with UVAB as it stimulated maximal furin expression in the cells (Figure 3.4). As cell viability was similar to that of untreated controls, we used CHX at 100 μM in this study.

The calculated half-life of furin in the un-irradiated HaCaT and Colo 16 cells was 6.0 h and 17.0, respectively. While the calculated half-life of furin in the UVAB-irradiated HaCaT cells was 5.6 h, it was much shorter in UVAB-irradiated Colo 16 cells (8.1 h) (Figures 3.7 and 3.8). This result suggests that furin is turned over more rapidly in HaCaT cells compared to Colo 16 cells and its levels may respond to external stimuli much faster than seen in the SCC cell line. Further studies on this may yield useful information on the effect of UVR on these cellular processes. Secondly, UVR has no

effect on the half-life of furin in HaCaT cells which differed to that seen in Colo 16 cells. It is unclear if UV has an effect on furin turnover, and further experiments would be needed to confirm if this is the case. Of interest is that in a study performed by Yu *et al*. furin levels in A6 (distal nephron cells) were unaffected by CHX treatment (270).

It has been shown that furin processes and activates enzymes such as TACE (151, 156, 158) and MMPs (151, 169, 266, 267). TACE is in turn known to be involved in the processing of TNFα (125, 136-138, 271). While MMPs are elevated when these cells have been exposed to UVB radiation, and their expression is further enhanced if either IL-1α (MMP-9) (217) or TNFα (MMP-2) (216) is present. IL-1α is a major epidermal cytokine that is constitutively synthesized by keratinocytes and released following injurious stimuli like UV-irradiation (236, 237, 272-274). Recently Bashir *et al*. (77) showed that IL-1α synergistically induced TNFα in both UVB-irradiated keratinocytes and fibroblasts. As IL-1α stimulates TNFα release from irradiated cells (77, 275-277), I investigated if this cytokine increased TNFα release from the cells by either increasing the cellular levels of TNFα and/or TACE (Chapter 5) or by enhancing furin levels.

The results showed that IL-1α had a suppressive effect on furin expression in HaCaT and Colo 16 cells but additive effect in HEK cells (Figure 3.9). When IL-1α was added to the UVAB-irradiated cells in the presence of CHX, the half-life of furin protein was similar to that seen with CHX-treated UVAB-irradiated cells. The calculated half-life of furin in HaCaT (Figure 3.10) and Colo 16 cells (Figure 3.11) grown in the presence of IL-1α were calculated to be 4.3 h and 8.3 h, respectively. From the results obtained, it appears that neither UV and/or IL-1α affects the rate of furin turnover in these cells. While the results from HaCaT cells (Figures 3.7 and 3.10) support this suggestion,

results from Colo16 cells (Figures 3.8 and 3.11) do not. The value determined for the un-irradiated controls need to be re-examined to see if these values are correct. If it is, it suggests that UV stimulates the turnover of furin in these cells. The significance of which is not clear and further studies on this process would be warranted.

The effects of various wavelengths of UV on melanocytes and other types of skin cells in culture have been studied, but little is known about gene expression patterns following exposure of human skin to different types of UVR (242). In order to observe if an increase in mRNA induction was associated with increased protein expression, I investigated furin gene expression in these cells using qRT-PCR. qRT-PCR is a highly sensitive and reproducible method and thus was used to analyze mRNA levels of furin in HaCaT and Colo 16 cells following exposure to UVR. Pearton *et al.* (156) observed the mRNA from furin and other PC family members in foreskin epidermis and keratinocyte cell cultures. Skiba *et al*. (136) showed that UVA (2 kJ/m^2) and UVB (2 kJ/m^2)-irradiation caused a significant increase in furin mRNA in HaCaT cells, with higher levels seen for UVB-irradiation.

A time course of the effect of UVB on furin mRNA expression in HaCaT and Colo 16 cell lines was examined (Figure 3.12). Furin mRNA levels were found to be maximal at 24 h in HaCaT cells and 12 h for Colo 16 cells. This differed to results obtained by Skiba *et al*. (136) who showed that peak furin mRNA levels were detected immediately at 0 h (~6 fold) post UVB (2 kJ/m^2) exposure in HaCaT cells. Though the dose of UVB radiation and the primer sequences were was same, the difference in results may be because of the following (i) the different methods (SYBR ® Green ER™ qRT-PCR used in this study compared to the TaqMan™ RT-PCR method used by Skiba *et al*. (136))

and (ii) the different methods of analysis (Pfaffl correction method used in my study compared to the $\Delta\Delta C_T$ method) used in earlier studies.

While little is known about the effect of UVR on furin mRNA, its expression has been seen in cells and tissues. Schalken *et al*. (278) observed a high furin expression in advanced lung tumours, specifically in non-small-cell lung carcinoma (non-SCLCs) but not in SCLCs. Mbikay *et al*. (279) showed that the level of furin mRNA in SCC and adenosarcomas was ~3-fold higher than in SCLCs. Cheng e*t al*. (280) showed that furin mRNA was readily detected by RT-PCR in human breast cancer cells but was undetectable in normal breast tissues. Recently, Spencer *et al*. (281) confirmed furin mRNA expression by RT-PCR in epidermal keratinocytes and melanocytes.

I also investigated the effect other UV types and doses had on furin gene expression 24 h post-irradiation (Figure 3.13). It can be seen that UVB induced maximum furin mRNA levels in both HaCaT and Colo 16 cells compared to that of UVA- and UVAB-irradiation. Of interest is that UVB-irradiation also results in the greater stimulation of furin protein levels in the cells (Figure 3.4). The levels of furin protein are much higher in UV-irradiated HaCaT than in Colo 16 cells. Furin mRNA levels were also higher in HaCaT cells compared to Colo 16 cells. Therefore, these results suggest that following exposure to UVB-irradiation (24 h post exposure), increased furin protein levels may be due to the corresponding increased furin mRNA levels. Although UVR has an effect on furin gene expression, a weak correlation was apparent between furin protein expression and its corresponding mRNA levels in both HaCaT ($r^2 = 0.581$) and Colo 16 ($r^2 = 0.399$) cells 24 h post-irradiation (Figure 3.14).

While it was seen at 24 h that the correlation between furin mRNA and protein levels was weak, it is unknown if there was a stronger correlation at other time points. Therefore, this confirms that increased mRNA induction may be an important determinant in cellular responses to UVR (136). This may closely reflect recent studies by Choi *et al*. (242) who showed that gene expression patterns induced by UVA or UVB are distinct-UVB eliciting dramatic increase in a large number of genes involved in pigmentation as well as in other cellular functions, whereas UVA had little or no effect on these. The expression patterns characterize the distinct responses of the skin to UVA or UVB, and identify several potential previously unidentified factors involved in UV-induced responses of human skin. Paracrine factors expressed by keratinocytes and/or fibroblasts that affect skin pigmentation and other skin inflammatory conditions might be regulated differently by UV, as might their corresponding receptors expressed on melanocytes (242).

In my study, furin mRNA levels were unaffected by CHX (Figure 3.15). This was expected as CHX affects only protein synthesis of furin and not mRNA transcription. Finally the effect of IL-1α on furin mRNA expression was also investigated post UVAB-irradiation (Figure 3.16). UVAB dose was chosen because it induced highest furin protein levels in HaCaT cells (Figure 3.4). The addition of IL-1α slightly reduced these levels in HaCaT and Colo 16 cells (Figure 3.9). IL-1α added to UVAB-irradiated cells increased furin mRNA levels at 16 h (5.7-fold) in HaCaT cells (Figure 3.16) and 4 h (2.6-fold) in Colo 16 cells compared to treated un-irradiated controls. Of interest is that furin mRNA levels in IL-1α treated UVAB-irradiated cells was 10-fold less than that seen in the same irradiated cells (Figure 3.13) which suggests that IL-1α suppresses

furin mRNA expression. Furin mRNA levels in IL-1α treated sham-irradiated cells were reduced by 29% when compared to that of untreated corresponding cells (results not shown). Further studies on the effect of IL-1α on furin mRNA expression needs to be undertaken in order to fully understand the effect it has on this process.

3.3.1 Conclusion

3.3.1.1 Effect of UVR on furin

Furin is a ubiquitously expressed proprotein convertase (PC) that plays a vital role in numerous disease processes including cancer metastasis, bacterial toxin and viral propagation (144, 146, 156, 167, 280, 282). Previous reports have shown that UVR induced furin mRNA expression but its protein expression had not been investigated (136). Skiba *et al*. (136) showed that mRNA alterations of putative genes involved in the UV response pathway were wavelength- and dose-dependent. In this study, we further investigated the effect of UVR on protein expression under different treatment and conditions (UVR and/or IL-1α) and expanded on the mRNA expression of furin in keratinocyte-derived cell lines.

In this study we observed that UVR up-regulates furin mRNA and protein expression in these keratinocyte-derived cells. The half-life of this protein was much longer in Colo 16 cells which suggests that these tumour cells harbor furin protein for much longer which may contribute to increasing its metastatic potential (174). Higher furin levels observed in tumour cells reflect these cell's metastatic potential as one of the proteases they activate, the MMPs, cleave the ECM, allowing metastasis to occur (265). Addition of the pro-inflammatory cytokine, IL-1α had a slightly suppressive effect on furin

protein and mRNA levels in HaCaT and Colo 16 cells. These results suggest that increase in TNFα released from UV-irradiated cells grown in the presence of IL-1α is due to increased transcription of this cytokine (77) and not because of increase in furin protein levels.

Of interest is that apart from UVAB-, UVB-irradiation also results in the greater stimulation of furin protein levels in the cells. The levels of furin protein and mRNA levels are much higher in HaCaT cells than in Colo 16 cells which suggest that following exposure to UVB-irradiation (24 h post exposure), increased furin protein levels may be due to increased furin mRNA levels. In order to achieve complete inhibition of protein/mRNA expression of furin and to see the subsequent effect this may have in the cells, siRNA (small interfering RNA) should be investigated. The ability of siRNA to reduce furin levels in the cell may in turn decrease the activation of TACE which may in turn reduce the release of TNFα. Tellier *et al*. (171) have used siRNAs strategies targeting furin and other genes which resulted in the significant inhibition of the activation of their proposed signalling pathway.

In order to investigate the effect of various treatments on the activity of furin in processing various biological substrates (TACE and/or MMP and other growth factors), the fluorogenic tetrapeptide boc-Arg-Val-Arg-Arg-MCA (Boc-RVRR-MCA) should be used (283-286). These experiments will confirm if changes in activity in the irradiated cells are due to corresponding changes in the levels of furin in the cell or its kinetic parameters.

3.3.1.2 Comparing cell types

There are also differences between the effect of UV types and doses on furin expression in the keratinocyte cell lines examined in this study as shown in Table 3.1.

3.3.1.2.1 HaCaT vs HEK cells

The effect of UVB-irradiation on cell viability was more sensitive on HEK than HaCaT cells. While furin protein levels were much higher in HaCaT cells than in HEK, the effect of IL-1α was slightly suppressive in HaCaT cells and had the opposite effect in HEK cells. In the studies done in this chapter, the response of HaCaT cells to UVR differs to that of HEK which suggests that these immortalized cell lines may not be a suitable model for studying keratinocytes. HEK cells were not available in sufficient quantities and future studies should repeat some of these experiments in order to obtain a better understanding on what is happening to keratinocytes located *in situ* on the skin.

3.3.1.2.2 Colo 16 vs HEK cells

HEK cells exhibit a different profile to that of the Colo 16 cells which is a SCC cell line. The effect of UVB-irradiation on cell viability was most sensitive in the Colo 16 cells than HEK cells. While moderate furin levels were observed in Colo 16 cells, very little was seen in HEK cells. The effect of IL-1α was suppressive on the furin protein levels in Colo 16 cells with the opposite effect seen in HEK cells.

	Experiments	HEK	HaCaT	Colo 16
1	Effect of UVB on cell viability	XX	X	XXX
2	Furin protein expression	X	XXX	XX
3	Furin half-life	-	XX	XXX
4	Effects of IL-1α on furin protein expression	XX	XX	XX
5	Maximal furin mRNA post UVB-irradiation	-	XXX (24 h)	XX (12 h)
6	Furin mRNA expression (UVR)	-	XXX	XX
7	Furin mRNA vs protein levels	-	XX	X

Table 3.1 Effect of UVR on the expression of furin in keratinocyte-derived cells. Effect of the response is represented by X, XX, XXX and (-) where and higher the X, greater the response and (-) represents no response (study not done).

3.3.1.2.3 HaCaT vs Colo 16 cells

The profile of HaCaT cells in response to UVR more closely resembled that of Colo 16 cells than HEK cells. Colo 16 cells were shown to be more sensitive to UVB radiation than were HaCaT cells. While HaCaT cells expressed the highest amounts of furin protein followed by Colo 16 cells, IL-1α had a slight suppressive effect on furin expression in both cell lines. While furin mRNA expression was higher in UVB-irradiated HaCaT and Colo 16 cells (24 h post-exposure), the highest levels were observed in HaCaT cells (24 h) compared to Colo 16 cells (12 h). Addition of IL-1α increased furin mRNA expression in UVAB-irradiated HaCaT cells but caused the opposite effect in Colo 16 cells. Since no significant effect of IL-1α was observed on furin levels, it suggests that this cytokine does not directly act on furin but may do so on either TACE or TNFα of the proposed pathway (Figure 6.1). There was a moderate correlation between furin mRNA and protein levels in Colo 16 cells, but it was stronger in HaCaT cells.

The reason for the similarities between HaCaT and Colo 16 cells could be because HaCaT cells have a defective p53 and as such the direct effects of UVB on DNA and the related cellular repair mechanisms did not result in the cell stopping at the G1 cell cycle checkpoint until this damage had been repaired (287). There is a possibility of the HaCaT cells being a precancerous cell and higher furin levels could have occurred as part of the immortalization of these cells. With regard to the tested parameters in this study, the profile of the HaCaT cells, which are themselves non-cancerous, can potentially lead to malignant skin cancers such as SCC as in case of solar keratosis. The profile of the Colo 16 cells suggests that differences in furin protein and/or mRNA are a

result of tumorigenesis. By drawing a comparison of the effect of UVR on the expression and/or activity of furin in different SCC cell lines (HNSCC) to that of HEK cells would help in determining the cell's metastatic nature and invasiveness since furin is ubiquitously distributed in cells (144, 288). Subsequent studies on MMPs (Chapter 4) and TACE and/or TNFα (Chapter 5) will look further on the role of furin in the cells.

Chapter Four:

Effect of UVR on furin activation of MMPs in human keratinocyte cell lines

4.1 Introduction

Furin is a PC localized to the constitutive secretory pathway (144, 226) and is ubiquitously distributed in cells (144, 288). It is activated through phosphorylation of basic amino acid sites (144, 288) and has been shown to activate a range of enzymes, including MMPs from their respective preproforms (167, 168, 175, 288). MMPs are important in tumour progression, promoting invasion and immune escape (187). They are involved in modifying matrix structure, growth factor availability and the function of cell surface signalling systems, with consequent effects on cellular differentiation and apoptosis (187). They play central roles in morphogenesis, wound healing, tissue repair and remodeling in response to injury and in the progression of cancer (187). The increasing diversity in both substrates and functions of MMPs makes these enzymes central regulators in the complex tumour ecosystem composed of cancer cells and their microenvironment (188).

Analogous to most pro-proteins, direct proteolysis is considered to be the principal way that proMMPs are activated (289). About one-third of MMPs-including all membrane-bound MMPs-contain an RXXR or RRKR sequence between the pro- and catalytic domains, which serves as a target sequence for PCs or furin (289). The discovery of MMPs as a significant group of cancer-associated PC substrates highlight the key role played by PCs in cancer development and progression (168). In these processes, the degradation of basement membrane is the critical event (290). The basement membrane is essentially composed of type IV collagen, which is the molecule that gelatinases (MMP-2 and -9) preferentially degrade (290).

MMP-2 is associated closely with organ growth, endometrial cycling, wound healing, bone remodeling, tumour invasion and metastasis (291). Recently, membrane type MT1-MMP was identified as a potential physiological activator of MMP-2 (218). Like all other MMPs, MT1-MMP possesses a pro-domain which must be removed for the enzyme to acquire its catalytic potential. The presence of a typical recognition motif (RXKR) for the furin-like convertases at the end of its pro-domain suggests a potential role for these proteinases in MT1-MMP processing (218). This concept was supported by Sato *et al*. (292), who demonstrated that, recombinant MT1-MMP was efficiently cleaved *in vitro* by purified soluble furin.

Bassi *et al*. (168) showed that MMP-2 and furin are expressed in different cell types, that is, stromal and epithelial, respectively, and that the interaction between them, one secreting the proMMP, and the other cell type providing the machinery to activate this proMMP, results in enhanced cell invasiveness (168). In order to evaluate the implication of furin in pro MT1-MMP processing, Maquoi *et al*. (175) treated HT1080 cells with a synthetic furin inhibitor (Dec RVKR cmk) and monitored their ability to activate proMMP-2 as well as their invasive potential. Dec RVKR cmk decreased proMT1-MMP processing as well as proMMP-2 activation and cell invasiveness and provided evidence that furin is a key factor in the maturation of MMPs associated with the invasive and metastatic potential of tumour cells (175).

Bassi *et al*. (268) showed that the addition of Dec RVKR cmk to furin-over expressing SCC cells resulted in an inhibition of furin-mediated MT1-MMP processing. Reduced MT-MMPs processing resulted in reduced invasion *in vitro* and *in vivo* (172, 173, 268,

293). Cao *et al*. (294) showed that in co-transfection systems, furin cleaved MMP-2 in the TGN, generating an inactive metalloprotease. Recently, Koo *et al*. (295) demonstrated MT1-MMP-independent propeptide processing of MMP-2 in HEK293F and various tumour cell lines, and showed that PCs such as furin can mediate the processing of MMP-2 intracellularly. It has been shown that MMPs with a furin cleavage site are processed intracellularly before secretion (6, 218, 296-298). This suggests that PC-mediated processing may be a major mechanism for the activation of proMMP-2 in PC-overexpressing cells (e.g. tumour cell lines), whereas, PCs are likely to act alongside MT-MMPs for proMMP-2 activation in cells expressing high levels of MT-MMPs (295).

Compared to MMP-2, the physiological activation mechanism of MMP-9 is not clear. MMP-9 (179, 200, 201), has been reported to play an important role in the pathophysiologies of many skin conditions, including tumour invasion and metastasis (179, 181, 202), wound healing (203, 204), and angiogenesis (201, 205). ProMMP-9 is expressed shortly after cutaneous trauma, and its concentration declines with the progression of healing (217, 299). MMP-9 is almost always associated with inflammatory conditions (217). Proteolytic activation of proMMP-9, is an irreversible process and, is mediated through cleavage of the prodomain, which leads to the dissociation of the cysteine in the N-terminal domain from the Zn atom, a process called the “cysteine-switch” (300). Active MMP-9, has been found in many types of metastatic cancers in humans (301). Watanabe *et al*. (290) produced active MMPs directly from cells by inserting a furin-recognition sequence in the prodomain. This activation mechanism was later applied to MMP-9 and these results showed that transfection of

this mutant gene into cultured CHO-K1 mammalian cells resulted in the direct production of active MMP-9 *in vitro* and *in vivo* (290). These results suggested that as furin is distributed nearly in all tissues (278), active MMP-9 can be produced from almost all cells in the body (290). Moreover, Han *et al*. (217) recently showed that the proteolytic activation of pro-MMP-9 in skin inflammatory diseases occurs via a pathway including IL-1α.

Therefore, furin or other PCs are likely to be the physiological activators of this group of metalloproteases. Recent studies using PC inhibitors have demonstrated that increased furin expression is associated with enhancement of metastatic spread and tumour cell proliferation (144, 227), probably as a result of the activation of MMP involved in ECM degradation (169, 266). Exposure to UVR has been shown to elevate MMP activity in human skin cells (214). This suggests that sunlight is a major factor in photoageing (167, 175),(89, 302). In the epidermis, Fisher *et al*. (80, 303) recently reported the induction of MMP-9 mRNA after UVB-irradiation of human skin *in vivo*. Onoue *et al*. (179) has suggested that MMP-9 secreted from keratinocytes after UVB-irradiation might result from apoptotic events. The role played by MMP-9 in the apoptotic pathway induced by UVB-irradiation is unclear. Steinbrenner *et al*. (209) investigated the effect of UVA-irradiation on the expression and secretion of MMP-2 and -9, in NHEK cells *in vitro*. They found that UVA-irradiation decreased the steady-state mRNA levels of both MMPs in a dose-dependent manner and reduced the gelatinolytic activity of both enzymes in cell culture supernatants. However, the specific roles of the gelatinases, including their expression patterns following UVR is not known (179).

4.1.1 Aim and hypothesis

Furin has been shown to play a role in the activation of the gelatinases, MMP-2 and -9 (177). Thus, we wish to investigate the role furin plays in the maturation and activation of these gelatinases in skin cells in response to UVR. The aim of this study was to determine if changes in the activity and expression of MMP-2 and-9 in cells exposed to UV-irradiation were related to changes in furin activity and/or expression. In order to understand the effects of UVR on different keratinocyte-derived cell lines; HEK, HaCaT and Colo16 cells were examined. It is unknown what effects tumorigenesis has on the MMPs. Colo16 cells were chosen to investigate what effect tumorigenesis have on the cellular response to UV exposure in keratinocytes.

4.2 Results

4.2.1 MMP-2 and MMP-9 protein activity and expression

4.2.1.1 Protein activity

The effect of UVR on the enzymatic activity of MMP-2 and -9 in keratinocyte-derived cell lines (HEK, HaCaT and Colo 16 cells) was investigated. In order to quantify changes in MMP activity, gelatin zymography (see section 2.7) was performed. In all the cell lines examined, two forms of MMP were detected, MMP-2 (72 kD) and MMP-9 (92 kD).

An aliquot (50 µl) of microconcentrated conditioned media (Section 2.7.2) was added to each lane in the zymograph. From the resultant image, fluorescent quantification of the bands was made using the Quantity one image analysis software. The level of cell protein in culture plates has been measured to determine the activity of these

gelatinases. The level of enzyme activity was expressed as au/mg cell protein where au represents the quantification of the bands found on the zymograph. A representative zymograph of the effect of UVB on MMP activity in HEK cells at different time points is shown in (Figure 4.1).

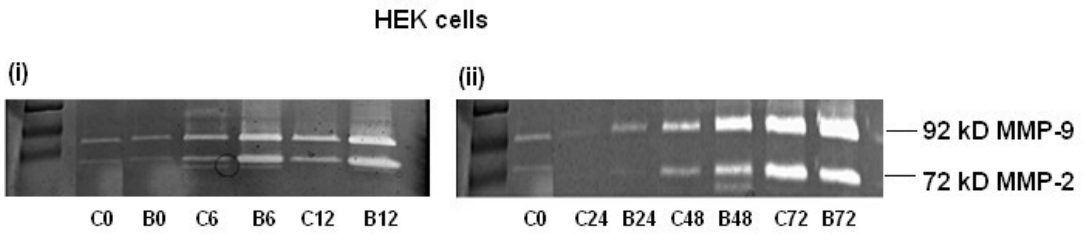

Figure 4.1 A representative zymograph showing the effect of UVB-irradiation on gelatinolytic activity of MMP-2 and -9 in conditioned media of HEK cells collected at 0, 6, 12 h (i) and 0, 24, 48 and 72 h (ii) after UVB-irradiation. In each lane, 50 µl of microconcentrated conditioned media was added. Samples represent sham-irradiated cells or controls (C) and UVB-irradiated cells (B).

In HEK cells, 9.0 au/mg cell protein of MMP-2 was secreted from sham-irradiated control cells at 0 h. Significant ($p<0.05$) levels of MMP-2 activity was released from these control cells between 6-72 h with highest activity seen at 72 h (2285.5 au/mg cell protein), which was a 252.8-fold increase when compared to that at 0 h (Figure 4.2i). However, when these cells were exposed to UVA, MMP-2 levels remained at low levels except for a slight increase seen at 72 h (1069.9 au/mg cell protein). It should be

noted that while this was higher than that seen at UVA-irradiated cells at 0 h, it was less than that observed in the untreated controls at 72 h. UVA-irradiation caused a dose-dependent decrease of MMP-2 gelatinolytic activity over the 72 h time period. There was a biphasic induction of MMP-2 activity following UVB radiation. MMP-2 was released in significant ($p<0.05$) amounts between 0-24 h with maximal release observed at 6 (2842.7 au/mg cell protein) and 12 h (13489.9 au/mg cell protein). UVAB-irradiation of the HEK cells also induced significantly increased activity of MMP-2 at 6, 48 and 72 h but in general this was less than that seen for UVB. Total MMP-2 released was 2866.4, 2596.5 and 4031.3 au/mg cell protein at 6, 48 and 72 h, respectively. In general, UVB-induced maximum MMP-2 activity into the conditioned cultured media of HEK cells.

In HEK cells, 561.2 au/mg cell protein of MMP-9 was secreted from sham-irradiated control cells at 0 h. Significant ($p<0.05$) levels of MMP-9 activity was released from these control cells between 6-72 h with highest activity at 72 h (3522.1 au/mg cell protein) which was a 6.2-fold increase when compared to that at 0 h (Figure 4.2ii). However, when these cells were exposed to UVA, MMP-9 levels were released at low levels except for a slight increase seen at 12 h (1798.2 au/mg cell protein). As with that seen for MMP-2 activity, UVA-irradiation caused a reduction in the level of MMP-9 activity released from the cells compared to the un-irradiated controls at the same time points. There was a biphasic induction of MMP-9 activity following UVB radiation. MMP-9 was released in significant ($p<0.05$) amounts between 0-24 h with maximal release occurring at 12 h (15392.0 au/mg cell protein). Relatively similar levels of

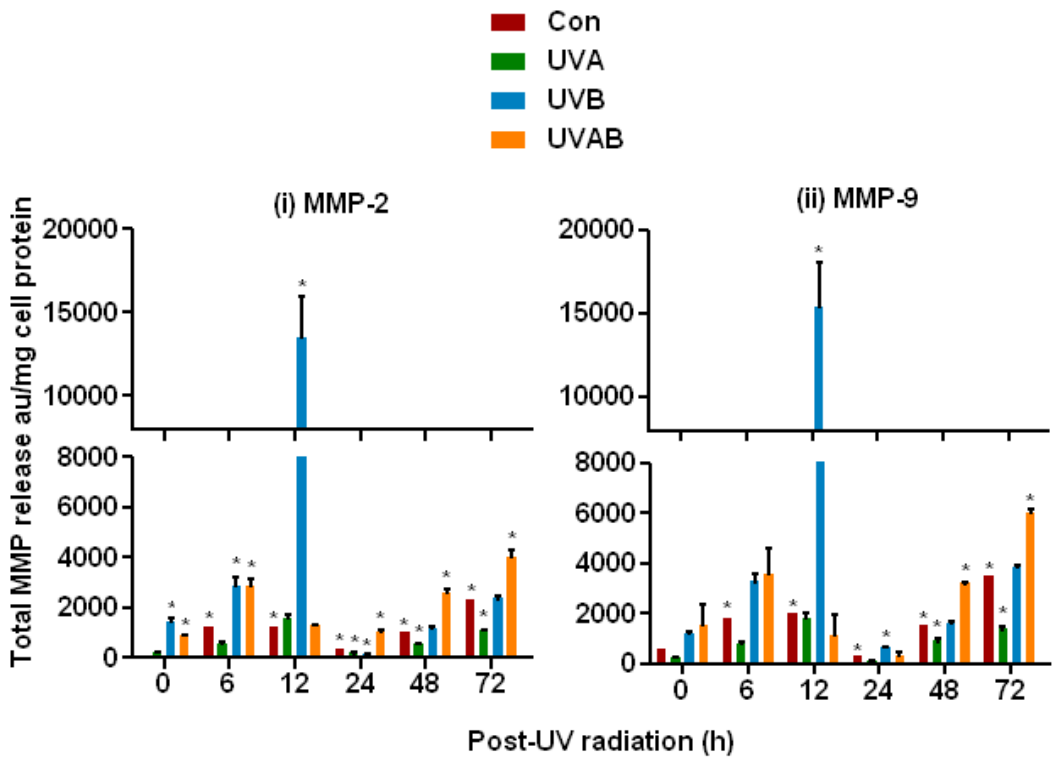

Figure 4.2 A time course of the effect of UVR on the activity of MMP-2 (i) and MMP-9 (ii) secreted from HEK cells. The cells were exposed to sham-irradiation or controls (Con), UVA-irradiation (A), UVB-irradiation (B) and UVAB-irradiation (UVAB). The media samples were collected 0, 6, 12, 24, 28 and 72 h post-irradiation. Results expressed are the mean ± SEM of three separate experiments. Statistical significance of the effect of UVR on MMP protein activity is represented as $p<0.05$ (*).

MMP-9 activity was observed at 6 and 72 h (~3500 au/mg cell protein). UVAB-irradiation of the HEK cells also induced significantly increased activity of MMP-9 at 6, 48 and 72 h but in general was less than that seen for UVB. Total MMP-9 released was 3585.0, 3197.1 and 5999.8 au/mg cell protein at 6, 48 and 72 h, respectively. In general, UVB-irradiation induced maximum MMP-9 activity into the conditioned cultured media of HEK cells.

In HaCaT cells, 49.0 au/mg cell protein of MMP-2 was secreted from sham-irradiated control cells at 0 h. Significant ($p<0.05$) levels of MMP-2 activity was released from these control cells between 6-72 h with highest activity at 48 h (313.0 au/mg cell protein) which was a 6.4-fold increase when compared to that at 0 h (Figure 4.3i). The secretion of MMP-2 activity in response to UVA-irradiation remained low over the 72 h time period with a significant ($p<0.05$) increase seen at 6 h (287.5 au/mg cell protein). Minimal MMP-2 secretion was observed in response to UVB-irradiation with the highest increase seen at 48 h (203.9 au/mg cell protein). UVAB-irradiation induced maximal activity of MMP-2 at 72 h (378.9 au/mg cell protein).

In HaCaT cells, 172.8 au/mg cell protein of MMP-9 was secreted from sham-irradiated control cells at 0 h. Significant ($p<0.05$) levels of MMP-9 activity was released from these control cells between 6-72 h with highest activity at 12 h (200.0 au/mg cell protein) which was a 1.2-fold increase when compared to that at 0 h (Figure 4.3ii). The secretion of MMP-9 activity in response to UVA-irradiation remained low over the 72 h time period with a significant ($p<0.05$) increase seen at 6 h (467.5 au/mg cell protein).

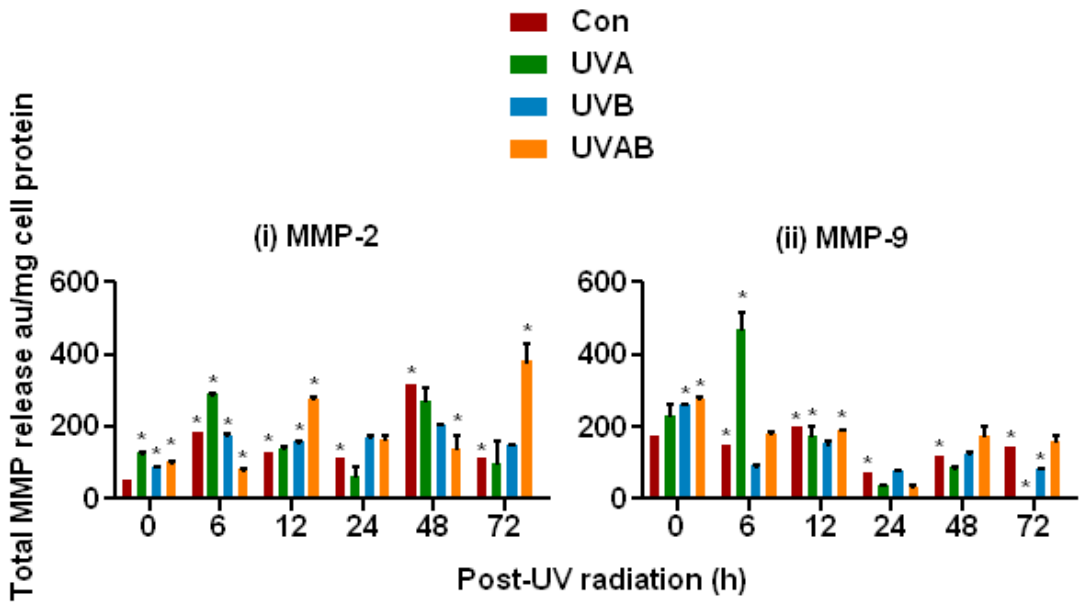

Figure 4.3 Time course of the effect of UVR on the activity of MMP-2 (i) and MMP-9 (ii) secreted from HaCaT cells. The cells were exposed to sham-irradiation or controls (Con), UVA-irradiation (A), UVB-irradiation (B) and UVAB-irradiation (UVAB). The media samples were collected 0, 6, 12, 24, 28 and 72 h post-irradiation. Results expressed are the mean ± SEM of three separate experiments. Statistical significance of the effect of UVR on MMP protein activity is represented as $p<0.05$ (*).

Minimal MMP-9 secretion was observed in response to UVB- and UVAB-irradiation with the highest increase observed immediately after sham-irradiation at 0 h (260.4 and 277.9 au/mg cell protein, respectively). In general, the level of MMP-2 and 9 shed from the cells was relatively low in the 72 h period following exposure to UV-irradiation compared to that from HEK cells.

In Colo 16 cells, MMP-2 activity was relatively constant throughout the time course tested with 11.7 au/mg cell protein of MMP-2 secreted from sham-irradiated control cells at 0 h (Figure 4.4i). Significant ($p<0.05$) levels of MMP-2 activity was released from these control cells between 6-72 h with highest activity at 48 h (101.1 au/mg cell protein) which was a 8.6-fold increase when compared to that at 0 h. Minimal MMP-2 activity was released when the cells were exposed to UVA-irradiation as no significant differences in MMP levels between time points were detected. There was a biphasic induction of MMP-2 activity following exposure to UVB-irradiation with significant activity observed at 24 h (1998.1 au/mg cell protein). UVAB-irradiation of the Colo 16 cells also induced a slight increase (not statistically significant) in the activity of MMP-2 at 24 h (567.7 au/mg cell protein) but in general this was less than that seen for UVB.

In Colo 16 cells, 59.4 au/mg cell protein of MMP-9 was secreted from sham-irradiated control cells at 0 h (Figure 4.4ii). Highest levels of MMP-9 activity was released from control cells at 24 h (355.5 au/mg cell protein) which was a 5.9-fold increase to that seen at 0 h. Minimal MMP-9 activity was released from the cell when they were exposed to UVA-irradiation as no significant differences in MMP levels

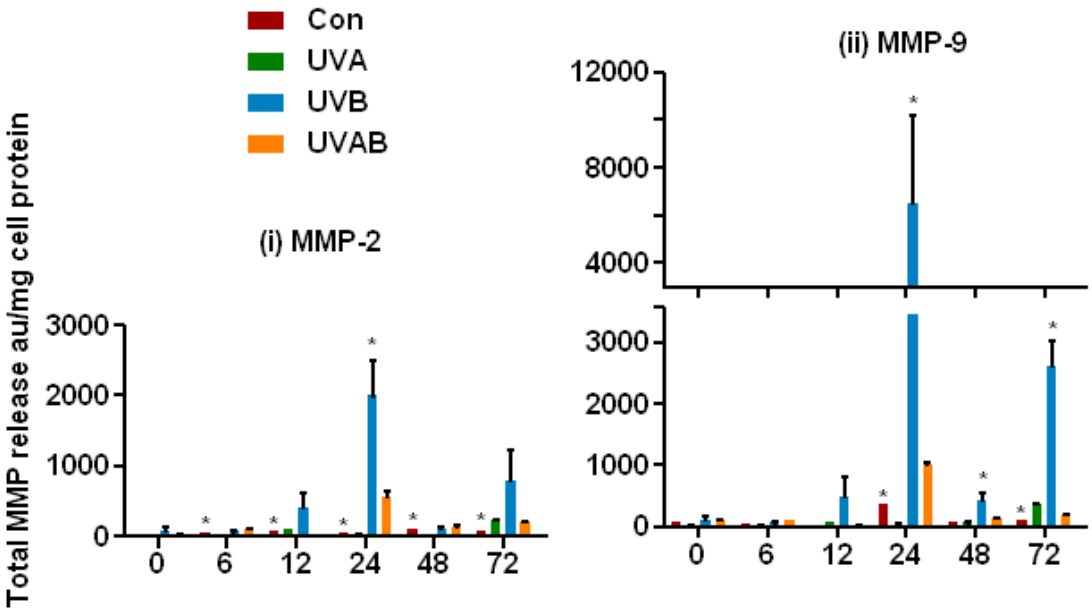

Figure 4.4 Time course of the effect of UVR on the activity of MMP-2 (i) and MMP-9 (ii) secreted from Colo 16 cells. The cells were exposed to sham-irradiation or controls (Con), UVA-irradiation (A), UVB-irradiation (B) and UVAB-irradiation (UVAB). The media samples were collected 0, 6, 12, 24, 28 and 72 h post-irradiation. Results expressed are the mean ± SEM of three separate experiments. Statistical significance of the effect of UVR on MMP protein activity is represented as $p<0.05$ (*).

between time points were detected. There was a biphasic induction of MMP-9 activity following exposure to UVB-irradiation with significant activity observed at 24 h and 72 h (6512.8 and 2605.9 au/mg cell protein, respectively). UVAB-irradiation of the Colo 16 cells slightly increased in the release of MMP-9 at 24 (1005.6 au/mg cell protein) from the cells but in general it was less than that seen for UVB.

In conclusion, these results suggest that MMP-2 and -9 secretion was not stimulated by UVA-irradiation in these keratinocyte-derived cell lines. On the other hand, UVB-irradiation resulted in enhanced secretion of MMP-2 and -9 from these cells. UVAB-irradiation also caused the cells to release high levels of gelatinolytic activity, but this was less compared to that seen following UVB-irradiation. In general, effect of UV-irradiation on the release of MMP activity was similar in HEK and Colo 16 cells unlike that seen in HaCaT cells.

4.2.1.2 Cellular expression of MMP protein

4.2.1.2.1 Effects of UVR on MMP-2 protein expression

The effect of UVR on the cellular expression of MMP-2 in HaCaT and Colo 16 cells was determined. In order to quantify changes in the MMP-2 levels in the cells, western blots (Section 2.5) of cell lysates were run and probed with a rabbit anti-MMP-2 antibody. In the cell lines examined, two forms of MMP-2 were detected, proMMP-2 (72 kD) and active MMP-2 (64 kD). A representative blot of the effect of UVR on cellular MMP-2 levels is seen in Figure 4.5. In these blots, 50 µg cell lysates was added per lane and β-actin was used to monitor the amount of protein added per lane.

From the resultant image, fluorescent quantification of the bands was made using the Quantity one image analysis software. The amount of MMP-2 in control (un-irradiated) cells was given a value of 100 (pro form + active form) and from that, the changes in proMMP-2 and active MMP-2 levels could be calculated in the irradiated samples, and these were expressed as a percentage of that found in control cells.

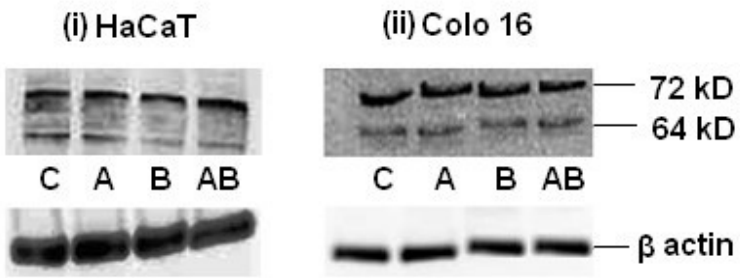

Figure 4.5 Representative western blots to show the effect of UVR on the expression of proMMP-2 and active MMP-2 in HaCaT (i) and Colo 16 cells (ii). The cells were exposed to sham-irradiation or controls (C), UVA (A), UVB (B) and UVAB (AB) radiation and after 24 h, 50 μg of cell lysates were run on western blots. β-actin was used as a loading control.

In HaCaT cells, the majority of MMP-2 found in un-irradiated cells was in the proform (64%). The expression of proMMP-2 was significantly ($p<0.05$) lower in UVA-irradiated cells (48%), while those in UVB- (63.2%) and UVAB-irradiated cells

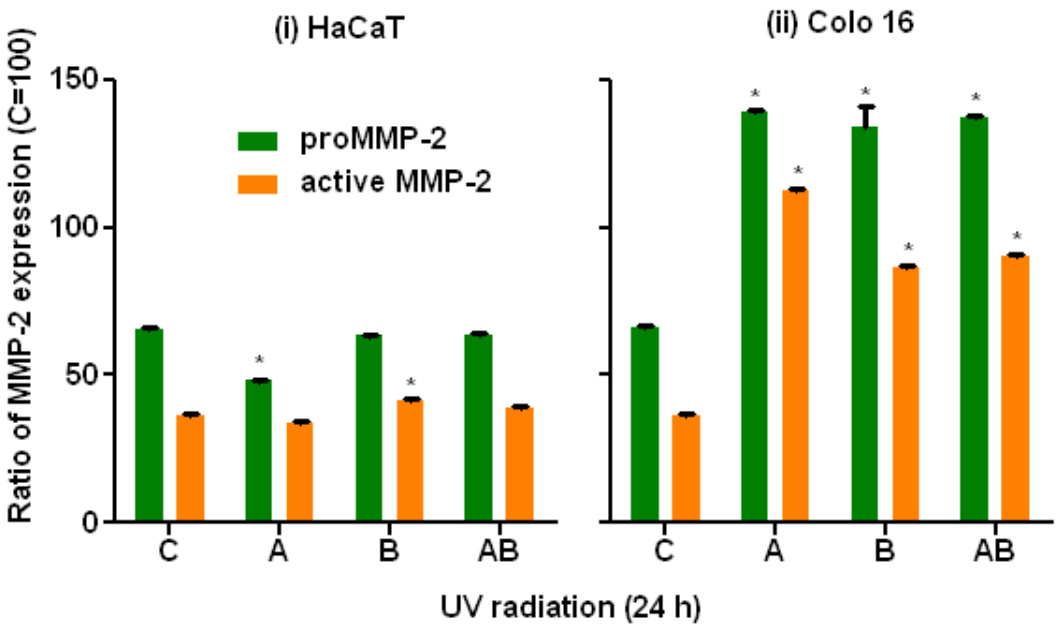

Figure 4.6 Effect of UVR on the expression of proMMP-2 and active MMP-2 in HaCaT (i) and Colo 16 cells (ii). Cells were exposed to sham-irradiation or controls (C), UVA (A), UVB (B) and UVAB (AB) radiation and cellular proteins were extracted 24 h post-irradiation. Results expressed are the mean ± SEM for three separate experiments. Statistical significance of the effect of UVR on the expression of MMP-2 levels was shown as $p<0.05$ (*).

(63.5%) were similar to that of sham-irradiated controls (Figure 4.6i). Active MMP-2 expression in UVA- (34%) and UVAB-irradiated cells (39%) were similar to that of sham-irradiated controls (36%) but was higher in UVB-irradiated cells (41.3%). The level of total MMP-2 (proMMP-2 and active MMP-2) was 20% lower in UVA-irradiated cells while those in UVB- and UVAB-irradiated cells were similar to that seen in un-irradiated controls. In general MMP-2 levels in HaCaT cells did not change when the cells were exposed to UVR.

In un-irradiated Colo 16 cells, most of the MMP-2 (64%) was in the proform (Figure 4.6ii). However, when the cells were exposed to UVR, the levels of both pro and active MMP-2 were higher than that seen in sham-irradiated cells. This was different to that seen in HaCaT cells. The highest induction of proMMP-2 protein was seen in UVA-irradiated cells (139.3%) while significant increases in UVB- and UVAB-irradiated cells (~135%) were also observed when compared to the un-irradiated controls. Active MMP-2 expression was highest in UVA-irradiated cells (112.3%), while that in UVB- (86.3%) and UVAB-irradiated cells (90%) were also much higher than that seen in the sham-irradiated controls. The expression of total MMP-2 levels increased to 2.5-fold in UVA-irradiated cells, they were also elevated (2.2-fold) in both the UVB- and UVAB-irradiated cells compared to that observed in sham-irradiated cells.

In conclusion, proMMP-2 expression was higher than that of the active form in both cell lines. UVR induced higher proMMP-2 and active MMP-2 levels in Colo 16 cells compared to that seen in HaCaT cells, where reduced levels were observed.

4.2.1.2.2 Effect of UVR on MMP-9 protein expression

The effect of UVR on the cellular expression of MMP-9 in HaCaT and Colo 16 cells was determined. In order to quantify changes in the MMP-9 levels in the cells, western blots (Section 2.5) of cell lysates were run and probed with an anti-MMP-9 antibody. In the cell lines examined, two forms of MMP-9 were detected, proMMP-9 (92 kD) and active MMP-9 (82 kD). A representative blot of the effect of UVR on cellular MMP-9 levels is seen in Figure 4.7. In these blots, 50 μg cell lysates was added per lane and β-actin was used to monitor the amount of protein added per lane. The level of protein in each sample was compared to that in un-irradiated controls (pro and active MMP-9 = 100%) and is expressed as a percentage of that found in the un-irradiated controls (Figure 4.8).

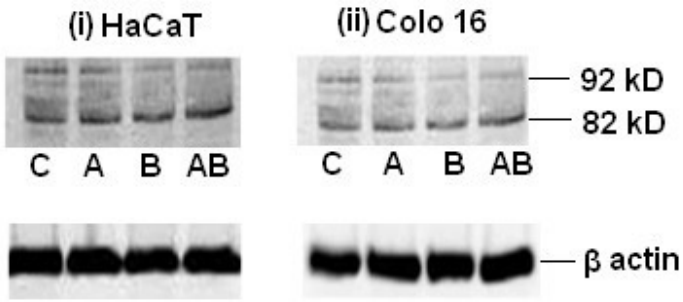

Figure 4.7 Representative western blots to show the effect of UVR on the expression of proMMP-9 and active MMP-9 in HaCaT (i) and Colo 16 cells (ii). The cells were exposed to sham-irradiation or controls (C), UVA (A), UVB (B) and UVAB (AB) radiation and after 24 h, 50 μg of cell lysates were run on western blots. β-actin was used as a loading control.

In HaCaT cells, MMP-9 is predominantly found in the active form (71%) in the un-irradiated controls (Figure 4.8i). The expression of proMMP-9 increased in response to UVR when compared to sham-irradiated controls. The greatest increases of proMMP-9 expression were observed in UVB- (36%) and UVAB-irradiated cells (48%). While active MMP-9 levels were high in response to UVA- (80%) and UVAB-irradiation (121%), a reduction was seen following exposure to UVB-irradiation (60%). While there were no changes observed in the expression of total MMP-9 (proMMP-9 and active MMP-9) levels in UVA- and UVB-irradiated cells, they were increased 1.7-fold in UVAB-irradiated cells.

In un-irradiated Colo 16 cells, the majority of the MMP-9 was in the proform (56%) unlike that seen in HaCaT cells (Figure 4.8ii). Lower levels of MMP-9 protein were seen in UVA-irradiated cells (41%) compared to the sham-irradiated controls while higher levels were observed in both the UVB- and UVAB-irradiated cells (67%). The level of active MMP-9 expression in the UVA-irradiated cells (44%) was similar to sham-irradiated controls. Higher levels of active MMP-9 were seen in UVB- (51.2%) and UVAB-irradiated cells (49%). While total MMP-9 levels decreased in UVA-irradiated cells (20%) when compared to sham-irradiated controls, overall the MMP-9 levels slowly elevated in UVB- and UVAB-irradiated cells. In conclusion active MMP-9 was the predominant form observed in HaCaT cells while in Colo 16 cells, it was the proform.

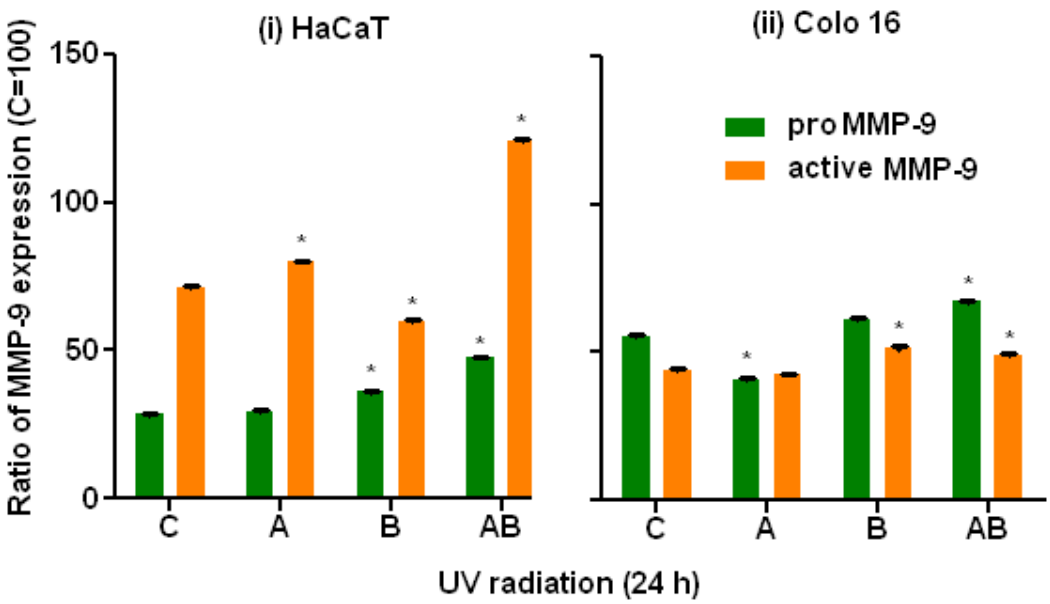

Figure 4.8 Effect of UVR on the expression of proMMP-9 and active MMP-9 in HaCaT (i) and Colo 16 cells (ii). Cells were exposed to sham-irradiation or controls (C), UVA (A), UVB (B) and UVAB (AB) radiation and cellular proteins were extracted 24 h post-irradiation. Results expressed are the mean ± SEM for three separate experiments. Statistical significance of the effect of UVR on the expression of MMP-9 levels was shown as $p<0.05$ (*).

4.2.1.3 IL-1α effects

IL-1α is seen in increased levels in skin inflammatory conditions (217). Although the proteolytic activation of pro MMP-9 has been documented in many pathologic conditions, the cellular factors that control this process have not been identified. Han *et al*. (217) recently showed that the proteolytic activation of proMMP-9 in skin inflammatory diseases likely occurs via a pathway including IL-1α. Therefore in this study, effect of IL-1α on MMP-2 and-9 activity in UV-irradiated HaCaT and Colo 16 cells was determined using gelatin zymography (Section 2.7).

4.2.1.3.1 MMP protein activity

In all the cell lines examined, two forms of MMP were detected, MMP-2 (72 kD) and MMP-9 (92 kD). The level (50 µl) of microconcentrated conditioned media (Section 2.7.2) added to each lane in the zymogen was similar. The level of cell protein in cultures has been measured in order to express the MMP activity per mg culture protein. A representative zymograph for HEK cells in IL-1α treated UV-irradiated cells are shown in Figure 4.9.

In HEK cells, the level of MMP-2 activity released from the sham-irradiated cells was 321.1 au/mg cell protein. Following the addition of IL-1α, the level of activity released from the cell increased to 765.4 au/mg cell protein (Figure 4.10i). Similar results were also seen in the UVA- and UVB-irradiated HEK cells treated with IL-1α compared to the corresponding untreated irradiated cells (179.2, 133.2 and 1015.0 au/mg cell protein of MMP-2 was released in UVA-, UVB- and UVAB-irradiated cells, respectively). On

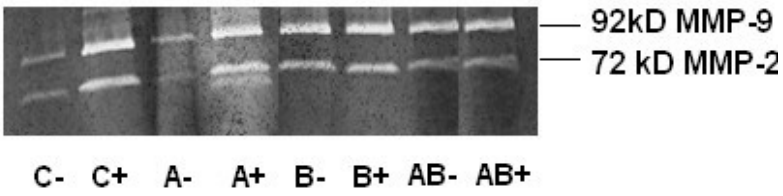

Figure 4.9 A representative zymograph showing the effect of IL-1α on the gelatinolytic activity of MMP-2 and MMP-9 in conditioned media of UV-irradiated HEK cells collected 24 h post UV-irradiation. In each lane, 50 µl of microconcentrated conditioned media was added. The cells were exposed to sham-irradiation or controls (C), UVA (A), UVB (B) and UVAB (AB) radiation in the presence (+) or absence (-) of IL-1α.

the addition of IL-1α, maximal increase was observed in UVA-irradiated cells (1023.3 au/mg cell protein), followed by UVB-irradiated cells (700.0 au/mg cell protein). On the other hand, MMP-2 levels released from the cell decreased by 94% in UVAB-irradiated cells in the presence of IL-1α.

A similar finding was observed for MMP-9 activity. The addition of IL-1α to these cells saw an increase in activity from 277.1 au/mg cell protein to 1084.7 au/mg cell protein (Figure 4.10i). Following the addition of IL-1α, there was a significant increase of MMP-9 activity in UV-irradiated cells compared to their corresponding untreated irradiated cells (87.8, 623.3 and 311.3 au/mg cell protein of MMP-9 were released in UVA-, UVB- and UVAB-irradiated cells, respectively).

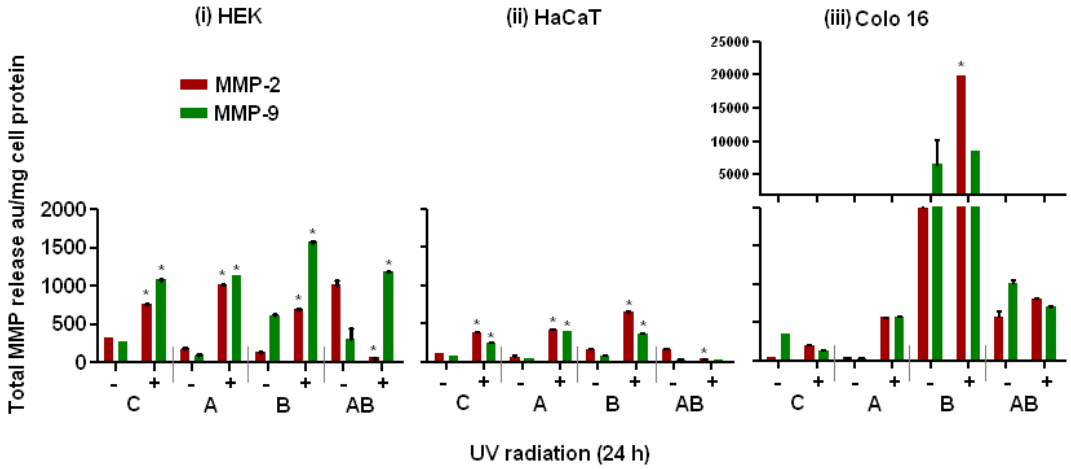

Figure 4.10 The effect of IL-1α on the activity of MMP-2 and -9 secreted in 24 h post-irradiated conditioned media of HEK (i), HaCaT (ii) and Colo 16 cells (iii). Cells were exposed to sham-irradiation or controls (C), UVA (A), UVB (B) and UVAB (AB) radiation in the presence (+) or absence (-) of IL-1α. Results expressed are the mean ± SEM for three separate experiments. Statistical significance of the effect of IL-1α on the activity of MMP-2 and-9 was shown as $p<0.05$ (*).

On the addition of IL-1α, maximal increase was seen in UVB-irradiated cells (1576.0 au/mg cell protein), followed by UVAB-irradiated cells (1198.4 au/mg cell protein). UVA-irradiation in the presence of IL-1α induced the least level of MMP-9 (1148.5 au/mg cell protein) activity.

In general, IL-1α added to UV-irradiated HEK cells resulted in an increase in MMP activity compared to that seen for UV-irradiated cells except for MMP-2 levels in UVAB-irradiated cells where the opposite effect was seen.

In HaCaT cells, the addition of IL-1α to sham-irradiated controls resulted in an increase in the level MMP-2 activity released from the cell from 111.0 au/mg cell protein to 387.5 au/mg cell protein (Figure 4.10ii). Following the addition of IL-1α, there was a significant ($p<0.05$) increase of MMP-2 activity released from UV-irradiated cells compared to their corresponding irradiated untreated cells (60.5, 168.6 and 162.5 au/mg cell protein of MMP-2 were released in UVA-, UVB- and UVAB-irradiated cells, respectively). On the addition of IL-1α, maximal increase was seen in UVB-irradiated cells (646.7 au/mg cell protein), followed by UVA-irradiated cells (421.7 au/mg cell protein). On the other hand the levels of MMP-2 released from the UVAB-irradiated cells decreased by 79% in the presence of IL-1α.

The addition of IL-1α to the sham-irradiated cells saw an increase in the level of MMP-9 activity released from the cell from 72.4 au/mg cell protein to 243.6 au/mg cell protein (Figure 4.10ii). Similar results were also seen in the UVA- and UVB-irradiated HaCaT cells treated with IL-1α compared to the corresponding untreated irradiated cells (35.7, 77.0 and 30.3 au/mg cell protein of MMP-9 were released in UVA-, UVB- and

UVAB-irradiated cells, respectively). On the addition of IL-1α, maximal increase in its release was observed in UVA-irradiated cells (391.2 au/mg cell protein), followed by UVB-irradiated cells (359.3 au/mg cell protein). On the other hand the release of MMP-9 fell by 1.3% in UVAB-irradiated cells in the presence of IL-1α.

In general, IL-1α added to UV-irradiated HaCaT cells resulted in an increase in MMP activity compared to that seen for UV-irradiated cells except in UVAB-irradiated cells where the opposite effect was seen.

In Colo 16 cells, the level of MMP-2 activity released from sham-irradiated controls was 43.7 au/mg cell protein. Following the addition of IL-1α, this increased to 191.9 au/mg cell protein (Figure 4.10iii). Following the addition of IL-1α, there was a significant ($p<0.05$) increase of MMP-2 activity released from UV-irradiated cells compared to their corresponding untreated irradiated cells (34.2, 1998.1 and 567.7 au/mg cell protein of MMP-2 were released in UVA-, UVB- and UVAB-irradiated cells, respectively). On the addition of IL-1α, maximal increase was observed in the level of MMP-2 released from UVB-irradiated cells (19864.2 au/mg cell protein), followed by UVAB-irradiated cells (810.7 au/mg cell protein), while the least was seen in the UVA-irradiated cells (559.3 au/mg cell protein).

The addition of IL-1α to the sham-irradiated cells saw a 65% decrease in MMP-9 activity (Figure 4.10iii). This differed to what was observed in HEK and HaCaT cells (28.7, 6512.8 and 1005.6 au/mg cell protein of MMP-9 were released in UVA-, UVB- and UVAB-irradiated cells, respectively). While maximal increase was induced by UVB-irradiation in the presence of IL-1α (8589.2 au/mg cell protein)

followed by UVAB-irradiation in the presence of IL-1α (697.3 au/mg cell protein), while the least induction was seen in UVA-irradiated cells (574.1 au/mg cell protein).

In general, the addition of IL-1α to UV-irradiated Colo 16 cells saw an increase in MMP-2 activity. MMP-9 activity was high in UVA- and UVB-irradiated cells in the presence of IL-1α except in UVAB-irradiated cells where the opposite effect was seen.

In conclusion, these results show that IL-1α increased MMP-2 and -9 activity in the UVA- and UVB-irradiated cell lines (HEK, HaCaT and Colo 16). Variation in MMP levels was observed in UVAB-irradiated cells in the presence of IL-1α (MMP-2 activity decreased in HEK cells, MMP-2 and -9 activity decreased in HaCaT cells and MMP-9 activity decreased in Colo 16 cells). The reason for this variation is not clear.

4.2.1.3.2 Cellular expression of MMP protein

In this study, the effect of IL-1α on the expression of MMP-2 and -9 in UV-irradiated HaCaT and Colo 16 cells were determined using western blots (Section 2.5). In the blots, 50 μg of cell lysates was added per lane, the pro (72 and 92 kD) and active (64 and 82 kD) forms of MMP-2 and -9 protein levels were quantified, respectively. β-actin was used to quantify the amount added per lane. The level of protein in each sample was compared to that in un-irradiated controls (pro and active MMP-9 = 100%) and is expressed as a %.

In HaCaT cells, there was no significant effect of IL-1α on the expression of proMMP-2 in sham-irradiated controls (Figure 4.11i). Following the addition of IL-1α to UV-irradiated cells proMMP-2 levels were significantly higher compared to

IL-1α-treated sham-irradiated controls (proMMP-2 levels were elevated 20-28% in these treated irradiated cells). When compared to the corresponding untreated irradiated cells, proMMP-2 levels were 2-, 1.2- and 1.3-fold higher in the respective IL-1α-treated UVA-, UVB- and UVAB-irradiated cells.

There was no significant effect of IL-1α on the expression of active MMP-2 in sham-irradiated controls. Active MMP-2 levels were relatively constant in the presence of IL-1α in UV-irradiated cells compared to IL-1α treated sham-irradiated controls. The active MMP-2 levels were the same in IL-1α treated UVB and UVAB-irradiated cells compared to their corresponding untreated irradiated counterparts. Only the active MMP-2 levels in treated UVA-irradiated cells fell to 5% compared to the corresponding untreated irradiated cells. Total MMP-2 (pro and active form) levels in IL-1α-treated UV-irradiated cells were elevated 20% in both the UVB- and UVAB-irradiated cells but were unchanged in UVA-irradiated cells compared to un-irradiated controls. In general, the highest levels of MMP-2 expression were seen in UVAB-irradiated cells which had been treated with IL-1α.

The addition of IL-1α to sham-irradiated controls induced a 1.9-fold increase in the expression of MMP-9 in these cells (Figure 4.11ii). ProMMP-9 levels were significantly ($p<0.05$) higher in IL-1α-treated UV-irradiated cells when compared to treated sham-irradiated controls (they were 4-, 8.4- and 10-fold higher in treated UVA-, UVB- and UVAB-irradiated cells, respectively). ProMMP-9 levels were 6.1-, 12.1- and 11-fold higher in IL-1α treated UVA-, UVB- and UVAB-irradiated cells, respectively compared to the corresponding untreated irradiated cells.

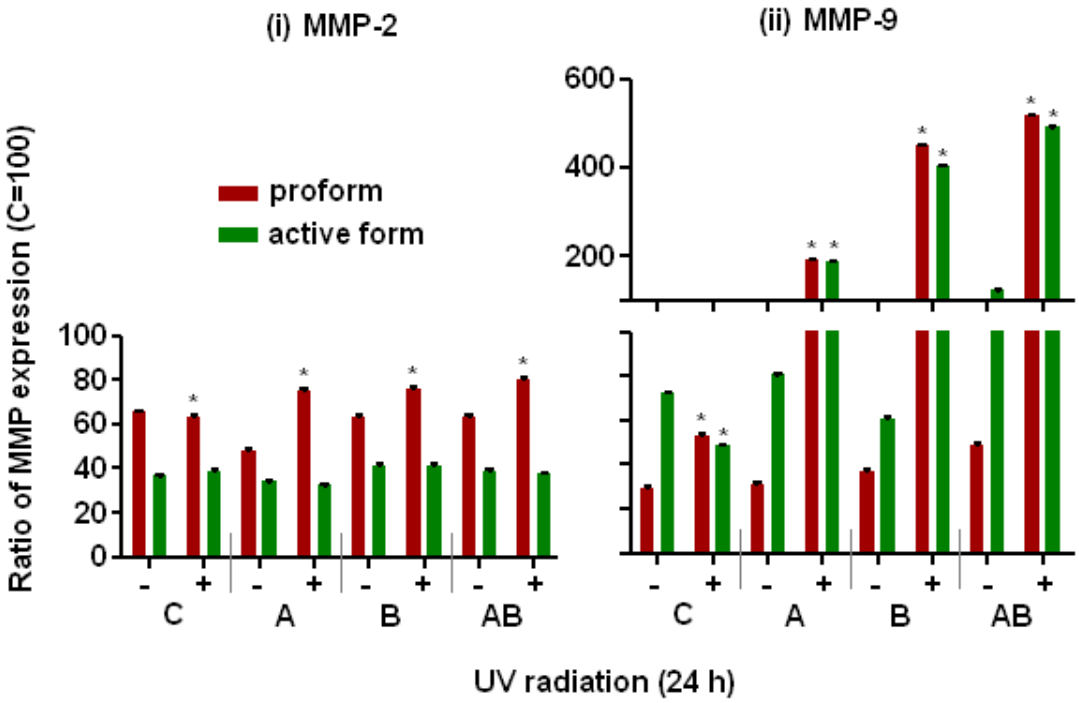

Figure 4.11 The effect of IL-1α on the expression of MMP-2 (i) and -9 (ii) in UVR-irradiated HaCaT cells. Cells were exposed to sham-irradiation or controls (C), UVA (A), UVB (B) and UVAB (AB) radiation in the presence (+) or absence (-) of IL-1α. Results expressed are the mean ± SEM for three separate experiments. Statistical significance of the effect of IL-1α on the expression of MMP-2 and-9 levels was shown as $p<0.05$ (*).

The active form of MMP-9 was 35% lower when IL-1α was added to the sham-irradiated HaCaT cells compared to the untreated controls. The levels of active MMP-9 were elevated in UV-irradiated cells treated with IL-1α compared to the IL-1α-treated sham-irradiated cells (the levels were 4-, 9- and 10.4-fold higher in UVA-, UVB- and UVAB-irradiated cells, respectively). When compared to the corresponding untreated irradiated cells, active MMP-9 levels were 2.3-, 6.6- and 4.0-fold higher in IL-1α treated UVA-, UVB- and UVAB-irradiated cells. Total MMP-9 levels (pro and active form) in the treated UV-irradiated cells were higher when compared to treated sham-irradiated controls. The greatest increase was 10-fold in UVAB-, followed by UVB- (9-fold) and UVA- irradiated cells (4-fold).

These results above suggest that in UV-irradiated HaCaT cells, addition of IL-1α has a greater stimulatory effect on MMP-9 than on MMP-2. The greatest increase of MMP-9 expression was seen in treated UVAB-irradiated cells.

In Colo 16 cells, there was no significant effect of IL-1α on the expression of proMMP-2 in sham-irradiated controls (Figure 4.12i). Following the addition of IL-1α to UV-irradiated cells proMMP-2 levels were significantly higher compared to IL-1α treated sham-irradiated controls (the levels were 1.6-, 2- and 2.1-fold higher in UVA-, UVB- and UVAB-irradiated cells, respectively). Following the addition of IL-1α to UV-irradiated cells proMMP-2 levels significantly fell by 25% in UVA-irradiated cells and ~2% in UVB- and UVAB-irradiated cells compared to the corresponding untreated irradiated cells.

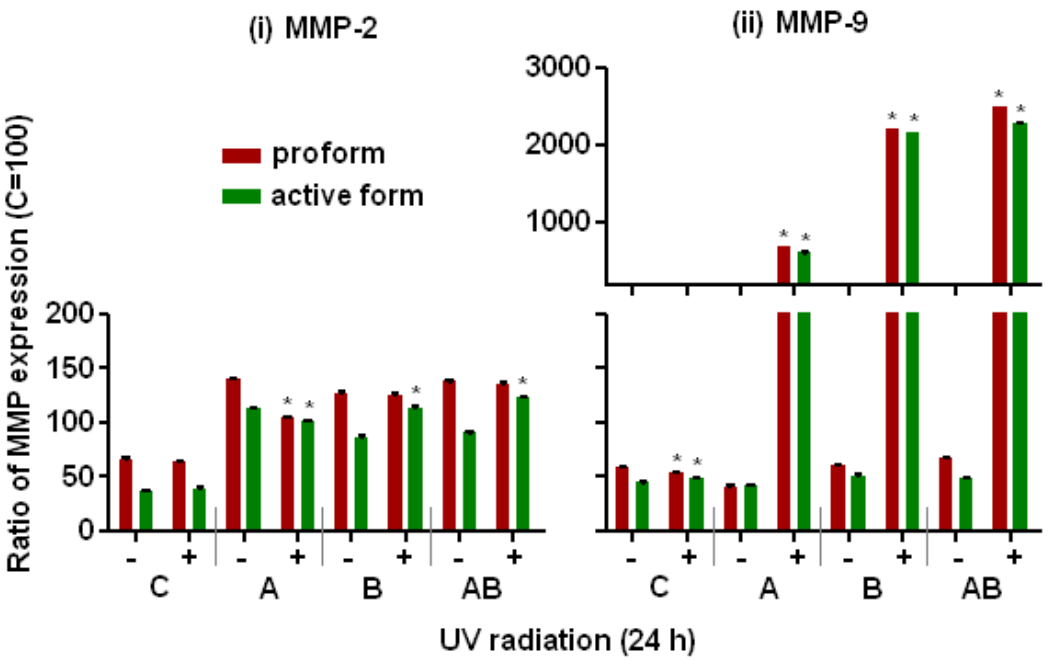

Figure 4.12 The effect of IL-1α on the expression of MMP-2 (i) and -9 (ii) in UVR-irradiated Colo 16 cells. Cells were exposed to sham-irradiation or controls (C), UVA (A), UVB (B) and UVAB (AB) radiation in the presence (+) or absence (-) of IL-1α. Results expressed are the mean ± SEM for three separate experiments. Statistical significance of the effect of IL-1α on the expression of MMP-2 and-9 levels was shown as $p<0.05$ (*).

On the other hand, active MMP-2 levels were relatively constant in the presence and/or absence of IL-1α in sham-irradiated cells. The active form of MMP-2 was significantly increased by 63%, 76% and 84.4% in IL-1α treated UVA-, UVB- and UVAB-irradiated cells, respectively when compared to treated sham-irradiated controls. While active MMP-2 levels fell by 11% in UVA-irradiated cells, it increased by ~1.3-fold in UVB- and UVAB-irradiated cells compared to the corresponding untreated irradiated cultures. While total MMP-2 (pro and active form) levels in IL-1α treated UVA-irradiated cells was elevated 2-fold compared to sham-irradiated controls; it was elevated 2.4-fold and 2.6-fold in UVB- and UVAB-irradiated cells, respectively. In general, on the addition of IL-1α, UVAB-irradiation induced higher levels of MMP-2 expression which was similar to that observed in HaCaT cells (Figure 4.11i).

In Colo 16 cells, the addition of IL-1α to sham-irradiated controls resulted in an 8% decrease in the expression of MMP-9 in these cells (Figure 4.12ii). ProMMP-9 levels were significantly ($p<0.05$) higher in IL-1α treated UV-irradiated cells when compared to treated sham-irradiated controls (they were 13-, 41.6- and 47-fold higher in treated UVA-, UVB- and UVAB-irradiated cells, respectively compared to treated sham-irradiated cells). The proMMP-9 levels were 17-, 36.6- and 37.3-fold higher in UVA-, UVB- and UVAB-irradiated cells, respectively when compared to the corresponding untreated irradiated cells.

On the other hand, active MMP-9 levels were relatively constant in the presence and/or absence of IL-1α in sham-irradiated cells. Active MMP-9 levels in IL-1α-treated UV-irradiated cells were significantly ($p<0.05$) higher compared to treated

sham-irradiated controls (the levels were 13-, 46- and 49-fold higher in UVA-, UVB- and UVAB-irradiated cells, respectively). When compared to the corresponding untreated irradiated cells, active MMP-9 levels were 14.6-, 42.4- and 47.4-fold higher in UVA-, UVB- and UVAB-irradiated cells, respectively. The total levels of MMP-9 (pro and active form) in IL-1α treated UV-irradiated cells were higher compared to sham-irradiated controls. Maximal levels were observed in UVAB-(48-fold), followed by UVB- (44-fold) and UVA-irradiated cells (13-fold) when compared to the treated sham-irradiated controls. In general, on the addition of IL-1α, UVAB-irradiation induced higher levels of MMP-9 expression.

These results suggest that in UV-irradiated Colo 16 cells, addition of IL-1α has a greater stimulatory effect on the cellular expression of MMP-9 than on MMP-2 and greatest increase was seen in treated UVAB-irradiated cells. This was similar to results observed in HaCaT cells.

4.2.1.4 Inhibitor studies

MMPs have been shown to be important in tumour progression, promoting invasion and immune escape (187). Furin has been shown to activate MMPs from their respective preproforms (136, 151, 168, 288). Recent studies using PC inhibitors have demonstrated that increased furin expression is associated with enhancement of metastatic spread and tumour cell proliferation (144, 227), probably as a result of the activation of MMP involved in ECM degradation (169, 266). I investigated the effect various inhibitors had on MMP activity in UV-irradiated cells. These were the furin inhibitor (Dec RVKR cmk), metalloprotease inhibitor (1, 10 phe), and

2R-2-[(4-Biphenylsulfonyl) amino]-3-phenylpropionic acid (MMP-2/-9 specific inhibitor) (MMPI).

4.2.1.4.1 Cell viability

Before undertaking inhibition studies we needed to confirm that the concentrations of the inhibitors used were not cytotoxic. As UVAB-irradiation induced high levels of MMP-2 and -9 expression in HaCaT and Colo 16 cells (Figures 4.6 and 4.8), it was chosen as the type of dose in these experiments.

4.2.1.4.1.1 Furin inhibitor (Dec RVKR cmk)

Dec RVKR cmk is a specific and potent inhibitor of furin (156, 158, 167, 175, 227). The concentration of this inhibitor used in this was 100 μM. The effect of Dec RVKR cmk on HaCaT and Colo 16 cell viability was determined 24 h post-irradiation using the trypan-blue exclusion assay (Section 2.4).

In HaCaT cells, the viability of attached cells in the untreated controls was 93%, however, in the presence of Dec RVKR cmk, this fell 70% in treated sham-irradiated cells (Figure 4.13i). The viability of untreated UVAB-irradiated attached cells was 60.3%, which fell slightly to 60% in the presence of Dec RVKR cmk. The level of attached dead cells was <20% across all treatments and conditions except for untreated UV-irradiated cells (21%). The number of detached viable cells was <5% in response to the different treatments and does. There were less dead detached cells observed in the untreated sham-irradiated cultures compared to the Dec RVKR cmk-treated controls (12%) and UV-irradiated cells (18%). The results

show that 100 μM Dec RVKR cmk did not significantly affect the viability of UVAB-irradiated HaCaT cells.

In Colo 16 cells, the viability of attached cells in the untreated controls was 90%, whereas this fell to 70% when Dec RVKR cmk was added to these cells (Figure 4.13ii). The viability of untreated UVAB-irradiated attached cells was 49% but in the presence of Dec RVKR cmk, it was 48%. The number of attached dead cells was <20% under all treatments and conditions. The percentage of detached viable cells was negligible (<5%) in all experimental conditions. There were less dead detached cells observed in the untreated sham-irradiated cultures compared to Dec RVKR cmk-treated controls (25%) and UV-irradiated cells (~30%).

In general, while Dec RVKR cmk had a slight effect on the viability of un-irradiated cells it did not have an effect on the UV-irradiated cultures.

4.2.1.4.1.2 Metalloprotease inhibitor (1, 10 phe)

1, 10 phe is a broad spectrum metalloprotease inhibitor (304, 305). The effect of different concentrations of 1, 10 phe on the cell viability of sham-irradiated and UV-irradiated HaCaT cells can be seen in Figure 4.14.

The viability of attached cells in sham-irradiated cultures treated with 100 μM of 1, 10 phe fell from 90% to 77% (Figure 4.14i). Increasing concentrations of 1, 10 phe resulted in a drop in the number of adhered viable cells in these cultures. There was an increase in the number of attached dead cells in the cultures when higher inhibitor concentrations were used. In cells treated with 500 μM of 1, 10 phe, 42% dead attached

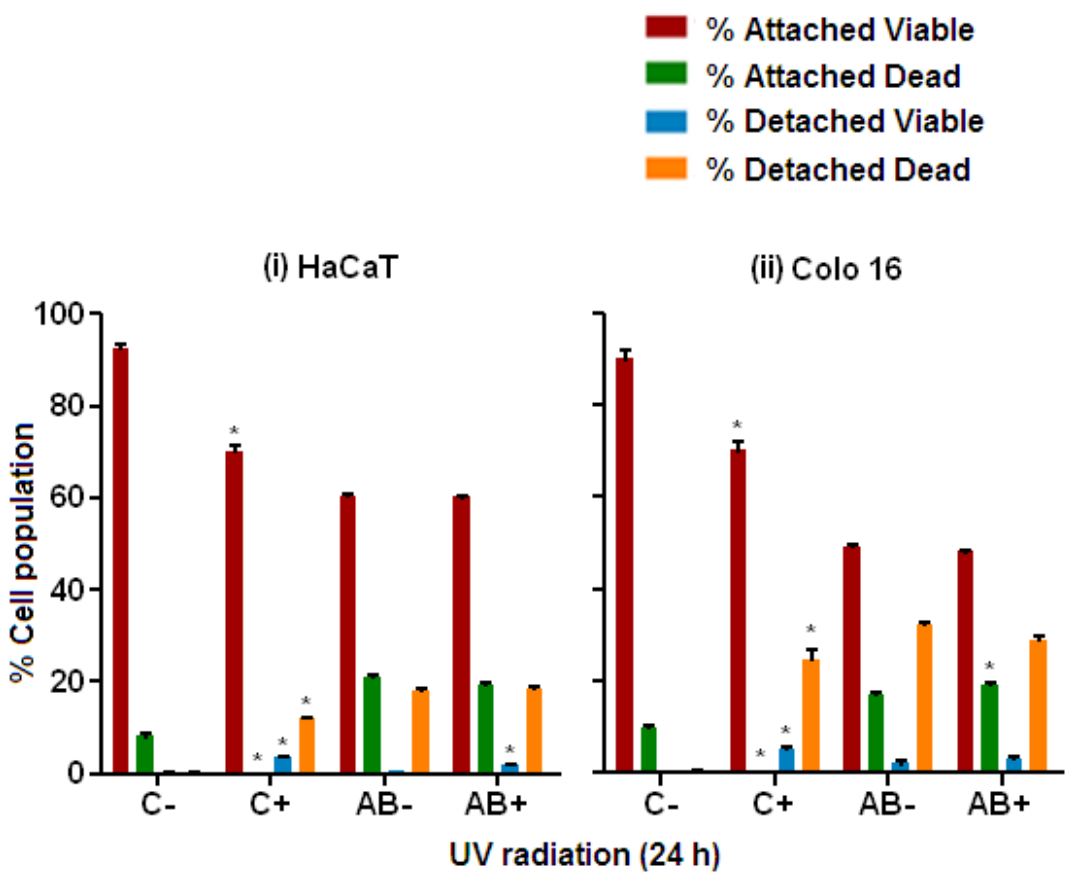

Figure 4.13 Effect of Dec RVKR cmk on the viability of UVAB-irradiated HaCaT (i) and Colo 16 cells (ii). Cells were exposed to sham-irradiation or controls (C) or UVAB-irradiation (UVAB) in the presence (+) and absence (-) of Dec RVKR cmk (100 μM). Cell viability was determined 24 h post-irradiation. Results expressed are the mean ± SEM for three separate experiments. Statistical significance of the effect of Dec RVKR cmk on cell populations was represented as $p<0.05$ (*).

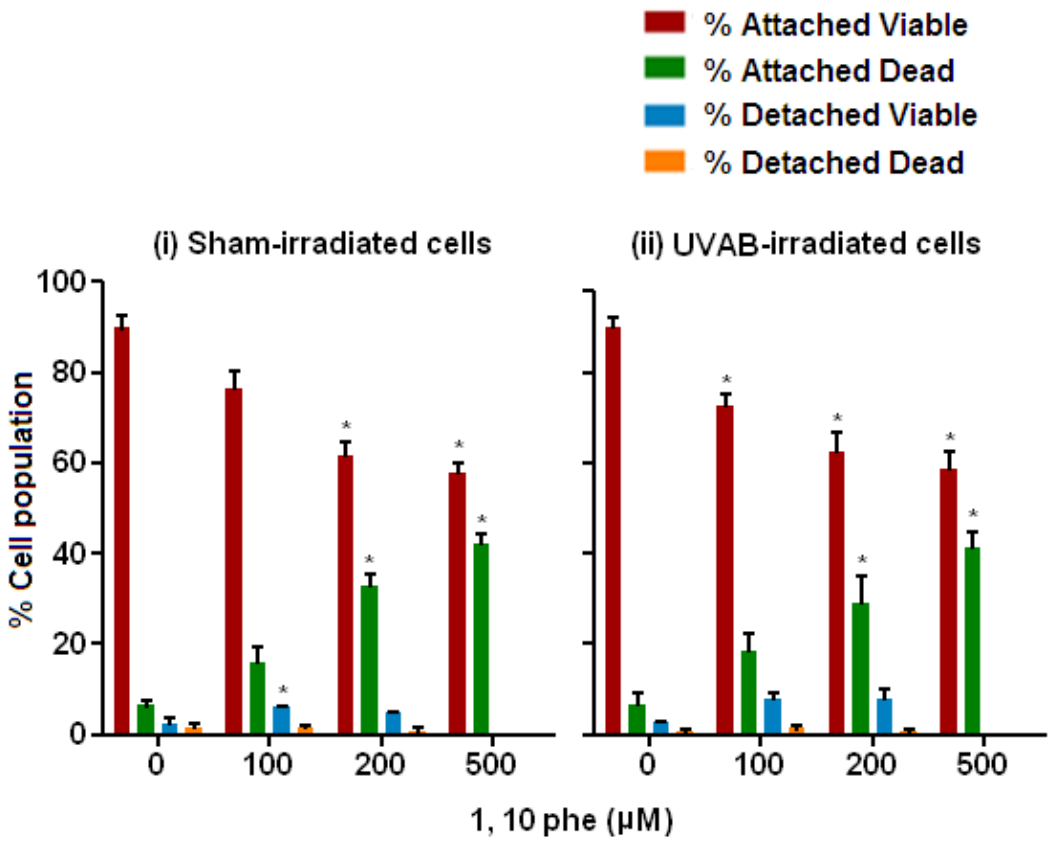

Figure 4.14 Effect of 1, 10 phe on the viability of sham-irradiated HaCaT cells (i) and UVAB-irradiated HaCaT cell cultures (ii). The cells were treated with 100, 200 and 500 µM of 1, 10 phe inhibitor and cell viability was determined 24 h post UVAB-irradiation. Results expressed are the mean ± SEM for three separate experiments. Statistical significance of the effect of 1, 10 phe on cell groups was represented as $p<0.05$ (*).

cells was observed. The number of detached viable and dead cells was <10% irrespective of the dose used.

A similar trend was observed in UVAB-irradiated HaCaT cells. The viability of attached cells in sham-irradiated cultures treated with 100 μM of 1, 10 phe fell from 90% to 73% (Figure 4.14ii). The viability of these cultures significantly fell when they were treated with 200 or 500 μM of 1, 10 phe. There was an increase in the number of attached dead cells in the cultures when the higher inhibitor concentrations (200 or 500 μM) were used. In cells treated with 500 μM of 1, 10 phe, 41% attached dead cells was observed. The number of detached viable and dead cells was <10% irrespective of the dose used.

These results suggest that, at a concentration of 100 μM, maximal viability of the cells was observed. UV-irradiated cultures showed a similar profile to that of sham-irradiated cells. Therefore, this dose was confirmed for use in further experiments described in this chapter.

4.2.1.4.1.3 MMP inhibitor (MMPI)

2R-2-[(4-Biphenylsulfonyl) amino]-3-phenylpropionic acid (MMPI) is a specific and potent inhibitor of MMP-2 and -9 (183, 306-308). The concentration of this inhibitor (5 μM) was recommended by the manufacturer. The effect of MMP inhibitor on the cell viability of HaCaT and Colo 16 cells exposed to UV-irradiation is seen in Figure 4.15. Cell cultures were pretreated for 1 h with 5 μM of MMPI (Section 2.3.2) and cell viability was measured 24 h post-irradiation (Section 2.4).

In HaCaT cells, the viability of attached cells in untreated sham-irradiated cells (92.5%) fell by 12.5% following the addition of MMPI (Figure 4.15i). The viability of untreated UVAB-irradiated attached cells (60.3%) fell slightly to 56% in the presence of MMPI. The level of attached dead cells was less in untreated and treated controls but was ~20% in both the untreated and treated UV-irradiated cells. The number of detached viable cells was <5% in response to the different treatments and does. There were less dead detached cells observed in the untreated sham-irradiated cultures compared to MMPI treated sham- (8%) and UV-irradiated cells (18%). The results show that 5 μM MMPI did not significantly affect the viability of HaCaT cells.

In Colo 16 cells, the viability of attached cells in untreated sham-irradiated cells (90%) fell by 10% following the addition of MMPI (Figure 4.15ii). The viability of untreated UVAB-irradiated attached cells (50%) fell slightly to 47% in the presence of MMPI. The level of attached dead cells was <20% across all treatments and conditions. The number of detached viable cells was <5% in untreated controls. There were more detached dead cells observed in treated sham-irradiated cultures (16%) when compared to their untreated counterparts. The percentage of detached dead cells was significantly high in MMPI-untreated UV- (32%) and treated UV-irradiated cells (30%).

These results suggest that MMPI had a slight effect on attached viable and detached dead cells in UV-irradiated HaCaT and Colo 16 cells.

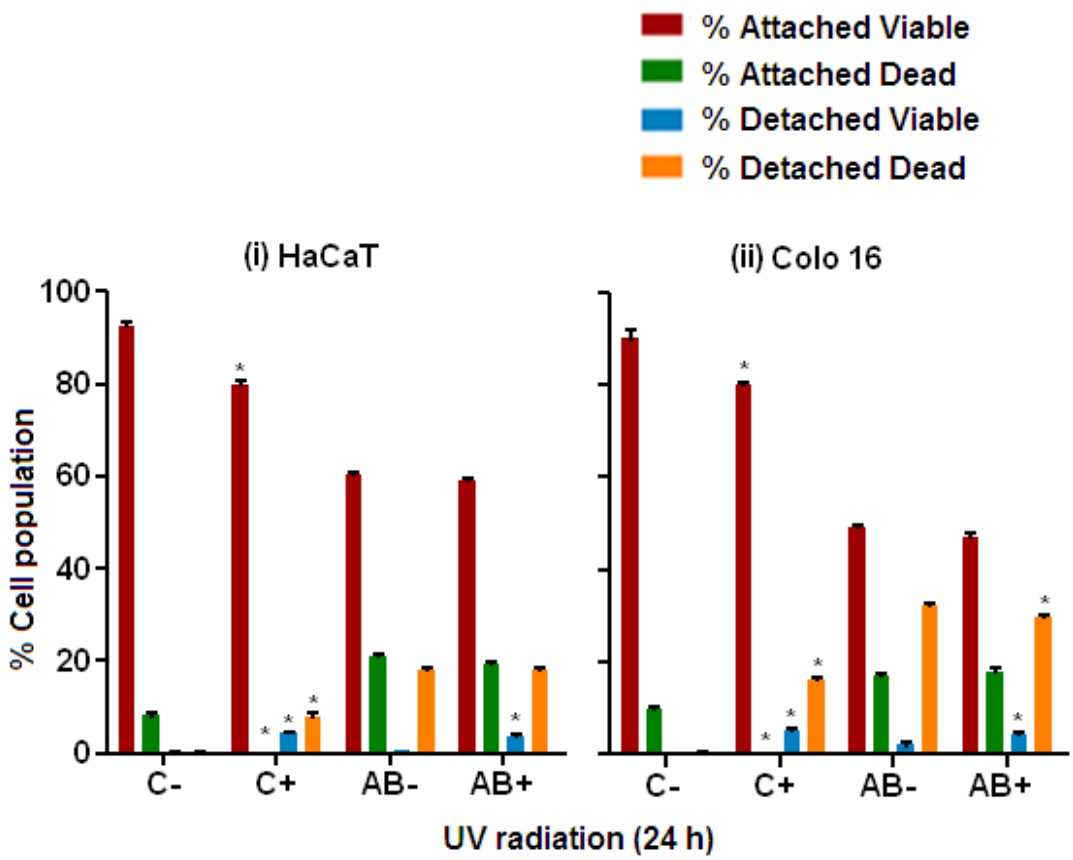

Figure 4.15 Effect of MMPI on the viability of UVAB-irradiated HaCaT (i) and Colo 16 cells (ii). Cells were exposed to sham-irradiation or controls (C) or UVAB-irradiation (UVAB) in the presence (+) and absence (-) of MMPI (5 μM). Cell viability was determined 24 h post-irradiation. Results expressed are the mean ± SEM for three separate experiments. Statistical significance of the effect of MMPI on cell groups was represented as $p<0.05$ (*).

4.2.1.4.2 Effects of inhibitors on MMP protein activity

This study was done to observe the effect of the different inhibitors on MMP-2 and -9 activity in UV-irradiated HaCaT and Colo 16 cells. Based on the results from the previous section, the inhibitors tested in these experiments were used at the following concentrations: Dec RVKR cmk, 100 μM; 1, 10 phe, 100 μM; and MMPI, 5 μM. In both the cell lines examined, two forms of MMP were detected, MMP-2 and MMP-9. The amount of microconcentrated conditioned media (Section 2.7.2) (50 μl) added to each lane in the zymogen was similar. The level of cell protein in cultures has been measured to express the MMP activity per mg culture protein.

4.2.1.4.2.1 Dec RVKR cmk

A representative zymograph showing the effects of Dec RVKR cmk on MMP-2 and -9 shed from HaCaT and Colo 16 cells is shown in Figure 4.16.

In HaCaT cells, MMP-2 activity released from the sham-irradiated controls was 111.0 au/mg cell protein. Following the addition of Dec RVKR cmk, the level of activity released from the cells fell by 27% (Figure 4.17i). Similar results were also seen in the UV-irradiated cells treated with Dec RVKR cmk compared to the corresponding untreated irradiated cells. The levels of MMP-2 released from the cells fell by 47%, 17% and 49% in treated UVA-, UVB- and UVAB-irradiated cells, respectively when compared to the corresponding untreated irradiated cohorts.

MMP-9 activity released from the sham-irradiated cells was 72.4 au/mg cell protein. On the addition of Dec RVKR cmk to these cells, complete inhibition of MMP-9 activity

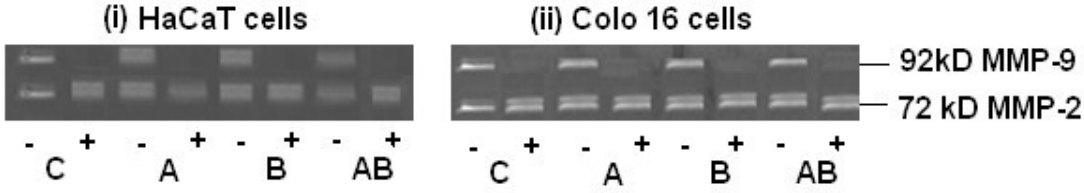

Figure 4.16 A representative zymograph showing the effect of Dec RVKR cmk on the gelatinolytic activity of MMP-2 and -9 secreted into conditioned media of UV-irradiated HaCaT (i) and Colo 16 cells (ii) 24 h post-irradiation. In each lane, 50 μl of microconcentrated conditioned media was added. The cells were exposed to sham-irradiation or controls (C), UVA (A), UVB (B) and UVAB (UVAB) radiation in the presence (+) or absence (-) of Dec RVKR cmk.

was observed (Figure 4.17ii). Similar results were also seen in the UVA-, UVB- and UVAB-irradiated cells treated with Dec RVKR cmk compared to the corresponding untreated irradiated cells. The absence of MMP-9 activity was also seen in the representative zymograph (Figure 4.16i) where absence of these gelatinolytic bands in treated sham and UV-irradiated samples was shown.

In Colo 16 cells, MMP-2 activity released from the sham-irradiated controls was 43.7 au/mg cell protein. Following the addition of Dec RVKR cmk, the level of activity released from the cells fell by 21% (Figure 4.17i). Similar results were also seen in the UV-irradiated cells treated with Dec RVKR cmk compared to their corresponding untreated irradiated cells. The levels of MMP-2 released from the cells fell by 35.4%,

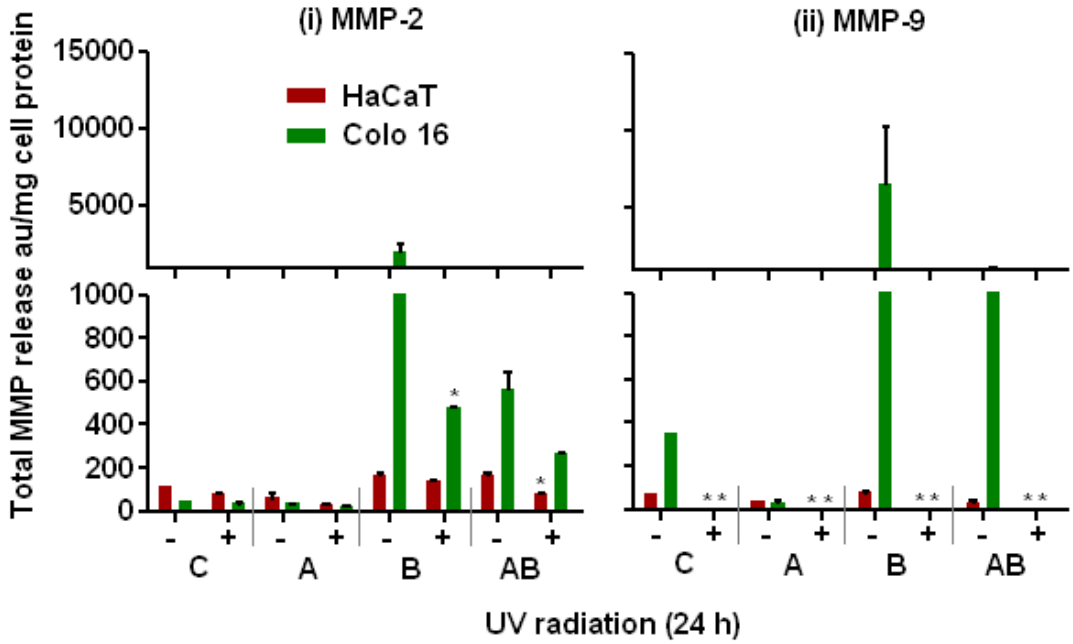

Figure 4.17 The effect of Dec RVKR cmk on the activity of MMP-2 (i) and MMP-9 (ii) secreted into conditioned media of HaCaT and Colo 16 cells. Cells were exposed to sham-irradiation or controls (C), UVA (A), UVB (B) and UVAB (AB) radiation in the presence (+) or absence (-) of Dec RVKR cmk and samples were collected 24 h post-treatment. Results expressed are the mean ± SEM for three separate experiments. Statistical significance of the effect of Dec RVKR cmk on MMP-2 and-9 activity in cell cultures is shown as $p<0.05$ (*).

MMP-9 activity released from the sham-irradiated cells was 356.0 au/mg cell protein. Following the addition of Dec RVKR cmk to these cells, complete inhibition of 76% and 53% in treated UVA-, UVB- and UVAB-irradiated cells, respectively when compared to their corresponding untreated cohorts. MMP-9 activity was observed (Figure 4.17ii). Similar results were also seen in the UVA-, UVB- and UVAB-irradiated cells treated with Dec RVKR cmk compared to their corresponding untreated irradiated cells.

In conclusion, Dec RVKR cmk inhibited both MMP-2 and -9 activity in treated UV-irradiated cells compared to their untreated counterparts. This result suggests that furin is involved with their activation.

4.2.1.4.2.2 1, 10 phe

A representative zymograph showing the effects of 1, 10 phe on MMP-2 and -9 shed from HaCaT and Colo 16 cells is shown in Figure 4.18.

In HaCaT cells, MMP-2 activity released from the treated sham-irradiated controls was 109.1 au/mg cell protein. Following the addition of 1, 10 phe, the level of activity released from the cells decreased by 26.4% (Figure 4.19i). Of interest was that, while there was a drop in the level of MMP-2 released from treated UV-irradiated cells compared to their untreated counterparts, this was not statistically significant. The level of MMP-2 activity released from the cell fell by 12%, 4% and 8% in treated UVA-, UVB- and UVAB-irradiated cells, respectively when compared to their corresponding untreated irradiated cohorts.

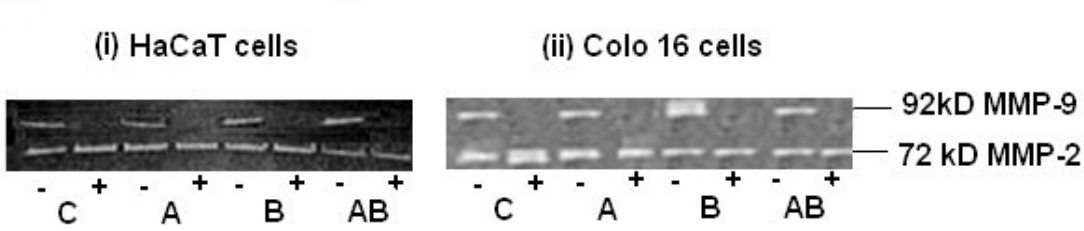

Figure 4.18 A representative zymograph showing the effect of 1, 10 phe on the activity of MMP-2 and MMP-9 secreted into conditioned media of UV-irradiated HaCaT (i) and Colo 16 cells (ii) 24 h post-irradiation. In each lane, 50 µl of microconcentrated conditioned media was added. The cells were exposed to sham-irradiation or controls (C), UVA (A), UVB (B) and UVAB (UVAB) radiation in the presence (+) or absence (-) of 1, 10 phe.

MMP-9 activity released from the sham-irradiated controls was 70.3 au/mg cell protein. On addition of 1, 10 phe to these cells, complete inhibition of MMP-9 activity was observed (Figure 4.19ii). Similar results were also seen in the UVA-, UVB- and UVAB-irradiated cells treated with 1, 10 phe compared to the corresponding untreated irradiated cells. The absence of MMP-9 activity was also seen in the representative zymograph (Figure 4.18i) where gelatinolytic bands were not present in the treated sham- and UV-irradiated samples.

In Colo 16 cells, MMP-2 activity released from the treated sham-irradiated controls was 46.4 au/mg cell protein. Following the addition of 1, 10 phe, the level of activity

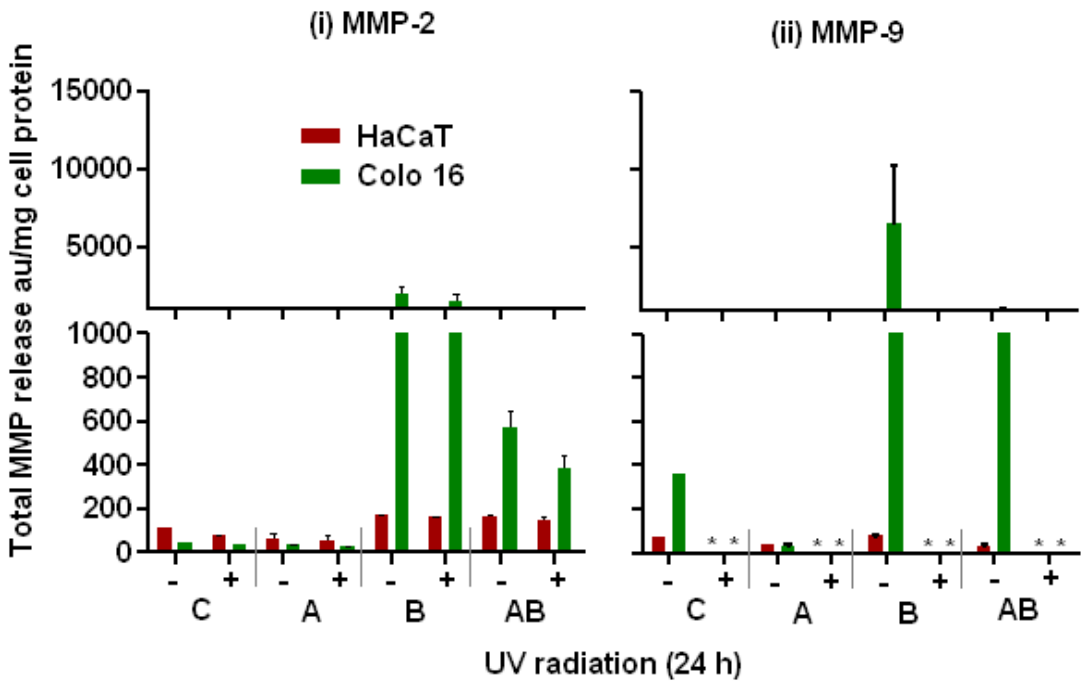

Figure 4.19 The effect of 1, 10 phe on the activity of MMP-2 (i) and MMP-9 (ii) secreted into conditioned media of HaCaT and Colo 16 cells. Cells were exposed to sham-irradiation or controls (C), UVA (A), UVB (B) and UVAB (AB) radiation in the presence (+) or absence (-) of 1, 10 phe and samples were collected 24 h post-treatment. Results expressed are the mean ± SEM for three separate experiments. Statistical significance of the effect of 1, 10 phe on MMP-2 and-9 activity in cell cultures is shown as $p<0.05$ (*).

released from the cells decreased by 25% (Figure 4.19i). Of interest was that, while there was a drop in the level of MMP-2 released in treated UV-irradiated cells compared to their untreated counterparts, it was not statistically significant. The levels of MMP-2 released from the cells fell by 27%, 25% and 33% in treated UVA-, UVB- and UVAB-irradiated cells, respectively when compared to their corresponding untreated irradiated cohorts.

MMP-9 activity released from the sham-irradiated controls was 362.1 au/mg cell protein. On addition of 1, 10 phe to these cells, complete inhibition of MMP-9 activity was observed (Figure 4.19ii). Similar results were also seen in the UVA-, UVB- and UVAB-irradiated cells treated with 1, 10 phe compared to the corresponding untreated irradiated cells. The absence of MMP-9 activity were also seen in the representative zymograph (Figure 4.18ii) where the absence of these gelatinolytic bands in treated sham- and UV-irradiated samples were observed. These results show that when 1, 10 phe was added to Colo 16 cells, complete absence of MMP-9 activity was observed in the treated UV-irradiated cells irrespective of the UV doses. This was similar to that seen in HaCaT cells.

In conclusion, 1, 10 phe significantly reduced MMP-2 activity shed from the cells. In general, UVB-irradiation induced maximal release of MMP-2 and -9 activity in both cell lines. 1, 10 phe completely inhibited the activity of MMP-9 and significantly reduced that of MMP-2 shed from both UV-irradiated cells irrespective of the type used, which suggests that both MMPs are metalloproteases.

4.2.1.4.2.3 MMPI

UVB-irradiation was shown to induce significant levels of MMP-2 and-9 activity in HaCaT cells (Figure 4.3) and highest levels of MMP-2 and -9 activity in Colo 16 cells (Figure 4.4). A similar result was seen in Figures 4.17 and 4.19. MMPI at 5 μM was shown to have no significant effect on cell viability (Figure 4.15) and as such its effect at this UV dose on MMP-2 and -9 activity was investigated.

A representative zymograph showing the effects of MMPI on MMP-2 and -9 shed from HaCaT and Colo 16 cells is shown in Figure 4.20.

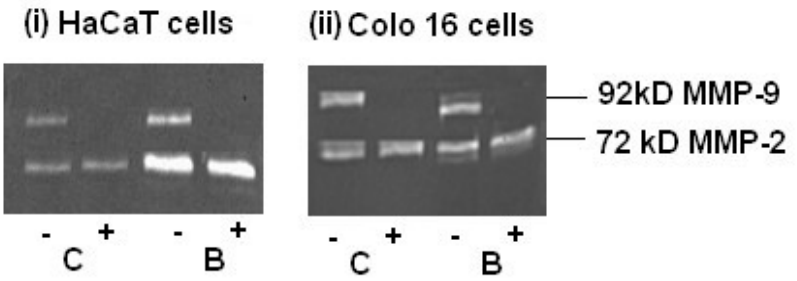

Figure 4.20 A representative zymograph showing the effect of MMPI on the activity of MMP-2 and MMP-9 secreted into conditioned media of HaCaT (i) and Colo 16 cells (ii) collected 24 h post UV-irradiation. In each lane, 50 μl of microconcentrated conditioned media was added. The cells were exposed to sham-irradiation or controls (C) or UVB-irradiation (B) in the presence (+) or absence (-) of MMPI.

In HaCaT cells, MMP-2 activity released from the treated sham-irradiated controls was 112.4 au/mg cell protein. Following the addition of MMPI, the level of activity released from the cells was significantly decreased by 67% (Figure 4.21i). Similar results were also seen in the UVB-irradiated cells treated with MMPI compared to their corresponding untreated irradiated cells. The levels of MMP-2 released from these cells fell by 21%.

MMP-9 activity released from the sham-irradiated controls was 71.2 au/mg cell protein. Following the addition of MMPI, complete inhibition of MMP-9 activity was observed (Figure 4.21ii). Similar results were also seen in the UVB -irradiated cells treated with MMPI compared to their corresponding untreated irradiated cells. The absence of MMP-9 activity was also seen in the representative zymograph (Figure 4.20ii) where the absence of these gelatinolytic bands in treated sham- and UV-irradiated samples was observed.

In Colo 16 cells, MMP-2 activity released from the treated sham-irradiated controls was 42.6 au/mg cell protein. Following the addition of MMPI, the level of activity released from the cells was significantly decreased by 60% (Figure 4.21i). Similar results were also seen in the UVB-irradiated cells treated with MMPI compared to their corresponding untreated irradiated cells. The levels of MMP-2 released from these cells fell by 91.3%.

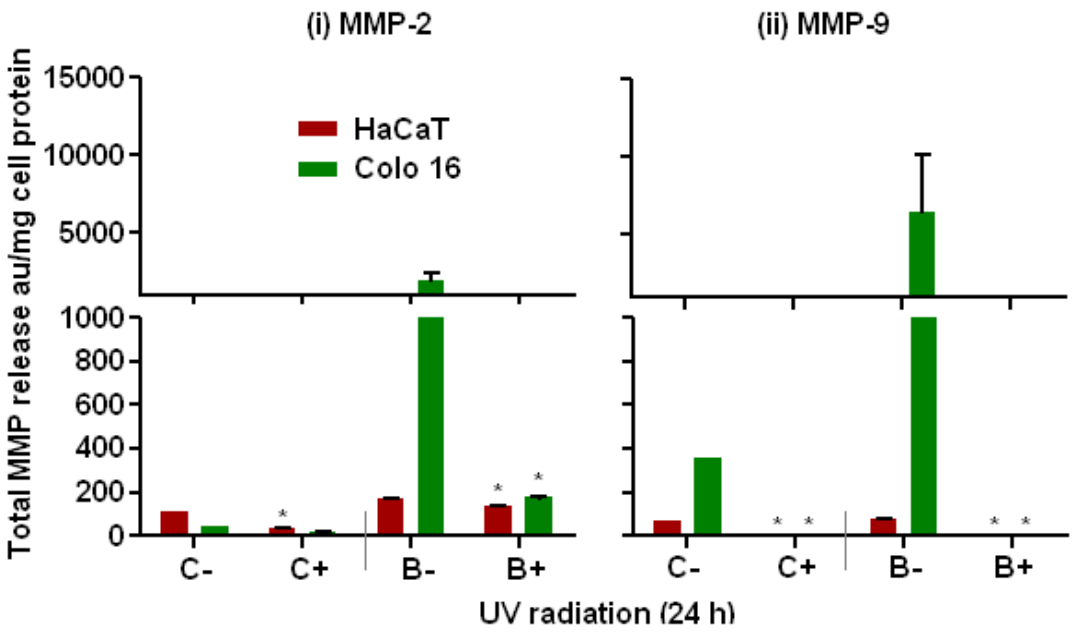

Figure 4.21 The effect of MMPI on the activity of MMP-2 (i) and MMP-9 (ii) secreted into conditioned media of HaCaT and Colo 16 cells. Cells were exposed to sham-irradiation or controls (C) and UVB (B) radiation in the presence (+) or absence (-) of MMPI and samples were collected 24 h post-treatment. Results expressed are the mean ± SEM for three separate experiments. Statistical significance of the effect of MMPI on MMP-2 and-9 activity in cell cultures is shown as $p<0.05$ (*).

MMP-9 activity released from the sham-irradiated controls was 352.3 au/mg cell protein. Following the addition of MMPI to these cells, complete inhibition of MMP-9 activity was observed (Figure 4.21ii). Similar results were also seen in the UVB-irradiated cells treated with MMPI compared to their corresponding untreated irradiated cells. The absence of MMP-9 activity was also seen in the representative zymograph (Figure 4.20ii) where the absence of these gelatinolytic bands in treated sham- and UV-irradiated samples was observed. These results show that when MMPI was added to Colo 16 cells, no MMP-9 activity was observed in treated UV-irradiated cells. This result was similar to that seen in HaCaT cells.

In conclusion, MMPI significantly reduced the secretion of MMP-2 activity from both cells under all conditions. In general, higher levels of MMP-2 and -9 activity was shed from treated UV-irradiated Colo 16 cells compared to HaCaT cells which was similar to that seen previously in Figures 4.3 and 4.4. MMPI completely inhibited the activity of MMP-9 and significantly reduced that of MMP-2 shed from both UV-irradiated cells.

4.2.1.4.3 Effect of MMPI on MMP expression

This study was done to observe the effect of MMPI on the expression of MMP-2 and -9 protein levels in UV-irradiated HaCaT and Colo 16 cells. UVAB induced high levels of MMP-2 and -9 expression in HaCaT and Colo 16 cells either in the presence or absence of IL-1α (Figures 4.6, 4.8, 4.11 and 4.12). Therefore, UVAB was chosen as the UVR to determine the effect MMPI has on MMP protein expression in cells treated in the presence and absence of IL-1α.

In the western blots, 50 μg of cell lysates was added per lane, the pro and active forms of MMP-2 and -9 protein levels were quantified, respectively. β-actin was used to quantify the amount added per lane. A representative blot for the effect of MMPI on MMP expression in treated UV-irradiated HaCaT cells in the presence and absence of IL-1α is seen in Figure 4.22. The level of protein in each sample was compared to that in un-irradiated controls (pro and active MMP-9 = 100%) and is expressed as a percentage of this value.

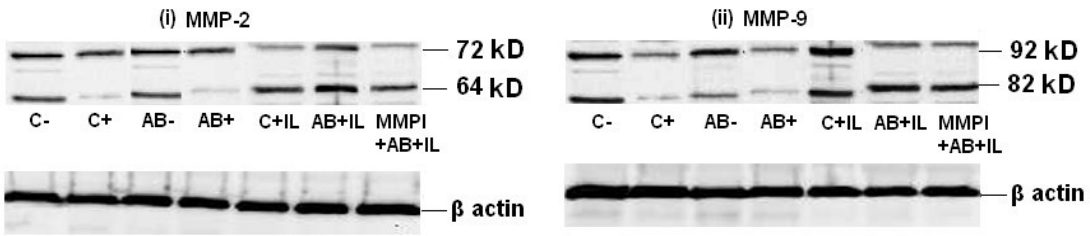

Figure 4.22 A representative western blot showing the effect of MMPI on pro and active MMP-2 (i) and pro and active MMP-9 (ii) expression in UV-irradiated HaCaT cells in the presence and/or absence of IL-1α. In each lane, 50 μg of cell lysate was added and β-actin was used to monitor the amount of protein added per lane. The cells were exposed to sham-irradiation or controls (C) or UVAB-irradiation (AB) in the presence (+) or absence (-) of MMPI (MMPI) and/or IL-1α (IL).

In HaCaT cells, the expression of proMMP-2 in the untreated sham-irradiated cells was 64.4%. Following the addition of MMPI, the expression of proMMP-2 significantly ($p<0.05$) decreased by 21% in these cells (Figure 4.23i). Similar results were also seen in the UVAB-irradiated cells treated with MMPI compared to their corresponding untreated irradiated cells. The levels of proMMP-2 fell by 26% in these cells. On addition of IL-1α, proMMP-2 levels in MMPI treated UV-irradiated cells significantly fell by 45.2% compared to untreated UV-irradiated cells.

On the other hand expression of active MMP-2 in untreated sham-irradiated controls was 35.7%. Following the addition of MMPI, the expression of active MMP-2 significantly fell by 13.2% (Figure 4.23i). Similar results were also seen in the UVAB-irradiated cells treated with MMPI compared to their corresponding untreated irradiated cells. The levels of active MMP-2 fell by 25.3% in these cells. On addition of IL-1α, active MMP-2 levels in MMPI-treated UV-irradiated cells significantly fell by 31% compared to untreated UV-irradiated cells.

The levels of total MMP-2 levels (pro and active form) in the MMPI-treated sham- and UV-irradiated cells fell by 20% and 10%, respectively compared to their untreated counterparts. Following addition of IL-1α, levels reduced by 50% in the treated UV-irradiated cells compared to untreated UV-irradiated cells.

In HaCaT cells, the expression of proMMP-9 in the untreated sham-irradiated controls was 29.5%. Following the addition of MMPI, the expression of proMMP-9 significantly ($p<0.05$) decreased by 37% in these cells (Figure 4.23ii). Similar results were also seen

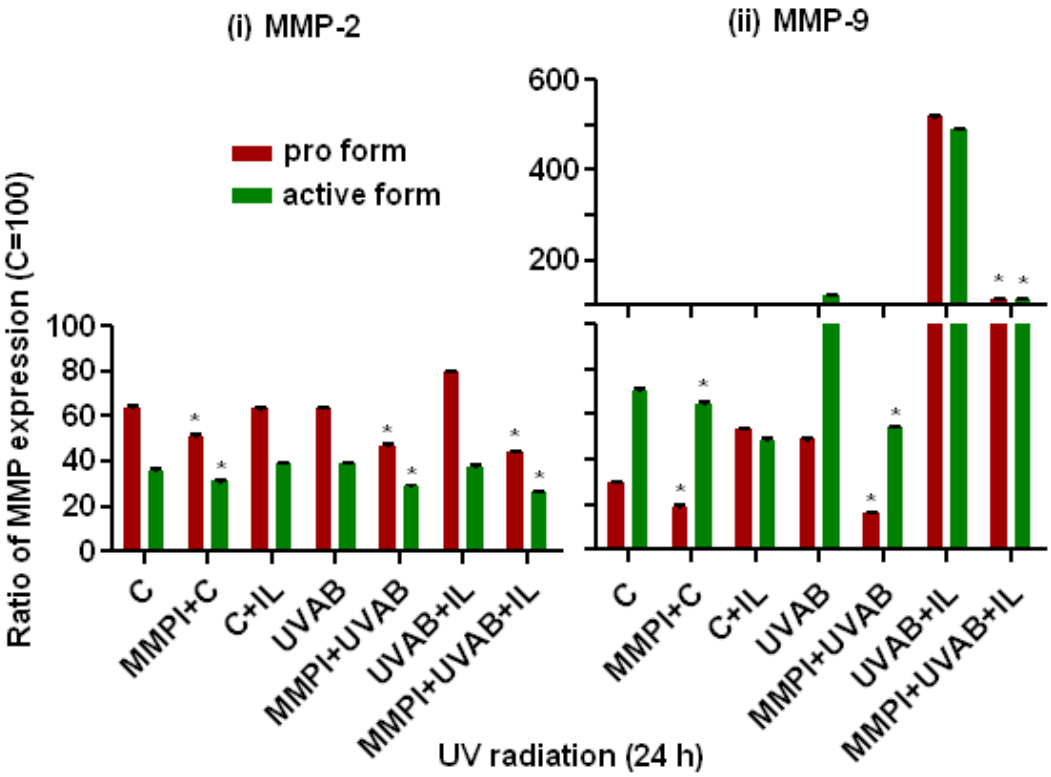

Figure 4.23 Effect of MMPI on the expression of MMP-2 (i) and MMP-9 (ii) in UV-irradiated HaCaT cells in the presence and/or absence of IL-1α. Results expressed are the mean ± SEM for three separate experiments. Statistical significance for MMPI treatment on MMP expression in cell cultures is shown as $p<0.05$ (*).

in the UVAB-irradiated cells treated with MMPI compared to their corresponding untreated irradiated cells. The levels of proMMP-9 fell by 67% in these cells. On addition of IL-1α, proMMP-9 levels in MMPI-treated UV-irradiated cells significantly fell by 78% compared to the untreated UV-irradiated cells.

On the other hand expression of active MMP-9 in the untreated sham-irradiated controls was 70.7%. On the addition of MMPI, the expression of active MMP-9 significantly fell by 8.5% (Figure 4.23ii). Similar results were seen in the UVAB-irradiated cells treated with MMPI compared to their corresponding untreated irradiated cells. In these cells the levels of active MMP-9 fell by 56%. When IL-1α was added to the MMPI treated UV-irradiated cells active MMP-2 levels significantly fell by 77% compared to the untreated UV-irradiated cells. The levels of total MMP-9 (pro and active form) in the MMPI-treated sham- and UV-irradiated cells fell by 20% and 60%, respectively compared to their untreated counterparts. These levels fell by 80% when the UV-irradiated cells in the presence of IL-1α were treated with MMPI.

In Colo 16 cells, the expression of proMMP-2 in untreated sham-irradiated controls was 64% (Figure 4.24i). Following the addition of MMPI, the expression of proMMP-2 significantly ($p<0.05$) decreased by 13% in these cells. Similar results were also seen in the UVAB-irradiated cells treated with MMPI compared to their corresponding untreated irradiated cells. In these cells the levels of proMMP-2 fell by 65%. Following the addition of IL-1α, proMMP-2 levels in MMPI treated UV-irradiated cells significantly fell by 49% compared to the untreated UV-irradiated cells.

On the other hand the expression of active MMP-2 in the untreated sham-irradiated controls was 36%. Following the addition of MMPI, the expression of active MMP-2 significantly fell by 25% (Figure 4.24i). Similar results were also seen in the UVAB-irradiated cells treated with MMPI compared to their corresponding untreated irradiated cells. The levels of active MMP-2 fell by 79% in these cells. Following the addition of IL-1α, active MMP-2 levels in the MMPI treated UV-irradiated cells significantly fell by 48.3% compared to untreated UV-irradiated cells. The levels of total MMP-2 levels (pro and active form) in the MMPI treated sham- and UV-irradiated cells fell by 20% and 70%, respectively compared to their untreated counterparts. Following the addition of IL-1α, the MMP-2 levels fell by 50% in the treated UV-irradiated cells compared to the untreated UV-irradiated cells.

In Colo 16 cells, the expression of proMMP-9 in the untreated sham-irradiated controls was 56% (Figure 4.24ii). Following the addition of MMPI, the expression of proMMP-9 significantly ($p<0.05$) decreased by 21.4% in these cells. Similar results were seen in the UVAB-irradiated cells treated with MMPI compared to their corresponding untreated irradiated cells. The levels of proMMP-9 fell by 45% in these cells. On addition of IL-1α, proMMP-9 levels in the MMPI-treated UV-irradiated cells significantly fell by 68% compared to the untreated UV-irradiated cells.

The expression of active MMP-9 in the untreated sham-irradiated controls was 44%. Following the addition of MMPI, the expression of active MMP-9 significantly fell by 23% in these cells (Figure 4.24ii). Similar results were seen in the UVAB-irradiated

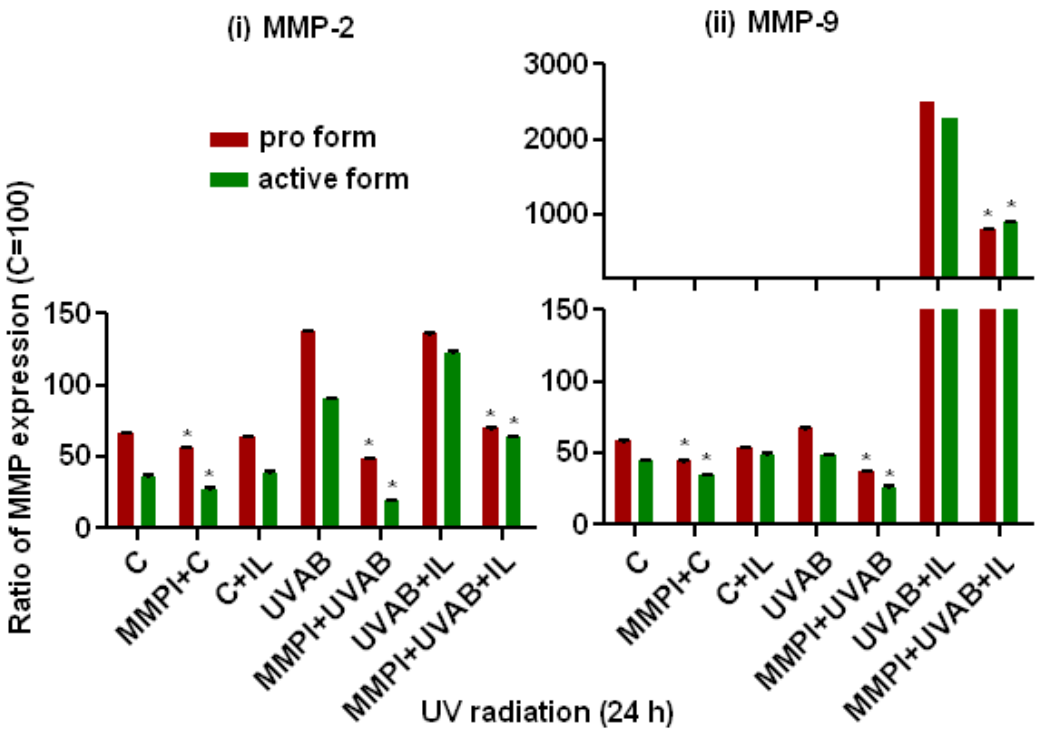

Figure 4.24 Effect of MMPI on the expression of MMP-2 (i) and MMP-9 (ii) in UV-irradiated Colo 16 cells in the presence and/or absence of IL-1α. Results expressed are the mean ± SEM for three separate experiments. Statistical significance for MMPI treatment on MMP expression in cell cultures is shown as $p<0.05$ (*).

cells treated with MMPI compared to their corresponding untreated irradiated cells. The levels of active MMP-9 fell by 46% in these cells. On addition of IL-1α, active MMP-9 levels in the MMPI-treated UV-irradiated cells significantly fell by 60% compared to untreated UV-irradiated cells. The level of total MMP-9 (pro and active form) in the MMPI-treated sham- and UV-irradiated cells fell by 20% and 50%, respectively compared to their untreated counterparts. These levels fell by 60% in the treated UV-irradiated cells in the presence of IL-1α compared to untreated UV-irradiated cells in the presence of IL-1α. In general, the expression of both MMP-2 and -9 expression was significantly reduced in MMPI-treated UV-irradiated HaCaT and Colo 16 cells in the presence and /or absence of IL-1α.

4.2.2 MMP-2 and MMP-9 mRNA expression

4.2.2.1 Time course of furin, MMP-2 and MMP -9

The aim of this study was to observe the effect UVB radiation had on MMP-2 and -9 mRNA expression in HaCaT and Colo 16 cells. Steady state mRNA levels of MMP-2 and -9 were assessed by qRT-PCR to observe if transcriptional regulation is occurring. Skiba *et al*. (136) showed that qRT-PCR is a useful tool in the analysis of quantitative changes of mRNA levels in cultured HaCaT cells after UV exposure.

As furin activates the gelatinases, MMP-2 and -9 (177), a time course (0-32 h) of its gene expression as well as those of MMP-2 and-9 in UVB-irradiated HaCaT and Colo 16 cells was investigated (Figure 4.25). Results from this experiment were used to determine if there is a relationship between the mRNA levels of these three proteases.

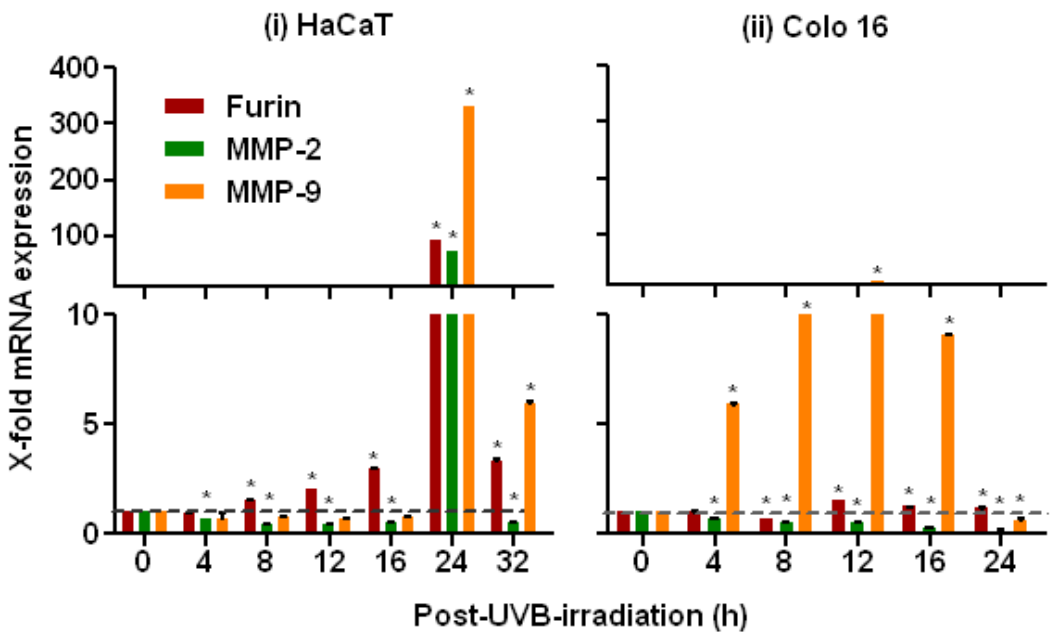

Figure 4.25 Time course of furin, MMP-2 and -9 mRNA induction/expression in UVB-irradiated HaCaT (i) and Colo 16 cells (ii). Control mRNA levels (=1) are represented as a dotted line. Results expressed are the mean ± SEM for three separate experiments. Statistical significance of the effect of UVB on furin, MMP-2 and -9 mRNA mRNA levels is shown as $p<0.05$ (*).

In this study, un-irradiated controls cells were given the value of unity at 0 h and mRNA expression was expressed as ratio to this value at the time points examined.

Results from this study show that in UVB-irradiated HaCaT cells, furin mRNA levels slowly increased with time reaching 3-fold at 16 h before rapidly increasing to a maximal level (91-fold) at 24 h before falling back to 3-fold at 32 h (Figure 4.25i). MMP-2 mRNA expression was relatively constant for the first 16 h post-irradiation, then rose to 73-fold at 24 h before falling to 50% at 32 h. MMP-9 gene expression was observed in HaCaT cells 4-32 h post UVB-irradiation. MMP-9 mRNA levels were maximal at 24 h (330-fold) post UVB-irradiation before falling to 6-fold at 32 h. Fisher *et al*. (80, 303) recently reported the increased induction of MMP-9 mRNA after UVB-irradiation of human skin *in vivo*. When plots of furin, MMP-2 and MMP-9 mRNA levels were constructed, an apparent strong correlation was observed between furin and MMP-2 ($r^2 = 0.999$), furin and MMP-9 ($r^2 = 0.999$), and MMP-2 and -9 ($r^2 = 1$) mRNA in UVB-irradiated HaCaT cells (Figure 4.26). It should be noted that due to the high values seen at 24 h, this heavily influences these curves and as such this value may not be correct.

Furin mRNA levels in UVB-irradiated Colo 16 cells, were higher than that seen in un-irradiated controls over the period 12-24 h with maximal levels observed at 12 h (1.5-fold) (Figure 4.26ii). The expression of the MMP-2 mRNA in UVB-irradiated Colo 16 cells was detected in very minimal amounts and remained fairly constant throughout the 24 h period. No dramatic increase in mRNA levels between time points were detected. However, in the UVB-irradiated Colo 16 cells, MMP-9 mRNA levels reached

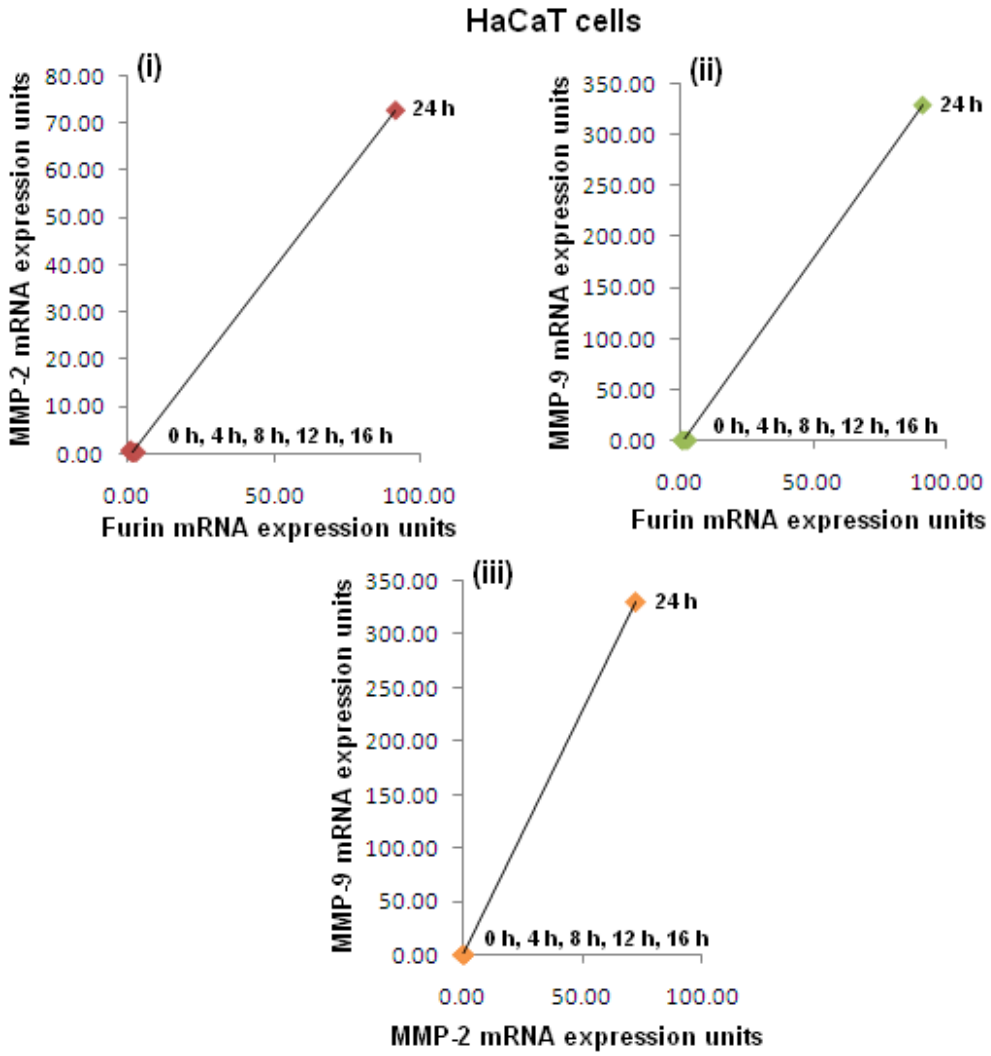

Figure 4.26 Correlation between the expression of furin and MMP-2 (i) and furin and MMP-9 (ii) and MMP-2 and -9 mRNA (iii) in UVB-irradiated HaCaT cells. The levels of furin, MMP-2 and -9 mRNA expressed in the cell extracts for UVB-irradiation were expressed as a ratio to that observed in sham-irradiated cells, the later was given a value of unity.

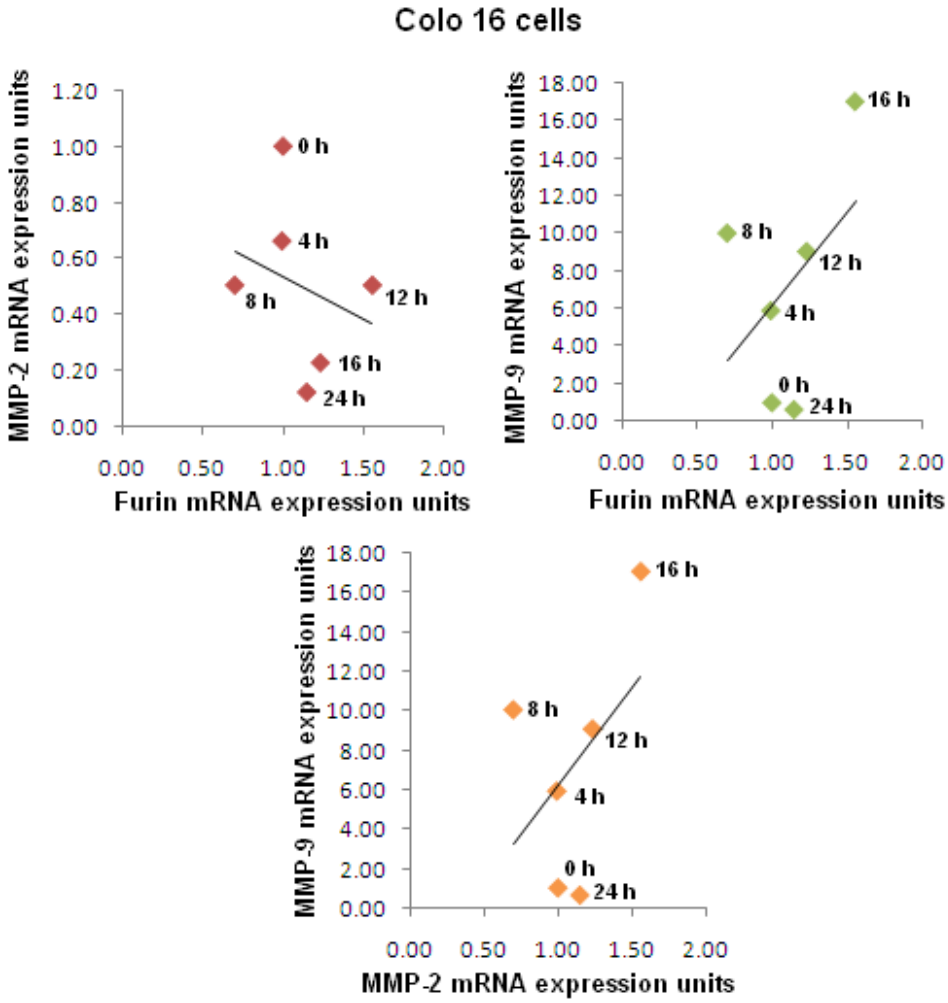

Figure 4.27 Correlation between the expression of furin and MMP-2 (i) and furin and MMP-9 (ii) and MMP-2 and -9 mRNA (iii) in UVB-irradiated Colo 16 cells. The levels of furin, MMP-2 and -9 mRNA expressed in the cell extracts for UVB-irradiation were expressed as a ratio to that observed in sham-irradiated cells, the later was given a value of unity.

maximal levels at 12 h (17-fold) after which they fell back to 9-fold at 16 h before falling by 40% to at 24 h post-irradiation. Following re-examination of the time points over the first 16 h it was found that when the plots of furin, MMP-2 and MMP-9 mRNA levels were constructed, no correlation was observed between the mRNA of these proteases in UVB-irradiated Colo 16 cells (Figure 4.27). This suggests that the result obtained in Figure 4.26 was heavily influenced by the 24 h time point. Therefore in light of this, it is unlikely that the expression of the mRNA of these proteins is related.

In conclusion, furin and MMP-2 mRNA was detected at low levels in UVB-irradiated HaCaT cells, except for a dramatic increase at 24 h. A similar finding was observed in Colo 16 cells. On the other hand, MMP-9 mRNA levels appeared to be high in both these cells post UVB-irradiation. While a strong correlation was observed among these proteases in HaCaT cells, the opposite effect was seen in Colo 16 cells.

4.2.2.2 Effects of UVR

MMP-2 and -9 mRNA was shown to be induced by UVB-irradiation in both HaCaT and Colo 16 cells (Figure 4.25). I extended that study to see if UVA and UVAB-irradiation had an effect on MMP-2 and -9 mRNA levels in the cell. I chose 24 h post-irradiation as the time point to perform this study.

In HaCaT cells, maximum induction of MMP-2 mRNA was observed in UVB-irradiated cells (73-fold) (Figure 4.28i). While MMP-2 mRNA levels were slightly increased (1.2-fold) in the UVA-irradiated cells, the levels were similar to that

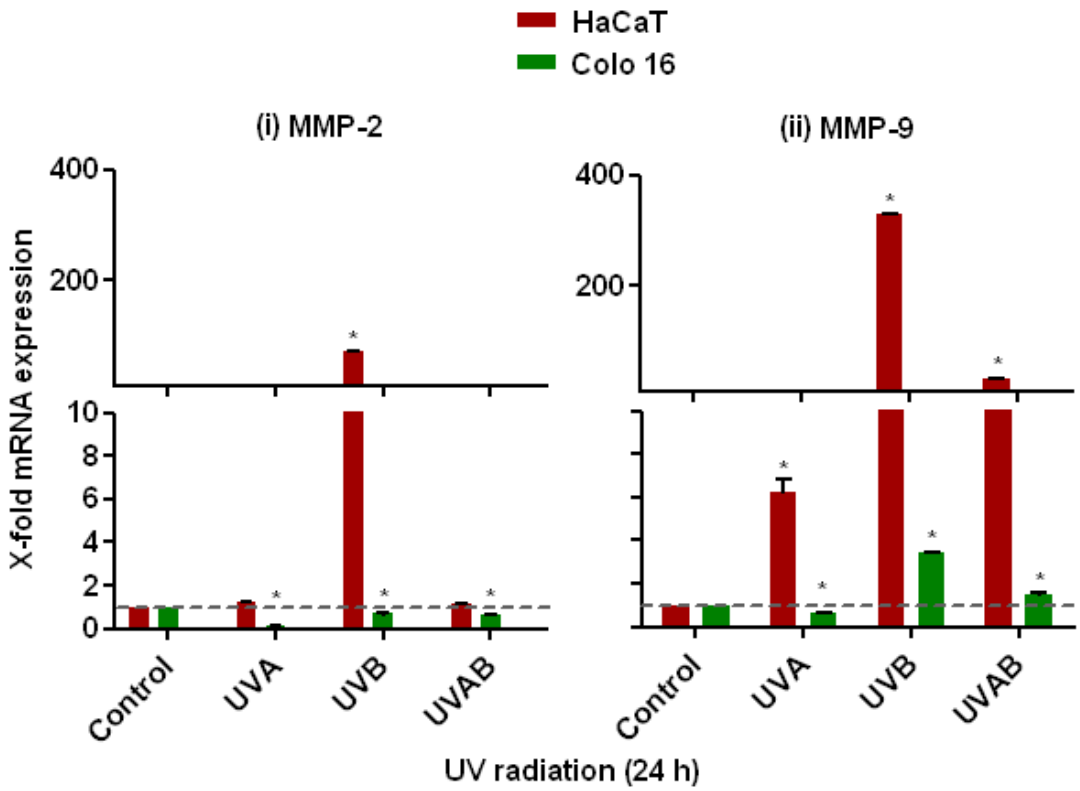

Figure 4.28 Effect of UVR on MMP-2 (i) and -9 mRNA induction/expression (ii) in HaCaT and Colo 16 cells. Cells were exposed to no-irradiation (controls), UVA, UVB and UVAB radiation and mRNA expression measured 24 h post-irradiation. Control mRNA levels (=1) are represented as a dotted line. Results expressed are the mean ± SEM for three separate experiments. Statistical significance of the effect of UVR on MMP-2 and -9 mRNA levels was shown as $p<0.05$ (*).

of controls in UVAB-irradiated cells HaCaT cells. However, maximal induction of MMP-2 mRNA was observed in response to UVB-irradiation.

On the other hand, maximal MMP-9 mRNA expression was seen in UVB-irradiated cells (330-fold) (Figure 4.28ii). MMP-9 mRNA levels were 6- and 31-fold higher in UVA- and UVAB-irradiated cells, respectively compared to that seen in the untreated controls. These results agreed with previous studies which showed that UVB radiation induced the expression of MMP-9 mRNA (80, 303).

In Colo 16 cells, MMP-2 mRNA levels were significantly lower irrespective of the UV doses when compared to the sham-irradiated controls. MMP-2 mRNA levels fell by 90%, 30% and 40% in UVA-, UVB- and UVAB-irradiated cells, respectively compared to the un-irradiated controls (Figure 4.28i). On the other hand, maximal MMP-9 mRNA expression was seen in UVB-irradiated cells (3.5-fold) (Figure 4.28 (ii)). While MMP-9 mRNA levels were decreased by 40% in the UVA-irradiated cells, it increased by 1.5-fold in UVAB-irradiated cells when compared to the sham-irradiated controls. However, the highest levels of MMP-9 mRNA expression were seen in UVB-irradiated cells.

Of interest was that, in both these cells, the highest expression of MMP-2 and -9 mRNA was induced by UVB-irradiation. The levels of MMP-2 and -9 mRNA were low in UVA-irradiated cells which was similar to that seen by Steinbrenner *et al*. (209) who showed that the steady-state mRNA level of MMP-2 and-9 was dose-dependently down-regulated 24 h after UVA-irradiation (300 kJ/m^2) in the NHEK cells.

4.2.2.3 IL-1α effects

4.2.2.3.1 Furin, MMP-2 and-9 mRNA expression

Following the addition of IL-1α, variation in MMP protein activity was observed in UVAB-irradiated cells (Figure 4.10). Similarly the addition of IL-1α caused maximal increase of MMP-2 and -9 protein expression in UVAB-irradiated HaCaT and Colo 16 cells (Figures 4.11 and 4.12). Therefore, UVAB radiation was chosen as the type of dose to observe the time course effect IL-1α has on furin, MMP-2 and -9 mRNA expression in irradiated HaCaT and Colo 16 cells.

The mRNA levels were measured using qRT-PCR (Section 2.9). In this method, the relative expression of the internal control gene (β actin) and target gene (furin, MMP-2 and -9) for each UV-irradiated sample with IL-1α at different time points was compared against the un-irradiated sample with IL-1α at 0 h. This was calculated using the Pfaffl Correction method (Appendix A.8) (225).

In HaCaT cells, furin mRNA levels fell below that of the sham-irradiated controls over the first 12 h before increasing to reach a maximal value at 16 h (5.3-fold) before falling to 4.2-fold at 24 h (Figure 4.29i). The expression of MMP-2 mRNA in these cells was reduced from 4-12 h after which it increased to 2-fold at 16 h before falling at 24 h to 82% that seen at 0 h following UVAB-irradiation. MMP-9 mRNA levels steadily decreased by 30% at 4 h before falling by 90% at 24 h in these cells. When plots of furin, MMP-2 and MMP-9 mRNA levels were constructed, a weak correlation between furin and MMP-2 ($r^2 = 0.258$), moderate correlation between furin and MMP-9

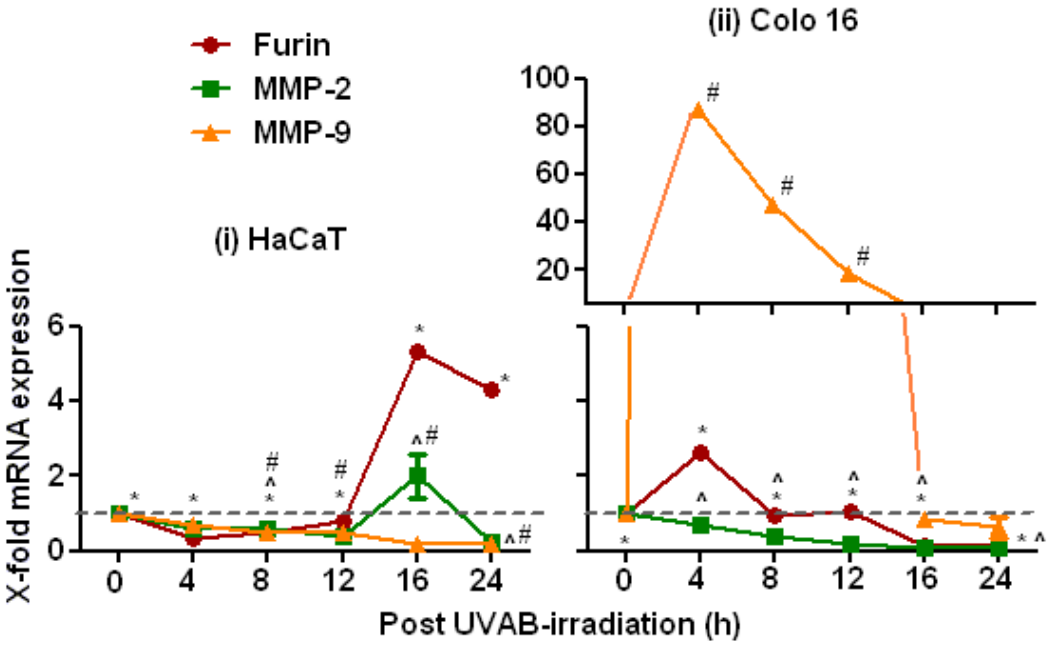

Figure 4.29 Time course of the effect of IL-1α on the expression of furin, MMP-2 and MMP-9 mRNA induction/expression in UVAB-irradiated HaCaT (i) and Colo 16 cells (ii). Cells were exposed to UVAB radiation and mRNA expression measured over 24 h post-irradiation. Control mRNA levels (=1) were represented as a dotted line. Results expressed are the mean ± SEM for three separate experiments. Statistical significance of the effect of UVAB radiation in the presence of IL-1α on gene expression is shown as $p<0.05$ for furin (*), for MMP-2 (^) and for MMP-9 (#).

(r^2 = 0.571), and no correlation between MMP-2 and -9 (r^2 = 0.002) mRNA in UV-irradiated HaCaT cells was observed (results not shown).

In Colo 16 cells, mRNA expression of furin fell following UV exposure in the IL-1α treated cells and remained low over the 24 h period (Figure 4.29ii). No significant differences in MMP-2 mRNA levels were seen between the different time points. MMP-2 mRNA expression decreased by 40% at 4 h before falling by 92% at 24 h. The expression of MMP-9 mRNA, on the other hand rose immediately following irradiation reaching a maximum level at 4 h (87.3-fold) before falling back at 24 h to 40% that seen at 0 h. When plots of furin, MMP-2 and MMP-9 mRNA levels were constructed, a weak correlation between furin and MMP-2 (r^2 = 0.337), strong correlation between furin and MMP-9 (r^2 = 0.789), and no correlation between MMP-2 and -9 (r^2 = 0.080) mRNA in UV-irradiated HaCaT cells was observed (results not shown).

In conclusion, MMP-2 mRNA levels were low throughout the 24 h time period in both HaCaT and Colo 16 cells. Of interest was that addition of IL-1α increased the expression of MMP-9 mRNA from UVAB-irradiated HaCaT and Colo 16 cells compared to that of furin and MMP-2 mRNA. These results suggest that IL-1α plays an important role in the activity (Figure 4.10), protein (Figures 4.11 and 4.12) and mRNA expression of MMP-2 and -9. These results agree with that of Han *et al.* (217) who found that the activation of proMMP-9 in skin inflammatory diseases likely occurs via a pathway including IL-1α. However, the time course of MMP-2 and -9 mRNA induction from UVAB-irradiated cells in the presence of IL-1α do not appear to be related to each

other however there does appear to be association between the time course of MMP-9 and furin mRNA induction.

4.2.3 Cell migration

4.2.3.1 Effects of UVR

Liang *et al*. (309) showed that the *in vitro* scratch assay is suitable for studies on (a) the effects of cell-matrix and cell-cell interactions on cell migration, (b) mimic cell migration during wound healing *in vivo* and it is compatible with the imaging of live cells during migration to monitor intracellular events. Todaro *et al*. (310) showed that the *in vitro* scratch assay is a straightforward, easy, well-developed and economical method to study cell migration *in vitro*. In order to study the migration and invasion potential of MMP-2 and -9 in A549 lung cancer cells, Hung *et al*. (311) used the *in vitro* scratch assay. Therefore, the rationale behind performing cell scratch assays was to determine the role of MMPs in cell migration in these irradiated cells. This method is based on previous observation that, upon creation of a new artificial gap, so called ‘‘scratch’’, on a confluent cell monolayer, the cells on the edge of the newly created gap will move toward the opening to close the ‘‘scratch’’ until new cell-cell contacts are established again (310).

HaCaT and Colo 16 cells were grown to 90% confluence (Section 2.8) and the scratch was created in the center of the cell monolayer by the gentle removal of the attached cells using a sterile plastic pipette tip. The ability of the cells to migrate into the distance between the scratch was assessed at 0, 24 and 48 h. Cell migration was quantified by measuring the readings of distance for each sample and each experiment

was repeated three times. An average of the readings was calculated and the results were represented as the distance (in mm) the cells migrated compared to that travelled by untreated controls (Appendix A.4).

In this study, similar findings were observed for HaCaT and Colo 16 cells. A representative phase contrast image of a time course recovery of cell scratch in sham- irradiated Colo 16 cells is shown in Figure 4.30. The distance between the scratch was maximum at 0 h. which was taken immediately after the scratch was done (Figure 4.30i). The width of the scratch in HaCaT and Colo 16 cell assays ranged between 5.0-5.5 mm.

At 24 h, the cells had migrated into the scratch as seen by the black arrows in Figure 4.30ii. But at 48 h, more cells had migrated into the scratch and the distance between the cell fronts had closed (Figure 4.30iii). Distance between the cells was quantified and results were analyzed based on the cell migration of sham-irradiated cells (Figure 4.31). The results suggest that maximal cell migration occurred 48 h after incubation. Therefore, in this study, 48 h time frame was chosen for measuring cell migration.

4.2.3.2 Effects of inhibitors

Parsy *et al*. (312) used synthetic and physiological protease inhibitors to investigate the invasion of UCC cells using the Matrigel assay. This group also suggested that in two-dimensional culture (scratch test), MMPs may not play a significant role in wound healing. Results from previous studies have shown that addition of inhibitors, Dec

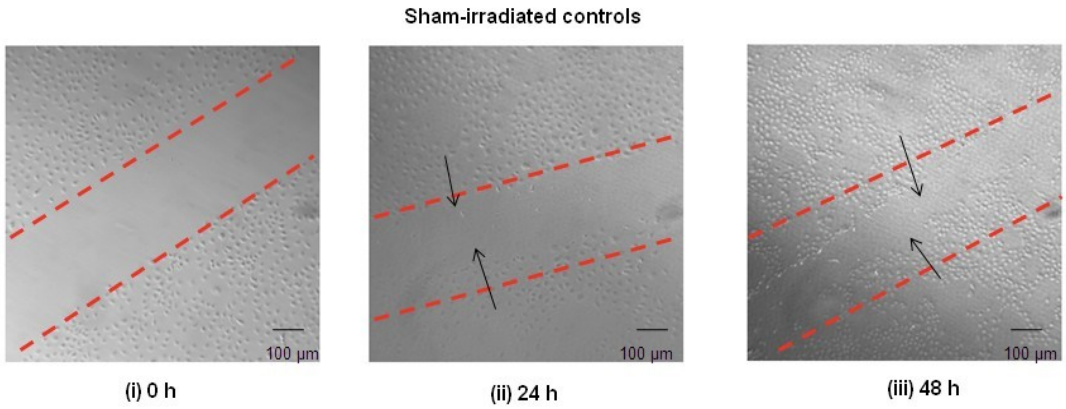

Figure 4.30 Measurement of individual cell migration in cell scratch assay. Sham-irradiated Colo 16 cells were "scratched" and images recorded 0, 24 and 48 h following treatment using phase-contrast microscopy. The red dotted lines mark the distance between the scratch. Black arrows represent the rate of cell migration.

RVKR cmk (Figure 4.17), 1, 10 phe (Figure 4.19) and MMPI (Figure 4.21) significantly reduces secretion of MMP-2 activity and completely inhibits MMP-9 activity in HaCaT and Colo 16 cells. The rationale behind this current study is to determine the effect These inhibitors have on MMP activity and the role they may play in cell migration. Therefore, the cell scratch assays were performed in the presence of Dec RVKR cmk, 1, 10 phe and MMPI. Cells were pretreated with these inhibitors and then exposed to UVR, 48 h after which, the distance cells migrated were quantified.

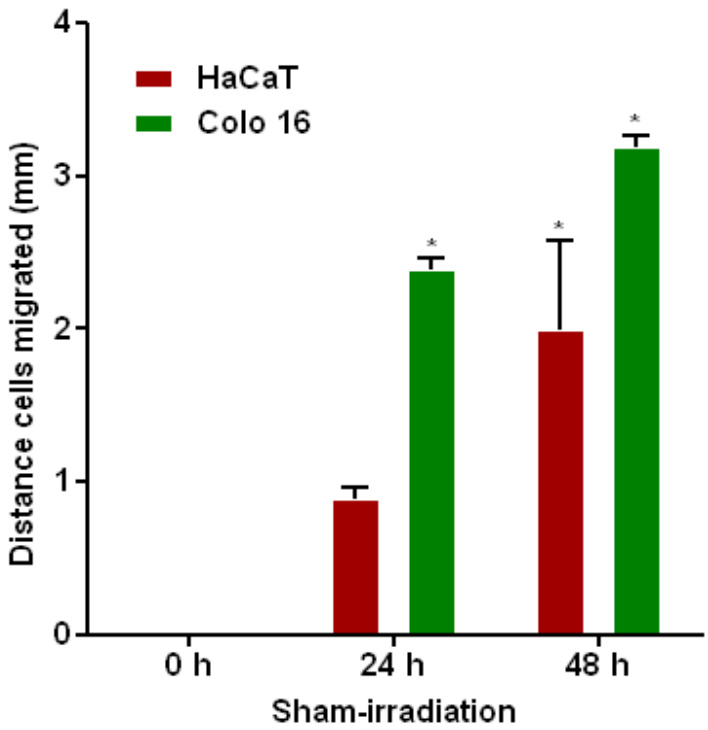

Figure 4.31 Effect of time course recovery on migration of sham-irradiated HaCaT and Colo 16 cells. Cell migration was determined 0, 24 and 48 h post treatment. Results expressed are the mean ± SEM for three separate experiments. Statistical significance is represented as $p<0.05$ for effect of different time courses on cell migration (*).

The effect of these inhibitors on MMP-9 activity secreted into the conditioned media of the cell scratch assay was evaluated by gelatin zymography (Section 2.7). The only difference was that the amount of cell proteins in cultures was not quantified as cells were permanently fixed with ethanol for the scratch assay analysis. Effect of the inhibitors on gelatinolytic activity of MMP-9 was authenticated by visual examination of these zymograms. The amount of microconcentrated conditioned media (50 µl) added per lane in the zymogen was similar.

4.2.3.2.1 Dec RVKR cmk

A representative phase contrast image showing the effect of Dec RVKR cmk on the migration of cells 48 h post UVAB-irradiation is shown in Figure 4.32. The distance between the cells was quantified and results were analyzed based on the effect of Dec RVKR cmk on cell migration of the UV-irradiated cells.

In HaCaT cells, the size of the scratch was 5.4 mm at 0 h (Figure 4.33i). After 48 h in culture the distance between the untreated sham-irradiated cells was 1.9 mm. The migration of UVA-, UVB- and UVAB-irradiated cells was reduced by 42.9%, 34.3% and 65.7%, respectively when compared to the untreated sham-irradiated cells. The migration of the cells treated with Dec RVKR cmk was significantly ($p<0.05$) reduced by 31.4% compared to the untreated sham-irradiated cells. Similar results were seen in the UV-irradiated cells treated with Dec RVKR cmk compared to their corresponding untreated irradiated cells. Cell migration was reduced by 40%, 17.4% and 98.3%

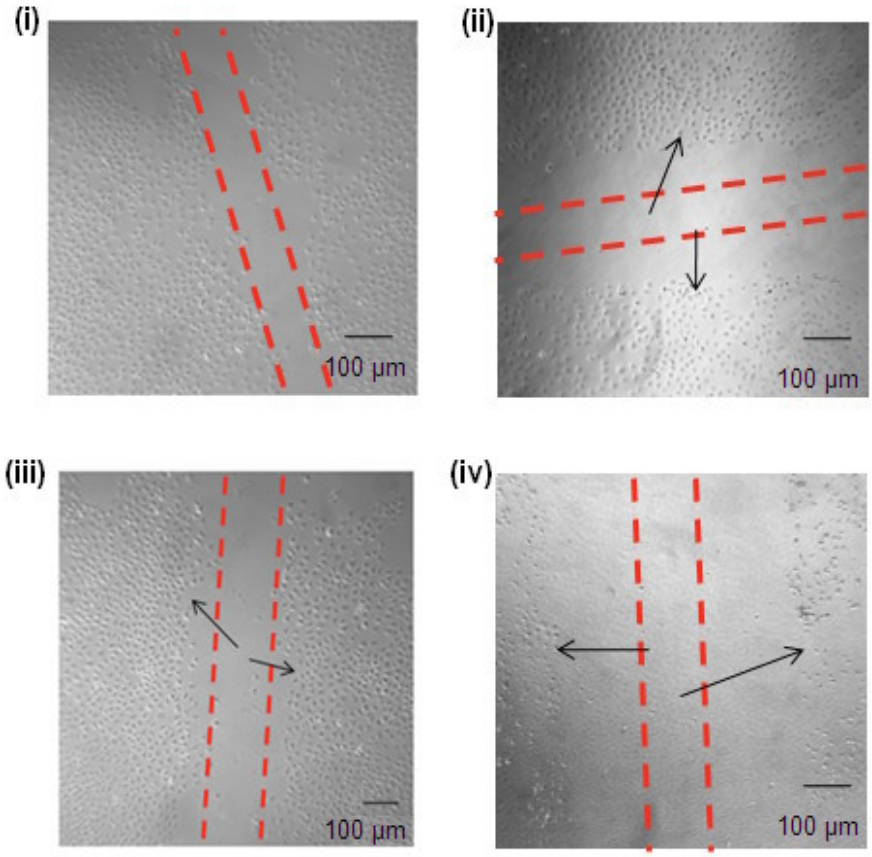

Figure 4.32 Cell scratch images showing the effect of Dec RVKR cmk on the migration of UV-irradiated Colo 16 recorded using the phase contrast microscopy 48 h post-irradiation. Cells were exposed to untreated sham-irradiated controls (i), treated sham-irradiated controls (ii), untreated UVAB-irradiated cells (iii) and treated UVAB-irradiated cells (iv). The red dotted lines mark the distance between the scratch. Black arrows represent the rate of cell migration.

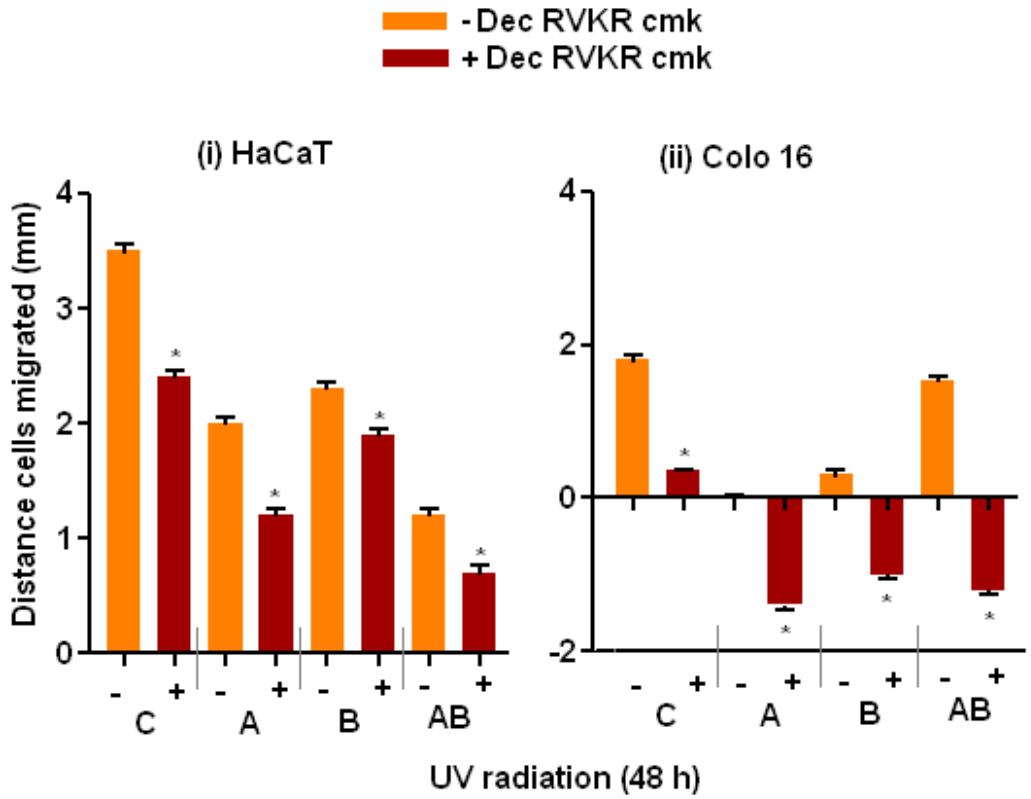

Figure 4.33 Effect of Dec RVKR cmk on the migration of UV-irradiated HaCaT (i) and Colo 16 cells (ii). Cell migration was determined 48 h post-UVR. Cells were exposed to sham-irradiation or controls (C), UVA (A), UVB (B) and UVAB (AB) radiation in the presence (+) or absence (-) of Dec RVKR cmk. Results expressed are the mean ± SEM for three separate experiments. Statistical significance for the effect of Dec RVKR cmk on cell migration of UV-irradiated cells is represented as $p<0.05$ (*).

in UVA-, UVB- and UVAB-irradiated cells, respectively compared to their untreated counterparts.

In Colo 16 cells, the size of the scratch was 5.0 mm at 0 h (Figure 4.33ii). After 48 h in culture the distance between the untreated sham-irradiated cells was 3.1 mm. The migration of UVA-, UVB- and UVAB-irradiated cells was reduced by 98.3%, 83.3% and 15%, respectively when compared to the untreated sham-irradiated cells. Following the addition of Dec RVKR cmk, the migration of these cells was significantly reduced by 80% compared to the untreated sham-irradiated cells. Similar results were seen in the UV-irradiated cells treated with Dec RVKR cmk compared to their corresponding untreated irradiated cells. Cell migration was reduced by 102%, 130% and 228% in Dec RVKR cmk treated UVA-, UVB- and UVAB-irradiated cells, respectively compared to their untreated counterparts. These treated UV-irradiated cells showed signs of regression.

Of interest, was that some of the Dec RVKR cmk-treated UV-irradiated cells detached during the 48 h period. This resulted in a widening of the distance between the cell front on scratch and the cells appeared to regress.

Complete loss of MMP-9 activity was observed when the conditioned media of the cell scratch assay was run on a gelatin zymograph. A representative zymograph showing the effect of Dec RVKR cmk on the activity of MMP-2 and -9 in the conditioned media of UV-irradiated HaCaT and Colo 16 cells is shown in Figure 4.34. This was similar to the zymographs seen in Figure 4.16.

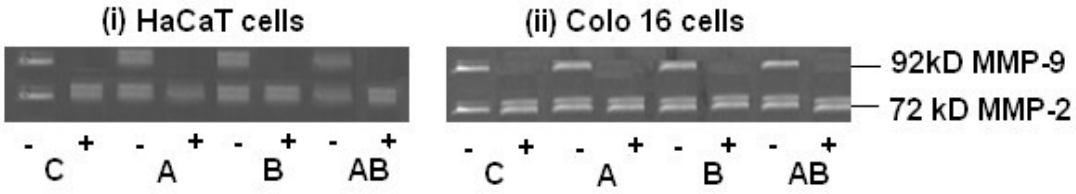

Figure 4.34 A representative zymograph showing the effect of Dec RVKR cmk on the gelatinolytic activity of MMP-2 and MMP-9 in conditioned media of UV-irradiated HaCaT (i) and Colo 16 cells (ii) collected 48 h post UV-irradiation. In each lane, 50 µl of microconcentrated conditioned media was added. The cells were exposed to sham-irradiation or controls (C), UVA (A), UVB (B) and UVAB (AB) radiation in the presence (+) or absence (-) of Dec RVKR cmk.

4.2.3.2.2 1, 10 phe

A representative phase contrast image showing the effect of 1, 10 phe on the migration of cells 48 h post UVAB-irradiation is shown in Figure 4.35. The distance between the cells was quantified and results were analyzed based on the effect of 1, 10 phe on cell migration of the UV-irradiated cells.

In HaCaT cells, the size of the scratch was 5.4 mm at 0 h (Figure 4.36i). After 48 h in culture the distance between the untreated sham-irradiated cells was 2.4 mm. The migration of UVA-, UVB- and UVAB-irradiated cells was reduced by 40.5%, 31.5%

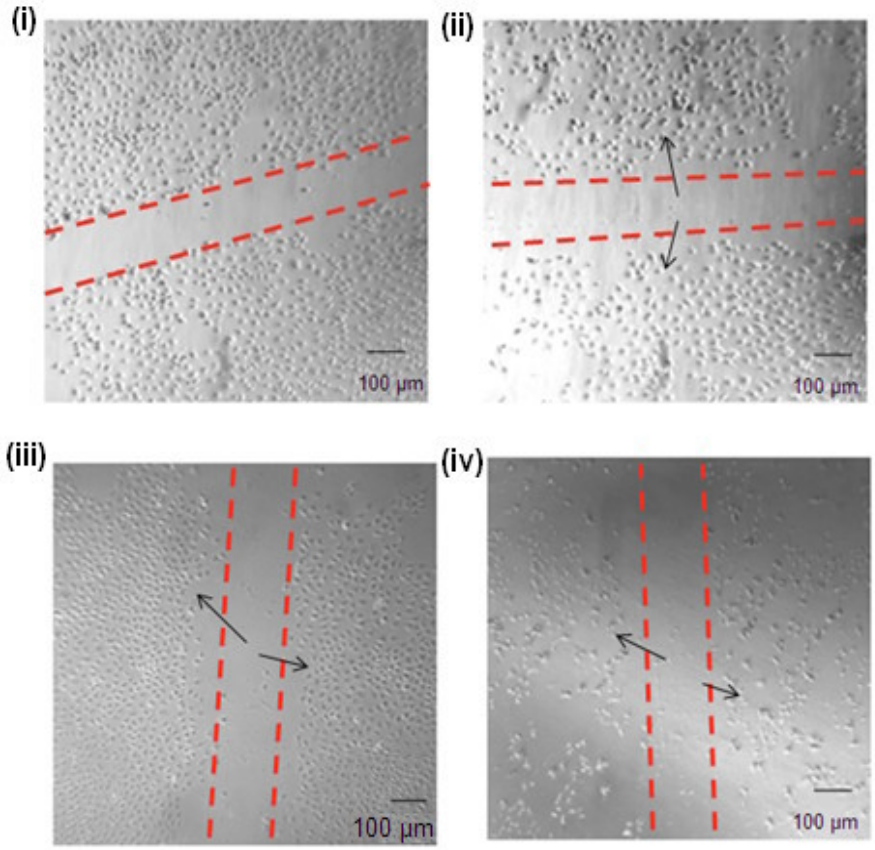

Figure 4.35 Cell scratch images showing the effect of 1, 10 phe on migration of UV-irradiated Colo 16 recorded using the phase contrast microscopy 48 h post-irradiation. Cells were exposed to untreated sham-irradiated controls (i), treated sham-irradiated controls (ii), untreated UVAB-irradiated cells (iii) and treated UVAB-irradiated cells (iv). The red dotted lines mark the distance between the scratch. Black arrows represent the rate of cell migration.

and 64.3%, respectively when compared to the untreated sham-irradiated cells. When 1, 10 phe was added, the migration of these cells was significantly ($p<0.05$) reduced by 32.1% compared to the untreated sham-irradiated cells. Similar results were seen in the UV-irradiated cells treated with 1, 10 phe compared to their corresponding untreated irradiated cells. Cell migration was reduced by 76%, 23% and 91% in UVA-, UVB- and UVAB-irradiated cells, respectively compared to their untreated counterparts.

In Colo 16 cells, the size of the scratch was 5.2 mm at 0 h (Figure 4.36ii). After 48 h in culture the distance between the untreated sham-irradiated cells was 3.5 mm. The migration of UVA-, UVB- and UVAB-irradiated cells was reduced by 98.2%, 81.6% and 6.1%, respectively when compared to the untreated sham-irradiated cells. Following the addition of 1, 10 phe, migration of these cells was significantly reduced by 63.2% compared to the untreated sham-irradiated cells. Similar results were seen in the UV-irradiated cells treated with 1, 10 phe compared to their corresponding untreated irradiated cells. Cell migration was reduced by 101%, 120% and 181% in 1, 10 phe treated UVA-, UVB- and UVAB-irradiated cells, respectively compared to their untreated counterparts. These treated UV-irradiated cells showed signs of regression. Of interest, was that the 1, 10 phe-treated UV-irradiated cells were detached over the 48 h period. This widened the distance between the cell front on scratch and the cells appeared to regress.

Complete loss of MMP-9 activity was observed when the conditioned media of the cell scratch assay was run on a gelatin zymograph. A representative zymograph showing the

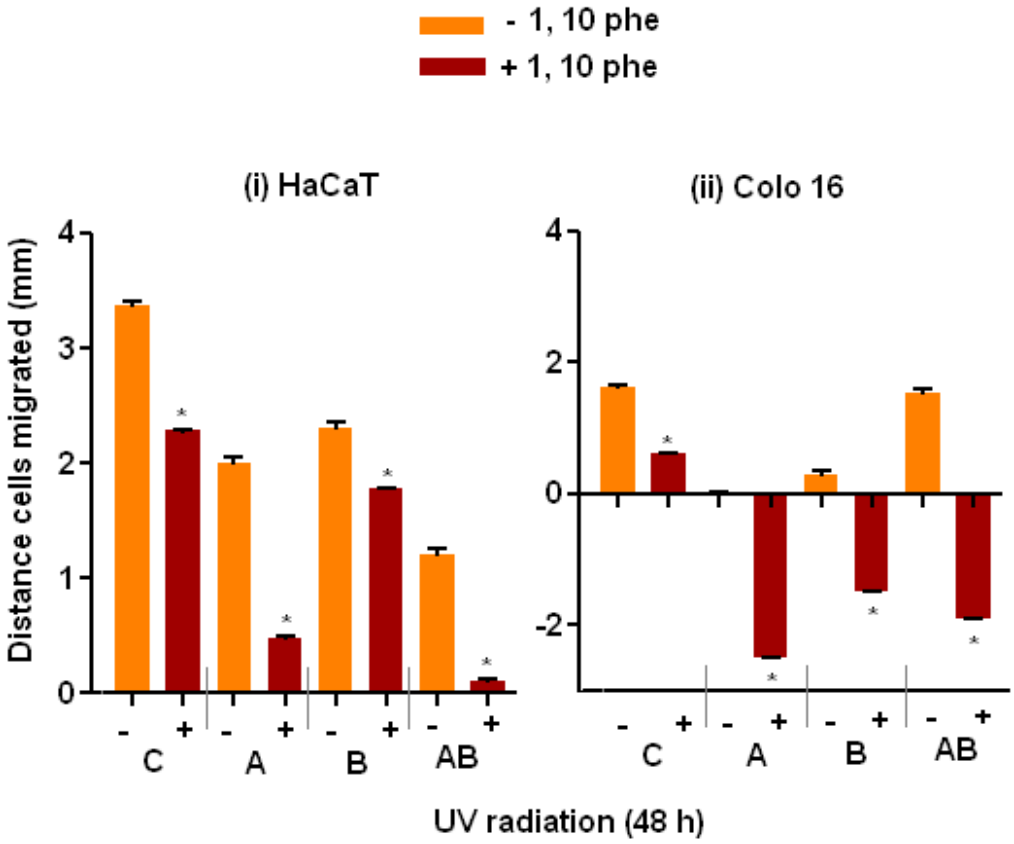

Figure 4.36 Effect of 1, 10 phe on the migration of UV-irradiated HaCaT (i) and Colo 16 cells (ii). Cell migration was determined 48 h post-UVR. Cells were exposed to sham-irradiation or controls (C), UVA (A), UVB (B) and UVAB (AB) radiation in the presence (+) or absence (-) of 1, 10 phe. Results expressed are the mean ± SEM for three separate experiments. Statistical significance for the effect of 1, 10 phe on cell migration of UV-irradiated cells is represented as $p<0.05$ (*).

effect of 1, 10 phe on the activity of MMP-2 and -9 in the conditioned media of UV-irradiated HaCaT and Colo 16 cells are shown in Figure 4.37. This was similar to the zymographs seen in Figure 4.18.

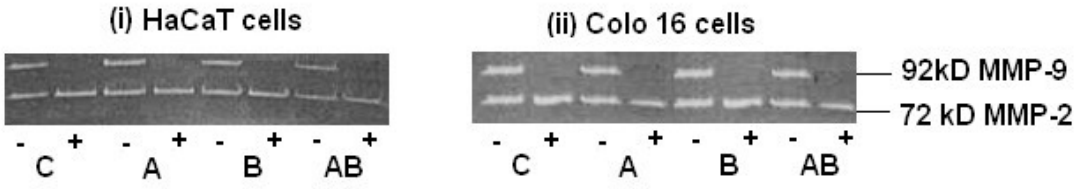

Figure 4.37 A representative zymograph showing the effect of 1, 10 phe on the gelatinolytic activity of MMP-2 and MMP-9 in conditioned media of UV-irradiated HaCaT (i) and Colo 16 cells (ii) collected 48 h post UV-irradiation. In each lane, 50 µl of microconcentrated conditioned media was added. The cells were exposed to sham-irradiation or controls (C), UVA (A), UVB (B) and UVAB (AB) radiation in the presence (+) or absence (-) of 1, 10 phe.

4.2.3.2.3 MMPI

A representative phase contrast image showing the effect of MMPI on the migration of cells 48 h post UVAB-irradiation is shown in Figure 4.38. The distance between the cells was quantified and results were analyzed based on the effect of MMPI on cell migration of the UV-irradiated cells.

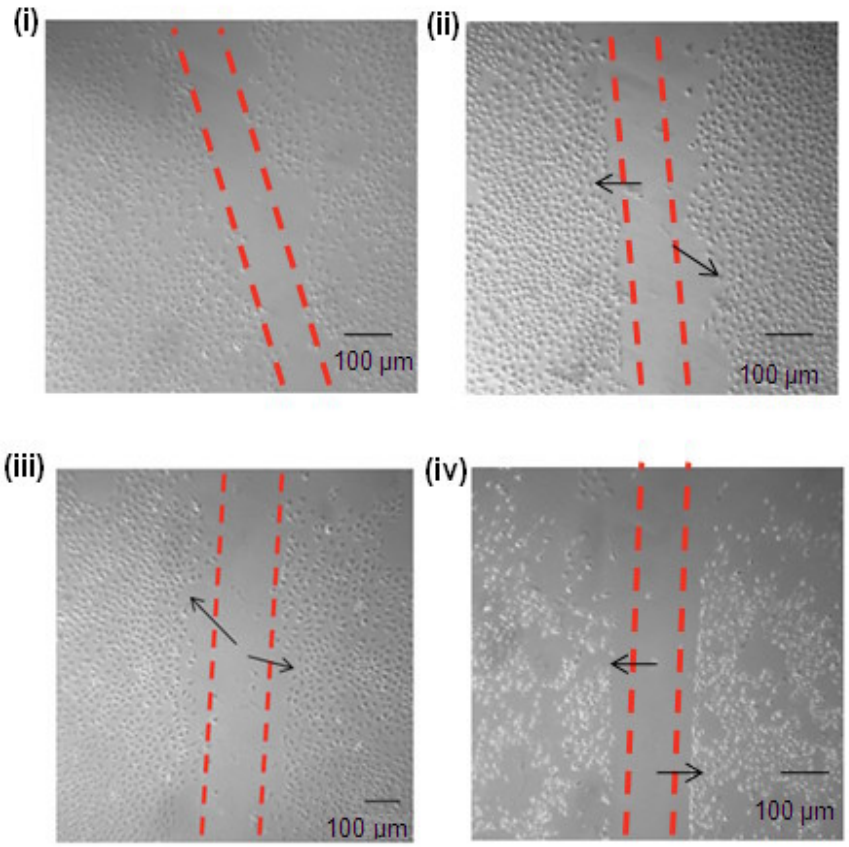

Figure 4.38 Cell scratch images showing the effect of MMPI on migration of UV-irradiated Colo 16 recorded using the phase contrast microscopy 48 h post-irradiation. Cells were exposed to untreated sham-irradiated controls (i), treated sham-irradiated controls (ii), untreated UVAB-irradiated cells (iii) and treated UVAB-irradiated cells (iv). The red dotted lines mark the distance between the scratch. Black arrows represent the rate of cell migration.

In HaCaT cells, the size of the scratch was 5.6 mm at 0 h (Figure 4.39i). After 48 h in culture the distance between the untreated sham-irradiated cells was 2.2 mm. The migration of UVA-, UVB- and UVAB-irradiated cells was reduced by 36.4%, 24.2% and 100%, respectively when compared to the untreated sham-irradiated cells. Following the addition of MMPI, the migration of these cells was significantly ($p<0.05$) reduced by 21.2% compared to the untreated sham-irradiated cells. Similar results were seen in the UV-irradiated cells treated with MMPI compared to their corresponding untreated irradiated cells. Cell migration was reduced by 76.2%, 36% and 40% in UVA-, UVB- and UVAB-irradiated cells, respectively when compared to their untreated counterparts.

In Colo 16 cells, the size of the scratch was 5.0 mm at 0 h (Figure 4.39ii). After 48 h in culture the distance between the untreated sham-irradiated cells was 2.1 mm. While the migration of UVA-irradiated cells increased by 6.5%, the migration of UVB- and UVAB-irradiated cells was reduced by 34.5% and 41.4%, respectively when compared to the untreated sham-irradiated cells. Following the addition of MMPI, the migration of these cells was significantly reduced by 31% compared to the untreated sham-irradiated cells. Similar results were seen in the UV-irradiated cells treated with MMPI compared to their corresponding untreated irradiated cells. Cell migration was reduced by 48.4%, 5.3% in UVA- and UVB-irradiated cells, respectively when compared to

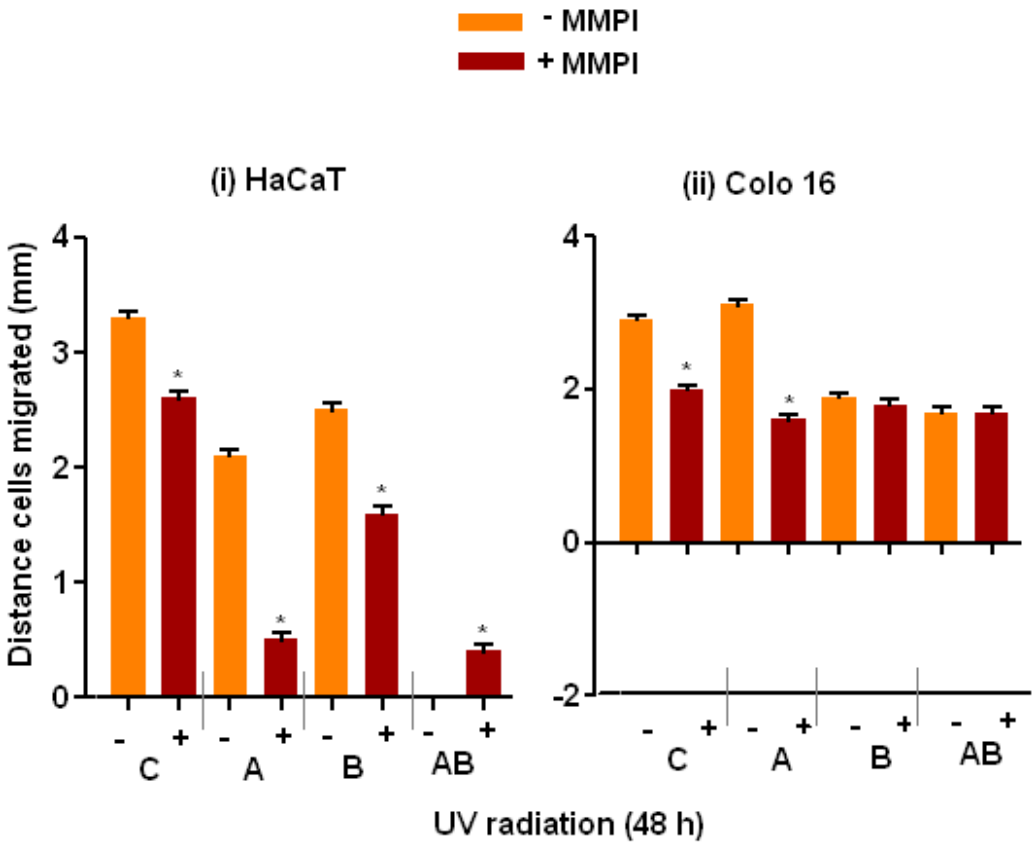

Figure 4.39 Effect of MMPI on the migration of UV-irradiated HaCaT (i) and Colo 16 cells (ii). Cell migration was determined 48 h post-UVR. Cells were exposed to sham-irradiation or controls (C), UVA (A), UVB (B) and UVAB (AB) radiation in the presence (+) or absence (-) of MMPI. Results expressed are the mean ± SEM for three separate experiments. Statistical significance for the effect of MMPI on cell migration of UV-irradiated cells is represented as $p<0.05$ (*).

their untreated counterparts. No change in cell migration was observed in MMPI-treated UVAB-irradiated cells when compared to their untreated counterparts.

Of interest, was that the MMPI-treated UV-irradiated cells showed some rate of migration. Complete loss of MMP-9 activity was observed when the conditioned media of the cell scratch assay was run on a gelatin zymograph. A representative zymograph showing the effect of MMPI on the activity of MMP-2 and -9 in the conditioned media of UV-irradiated HaCaT and Colo 16 cells is shown in Figure 4.40. This was similar to the zymographs seen in Figure 4.20.

.

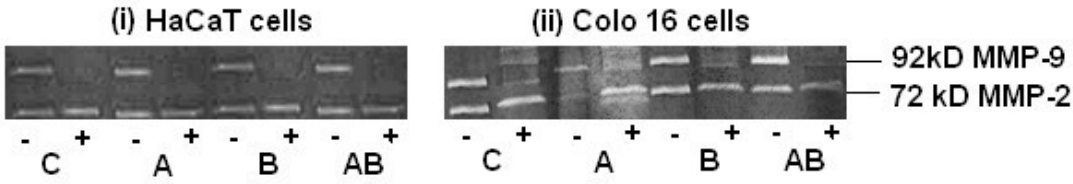

Figure 4.40 A representative zymograph showing the effect of UVR in the presence and/or absence of MMP inhibitor on gelatinolytic activity of MMP-2 and MMP-9 in conditioned media of HaCaT (i) and Colo 16 (ii) cells collected 24 h post UV-irradiation. In each lane, 50 µl of microconcentrated conditioned media was added. The cells were exposed to control or sham-irradiation (C) and UVB-irradiation (B) in the presence (+) or absence (-) of MMP inhibitor.

4.2.4 Summary

This study investigated the involvement of furin in the maturation and activation of MMP-2 and-9 in UV-irradiated skin cells. The level of MMP-2 and -9 activity in HaCaT cells (Figure 4.3) did not change in the 72 h period following exposure to UVR which differed to that seen in HEK (Figure 4.1) and Colo16 cells (Figure 4.4). Maximal MMP-2 and -9 activity was seen at 12 and 72 h in HEK and 24 and 72 h in Colo 16 cells. ProMMP-2 expression was higher than active MMP-2 in both HaCaT and Colo 16 cells (Figure 4.6). The level of active MMP-9 protein was only elevated in HaCaT cells exposed to either UVA or UVAB radiation. This result was not seen in Colo 16 cells (Figure 4.8). Of the other inhibitors used 1, 10 phe (Figure 4.19) and MMPI (Figure 4.21) both significantly decreased the activity of MMP-2 and -9 shed from UV-irradiated cells confirming that these proteases are matrix metalloproteases. When Dec RVKR cmk (furin inhibitor) was added to HaCaT and Colo 16 cells (Figure 4.17), there was a loss of MMP-9 activity in the media of the UV-irradiated cells, suggesting that furin is involved in its maturation.

Addition of IL-1α significantly increased MMP-9 activity (Figure 4.10), protein (Figures 4.11 and 4.12) and mRNA expression in HaCaT and Colo16 cells (Figure 4.29). The mRNA levels for furin, MMP-2 and -9 were maximal 24 h post UVB-irradiation in HaCaT cells after which they declined (Figure 4.25). In Colo 16 cells, maximal mRNA expression was seen at 12 h for furin, 0 h for MMP-2 and 12 h for MMP-9 post UVB-irradiation. There was a strong and positive correlation between furin and MMP mRNA levels in HaCaT (Figure 4.26) cells but not in Colo 16 cells (Figure 4.27). Cell migration assays performed 48 h post-UV irradiation showed that if

the MMPs were inhibited, the rate of cell migration was greatly reduced (Figures 4.33, 4.36 and 4.39). A similar finding was observed when the cells were treated with Dec RVKR cmk, suggesting that a reduction in MMP activity interferes with this process. Therefore, these results suggest that furin is the main PC involved in the processing of MMPs and inhibition of furin reduces MMP activity which suggests that specific inhibitors may have the potential to reduce the incidence of cancer spread and metastasis.

4.3 Discussion

In this chapter I investigated some of the cellular changes elicited by UVR on furin activation of MMPs in cultured keratinocyte-derived cell lines. In most of the experiments used in this study, only HaCaT and Colo 16 cells were used. HEK cells were not available in sufficient quantities and as such future studies should repeat such experiments using these cells.

4.3.1 MMP protein activity and expression

Both UVA and UVB radiation stimulate the expression and secretion of different MMPs *in vitro* and *in vivo* (80, 313-316). However, most of these *in vitro* studies have focused on fibroblasts (313-315). For human newborn foreskin keratinocytes (NHEK), which are the initial cellular target of UVR because of their location closer to the surface of the skin, much less data is currently available (209). In contrast to fibroblasts, the expression and secretion of MMP-1 in was slightly inhibited by UVA as well as by UVB-irradiation *in vitro* (316, 317). On the other hand, UVB-irradiation resulted in

enhanced expression and secretion of MMP-1, -3 and -9 in the epidermis and dermis (33, 80, 303). In keeping with these findings, the effect of UVA and/or UVB on the enzymatic activity of MMP-2 and -9 in my study was evaluated by using gelatin-zymography.

Kobayashi *et al*. (207) showed that both, MMP-2 and -9 gelatinases were detected in keratinocyte-conditioned media using zymography. The level of MMP-2 in the medium decreased after sequential passage, whereas MMP-9 was detected at a constant level. Onoue *et al*. (179) showed that in HNEK, secretion of MMP-2 remained at low levels under all conditions (24, 48 and 72 h) and MMP-9 secretion was stimulated by UVB-irradiation (7.5, 15, 30 or 60 mJ/cm^2). In my study, there was a biphasic shedding of both MMP-2 and -9 activity following UVB radiation in HEK cells. UVAB-irradiation of the HEK cells also induced significantly increased activity of both MMP-2 and -9 at 6, 48 and 72 h but in general was less than that seen for UVB (Figure 4.2).

While, the results from my study show that UVB-irradiation induced maximal MMP-9 activity similar to that seen in studies by Onoue *et al*. (179), major difference was seen with respect to MMP-2 activity which was also shown to be increased following a similar trend to that seen for MMP-9. Therefore, results from my study showed that UVB induces maximal gelatinolytic activity (MMP-2 and -9). UVAB also had an increased effect on the cells probably due to the fact that when cells were irradiated with UVA (40 kJ/m^2) and then immediately with 2 kJ/m^2 of UVB, the latter dose appeared to be of predominance, dominating the effect of UVA. There have been

reports showing the formation of apoptotic sunburn cells caused by UVB-irradiation (89). UVB-irradiation together with stimulation by high Ca^{2+} concentrations were also shown to cause apoptosis of keratinocytes in culture (302). In keeping with this finding, it can be said that the increase in MMP-2 and -9 secretions from keratinocytes after UVB-irradiation might result from cells undergoing apoptosis.

It is known that UVA-irradiation can induce the expression of a number of genes, including MMP-1 (316), MMP-2 and -3 (318) and heme oxygenase-1 (HO-1) (319) in human dermal fibroblasts. On the other hand, in epidermal keratinocytes the cellular effects of UVA-irradiation seems to be more diverse. The expression of MMP-1 and HO-1 in keratinocytes is only marginally affected by UVA (316, 320). In my study, UVA-irradiation of HEK cells caused a dose-dependent decrease of MMP-2 and -9 activity over the 72 h time period (Figure 4.2). These results agreed with studies by Onoue *et al*. (179) who suggested that MMP-9 activity was not induced by UVA (20 and 40 J/cm^2) in NHEK cells. Steinbrenner *et al*. (209) also suggested that irradiation of NHEK with a single dose of 30 J/cm^2 UVA reduced MMP-2 activity by 74% and MMP-9 activity by 66% compared to mock-irradiated cells 24 h post-irradiation.

Several cellular effects of UVA are mediated by singlet oxygen (O^-) (321-323). Applegate *et al*. (320) reported a 2.5-fold higher basal activity of the enzyme HO-1, which is involved in a cellular defence system against oxidative stress in NHEK compared with fibroblasts. Furthermore, the same authors measured a lower damage of cell membranes upon UVA-irradiation in NHEK compared with fibroblasts. Biologically, such a higher antioxidant capacity of NHEK makes sense, because these

cells are located in the upper layers of the skin and may represent the first line of defence against oxidative challenge. The UVA-induced down-regulation of MMPs in normal keratinocytes, seems contradictory, but is consistent with a hypothesis of different roles of the epidermal and the dermal compartment of the skin in the UV-induced ECM degradation similar to that seen previously (317). According to this hypothesis, the production of MMPs is directly enhanced by UVA-irradiation only in fibroblasts, whereas UV light is not able to increase MMP production of NHEK.

Bredin *et al*. (324) showed the presence of MMP-2 and -9 activity in human non-small cell lung cancer cell lines. Metastatic cancer cells including human hepatoma (HepG2), fibrosarcoma (HT1080), breast cancer (MCF-7 and MDA-MB-231), colon cancer (HCT 116) and melanoma A 2058 cells secrete large amounts of MMPs (325). In this study, effect of UVR in Colo 16 cells followed a similar pattern to that observed in HEK cells with UVB having a biphasic effect on MMP-2 (highest at 24 h) and -9 (highest at 24 and 72 h) activity, followed by an increase in response to UVAB (24 and 72 h) with UVA having very minimal effect (Figure 4.4). Roomi *et al*. (325) also suggested that when normal human dermal fibroblasts (NHDF) were co-cultured with melanoma, HepG2 or HT-1080 cells, there was a dramatic increase in MMP expression. Both MMP-2 and -9 expression increased significantly in HepG2 and HT-1080 cancer cells; while highest increases were seen in melanoma cells. Therefore, as part of future experiments, NHDF can be co-cultured with Colo 16 cells in order to determine if UVR further enhances the activity of these gelatinases.

Baumann *et al*. (326) showed the induction of MMP-9 in HaCaT cell line was less than that seen in ras-transfected tumorigenic HaCaT clones (A-5). Bachmeier *et al*. (327) showed that the conditioned media of the malignant II-4RT (malignant, tumorigenic human keratinocyte cell line) cells contain significantly more MMP-2 and -9 than that seen in HaCaT or A5 (benign, tumorigenic human keratinocyte cell line) cells. Similar to these findings, results represented in Figure 4.3 showed that the level of MMP-2 and -9 activity in HaCaT cells did not change in the 72 h period following exposure to UVR. Minimal gelatinolytic activity was observed in these non-tumorigenic cells. This differed to that seen in HEK and Colo16 cells. This was in line with studies by Steinbrenner *et al*. (209) who observed that in contrast to NHEK, the supernatants of HaCaT cells, only MMP-2 was found and its activity was not affected by UVA-irradiation.

In order to confirm the nature of the MMPs in the zymographs of keratinocyte-derived cell supernatants, western blotting was performed. This study helped to determine the cellular expression of MMP-2 and -9. Cell lysates were assessed by immunoblotting for the production of MMP using anti MMP-2 and anti MMP-9 antibodies so both pro and active forms of MMP-2 and -9 would be detected, respectively. Results from my study show that in HaCaT cells, the expression of total MMP-2 (pro and active form) levels decreased in UVA-irradiated cells (20%) compared to the sham-irradiated controls and no change in MMP-2 levels were seen in UVB- and UVAB-irradiated cells (Figure 4.6i). In Colo 16 cells, the expression of total MMP-2 levels was highest in UVA-irradiated cells (2.5-fold) compared to the sham-irradiated controls while those in the UVB- or UVAB-irradiated cells were only elevated 2.2-fold (Figure 4.16ii).

In conclusion, UVR induced higher proMMP-2 and active MMP-2 levels in the tumour cell line Colo 16 cells compared to that seen in the non-tumorigenic HaCaT cells where reduced levels were observed. This agreed to studies by Schmalfeldt *et al*. (328) who showed that total MMP-2 activity (pro and active form) and the ratio of activated MMP-2: proMMP-2 was higher in metastatic ovarian cells when compared to the primary tumour. This could suggest that conversion of proMMP-2 to active MMP-2 is an important step in the transition from a benign to a malignant tumour.

On the other hand, in HaCaT cells, there was no change in the expression of total MMP-9 (pro and active form) levels in UVA- and UVB-irradiated cells. MMP-9 levels increased to 1.7-fold in UVAB-irradiated cells compared to un-irradiated controls (Figure 4.8i). In Colo 16 cells, the expression of total MMP-9 levels decreased in UVA-irradiated cells (20%) compared to the sham-irradiated controls, while they were similar (1.1-fold) in the UVB- and UVAB-irradiated cells (Figure 4.8ii). Therefore, MMP-9 levels in UVA-irradiated cells was similar to studies by Steinbrenner *et al*. (209) who showed that MMP-9 protein expression of NHEK was down-regulated by UVA-irradiation. The results from my study suggest that while active MMP-9 was the predominant form seen in HaCaT cells, the proform was higher in the Colo 16 cells. A possible explanation is that an increase in the active enzyme form could lead to metastatic process and increased malignancy, for example, via enhanced angiogenic activity (329).

Total levels of MMP-2 and -9 (pro and active form) expression in HaCaT and Colo 16 cells is expressed as a percentage in Tables 4.1 and 4.2, respectively. Level of protein

UV type	0 μg IL-α				10 μg IL-1α			
	C	A	B	AB	C	A	B	AB
proMMP-2	64	48	63.2	63.5	62	75.1	76.2	80.3
active MMP-2	36	34	41.3	38.9	38	32.3	41.3	37.5
Total	100	81.9	104.5	102.4	100	107.4	117.5	117.8
proMMP-9	28.6	30.3	36.3	47.9	53	190.7	450	516.8
active MMP-9	71.4	80.6	60.8	121.4	47	187.5	403.6	490.2
Total	100	110.8	97.1	169.3	100	378.3	853.6	1007

Table 4.1 Effect of UVR on the expression of MMP-2 and -9 in IL-1α treated irradiated HaCaT cells.The pro and active forms of MMP-2 and -9 represent the average values of three separate experiments. Total levels (pro and active form) of protein in eachIL-1α untreated UV-irradiated cells have been compared to the untreated sham-irradiated cells(pro and active MMP-9 = 100%) and is expressed as a percentage. Total levels (pro and active form) of protein in eachIL-1α treated UV-irradiated cells have been compared to treated sham-irradiated cells(pro and active MMP-9 = 100%)and is expressed as a percentage.

UV type	0 μg IL-α				10 μg IL-1α			
	C	A	B	AB	C	A	B	AB
proMMP-2	64	139.4	127	137.3	62	104.2	125.2	135.4
active MMP-2	36	112.3	86.4	90.1	38	100.3	113.5	122.5
Total	100	251.7	213.4	227.4	100	204.5	238.7	257.8
proMMP-9	55.5	40.6	60.9	67.1	53	687.6	2206.2	2487.5
active MMP-9	44.5	42.7	51.2	48.7	47	607.3	2146.9	2284.6
Total	100	83.4	112.1	115.8	100	1294.9	4353.1	4772.1

Table 4.2 Effect of UVR on the expression of MMP-2 and -9 in IL-1α treated irradiated Colo 16 cells. The pro and active forms of MMP-2 and -9 represent the average values of three separate experiments. Total levels (pro and active form) of protein in eachIL-1α untreated UV-irradiated cells have been compared to the untreated sham-irradiated cells (pro and active MMP-9 = 100%) and is expressed as a percentage. Total levels (pro and active form) of protein in eachIL-1α treated UV-irradiated cells have been compared to treated sham-irradiated cells (pro and active MMP-9 = 100%)and is expressed as a percentage.

in each sample was compared to that in un-irradiated controls (pro and active MMP-9 = 100%) and is expressed as a percentage. The data from Table 4.1 show that the pro and active MMP-2 levels in UVA-irradiated HaCaT cells were lower when compared to the un-irradiated cells. Levels of MMP-2 were higher in UVB- and UVAB-irradiated cells. On the other hand, the pro and active forms of MMP-9 were the highest in UVAB-irradiated cells. The data from Table 4.2i show that the pro and active MMP-2 levels in UVA-irradiated Colo 16 cells were slightly higher when compared to UVB- and UVAB-irradiated cells. On the other hand, the pro and active forms of MMP-9 were the lowest in these cells.

Of interest, was that in Colo 16 cells, protein expression of MMP-9 (Figure 4.8ii) was not observed in significant amounts but increased MMP-9 activity (Figure 4.4) was observed. These results could be because very minimal amount of MMP-9 was present on the cell membrane but was shed in significant amounts into the media. Therefore, a better understanding of the protease cleavage mechanisms or use of a bank/cocktail of different protease inhibitors (e.g. serine, aspartic proteases) on MMPs will help in a better understanding of this mechanism.

4.3.2 Effects of IL-1α on MMP activity and expression

Although the proteolytic activation of proMMP-9 has been documented extensively in many pathologic conditions including inflammation and tumour metastasis, the cellular factors that control this process have not been identified. Because there is a close association between inflammation and MMP-9 activation in these conditions, we postulated that IL-1α may have a prominent role in the regulation of this process. Han *et*

al. (6, 330) previously identified TNFα to be a potent stimulator for MMP-9 activation in the human skin. On the basis of similar biologic functions and intracellular signalling pathways controlled by TNFα and IL-1α, Han *et al*. (217) recently showed that IL-1α has been identified as a potent factor inducing the proteolytic activation of proMMP-9 in human skin. Therefore in this study, effect of UVR in the presence and/or absence of IL-1α (10 ng/ml) on MMP-2 and-9 activity in keratinocyte-derived cells was determined.

Results from this study suggests that on addition of IL-1α, increased MMP activity was observed in UVA- and UVB-irradiated cells (HEK, HaCaT and Colo 16) (Figure 4.10). Variation in MMP activity was observed in UVAB-irradiated cells following the addition of IL-1α. Level of MMP-2 activity (65.4 au/mg cell protein) was decreased in HEK cells. While MMP-2 (34.3 au/mg cell protein) and -9 activity (29.6 au/mg cell protein) was reduced in HaCaT cells, MMP-9 activity (697.3 au/mg cell protein) was decreased in Colo 16 cells. The reason for this variation was not clear.

In order to investigate changes in cellular expression of MMP-2 and -9 in the presence of IL-1α, western blots were performed. These results suggested that following the addition of IL-1α to UVAB-irradiated HaCaT (Figure 4.11) and Colo 16 cells (Figure 4.12), MMP-9 levels were much higher than MMP-2 levels. Total levels of MMP-2 and -9 (pro and active form) expression in the presence and/or absence of IL-1α in these cells is expressed as a percentage in Tables 4.1 and 4.2. Level of protein in each sample was compared to that in un-irradiated controls (pro and active MMP-9 = 100%) and is expressed as a percentage. Results from Table 4.1 show that

level of the pro and active MMP-2 levels in UVA-irradiated HaCaT cells were slightly higher when compared to the IL-1α treated un-irradiated cells. Levels of MMP-2 were similar in UVB- and UVAB-irradiated cells. On the other hand, increasing levels of the pro and active forms of MMP-9 were observed in UV-irradiated cells when compared to the controls with the highest increase in UVAB-irradiated cells. The data from Table 4.2 show that the pro and active MMP-2 levels in UV-irradiated cells were higher when compared to that seen in IL-1α treated un-irradiated controls. The highest increase was observed in UVAB-irradiated cells. A similar finding was observed for the level of MMP-9 (pro and active form) expression in these cells.

Therefore, the results suggest that addition of IL-1α plays a role in MMP-9 activation which may contribute to the pathogenesis of inflammatory conditions such as cancer metastases and chronic wounds. IL-1α may promote the conversion of proMMP-9 into its active form as suggested by Han *et al*. (217) either by slowly inducing an activator or promoting down-regulation of an inhibitor such as TIMP-1. This conclusion was based on three facts: (1) TIMP-1 binds pro-MMP-9 at its C-terminus (331), (2) the activation of pro-MMP-9 by IL-1α correlates with downregulation of TIMP-1 (217) and (3) recombinant TIMP-1 can inhibit directly the skin-mediated conversion of pro-MMP-9 (332).

It should be noted that addition of IL-1α did not increase furin protein levels in the cells (Figure 3.10). Therefore, the fact that this pro-inflammatory cytokine causes MMP-9 stimulation via a “feed-through” mechanism from furin may be ruled out. In order to further investigate, if the factors responsible for the activation of proMMP-9 by human

skin cells are present in these pure cell cultures or may originate from other resident skin cells, co-culture experiments with fibroblasts should be performed as part of future experiments. Han *et al*. (217) investigated the possibility of cell-interactions as a cause for proMMP-9 activation but observed only the induction of proMMP-9 but not its proteolytic activation.

4.3.3 MMP mRNA expression

Fisher *et al*. (80, 303) recently reported the induction of MMP-9 mRNA after UVB-irradiation of human skin i*n vivo*. In this study, UVB-irradiation was shown to induce maximal MMP-2 and -9 activity (Figures 4.2, 4.3 and 4.4). In order to expand on this work by determining if transcriptional regulation occurred, the effect of UVB on MMP-2 and -9 mRNA expression in HaCaT and Colo 16 cells was determined. Steady-state mRNA levels of MMP-2 and -9 were assessed by qRT-PCR in order to find out if transcriptional regulation occurred. Skiba *et al*. (136) showed that qRT-PCR is a useful tool in the analysis of quantitative changes of mRNA levels in cultured HaCaT cells after UV exposure. This is a highly sensitive and reproducible method and thus was used to analyze mRNA levels of different genes of interest in HaCaT and Colo 16 cells following exposure to UVR.

Furin plays a potential role in the activation of the gelatinases, MMP-2 and -9 (177). Therefore, in order to quantify the gene expression of furin, MMP-2 and-9, a time course gene induction in response to UVB-irradiation was determined in HaCaT and Colo 16 cells (Figure 4.25). Results from this experiment helped to investigate the relationship between MMP-2 and -9 mRNA to furin mRNA levels. In UVB-irradiated

HaCaT cells, maximum induction of furin mRNA was seen at 24 h (90-fold) (Figure 4.25i). MMP-2 mRNA expression was relatively constant throughout the 32 h time course except for an increase observed at 24 h (73-fold). MMP-9 mRNA induction reached a maximum at 24 h (329.6-fold) post UVB-irradiation. While there are not many reports from literature about the effect of UVB on mRNA expression in Colo 16 cells, results from this study suggests that the expression of the furin gene in UVB-irradiated Colo 16 cells, was maximum at 12 h (1.6-fold). While, no dramatic increase of MMP-2 mRNA levels between timepoints was detected, MMP-9 showed maximum induction at 12 h. Therefore, in conclusion, in, HaCaT cells, furin and MMP-2 is detected at low levels except for a dramatic increase at 24 h. A similar trend was observed in Colo 16 cells. MMP-9 mRNA levels appeared to be high in both these cell lines post UVB-irradiation. This was similar to studies by Egeblad *et al*. (333) and Wagenaar-Miller *et al*. (334) who showed that the tumour tissue levels of MMP-9 are elevated compared with the corresponding normal tissue in a variety of cancer types, including breast, colon, and gastric cancers. Zucker *et al*. (335) also showed that in human colorectal adenocarcinomas, the MMP-9 mRNA and the MMP-9 plasma protein levels were increased when compared with normal individuals. Further evidence comes from reports by Zeng *et al*. (336) who showed increased levels of MMP-9 in liver metastasis.

When plots of furin, MMP-2 and MMP-9 mRNA levels were constructed, strong correlation was observed between furin and MMP-2, furin and MMP-9, and MMP-2 and -9 mRNA in UV-irradiated HaCaT cells (Figure 4.26). These results show that the 24 h time point heavily influences this outcome, and to confirm that this observation is

correct other time points would need to be investigated. On the other hand, in Colo 16 cells, weak correlation was observed between these genes of interest (Figure 4.27). In order to elucidate the effect of other UV types and doses on MMP-2 and -9 gene expression 24 h post-irradiation, the effects UVA and UVAB-irradiation on MMP-2 and -9 gene expression was determined.

In HaCaT cells, MMP-2 mRNA levels in UVA- and UVAB-irradiated cells were similar compared to sham-irradiated controls (Figure 4.28). On the other hand, MMP-9 mRNA levels were 6- and 31-fold higher in response to UVA and UVAB, respectively (Figure 4.26 (ii)). In Colo 16 cells, UVA- and UVAB-irradiation induced a significant decrease in MMP-2 mRNA levels, compared to sham-irradiated controls (Figure 4.26). While MMP-9 mRNA expression was lower in UVA-irradiated cells, it slightly increased in UVAB-irradiated cells. Results from this study agreed to previous reports by Steinbrenner *et al*. (209) who showed that the steady-state mRNA level of MMP-2 and -9 was dose-dependently down-regulated 24 h after UVA-irradiation (300 kJ/m^2). Of interest was that, in both these cell lines, the greatest expression of MMP-2 and -9 genes were induced by UVB-irradiation. The results of this present study further confirm previous studies where UVB radiation has been shown to be significant inducers of MMP-9 in skin cells (80, 303).

Results shown in Figure 4.10 showed that UVAB in the presence of IL-1α clearly decreases MMP-2 and/or -9 protein activity. Similarly, the results in Figures 4. 11 and 4.12 show that IL-1α caused maximal increase of MMP-2 and -9 protein expression in UVAB-irradiated HaCaT and Colo 16 cells, respectively. Therefore. UVAB radiation

was chosen as the type of dose to elucidate the effect of IL-1α on MMP-2 and -9 mRNA expression in HaCaT and Colo 16 cell lines. In order to investigate the association of these genes of interest against furin mRNA levels, a time course gene induction of furin, TACE and TNFα mRNA levels in response to UVAB-irradiation in the presence of IL-1α was determined.

In HaCaT cells, mRNA expression of furin was highest at 16 h (5.3-fold) when compared to sham-irradiated controls. The expression of the MMP-2 mRNA in these cells increased to 2-fold at 16 h before falling back at 24 h following UVAB-irradiation. MMP-9 mRNA levels on the other hand steadily decreased by 30% at 4 h before falling by 90% at 24 h in these cells. In Colo 16 cells, mRNA expression of furin steadily decreased compared to that of sham-irradiated controls. No differences in MMP-2 mRNA levels were seen between the different time points. MMP-9 mRNA expression rose immediately following irradiation reaching a maximum level at 4 h (87.3-fold) before falling back at 24 h to 40% that seen at 0 h. In conclusion, MMP-2 mRNA levels remained low over the 24 h time period in both HaCaT and Colo 16 cells. Of interest is that addition of IL-1α increased the expression of MMP-9 mRNA from UVAB-irradiated HaCaT and Colo 16 cells. These results suggest that IL-1α does play an important role in the activity (Figure 4.10), protein (Figures 4.11 and 4.12) and mRNA expression of MMP-2 and -9. This provides evidence that the activation of proMMP-9 in skin inflammatory diseases likely occurs via a pathway involving IL-1α.

However, when plots of furin, MMP-2 and MMP-9 mRNA levels were constructed, a weak correlation was observed between furin and MMP-2, furin and MMP-9, and

MMP-2 and MMP-9 mRNA in UV-irradiated HaCaT cells and moderate correlation between these genes of interest were observed in Colo 16 cells. The time course of MMP-2 and -9 mRNA induction from UVAB-irradiated cells in the presence of IL-1α does not appear to be related to furin and no direct association was evident between the time course of MMP-9 and furin mRNA induction.

4.3.4 Effect of inhibitors

Recent studies using PC inhibitors have demonstrated that increased furin expression is associated with enhancement of metastatic spread and tumour cell proliferation (144, 227), probably as a result of the activation of MMP involved in ECM degradation (169, 266). In order to investigate if there were changes in the secretion of MMP activity and protein expression by the irradiated cells, on the addition of inhibitors, various inhibitors were tested. These were the furin inhibitor (Dec RVKR cmk), metalloprotease inhibitor (1, 10 phe), and 2R-2-[(4-Biphenylsulfonyl)amino]-3-phenylpropionic acid (MMPI).

It was necessary to ensure that the doses of inhibitors used were not cytotoxic to the cells. Therefore, cell viability was performed to determine the effect of the different inhibitors in both, HaCaT and Colo 16 cells lines. Since UVAB induced significantly high levels of MMP-2 (Figure 4.6) and -9 (Figure 4.8) expression in these keratinocyte-derived cell lines, it was chosen as the type of dose to determine cell viability. The cells were exposed to UVAB-irradiation in the presence or absence of each of these inhibitors. In cell viability experiments using Dec RVKR cmk (Figure 4.13), a slight effect on the viability of un-irradiated cells was observed but not on the

UV-irradiated cultures. This was similar to results obtained by Koo *et al*. (295) who showed that cells including COS-1 and HEK293F did not undergo apoptosis at a dose of 100 μM which was confirmed by the MTT assay.

The effect of different concentrations of 1, 10 phe on sham-irradiated and UV-irradiated HaCaT cells was determined (Figure 4.14). At a concentration of 100 μM, maximal viability of the cells was observed. The viability of the UV-irradiated cultures were similar to that of the sham-irradiated cells. Therefore, this dose was chosen as it caused the minimal cell death. MMPI had a slight effect on attached viable and detached dead cells in UV-irradiated HaCaT cells. Therefore, the results from this study confirmed that the concentrations of each of these inhibitors used in this thesis did not significantly cause in cell death of these keratinocyte-derived cell lines.

The changes in MMP-2 and -9 activity in UV-irradiated HaCaT and Colo 16 cells, in the presence of each of the inhibitors was determined by gelatin-zymograph. In this study, the addition of Dec RVKR cmk significantly reduced the secretion of MMP-2 activity (Figure 4.17). This agreed to studies by Koo *et al*. (295) who investigated the effect of Dec RVKR cmk on proMMP-2 processing (COS-1, HCT116, HEK293F and MCF-7) cells. The results revealed that proMMP-2 processing was significantly reduced, suggesting that PCs are major processing enzymes for proMMP-2 in these cell types. Maquoi *et al*. (175) showed that Dec RVKR cmk (100 μm) induced a dose dependent reduction of MMP-2 activity in HT1080 cells.

In this study, higher levels of MMP-2 and -9 activity was observed in the treated UV-irradiated Colo 16 cells 24 h post-irradiation compared to HaCaT cells (Figure

4.17). This was similar to the results seen in Figures 4.3 and 4.4. UVB-irradiation induced maximal release of both MMP-2 and -9 in these cell lines. These results highlight that the furin inhibitor completely inhibited MMP-9 activity in both HaCaT and Colo 16 (Figure 4.17) which suggests that furin cleaves proMMP-9. Similar findings were observed for MMP-2 and -9 activity when the cells were treated with 1, 10 phe (Figure 4.19) and MMP inhibitor (Figure 4.21). These results confirm that these MMPs are metalloproteases. Ikeda *et al*. (306) also showed that the synthetic MMPI inhibited MMP activity in tumour tissues.

MMP inhibition might be an approach for the treatment of patients with chronic wounds and reduced angiogenesis. Therefore, in my study the changes in MMP-2 and -9 cellular protein expression in UVAB-irradiated HaCaT and Colo 16 cells, in the presence of the MMPI were elucidated. This study was done, in the presence and absence of IL-1α in order to determine if presence of this cytokine brought any changes to the expression of MMPs when cells were pretreated with the MMPI. Results from this study showed that MMPI reduced the expression of MMP-2 and -9 in UV-irradiated HaCaT (Figure 4.23) and Colo 16 cells (Figure 4.24) both in the presence and absence of IL-1α. At present, there is no information on the targets of MMPI apart from MMP-2 and/or -9 (306, 308). It is not yet known whether MMPI targets exclusively MMP-2and/or -9 or other proteases such as TACE and other members of the ADAM family.

4.3.5 Cell migration

Liang *et al*. (309) showed that the *in vitro* scratch assay is suitable for studies on the effects of cell-matrix and cell-cell interactions on cell migration, mimic cell migration

during wound healing *in vivo* and are compatible with imaging of live cells during migration to monitor intracellular events. Todaro *et al*. (310) showed that the *in vitro* scratch assay is a straightforward, easy, well-developed and economical method to study cell migration *in vitro*. In order to study the migration and invasion potential of MMP-2 and -9 in A549 lung cancer cells, Hung *et al*. (311) used the *in vitro* scratch assay and demonstrated that migration was enhanced at 48 h. Therefore, the rationale behind performing cell scratch assays in my study was to determine the role of MMPs in cell migration. This method was based on previous observation that, upon creation of a new artificial gap, so called ‘‘scratch’’, on a confluent cell monolayer, the cells on the edge of the newly created gap will move toward the opening to close the ‘‘scratch’’ until new cell–cell contacts are established again (310). In keeping with these findings, cell migration assays were performed on both sham-irradiated and UV-irradiated HaCaT and Colo 16 cells (Figure 4.30 and 4.31) at 0, 24 and 48 h. These results suggested that maximal cell migration occurred 48 h after incubation. Therefore, in this study, 48 h time frame was chosen for determining cell migration.

Parsy *et al*. (312) used synthetic and physiological a range of protease inhibitors (BB94, aprotinin, TIMP1 and TIMP2) and assessed the role of MT1-MMP invasion by the UCC cells by the Matrigel assay. On the contrary, the same group suggested that in a two-dimensional culture (scratch test), MMPs may not play a significant role in wound healing. Results from this study show that addition of inhibitors, Dec RVKR cmk (Figure 4.17), 1, 10 phe (Figure 4.19) and MMPI (Figure 4.21) significantly reduced the secretion of MMP-2 and completely inhibited that of MMP-9 activity in HaCaT and Colo 16 cells. Therefore, the effect of these inhibitors on cell migration was performed

to understand the involvement of MMPs in cell migration and their possible role in tumour metastasis.

When cells were pretreated with these inhibitors (Dec RVKR cmk and 1, 10 phe) and then exposed to UVR, cells completely stayed stationary, especially in Colo 16 cells where they were detached probably as they underwent apoptosis. Of interest was that when HaCaT and Colo 16 cells were treated with Dec RVKR cmk, migration was dramatically reduced, suggesting that a reduction in MMP activity interferes with this process further confirming the role of furin in MMP activity (Figure 4.33). In HaCaT cells, the average of the effect of UVA-, UVB- and UVAB-irradiation on the migration of cells was 56%, 67% and 33% when compared to the sham-irradiated cells which were expressed as 100%. On the other hand, in Colo 16 cells, the average of the effect of UVA-, UVB- and UVAB-irradiation on the migration of cells was 2%, 16% and 84% These results suggested that MMPs are involved and play a crucial role in cell migration. In HaCaT cells, the average of the effect of UVA-, UVB- and UVAB-irradiation on the migration of cells was 57%, 69% and 35% when compared to the sham-irradiated cells which were expressed as 100%. On the other hand, in Colo 16 cells, the average of the effect of UVA-, UVB- and UVAB-irradiation on the migration of cells was 31%, 35% and 88% Similar effect on the cells was seen in the presence of 1, 10 phe (Figure 4.36).

In the presence of MMPI (Figure 4.39), the rate of cell migration was significantly reduced in HaCaT cells. In these cells, the average of the effect of UVA- and UVB- irradiation on the migration of cells was 64% and 75% when compared to the

sham-irradiated cells which were expressed as 100%. Of interest was that UVAB-irradiation had no effect on cell migration, the reason for which is unclear. On the other hand, in Colo 16 cells, the average of the effect of UVA-, UVB- and UVAB-irradiation on the migration of cells was 108%, 67% and 59%. In these cells, the effect of MMPI was minimal unlike that seen in HaCaT cells. While UVA-irradiation had and increased effect on cell migration, UVB- and UVAB-irradiation reduced cell migration when compared to the sham-irradiated controls. Therefore, this suggests that MMPs play a crucial role in cell migration in HaCaT cells but not in Colo 16 cells.

The limitations of the *in vitro* scratch assay are that it takes a relatively longer time to perform than some other methods. Two to three days are needed for the formation of cell monolayer and then up to 48 h for cell migration to close the scratch. Last, relatively large amount of cells and chemicals will be required for the assay as it is usually performed in a tissue culture dish. Therefore, it is not a method of choice if the availability of cells (e.g. primary keratinocytes that are hard to get in sufficient amount were not used for this study) or cost of inhibitors is limiting. Despite these limitations of the method, overall, *in vitro* scratch assay is still often the method of choice to analyze cell migration in a laboratory because it is easy to set up, does not require any specialized equipment and all materials required for the assay are available in any laboratory that performs cell culture. Another way to expand on this study in future depending on funding and availability of resources would be to employ use of other well-established 3-D methods for chemotaxis such as the Boyden chamber assay, as no chemical gradient is established.

Interestingly, when conditioned media from the cell migration assays was tested by gelatin-zymography, we detained similar results to our previous experiment which showed the absence of MMP-9 on the zymographs (Figures 4.34, 4.37 and 4.40). This helped us to confirm our study about the effect of Dec RVKR cmk (Figure 4.16), 1, 10 phe (Figure 4.18) and specific MMP-2/-9 I (Figure 4.20) on MMP activity and expression.

4.3.6 Conclusion

4.3.6.1 Effect of UVR on furin activation of MMPs

Furin is a PC that has been shown to activate a range of enzymes, including MMPs from their respective preproforms (167, 168, 175, 288). MMPs are important in tumour progression, promoting invasion and immune escape (187). In this study, we investigated the role furin plays in the maturation and activation of these gelatinases in skin cells in response to UVR.

These results suggest that MMP-2 and -9 secretion was stimulated by UVB-irradiation and activity of these gelatinases was down-regulated by UVA-irradiation. In Colo 16 cells, protein expression of MMP-9 was not observed in significant amounts but increased MMP-9 activity was observed. This suggests that minimal amounts of MMP-9 was present on the cell membrane but was shed in significant amounts into the media. UVB-irradiation induced maximal mRNA expression of furin, MMP-2 and -9 in HaCaT and Colo 16 cells. Strong positive correlation was seen between furin and MMP-2 and -9 in HaCaT cells and moderate correlation was observed between these proteases in Colo 16 cells. IL-1α plays a very pivotal role in MMP activity, protein and

mRNA expression and facilitates activation of MMP-9. Obviously, much work will be necessary to understand the mechanism behind this process and support this concept.

Most MMPs are secreted as inactive proenzymes, and their proteolytic activity is regulated by zymogen activation and enzyme inhibition (337). Most PC inhibitors are compounds that act as competitive inhibitors. All of them contain the general cleavage motif RXK/RR that binds to the PC's active site impairing further interactions with their physiological substrates (227). In this study, we used the specific furin inhibitor Dec RVKR cmk in order to determine the role of furin in the expression and activity of MMPs. Previous studies have reported that this inhibitor exhibits reduced toxicity and has been widely used as an effective general PCs inhibitor (227). It inhibits furin and has a *K*i of 3.4 nM (338). These inhibitors are commercially available and have been used for inhibition studies in cell culture (227). In this study, Dec RVKR cmk significantly reduced both MMP-2 and -9 activity and slowed cell migration in UV-irradiated HaCaT and Colo 16 cells which confirmed the role of furin in the processing of MMPs. This agreed with previous studies where inhibition of furin activity with this inhibitor showed a significant decrease in both substrate processing and *in vitro* invasiveness (268). Moreover, the presence of MMP-9 in tumour metastasis was further demonstrated by MMP-9 gene knockout mice showing a decreased rate of tumour metastasis (203).

Increased furin expression is associated with enhancement of metastatic spread due to elevated expression and activation of MMPs. From these results it was evident that furin is a key factor involved in the maturation of MMPs associated with the invasive and

metastatic potential of tumour cells. At this point in time, there is no record in the literature of any cmk compound evaluated *in vivo* as a possible cytostatic or tumoricidal agent (227). Therefore, future development of specific furin inhibitors can consequently, reduce tumour progression and in turn decrease the incidence of skin cancer.

4.3.6.2 Comparing cell types

There are differences between the effect of UV types and doses on MMP activity and expression in the keratinocyte cell lines examined in this study as shown in Table 4.3.

4.3.6.2.1 HEK vs HaCaT and Colo 16 cells

UVB radiation induced maximum MMP-9 activity into the conditioned cultured media of HEK cells which was similar to that seen in Colo 16 cells but different to HaCaT cells. On addition of IL-1α, while increase in MMP-2 and -9 activity was observed in UVA- and UVB-irradiated cell lines (HEK, HaCaT and Colo 16), MMP-2 activity decreased in HEK cells, MMP-2 and -9 activity decreased in HaCaT cells and MMP-9 activity decreased in Colo 16 cells. These results suggest that the response of HaCaT cells to UVR differs to that of HEK which suggest that these immortalized cell lines may not be a suitable model for studying keratinocytes. HEK cells were not available in sufficient quantities and future studies should repeat some of these experiments in order to obtain a better comparison of the Colo 16 cells which is a tumour cell line to these primary keratinocytes.

	Experiments	HEK	HaCaT	Colo 16
1	MMP-2 and -9 protein activity	XXX	X	XX
2	MMP-2 and -9 cellular expression	-	XXX	XX
3	Effects of IL-1α on MMP-2 and -9 activity	X	XX	XX
4	Effects of IL-1α on MMP-2 and -9 protein expression	-	XX	XX
5	Effect of Dec RVKR cmk on MMP activity	-	XXX	XXX
6	Effect of 1, 10 phe on MMP activity	-	XXX	XXX
7	Effect of Specific MMPI on MMP activity	-	XXX	XXX
8	Effect of Specific MMPI on MMP -2 and -9 expression	-	XX	XX
9	MMP-2 mRNA expression	-	XX (24 h)	XX (4 h)
10	MMP-9 mRNA expression	-	XX (24 h)	XXX (12 h)
11	Furin mRNA vs MMP mRNA (correlation studies)	-	XXX	XX
12	Effects of IL-1α on MMP-2 expression	-	XX (16 h)	XX (4 h)
13	Effects of IL-1α on MMP-9 expression	-	XX (4 h)	XXX (4 h)
14	Effect of Dec RVKR cmk on cell migration	-	XX	XXX
15	Effect of 1, 10 phe on cell migration	-	XX	XXX
16	Effect of Specific MMPI on cell migration	-	XX	XXX

Table 4.3 Effect of UVR on the function of keratinocyte-derived cells. Effect of the response is represented by X, XX, XXX and (-) where (-) represents no response and the number of X's represent the intensity of the response with XXX being the highest.

4.3.6.2.2 HaCaT vs Colo 16 cells

The profile of HaCaT cells in response to UVR more closely resembled that of Colo 16 cells than HEK cells. While low levels of MMP-2 and -9 activity in response to UVR was observed in HaCaT cells, Colo 16 cells exhibited high levels of protein activity similar to that of HEK cells. ProMMP-2 expression was higher than that of the active form in both cell lines. UVR induced higher proMMP-2 and active MMP-2 levels in Colo 16 cells compared to that seen in HaCaT cells, where reduced levels were observed. Active MMP-9 was the predominant form observed in HaCaT cells while in Colo 16 cells, it was the proform. Effect of IL-1α had similar effect on both the cell lines. Increased MMP-2 and -9 activity was observed in UVA- and UVB-irradiated cell lines (HaCaT and Colo 16). Variation in the MMP levels was observed in UVAB-irradiated cells in the presence of IL-1α (while decrease in the level of MMP-2 and -9 activity was observed in HaCaT cells, decrease in the level of MMP-9 activity was seen in Colo 16 cells).

The addition of IL-1α has a greater stimulatory effect on MMP-9 than on MMP-2 with the greatest increase seen in treated UVAB-irradiated HaCaT and Colo 16 cells. While UVB-irradiation induced maximal mRNA expression of furin, MMP-2 and -9 in a time course study, UVA-irradiation down-regulated the mRNA expression of these genes in both the cell lines. Strong positive correlation was observed between these proteases in HaCaT cells while moderate correlation was seen in Colo 16 cells. MMP-2 mRNA levels were low throughout the 24 h time period in both HaCaT and Colo 16 cells. Of interest was that addition of IL-1α enhances MMP-9 mRNA expression in UVAB-irradiated HaCaT and Colo 16 cells. Dec RVKR cmk, 1, 10 phe and MMPI

inhibited MMP-9 activity and halted cell migration in both the UV-irradiated HaCaT and Colo 16 cells.

Chapter Five:

Effect of UVR on furin activation of TACE in human keratinocyte cell lines

5.1 Introduction

UV light is a physical carcinogen and UV-irradiation from sunlight has profound effects on the human skin, causing various biological events such as sunburn, inflammation, cellular/tissue injury, cell death, and skin cancer (253, 339). Much attention has been focused on the increasing rates of skin cancer due to excessive UV exposure in humans (40). UVR is also involved in the release of pro-inflammatory cytokines, of which TNFα has been implicated in tumorigenic activities (5). While, TNFα is known to be cytotoxic to some tumour cell lines, it can mediate UV-induced tumorigenesis in others (30, 118). Up-regulation of TNFα is a key early response to UVB by keratinocytes, and represents an important component of the inflammatory cascade in skin (77, 276). Bashir *et al*. (77) found that IL-1α, a cytokine also present in irradiated skin, substantially and synergistically enhanced the induction of TNFα by UVB radiation. The induction of TNFα by UVB with IL-1α is mediated through increased gene transcription (77). Previous studies have reported that UVA and UVB radiation appear to be significant inducers of TNFα transcription in epidermal cells *in vitro* and *in vivo* (115, 277, 340).

TNFα is released from the cells by proteolytic cleavage of its membrane-anchored precursor (341). TACE is the main protease responsible for the ectodomain shedding of TNFα (341). Black *et al*. (126) showed impaired shedding of TNFα from TACE-deficient mice which confirmed TACE's role in the processing this cytokine. As TNFα plays a major role in some acute as well as chronic inflammatory diseases, TACE represents an important and novel target for the design of specific synthetic inhibitors that might be used in a variety of inflammatory and immunological therapies (146,

219). Because of the wide physiological and pathological importance of TACE, much attention has been paid to its mechanism of activation (158).

Peiretti *et al*. (151) reported that furin is the major PC involved in TACE maturation and activation. TACE possesses the putative PC recognition sequence (RVKR), which is thought to be used to generate the mature enzyme (126, 147). In order to test the possibility whether PCs were involved in the maturation of TACE, Endres *et al*. (154) used the synthetic inhibitor Dec RVKR cmk and observed reduced levels of mature TACE in treated HEK293 cells compared to untreated cells. The development of selective inhibitors of PC may result in them being used in preventing or treating tumours (227). Existing evidence suggests that furin inhibitors may be useful chemotherapeutic agents (227, 266).

Although the role of TNFα in UV-induced skin has been well documented, the expression profile of genes involved in this proposed pathway has not been investigated. Skiba *et al*. (136) suggested that time-distinct gene induction of furin and TNFα may be involved in UV-induced cellular responses, but not for TACE. The effect UVR has on the expression and/or activity of furin and that of the proteases it activates in human keratinocyte cell lines is not known.

In this study the effect of UVA and/or UVB radiation on furin and TACE expression and/or activity and of the molecules they cleave in keratinocyte-derived cell lines was investigated.

5.1.1 Aim and Hypothesis

Some metalloproteases have been reported to be activated in epidermal cells following UV-irradiation (136, 262, 342). It is not known if UV-irradiation regulates the expression of TACE in the membrane of skin cells. Therefore, the aim of this study is to investigate the effect of UVR on the furin activation of TACE and to investigate if changes in activity are related to changes in furin expression and/or activity. Secondly, does UV light directly modulate the changes in expression and/or activity of TACE, thereby increasing TNFα release. The effect UV type and dose has on the release of TNFα from human keratinocyte-derived cells has also been examined as part of this study.

The effects of singular (UVA or UVB) and concurrent (combination of UVA and UVB herein referred to as UVAB) exposures of UVR were examined. In order to understand the effects of UVR on different keratinocyte-derived cell lines; primary keratinocytes (HEK), immortalized keratinocytes (HaCaT) and SCC-derived (Colo16) cells were examined. Based on previous findings (228, 229), we chose to use HaCaT cells as a model to study the effects of UV-irradiation on primary keratinocytes and draw a comparison between these two cell lines. As it is unknown if these pathways are increased as a result of tumorigenesis, Colo16 cells, a SCC cell line was also examined as part of this study.

5.2 Results

5.2.1 TNFα release

5.2.1.1 Effect of IL-1α

The up-regulation of TNFα is a key early response to UVB by keratinocytes, and represents an important component of the inflammatory cascade in the skin (77). Recently, Bashir *et al*. (77) found that IL-1α induced TNFα in UVB-irradiated keratinocytes and fibroblasts. Media samples were collected 24 h post-irradiation, and the level of TNFα present was calculated from the standard curve and was expressed as a function of cell protein level. The level of TNFα in the media of the irradiated cells was determined using ELISA (Section 2.6). The level of IL-1α supplementation (10 ng/ml) on the secretion of TNFα in cells exposed to UVR is seen in Figure 5.1.

In HEK cells, 223.6 ng/mg cell protein of TNFα was secreted from untreated control cells. However, when these cells were exposed to UVR, TNFα levels increased 1.3-fold, 3.4-fold and 14.1-fold in response to UVA-, UVB- and UVAB-irradiation, respectively. In sham-irradiated cells, the addition of IL-1α resulted in 2763.73 ng/mg cell protein of TNFα being secreted from these cells. This represented a 12.4-fold increase of that seen in untreated un-irradiated controls. However, following the addition of IL-1α to the UV-irradiated cells, the increase of TNFα secreted from the cells compared to sham-irradiated treated cells were 7.9-fold, 10.8-fold and 32.9-fold in response to UVA-, UVB- and UVAB-irradiation, respectively.

In HaCaT cells, low levels of TNFα were produced in untreated sham-irradiated controls (410.7 ng/mg cell protein). Following UVA-irradiation there was a reduction in the level of TNFα shed from the cell. There was an increase in the level of TNFα

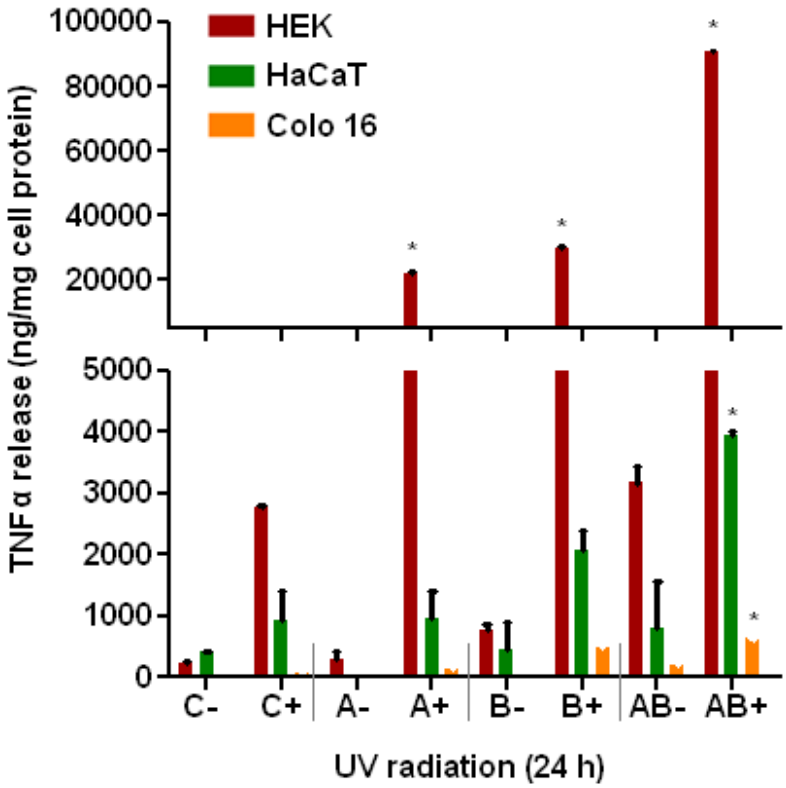

Figure 5.1 Effect of IL-1α (10 ng/ml) on TNFα shed from UV-irradiated HEK, HaCaT and Colo 16 cells. The cells were exposed to sham-irradiation or controls (C), UVA (A), UVB (B) and UVAB (AB) radiation in the presence (+) and/or absence (-) of IL-1α. Media samples were collected 24 h post-irradiation. Results expressed are the mean ± SEM for three separate experiments. Statistical significance of the effect of IL-1α on TNFα release is represented as $p<0.05$ for (*).

released from the cells following exposure to UVB- (1.1-fold) and UVAB-irradiation (1.9-fold) (Figure 5.1). The addition of IL-1α to the sham-irradiated cells, resulted in 935.5 ng/mg cell protein of TNFα being secreted from these cells which were 2.3-fold that seen in the untreated cells. UVA-irradiation induced similar levels of TNFα, compared to treated sham-irradiated cells. Higher levels of this cytokine were secreted following exposure to UVB- (2.2-fold) followed by a significant ($p<0.05$) increase in response to UVAB-irradiation (4.2-fold) compared to treated sham-irradiated cells.

In Colo 16 cells, 8.6 ng/mg cell protein of TNFα was secreted from the untreated control cells (Figure 5.1). Following exposure to UVA radiation, TNFα levels fell 80% compared to the un-irradiated controls. In cells exposed to UVB-or UVAB-irradiation TNFα levels increased 4.2-fold and 21.7-fold, respectively compared to the un-irradiated controls. In the sham-irradiated cells, the addition of IL-1α resulted in 81.9 ng/mg cell protein of TNFα being secreted which was 9.5-fold that seen in the untreated cells. Following UV-irradiation, the increase of TNFα secreted from the cells treated with IL-1α were 1.7-fold, 5.8-fold and 7.7-fold in response to UVA- and UVB- and UVAB-irradiation, respectively when compared to the sham-irradiated treated cells.

IL-1α increased the release of TNFα in sham-irradiated HEK and HaCaT cells but not Colo 16 cells. The greatest increase in TNFα release in all cell lines was induced by UVAB-irradiated cells treated with IL-1α. HEK cells shed the most TNFα while Colo 16 cells shed the least under all the examined conditions.

5.2.1.2 Effects of inhibitors

In order to investigate further the mechanisms by which IL-1α induces TNFα release from the irradiated cells, various inhibitors were tested. These were the protein synthesis inhibitor (CHX), metalloprotease inhibitor (1, 10 phe), furin inhibitor (Dec RVKR cmk) and 2R-2-[(4-Biphenylsulfonyl) amino]-3-phenylpropionic acid (MMPI). Each of the experiments was performed from the same batch of HaCaT and Colo 16 cells and was run simultaneously. The results were written up per individual inhibitor rather than as part of a larger group and as such the amount of TNFα released from sham-irradiated (controls) in the presence and/or absence of IL-1α was similar for all the four findings. In this study UVAB-irradiated cells were used as they were shown to secrete the greatest level of TNFα from the cells (Figure 5.1).

5.2.1.2.1 Effect of CHX on TNFα release

It has been shown previously that CHX at 100 μM had a minimal effect on cell viability of sham- and UVAB-irradiated HaCaT and Colo 16 cells (Figure 3.6). Therefore, CHX was added to the cells to determine if the cell contains a reservoir of pTNFα or continuously synthesizes this cytokine. If there was no significant reduction in the levels of TNFα released from the CHX-treated cells, it would suggest that the cell contains a reservoir of this cytokine.

The cells were pre-treated with CHX (100 μM) for 24 h prior to being exposed to UVAB radiation (Section 2.4.3), after which IL-1α (10 ng/ml) was added and the level of TNFα in the culture media 24 h post-irradiation was measured using an ELISA and expressed as a function of cellular protein levels.

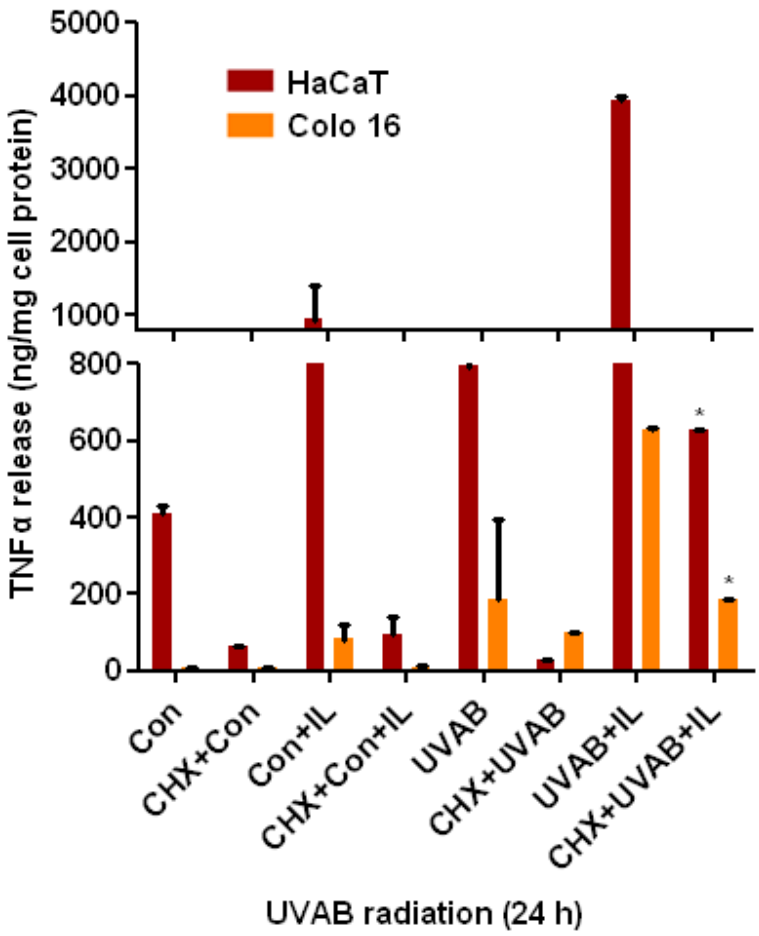

Figure 5.2 Effect of CHX on the release of TNFα from UVAB-irradiated HaCaT and Colo 16 cells treated with IL-1α. Cells were exposed to sham-irradiation or controls (C) and UVAB-irradiation (AB) in the presence (+) or absence (-) of CHX (100 μM) and/or IL-1α (IL) (10 ng/ml). Media samples were collected 24 h post-irradiation. Results expressed are the mean ± SEM for three separate experiments. Statistical significance of the effect of CHX on TNFα release is represented as $p<0.05$ (*).

In HaCaT cells, the amount of TNFα released from sham-irradiated cells was 410.7 ng/mg cell protein. When CHX was added to sham-irradiated HaCaT cells, there was an 80% inhibition in the level of TNFα shed from these cells (Figure 5.2). When IL-1α was added to sham-irradiated cells, there was a 2.3-fold increase in TNFα released compared to the corresponding untreated controls. However, when CHX was added to these treated un-irradiated cells, TNFα levels were reduced by 90%. In the UVAB-irradiated HaCaT cells, there was a 1.9-fold increase in the level of TNFα released (793.4 ng/mg cell protein) compared to un-irradiated controls. When CHX was added to these UVAB-irradiated cells, a 97% reduction in the amount of TNFα released from the cells was observed. While increased levels of TNFα (3936.7 ng/mg cell protein) were observed in IL-1α treated UVAB-irradiated cells (5.0-fold compared to untreated irradiated cells), the addition of CHX caused an 80% inhibition of the amount released.

In Colo 16 cells, the amount of TNFα released from sham-irradiated cells was 8.6 ng/mg cell protein (Figure 5.2). When CHX was added to these cells, a 23% inhibition in the level of TNFα shed from these cells was observed (Figure 5.2). When IL-1α was added to the sham-irradiated cells, a slight increase in TNFα (81.9 ng/mg cell protein) release was observed. However, when CHX was added to these treated un-irradiated cells, there was a 90% reduction in the level of TNFα released. UVAB-irradiation increased the level of TNFα released (187.3 ng/mg cell protein) from the cells 21.7-fold, compared to that seen in un-irradiated controls. The addition of CHX to these irradiated cells resulted in a 50% reduction in the level of TNFα released. However, when IL-1α was added to the UVAB-irradiated cells, 627.9 ng/mg cell protein TNFα

was released from the cell. The addition of CHX to these treated irradiated cells inhibited TNFα release by 70%.

These results obtained suggest that the cell does not contain a reservoir of proTNFα, and it is synthesized when required by the cell in response to external stimuli (e.g. UVAB-radiation and/or IL-1α).

5.2.1.2.2 Effect of 1, 10 phe on TNFα release

It is well known that TACE is a metalloprotease (125, 136-138, 271). The purpose of this experiment was to observe the effect 1, 10 phe (a metalloprotease inhibitor) has on the release of TNFα from UVAB-irradiated HaCaT and Colo 16 cells in the presence and/or absence of IL-1α.

It has been shown previously that maximal viability of the cells was observed at 100 μM of 1, 10 phe (Figure 4.14). Therefore, cells were pre-treated with 1, 10 phe (100 μM) for 24 h prior to being exposed to UVAB radiation (Section 2.4.3). Following UVAB-irradiation and addition of IL-1α (10 ng/ml), the level of TNFα in the cultured media 24 h post-irradiation was measured using an ELISA and expressed as a function of cell protein levels.

In HaCaT cells, the addition of 1, 10 phe caused a 93% reduction in the level of TNFα released from sham-irradiated cells (410.7 ng/mg cell protein) (Figure 5.3). While increased levels of TNFα was observed in IL-1α-treated sham-irradiated cells (935.5 ng/mg cell protein), the addition of 1, 10 phe resulted in a 91% inhibition. The level of TNFα released from UVAB-irradiated cells (793.4 ng/mg cell protein) was higher than

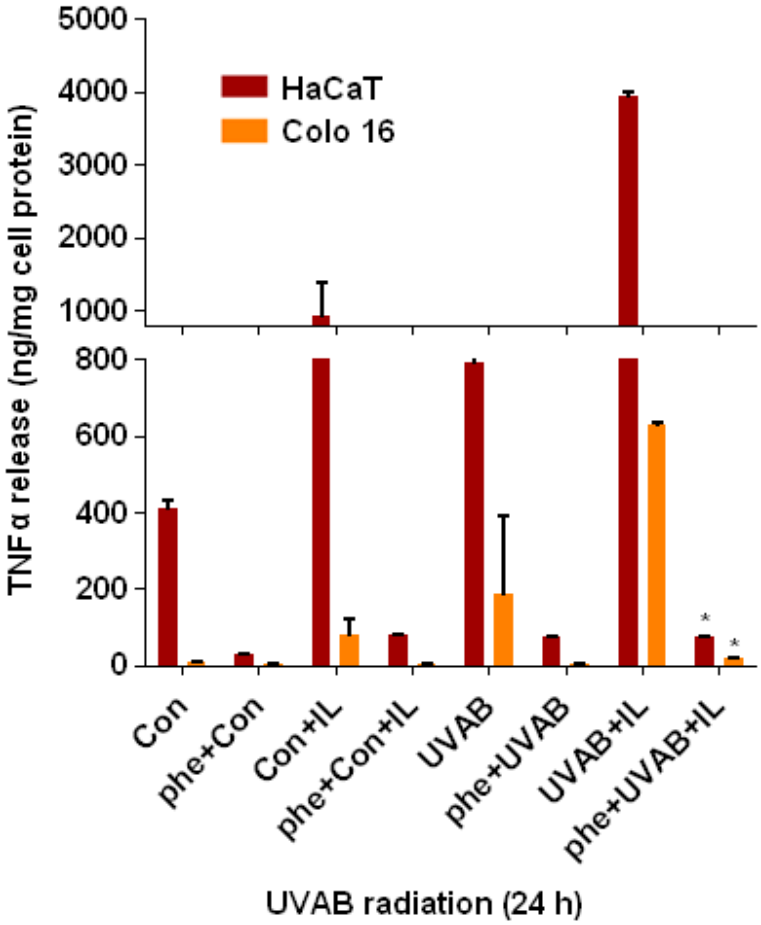

Figure 5.3 Effect of 1, 10 phe on the release of TNFα from UVAB-irradiated HaCaT and Colo 16 cells treated with IL-1α. Cells were exposed to sham-irradiation or controls (C) and UVAB-irradiation (AB) in the presence (+) or absence (-) of phe (100 µM) and/or IL-1α (IL) (10 ng/ml). Media samples were collected 24 h post-irradiation. Results expressed are the mean ± SEM for three separate experiments. Statistical significance of the effect of 1, 10 phe on TNFα release is represented as $p<0.05$ (*).

that seen for un-irradiated cells. When 1, 10 phe was added to these cells, the levels fell by 90%. The addition of IL-1α to the UVAB-irradiated cells induced TNFα levels 5.0-fold compared to the untreated irradiated cells. However, when 1, 10 phe was added to these cells, a 98% inhibition in the amount of TNFα released from the cells was observed.

In Colo 16 cells, the addition of 1, 10 phe caused a 75% reduction in the level of TNFα released from sham-irradiated cells (8.6 ng/mg cell protein) (Figure 5.3). While increased levels of TNFα was observed in IL-1α-treated sham-irradiated cells (81.9 ng/mg cell protein), the addition of 1, 10 phe resulted in a 97% inhibition. The level of TNFα released from UVAB-irradiated cells (187.3 ng/mg cell protein) was higher than that seen for un-irradiated cells. When 1, 10 phe was added to these cells, the levels fell by 99%. The addition of IL-1α to UVAB-irradiated cells increased TNFα levels 3.3-fold compared to the untreated irradiated cells. However, when 1, 10 phe was added to these cells, a 97% inhibition in the amount of TNFα released from the cells was observed.

In summary, the results obtained confirm that TACE is a metalloprotease as seen by the reduced levels of TNFα shed from the cells in the presence of 1, 10 phe.

5.2.1.2.3 Effect of Dec RVKR cmk on TNFα release

TACE is cleaved to its catalytically active form by the action of the proprotein convertase furin (144, 151, 154, 158). Therefore, in order to determine the effect furin has on the activation of TACE, Dec RVKR cmk was added to IL-1α treated UVAB-irradiated HaCaT and Colo 16 cells. A significant reduction in the level of

TNFα released from the cell would confirm that furin is involved in the activation of TACE.

Cells were pre-treated with Dec RVKR cmk (100 μM) for 24 h prior to being exposed to UVAB radiation (Section 2.4.3). Following UVAB-irradiation and addition of IL-1α (10 ng/ml), the level of TNFα in the cultured media 24 h post-irradiation was measured using an ELISA and expressed as a function of cellular protein levels.

In HaCaT cells, following the addition of Dec RVKR cmk, a 63% reduction in the level of TNFα released from sham-irradiated cells (410.7 ng/mg cell protein) was observed (Figure 5.4). While increased levels of TNFα was observed in IL-1α-treated sham-irradiated cells (935.5 ng/mg cell protein), a 87% inhibition was seen when Dec RVKR cmk was added to these cells. There was an increase in the level of TNFα released from UVAB-irradiated cells (793.4 ng/mg cell protein), but in the presence of Dec RVKR cmk these levels fell by 43%. The addition of IL-1α to UVAB-irradiated cells induced TNFα levels 5.0-fold compared to the untreated irradiated cells. However, when Dec RVKR cmk was added to the IL-1α-treated UVAB-irradiated cells, a 95% inhibition in the level of TNFα release was observed.

In Colo 16 cells, following the addition of Dec RVKR cmk a 23% reduction in the level of TNFα released from sham-irradiated cells (8.6 ng/mg cell protein) was observed (Figure 5.4). While increased levels of TNFα was observed in IL-1α-treated sham-irradiated cells (81.9 ng/mg cell protein), a 17% inhibition was seen when Dec RVKR cmk was added to these cells. It should be noted that due to the low endogenous

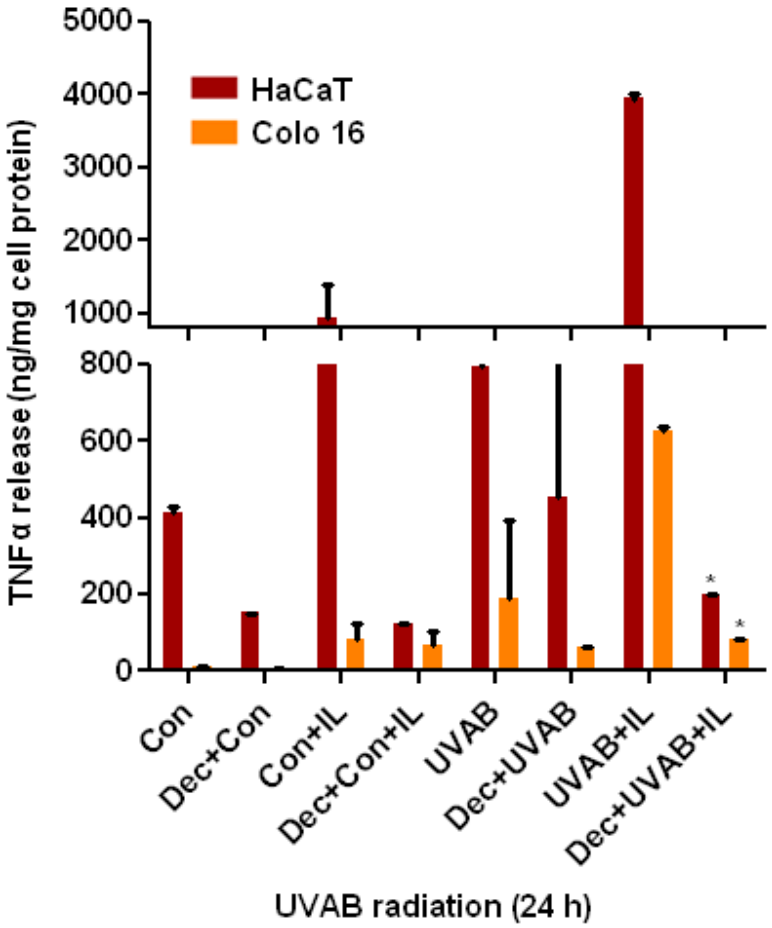

Figure 5.4 Effect of Dec RVKR cmk on release of TNFα from UVAB-irradiated HaCaT and Colo 16 cells treated with IL-1α. Cells were exposed to sham-irradiation or controls (C) and UVAB-irradiation (AB) in the presence (+) or absence (-) of Dec RVKR cmk (100 µM) and/or IL-1α (IL) (10 ng/ml). Media samples were collected 24 h post-irradiation. Results expressed are the mean ± SEM for three separate experiments. Statistical significance of the effect of Dec RVKR cmk on TNFα release is represented as $p<0.05$ (*).

levels of TNFα released from un-irradiated cells, the degree of inhibition observed did not seem high. There was an increase in the level of TNFα released from UVAB-irradiated cells (187.3 ng/mg cell protein), but following the addition of Dec RVKR cmk these levels fell by 66%. The addition of IL-1α to UVAB-irradiated cells induced TNFα levels 3.3-fold compared to the untreated irradiated cells. However, in the presence of Dec RVKR cmk, a 87% inhibition in TNFα release was observed in these IL-1α treated UVAB-irradiated cells.

These results show that Dec RVKR cmk inhibited TNFα release from the HaCaT and Colo 16 cells under all conditions tested which suggests that furin is involved in TACE activation and maturation.

5.2.1.2.4 Effect of MMP inhibitor (MMPI) on TNFα release

Some MMPs e.g. the gelatinases (MMP-2 and-9) have been shown to cleave pTNFα to yield the mature protein (343-345). The purpose of this experiment was to determine if MMPs also cleave TNFα from UVAB-irradiated HaCaT and Colo 16 cells in the presence and/or absence of IL-1α. Thus, in this study, ELISAs were performed using the 2R-2-[(4-Biphenylsulfonyl) amino]-3-phenylpropionic acid (MMP inhibitor = MMPI).

It has been shown previously that the concentration of this inhibitor (5 µM) was not cytotoxic to these cells (Figure 4.15). Cells were pre-treated with MMPI (5 µM) for 1 h prior to being exposed to UVAB radiation (Section 2.4.3). Following UVAB-irradiation and the addition of IL-1α (10 ng/ml), the level of TNFα released into

the cultured media 24 h post-irradiation was measured using an ELISA and expressed as a function of cellular protein levels.

In HaCaT cells, the amount of TNFα released from the sham-irradiated controls was 410.7 ng/mg cell protein. When the MMPI was added to these cells, there was a 91% inhibition of the amount of TNFα released from the cells (Figure 5.5). When IL-1α was added to the sham-irradiated cells, there was a 2.3-fold increase in the level of TNFα released from these cells compared to untreated controls. When these cells were irradiated with UVAB, 793.4 ng/mg cell protein of TNFα was released which was 1.9x than seen in the untreated un-irradiated controls. When MMPI was added to the UVAB-irradiated cells, a 93% reduction in TNFα release was observed. While IL-1α enhanced the level of TNFα released in UVAB-irradiated cells 5.0-fold to that seen in the untreated irradiated cells, MMPI caused a 26% drop in these levels after 8 h, 37% at 16 h and 45% at 24 h.

In Colo 16 cells, the amount of TNFα released from sham-irradiated cells was 8.6 ng/mg cell protein. When MMPI was added to these cells, there was a 2% inhibition of the amount of TNFα released from these cells (Figure 5.5). When IL-1α was added to sham-irradiated cells, there was a 9.5-fold increase in the level of TNFα released from these cells compared to untreated controls. When Colo 16 cells were irradiated with UVAB, 187.3 ng/mg cell protein of TNFα was released which was 21.7x than seen in the untreated un-irradiated controls. Following the addition of MMPI to the UVAB-irradiated cells, a 75% reduction in TNFα release was observed. While IL-1α enhanced the level of TNFα released in UVAB-irradiated cells 3.3-fold to that seen in the untreated

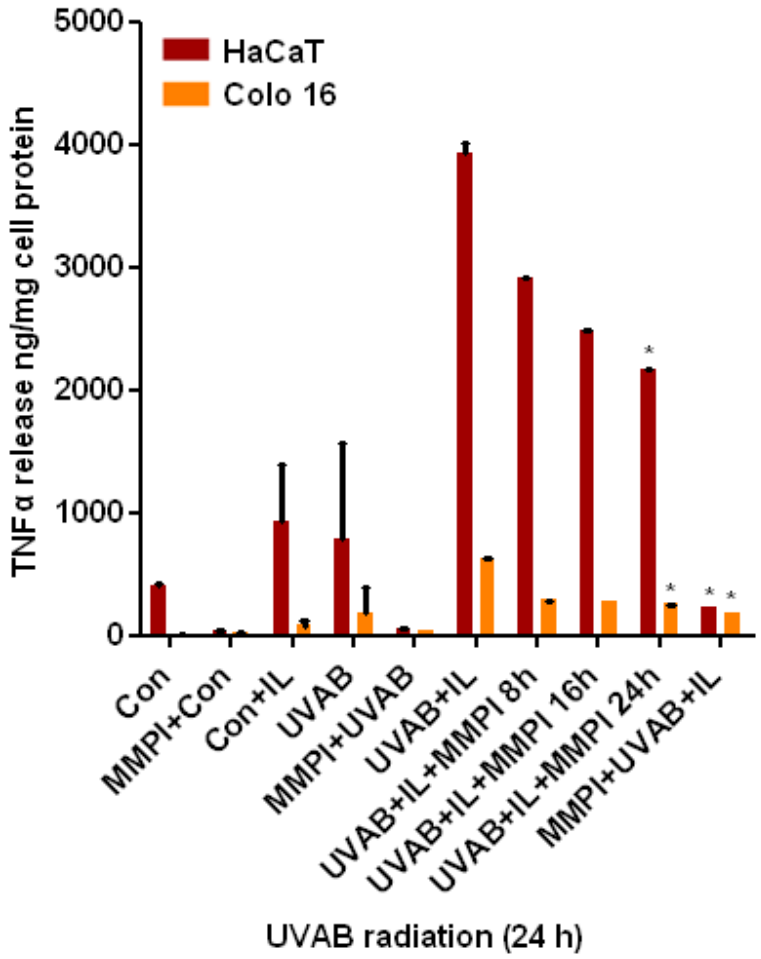

Figure 5.5 The effect of MMPI on the release of TNFα from UVAB-irradiated HaCaT and Colo 16 cells treated with IL-1α. Cells were exposed to sham-irradiation or controls (C) and UVAB-irradiation (AB) in the presence (+) or absence (-) of MMPI and/or IL-1α (IL). Results expressed are the mean ± SEM for three separate experiments. Statistical significance is represented as $p<0.05$ for the effect of MMPI on TNFα release (*).

irradiated cells, MMPI caused a 55% drop in these levels after 8 h, 56% at 16 h and 60% at 24 h. From this inhibition data, it is possible to determine the incubation time needed for MMPI to inhibit TNFα release by 50%. If the level of TNFα released at each of the time points (8, 16 and 24 h) are expressed as % of that released in the uninhibited cells, we can plot these values as seen in Figure 5.6.

In HaCaT cells it was not possible to determine the incubation time required for MMPI to induce a 50% inhibition of TNFα released from these cells. In Colo 16 cells, a 50% reduction in TNFα release from the cell was calculated to occur when the cells had been incubated with MMPI for 7.8 h. The results suggest that MMPs as well as TACE can cleave TNFα on these cells.

5.2.2 TACE protein expression

5.2.2.1 Effect of UVR

The effect of UVR on the expression of TACE in keratinocyte-derived cell lines (HEK, HaCaT and Colo 16 cells) was investigated using cell lysates run on western blots (Section 2.5). In all the cell lines examined, two forms of TACE were detected, proTACE (pTACE) and mature TACE (mTACE). Representative blots of the effect of UVR on TACE levels in the keratinocyte-derived cell lines are seen in Figure 5.7. The blots were probed with the ADAM 17 antibody which detects both pTACE and mTACE isoforms. In the western blots, 50 μg cell protein was added per lane and β-actin was probed to quantify the amount of protein present in each sample.

From the resultant image, fluorescent quantification of the bands was made using the Quantity one image analysis software. The amount of TACE in control (un-irradiated)

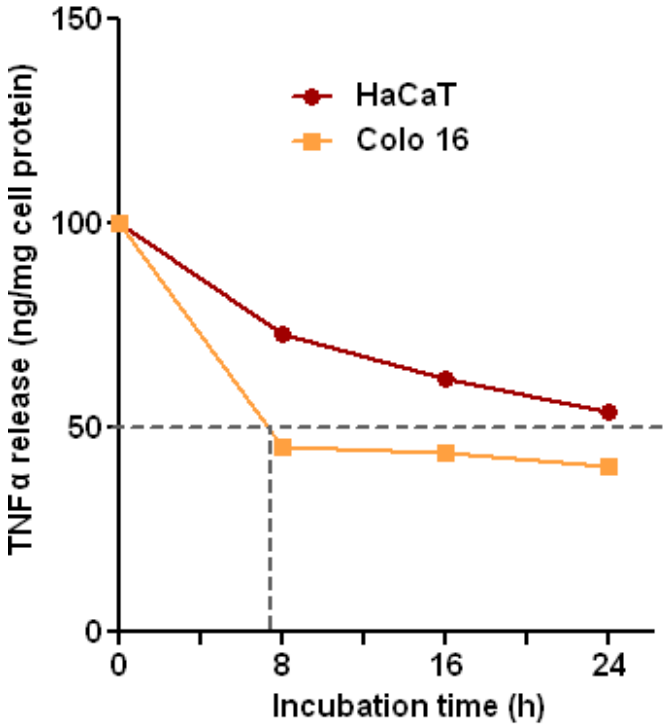

Figure 5.6 Time course on the effect of MMPI on the release of TNFα from UVAB-irradiated HaCaT and Colo 16 cells. Results expressed are the mean ± SEM for three separate experiments.

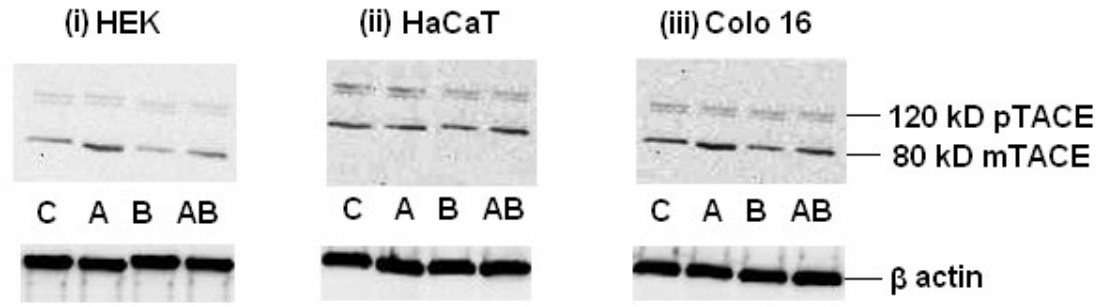

Figure 5.7 A representative western blot showing the effect of UVR on the expression of pTACE and mTACE in HEK (i), HaCaT (ii) and Colo 16 cells (iii). In each lane, 50 μg of cell lysate was added and β-actin was used to monitor the amount of protein added to each lane. Samples represent sham-irradiated cells or controls (C), UVA-irradiated cells (A), UVB-irradiated cells (B) and UVAB-irradiated cells (AB).

cells was given a value of 100 (pTACE + mTACE) and from that, the changes in pTACE and mTACE levels could be calculated in the irradiated samples, and these were expressed as a percentage of that found in control cells.

In HEK cells, the expression of pTACE in sham-irradiated controls was 42.8%, which was higher than that in cells exposed to UVA (17.8%), UVB (22.3%) and UVAB radiation (10.6%) (Figure 5.8i). mTACE expression was also lower in the UV-irradiated cells (irrespective of the UV type) when compared to that seen in sham-irradiated controls. The level of TACE (pTACE and mTACE) in the HEK cells decreased in

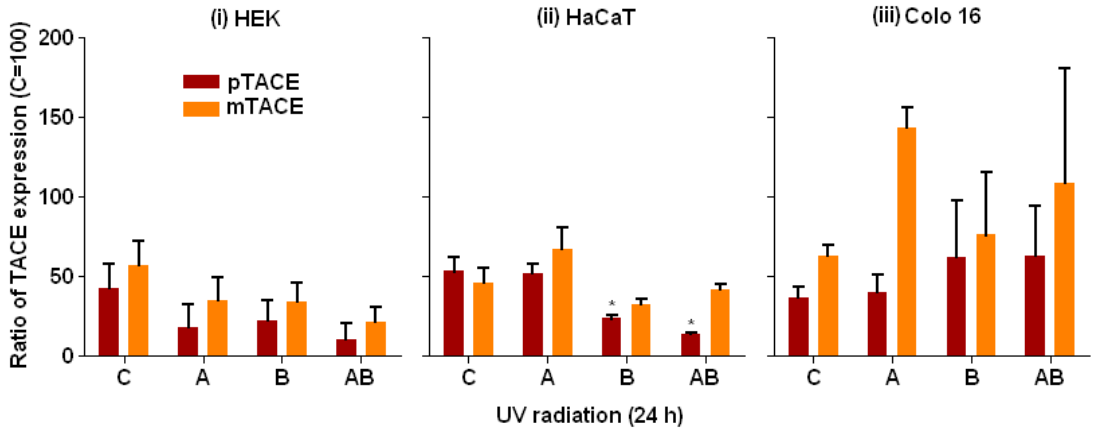

Figure 5.8 Effect of UVR on the expression of pTACE and mTACE in HEK (i), HaCaT (ii) and Colo 16 cells (iii). Cells were exposed to sham-irradiation or controls (C), UVA (A), UVB (B) and UVAB (AB) radiation and cellular proteins were extracted 24 h post-irradiation. Results expressed are the mean ± SEM for three separate experiments. Statistical significance of the effect of UVR on the expression of TACE compared to controls is shown as $p<0.05$ (*).

response to UVR (47% in UVA, 43% in UVB and by 68% in UVAB) when compared to the sham-irradiated controls. The main form of TACE found in all these cells was mTACE.

In the sham-irradiated HaCaT cells, there was slightly more pTACE (53.4%) compared to mTACE (46.6%) (Figure 5.8ii). While pTACE levels were similar in UVA-irradiated cells compared to un-irradiated controls, it fell in both UVB- (24%) and UVAB-irradiated cells (14%). On the other hand, mTACE expression was elevated in UVA-irradiated cells (67.7%) but lower in both UVB- (32.4%) and UVAB-irradiated cells (42.3%) when compared to the un-irradiated controls. The level of total TACE expression was 20% higher in UVA-irradiated cells but 40% lower in both UVB- and UVAB-irradiated cells when compared to that of the sham-irradiated controls. In these cells, mTACE was the predominant form seen in UV-irradiated HaCaT cells.

In Colo 16 cells, the predominant form of TACE was mTACE (63%) in the un-irradiated controls (Figure 5.8iii). There was a slight increase in pTACE levels in UVA- (40.2%), UVB- (62%) and UVAB-irradiated cells (63%) when compared to un-irradiated controls. mTACE levels increased to 143.5%, 76% and 109% in UVA-, UVB- and UVAB-irradiated cells, respectively when compared to the un-irradiated cells. The level of total TACE expression in Colo 16 cells increased 83% in UVA-irradiated cells, 38% in UVB-irradiated cells and 72% in UVAB-irradiated cells when compared to the sham-irradiated controls. The main form of TACE in all these cells was mTACE.

In conclusion, mTACE expression was higher than that of pTACE in all three keratinocyte-derived cell lines examined in this study. UVR-induced expression of pTACE and mTACE was higher in Colo 16 cells when compared to both HEK and HaCaT cells, where a reduction was seen. While UVR did change the expression of TACE in all three cell lines examined, these changes were not statistically significant.

5.2.2.2 Effect of Dec RVKR cmk on TACE levels

In this study, the furin inhibitor, Dec RVKR cmk was added to the cells to observe if furin was responsible for the processing of pTACE to mTACE. In these experiments, the cells were pre-treated with Dec RVKR cmk (100 μM) for 24 h before they were exposed to UVR (Section 2.4.3). At the end of this period, the cell lysates were run on western blots (Section 2.5) and the changes in TACE protein expression measured.

Representative western blots probed for TACE in UV-irradiated HaCaT and Colo 16 cells pretreated with Dec RVKR cmk are shown in Figure 5.9. It can be seen that in those cells treated with the furin inhibitor, irrespective of the UV type, only mTACE was present on the gels. This result suggests that furin is involved in the maturation of TACE in these cells.

In the control HaCaT cells, the predominant form of TACE was pTACE (53%) (Figure 5.10i). The addition of Dec RVKR cmk caused a slight reduction in pTACE levels but significantly ($p<0.05$) reduced mTACE levels (4.5%) in these cells. Similar results were also seen in the UV-irradiated HaCaT cells irrespective of the type used. In all cases, there was a significant reduction in the levels of mTACE in these irradiated cells when they were treated with Dec RVKR cmk. In general, the level of mTACE fell to ~10%

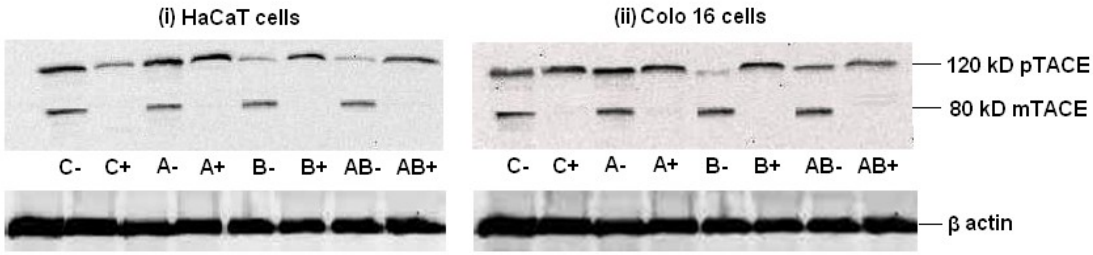

Figure 5.9 A representative western blot showing the effect of Dec RVKR cmk on the expression of TACE in UV-irradiated HaCaT (i) and Colo 16 cells (ii). In each lane, 50 µg of cell lysates was added. β-actin was used to monitor the amount of protein added to each lane. The cells were exposed to sham-irradiation or controls (C), UVA (A), UVB (B) and UVAB (AB) radiation in the presence (+) or absence (-) of Dec RVKR cmk.

that of the untreated cells irrespective of the UV dose. Of interest was that in UVB- and UVAB-irradiated cells, the level of pTACE were higher in those cells treated with Dec RVKR cmk than in the untreated cells. In UVA-irradiated cells, pTACE levels were lower in Dec RVKR cmk treated cells compared to the untreated cells.

In the control Colo 16 cells, the predominant form of TACE was mTACE (63%) (Figure 5.10ii). The addition of Dec RVKR cmk caused a slight reduction in pTACE

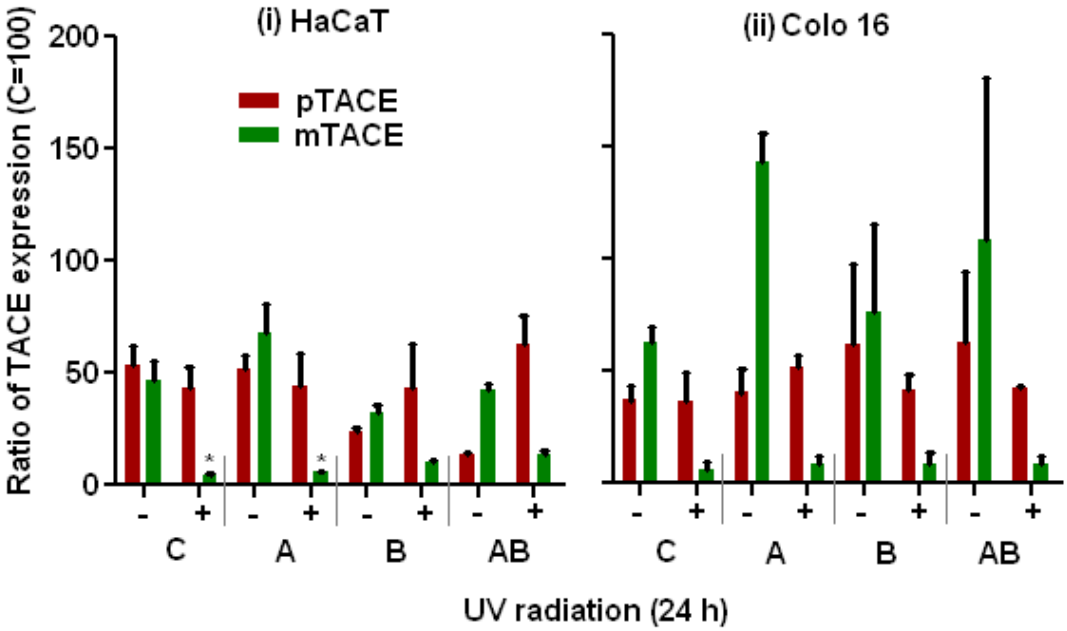

Figure 5.10 Effect of Dec RVKR cmk on the expression of TACE in UV-irradiated HaCaT (i) and Colo 16 cells (ii). Cells were exposed to sham-irradiation or controls (C), UVA (A), UVB (B) and UVAB (AB) radiation in the presence (+) or absence (-) of Dec RVKR cmk. Results expressed are the mean ± SEM for three separate experiments. Statistical significance is represented as $p<0.05$ for the effect of Dec RVKR cmk treatment (*).

levels but significantly ($p<0.05$) reduced mTACE levels (6.0%) in these cells. Similar results were also seen in the UV-irradiated Colo 16 cells irrespective of the type. In UVA-irradiated cells, the levels of pTACE were slightly higher in those cells treated with Dec RVKR cmk than in the untreated cells. In the UVB- and UVAB-irradiated cells, pTACE levels were lower in Dec RVKR cmk treated cells compared to the untreated cells. In all cases, there was a significant reduction in the levels of mTACE in these irradiated cells when they were treated with Dec RVKR cmk. In general, mTACE levels fell to ~8% to that of the untreated cells irrespective of the UV dose. On the contrary, the total levels of TACE in the treated UV-irradiated cells were about 40% that seen in the corresponding untreated cohorts.

Of interest was that while pTACE was not higher in every treated UV-irradiated cell, the corresponding mTACE levels were drastically reduced (irrespective of the type and dose). This may imply that in the absence of furin, pTACE may be the major form of TACE in the cells. In conclusion, these results suggest that furin is the main PC involved in the processing and activation of mTACE in HaCaT and Colo 16 cells and exposure to UV-irradiation has no effect on this process.

5.2.2.3 Effect of CHX on TACE levels

CHX was added to the cells to prevent the synthesis of TACE and from this we can calculate its half-life. In this study, the cells were pre-treated with CHX (100 μM) for 24 h prior to being exposed to UVAB radiation (Section 2.4.3). UVAB radiation was used as it was shown to induce high levels of TNFα release in irradiated cells (Figure 5.1). Following UVAB-irradiation, the cells were grown in culture for 24 h in the

presence of CHX. Cell lysates (50 µg) were run on western blots and TACE levels were quantified as described (Section 2.5). The level of TACE (pTACE and mTACE) in untreated control was 100%, and the values in the treated cells were expressed as a percentage of these values.

In un-irradiated HaCaT cells, most of TACE exists in its proform (51.7%), the rest being in the mature form (Figure 5.11i). When these cells were treated with CHX, the levels of both pTACE and mTACE fell (34.8% and 42.7%, respectively) when compared to the untreated controls. In the UVAB-irradiated HaCaT cells, the level of total TACE in the cell fell 46% compared to un-irradiated cells. The majority of TACE found in the UVAB-irradiated cells was in the mature form (41.2%) with only 13% being in the proform. When CHX was added to these irradiated cells, pTACE levels fell to 11%, while that of mTACE fell to 17%.

Based on the changes in the level of total TACE in the cell, its approximate half-life was calculated to be ~24 h. However in order to obtain a more accurate value, further time points would need to be investigated.

In un-irradiated Colo 16 cells, most of the TACE was present in the mature form (64%), with the rest being in the proform (Figure 5.11ii). When these cells were treated with CHX, the levels of both pTACE and mTACE fell (27.1% and 60%, respectively) when compared to untreated controls. In the UVAB-irradiated Colo 16 cells, the level of total TACE in the cell increased by 69% compared to the un-irradiated cells. The majority of TACE present was in the mature form (108%) with only 61% being in the proform. When CHX was added to the irradiated cells, pTACE levels fell to 37%, while

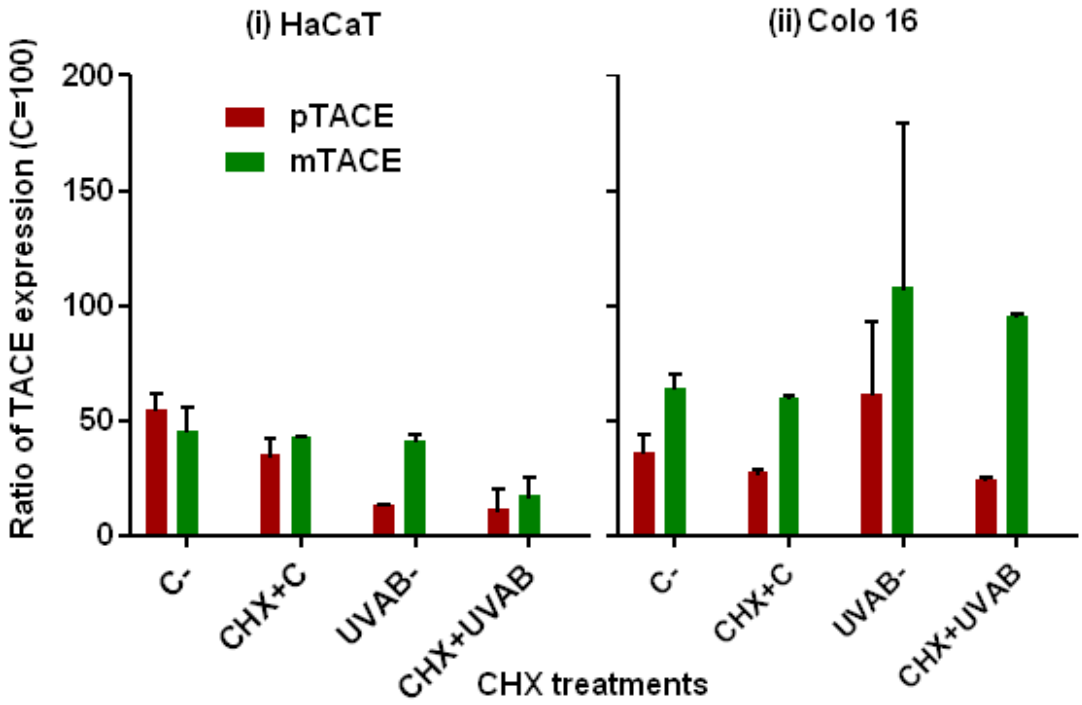

Figure 5.11 Effect of CHX on the expression of TACE in UVAB-irradiated HaCaT (i) and Colo 16 cells (ii). Cells were exposed to sham-irradiation or controls (C) and UVAB-irradiation (AB) in the presence (+) or absence (-) of CHX. Results expressed are the mean ± SEM for three separate experiments. No statistical significance was observed for the effect of CHX on TACE expression.

mTACE fell to 12.3%. Based on the changes in the level of total TACE in the cell, its approximate half-life was calculated to be 46 h. However, in order to obtain a more accurate value, further time points would need to be investigated.

In conclusion, these preliminary results suggest that TACE is not rapidly turned over in these cells and that CHX did not have a significant effect on the ratio of pTACE to mTACE in the cell, under the conditions examined.

5.2.2.4 Effects of IL-1α on TACE expression

Bashir *et al*. (77) recently showed that IL-1α stimulated the TNFα release from UVB-irradiated keratinocytes. TACE is the main metalloprotease responsible for the processing of TNFα (125, 136-138, 271). As a result of this I investigated the effect IL-1α had on the expression of TACE in these cells.

UVAB was shown to induce the maximal release of TNFα in HEK, HaCaT and Colo 16 cells (Figure 5.1). In this study I investigated the effect of UVR in the presence or absence of IL-1α on the expression of TACE. In order to quantify changes in the level of TACE in the cells, western blots (Section 2.5) of cell lysates were run.

In the control HEK cells, the predominant form of TACE was mTACE (58.1%). The addition of IL-1α caused a reduction in pTACE and mTACE levels (by 29% and 46%, respectively) in these cells (Figure 5.12i). Similar results were also seen in the UVA- and UVB-irradiated HEK cells treated with IL-1α compared to the corresponding irradiated untreated cells. However, in UVAB-irradiated cells treated with IL-1α, there

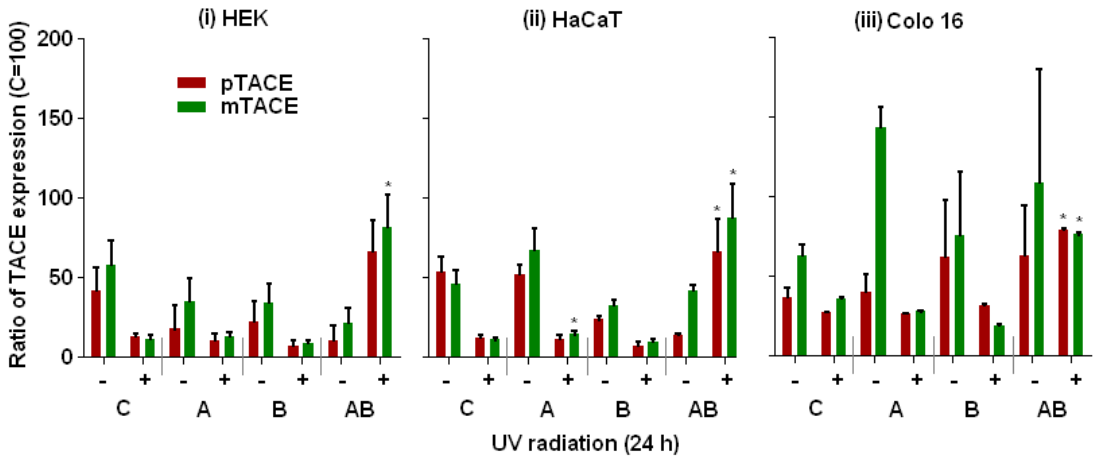

Figure 5.12 The effect of IL-1α on the expression of TACE in UVR-irradiated HEK (i), HaCaT (ii) and Colo 16 cells (iii). Cells were exposed to sham-irradiation or controls (C), UVA (A), UVB (B) and UVAB (AB) radiation in the presence (+) or absence (-) of IL-1α. Results expressed are the mean ± SEM for three separate experiments. No statistical significance was observed for effect of UVR on TACE expression in the absence of IL-1α. Statistical significance is represented as $p<0.05$ (*) for effect of UVR on TACE expression in the presence of IL-1α.

was an increase in pTACE (56%) and mTACE (60%) levels compared to that seen in the corresponding irradiated untreated cells. In general, while the level of total TACE (pTACE and mTACE) in the presence of IL-1α fell in sham- irradiated controls (75%), UVA- (54%) and UVB-irradiated cells (72%), it increased by 78% in the UVAB-irradiated cells compared to the corresponding untreated cells.

In the control HaCaT cells, the predominant form of TACE was pTACE (54.1%). The addition of IL-1α caused a reduction in pTACE and mTACE levels (by 42% and 35%, respectively) in these cells (Figure 5.12ii). Similar results were also seen in the UVA- and UVB-irradiated HEK cells treated with IL-1α compared to the corresponding irradiated untreated cells. However, in UVAB-irradiated cells treated with IL-1α, there was an increase in pTACE (67%) and mTACE (88%) levels compared to that seen in the corresponding irradiated untreated cells. In general, while the level of total TACE (pTACE and mTACE) in the presence of IL-1α fell in sham-irradiated controls (77%), UVA- (79%) and UVB-irradiated cells (71%), it increased by 275% in the UVAB-irradiated cells compared to the corresponding untreated cells.

In the control Colo 16 cells, the predominant form of TACE was mTACE (63.4%). The addition of IL-1α caused a reduction in pTACE and mTACE levels (by 9% and 28%, respectively) in these cells (Figure 5.12iii). Similar results were also seen in the UVA- and UVB-irradiated HEK cells treated with IL-1α compared to the corresponding irradiated untreated cells. However, in UVAB-irradiated cells treated with IL-1α, there was an increase in pTACE (79.3%) but not in mTACE (reduced by 33%) levels compared to that seen in the corresponding irradiated untreated cells. In general, the level of total TACE (pTACE and mTACE) in the presence of IL-1α fell in

sham-irradiated controls (37%), UVA- (70%), UVB- (63%) and UVAB-irradiated cells (9.4%).

These results suggest that IL-1α reduces the levels of both pTACE and mTACE in UVA- and UVB-irradiated HEK, HaCaT and Colo 16 cells, though it was not statistically significant. While IL-1α increased the levels of TACE in UVAB-irradiated HEK and HaCaT cells compared to their untreated irradiated counterparts, the opposite effect was seen in Colo 16 cells. The reasons for which are not clear.

5.2.2.5 Combined effects of CHX and IL-1α on TACE expression

IL-1α was shown to stimulate the expression of TACE in UVAB-irradiated cells (Figure 5.12). In this study, the effect of CHX on TACE expression in cells treated with IL-1α was determined.

Cells were pre-treated with CHX (100 μM) for 24 h prior to being exposed to UVAB radiation (Section 2.4.3). Following irradiation and treatment with IL-1α, the cells were grown in culture for 24 h in the presence or absence of CHX. At the end of this period, cell lysates (50 μg) were run on western blots and TACE levels were quantified (Section 2.5). The level of TACE (pTACE and mTACE) in untreated control was 100%, and the values in the treated cells were expressed as a percentage of these values.

In un-irradiated HaCaT cells both pTACE and mTACE levels were lower when the cells were treated with IL-1α or CHX and IL-1α (Figure 5. 13i). However, in the UVAB-irradiated cells, IL-1α stimulated the expression of both pTACE and mTACE.

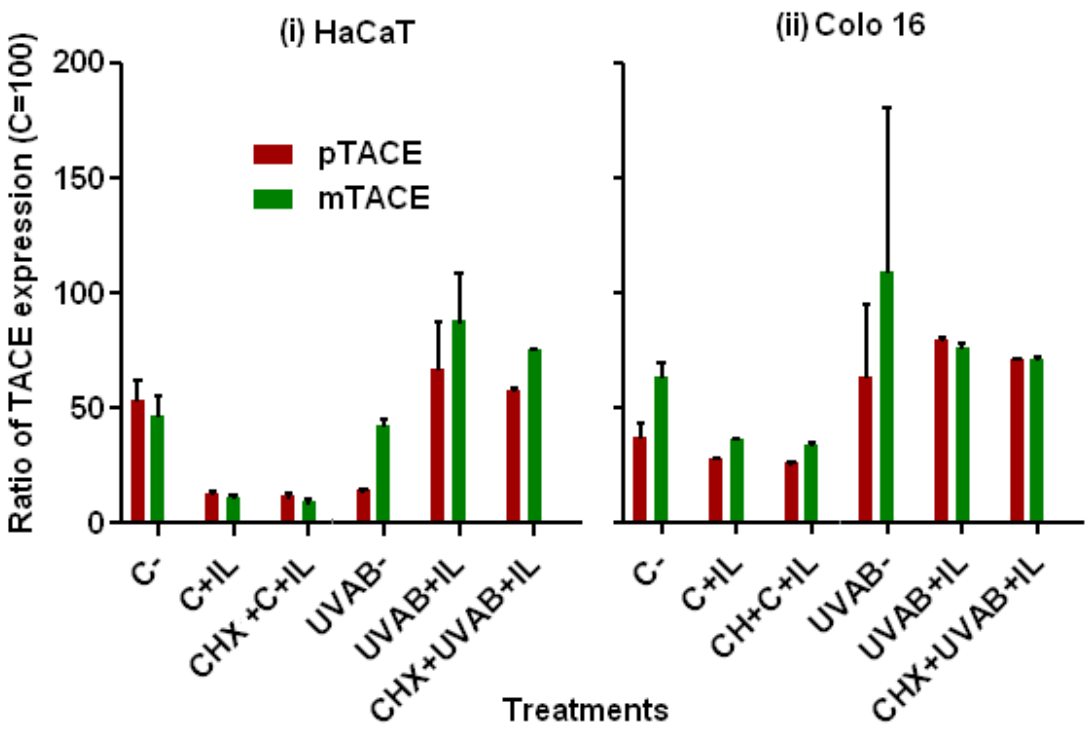

Figure 5.13 Effect of CHX on the expression of TACE in UVR-irradiated HaCaT (i) and Colo 16 cells (ii) treated with IL-1α. Cells were exposed to sham-irradiation or control (C) or UVAB-irradiation (AB) in the presence (+) or absence (-) of CHX (CHX) and/or IL-1α (IL). Results expressed are the mean ± SEM for three separate experiments. No statistical significance was observed for effect of CHX on TACE expression.

The addition of CHX to these irradiated cells caused a slight reduction in both pTACE and mTACE levels. The level of total TACE (pTACE and mTACE) in the presence of CHX and IL-1α decreased in both sham-irradiated controls (13%) and UVAB-irradiated cells (14%) compared to the corresponding cells only treated with IL-1α.

In un-irradiated Colo 16 cells both pTACE and mTACE levels were lower when the cells were treated with IL-1α or CHX and IL-1α (Figure 5. 13ii). In the UVAB- irradiated cells, IL-1α stimulated the expression of both pTACE and mTACE. The addition of CHX to these irradiated cells caused a slight reduction in the levels of both pTACE and mTACE. The levels of total TACE (pTACE and mTACE) in the presence of CHX and IL-1α decreased in sham-irradiated controls (6.3%) and UVAB-irradiated cells (9%) compared to the corresponding cells only treated with IL-1α.

In general, total TACE levels (pTACE and mTACE) were lower in the CHX-treated UVAB-irradiated cultures in the presence of IL-1α when compared to UVAB-irradiated cells treated only with IL-1α, though these changes were not statistically significant. The findings agree with that seen earlier (Figure 5.11) which suggests that the half-life of TACE in these cells is longer than that of furin (Chapter 3). However, in order to determine this value a time course study would need to be performed.

5.2.3 TACE and TNFα mRNA

UVR has been shown to be a potent inducer of TNFα gene expression in human keratinocytes (115). As well as up-regulating gene expression, UVR is also known to increase the amount of TNFα shed from the cells (Figure 5.1) (77, 121, 122, 136, 276,

346). TNFα is released from the surface of the keratinocytes by the action of TACE (125, 136-138, 271). Therefore, the aim of this study was to observe the effect of UVR on TACE and TNFα mRNA expression in HaCaT and Colo 16 cells. In order to quantify the gene expression of furin, TACE and TNFα qRT-PCR was used because of the low levels of mRNA detected in these cells (136).

5.2.3.1 Effects of UVR

In HaCaT or Colo 16 cells, the expression of TACE and TNFα in untreated control cells was given the value of unity (Figure 5.14). The relative expression of the internal control gene (β actin) and target gene (TACE and TNFα) for each UV-irradiated sample was compared against the un-irradiated sample. This was calculated using the Pfaffl Correction method (Appendix A.8) (225).

In HaCaT cells, only in the UVB-irradiated cells was there an increase (30%) in TACE mRNA levels seen 24 h post-irradiation (Figure 5.14i). In the UVA- and UVAB-irradiated cells, TACE mRNA expression fell 60% and 80%, respectively. This result differed to previous studies which showed that TACE mRNA levels were elevated in response to both UVA (8 kJ/m^2) or UVB (2 kJ/m^2) radiation (136). The expression of TNFα 24 h post-irradiation in HaCaT cells fell when they were exposed to UVA (90%), UVB (70%) or UVAB radiation (80%). These results differed to that seen previously where a rapid and strong induction of TNFα mRNA was observed post-exposure to UVA or UVB (136), and UVAB radiation (277, 340).

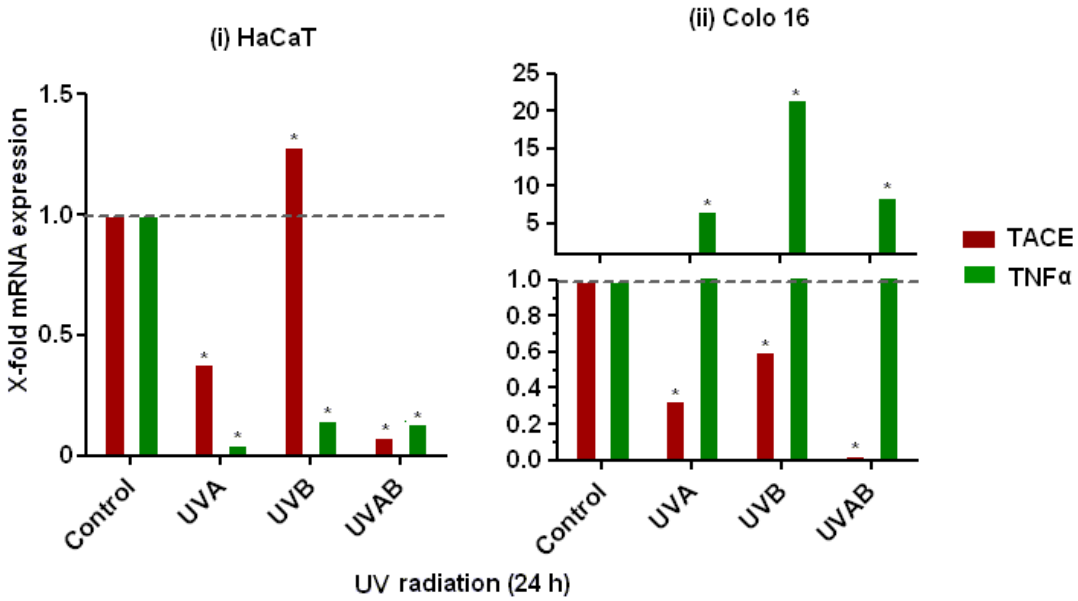

Figure 5.14 Effect of UVR on TACE (i) and TNFα mRNA induction/expression (ii) in HaCaT and Colo 16 cells. Cells were exposed to sham-irradiation (control), UVA, UVB and UVAB radiation and mRNA expression measured 24 h post-irradiation. Control mRNA levels (=1) are represented as a dotted line. Results expressed are the mean ± SEM for three separate experiments. Statistical significance of the effect of UVR on TACE and TNFα mRNA levels was shown as $p<0.05$ (*).

In UV-irradiated Colo 16 cells, there was a decrease in TACE mRNA levels seen 24 h post-irradiation (Figure 5.14ii). In the UVA-, UVB- and UVAB-irradiated cells, TACE mRNA expression fell 66% 39% and 97%, respectively compared to the un-irradiated controls. The highest levels of TACE mRNA were observed in the UVB-irradiated cells. The expression of TNFα 24 h post-irradiation in the Colo 16 cells was significantly higher when they were exposed to UVR (Figure 5.15ii). TNFα mRNA levels were 6.5-fold, 8-fold and 23-fold higher in UVA, UVB- and UVAB-irradiation, respectively when compared to that seen in the un-irradiated controls.

5.2.3.1.1 Time course of furin, TACE and TNFα

Following on from the results obtained in Figure 5.14, a time course of furin, TACE and TNFα mRNA expression post-irradiation was performed. Since, UVB induction of TACE and TNFα mRNA expression was the highest at 24 h (Figure 5.14), in order to further expand this study, a time course gene induction (0-32 h) in response to UVB-irradiation was determined in HaCaT and Colo 16 cells (Figure 5.15). Results from this experiment were used to determine if there is a relationship between the mRNA levels of these three proteases. In this study, un-irradiated controls cells were given the value of unity at 0 h and mRNA expression was expressed as ratio to this value at the time points examined.

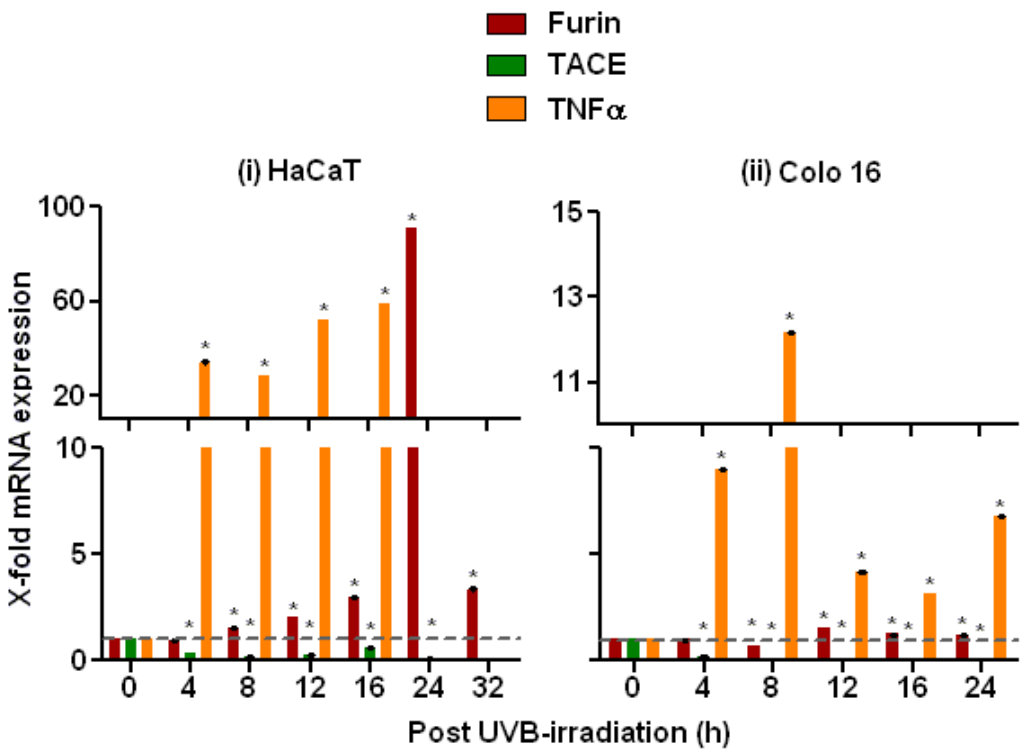

Figure 5.15 Time course of furin, TACE and TNFα mRNA induction/expression in UVB-irradiated HaCaT (i) and Colo 16 cells (ii). Control mRNA levels (=1) are represented as a dotted line. Results expressed are the mean ± SEM for three separate experiments. Statistical significance of the effect of UVB on furin, TACE and TNFα mRNA mRNA levels is shown as $p<0.05$ (*).

Results from this study show that in UVB-irradiated HaCaT cells, furin mRNA levels slowly increased with time reaching 2.9-fold at 16 h before rapidly increasing to a maximal level (91-fold) at 24 h before falling back to 3.3-fold at 32 h (Figure 5.15i). TACE expression was relatively constant throughout this period of time (32 h) with levels remaining close to unity. TNFα gene expression was observed in HaCaT cells 4-24 h post UVB-irradiation. TNFα mRNA levels were maximal at 16 h (59-fold) post UVB-irradiation, which was similar to results by Skiba *et al*. (136) who found that TNFα mRNA induction was bimodal in HaCaT cells with maximal levels seen at 16 and 24 h post UVB-irradiation. However, in this study a second peak at 24 h was not seen. Based on this information, correlation plots of furin, TACE and TNFα mRNA levels were constructed (Figure 5.16). It can be seen from this figure that there does not appear to be any apparent correlation between the mRNA of these proteins in the UVB-irradiated HaCaT cells.

Furin mRNA levels in UVB-irradiated Colo 16 cells, were higher than that seen in un-irradiated controls over the period 12-24 h with maximal levels seen at 12 h (1.5-fold) (Figure 5.15ii). The expression of TACE mRNA in UVB-irradiated Colo 16 cells was detected at minimal amounts and remained fairly constant throughout this 24 h period. However, in the UVB-irradiated Colo 16 cells, TNFα mRNA levels were rapidly induced reaching maximal levels by 8 h (12.1-fold) after which they fell back to 3-fold at 16 h before subsequently rising again to 6.7-fold at 24 h post-irradiation.

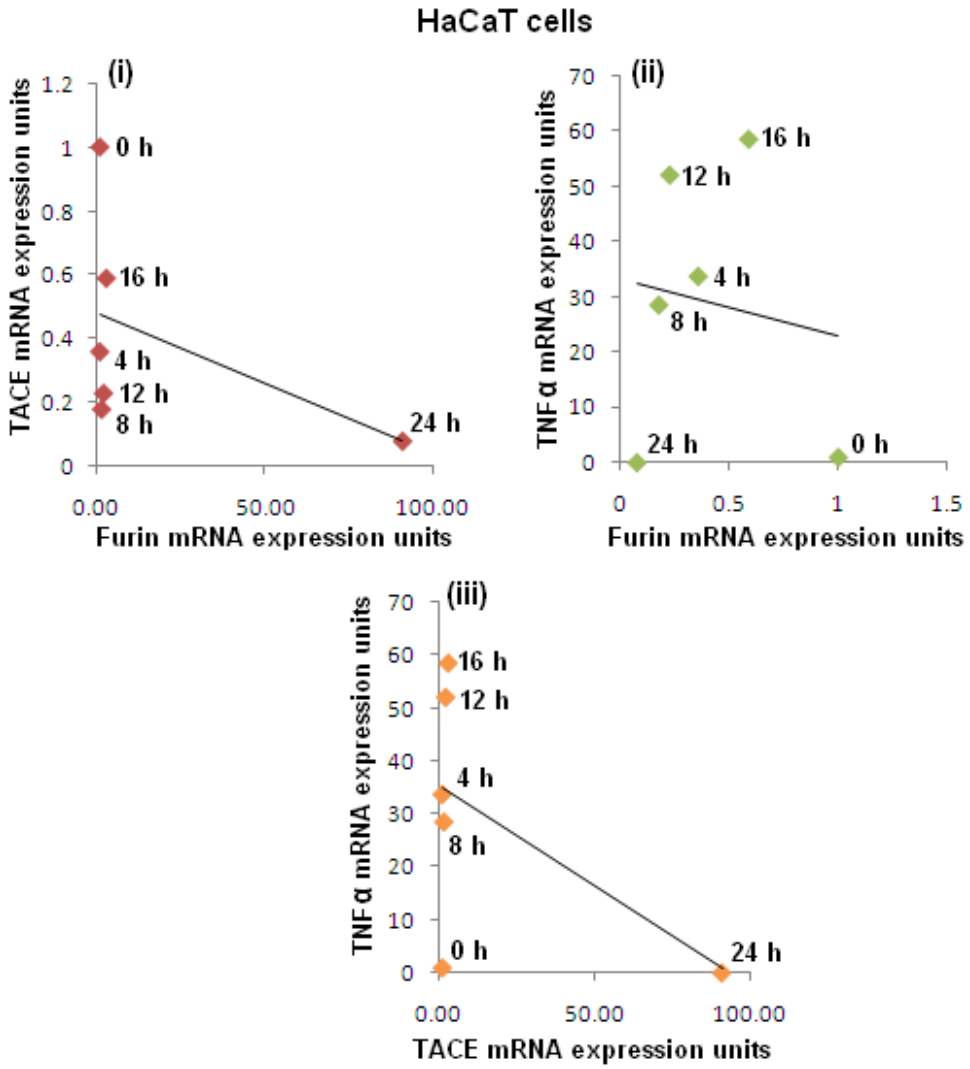

Figure 5.16 Correlation between the expression of furin and TACE (i), furin and TNFα (ii) and TACE and TNFα mRNA (iii) in UVB-irradiated HaCaT cells. The levels of furin, TACE and TNFα mRNA expressed in the cell extracts for each UV type were expressed as a ratio to that observed in sham-irradiated cells, the later was given a value of unity.

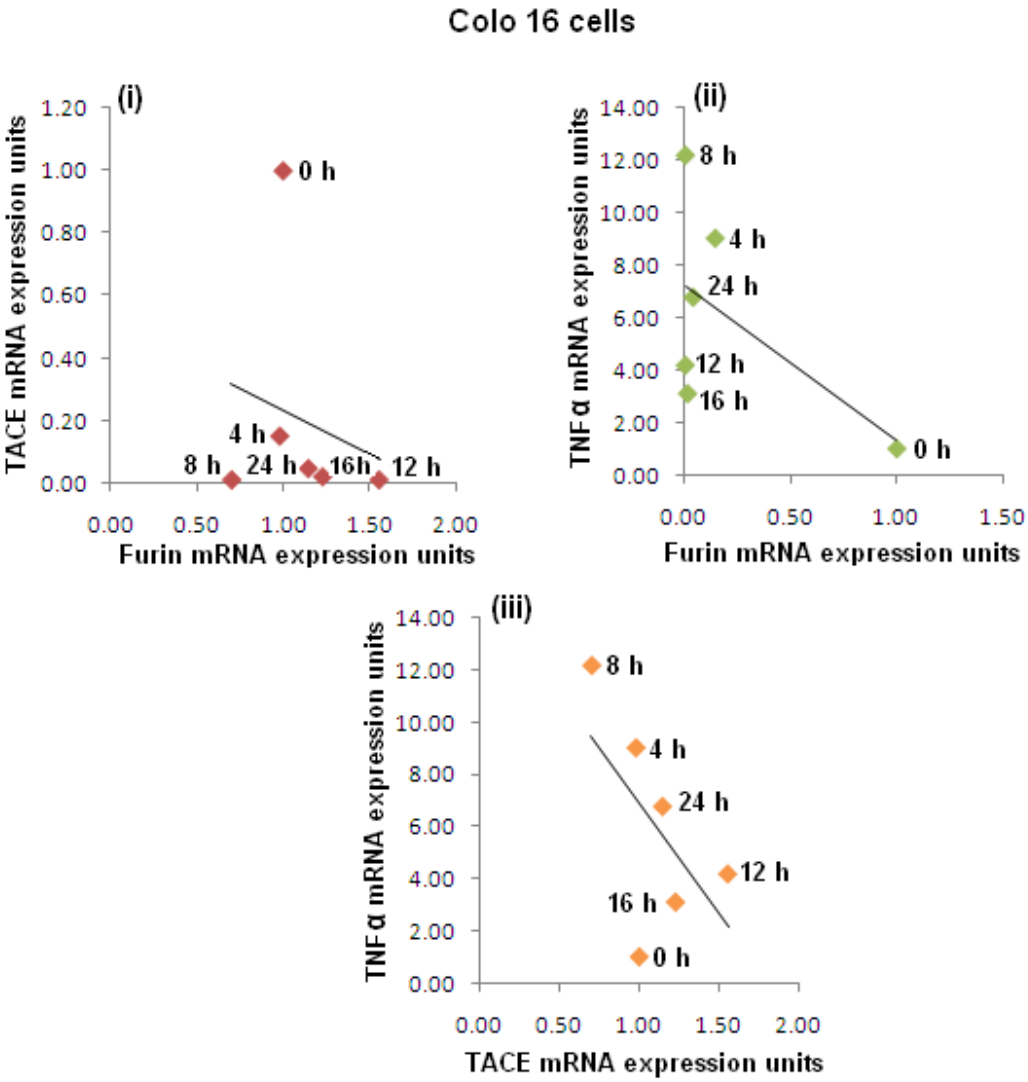

Figure 5.17 Correlation between the expression of furin and TACE (i), furin and TNFα (ii) and TACE and TNFα mRNA (iii) in UVB-irradiated Colo 16 cells. The levels of furin, TACE and TNFα mRNA expressed in the cell extracts for each UV type were expressed as a ratio to that observed in sham-irradiated cells, the later was given a value of unity.

Based on this information, correlation plots of furin, TACE and TNFα mRNA levels were constructed (Figure 5.17). It can be seen that a weak correlation was observed between furin and TNFα (r^2 = 0.321) and TACE and TNFα mRNA (r^2 = 0.351) but no correlation was observed between furin and TACE mRNA (r^2 = 0.042) in the UVB-irradiated Colo16 cells. In both HaCaT and Colo 16 cells, changes in the level of TACE, TNFα or furin mRNA expressed in UV-irradiated cells do not appear to be related to each other.

5.2.3.2 Effects of IL-1α on mRNA expression

The results from Figure 5.12 show that when IL-1α is added to the UV-irradiated cells it modulates TACE protein expression. IL-1α increased TACE levels in UVAB-irradiated HEK and HaCaT cells but not in irradiated Colo 16 cells. The addition of IL-1α also enhanced the release of TNFα in UV-irradiated keratinocyte-derived cell lines (Figure 5.1). We also observed that UVAB radiation induced the maximal release of TNFα from the cells. Therefore, we have used UVAB radiation to investigate the time course effect IL-1α has on furin, TACE and TNFα mRNA expression in irradiated HaCaT and Colo 16 cell lines.

In HaCaT cells, furin mRNA levels fell below that of the sham-irradiated controls over the first 12 h before increasing to reach a maximal value at 16 h (5.3-fold) before falling to 4.2-fold at 24 h (Figure 5.18i). The expression of TACE mRNA in these cells was reduced throughout the 24 h period following exposure to UVAB in the presence of IL-1α. TNFα mRNA levels on the other hand increased following exposure reaching

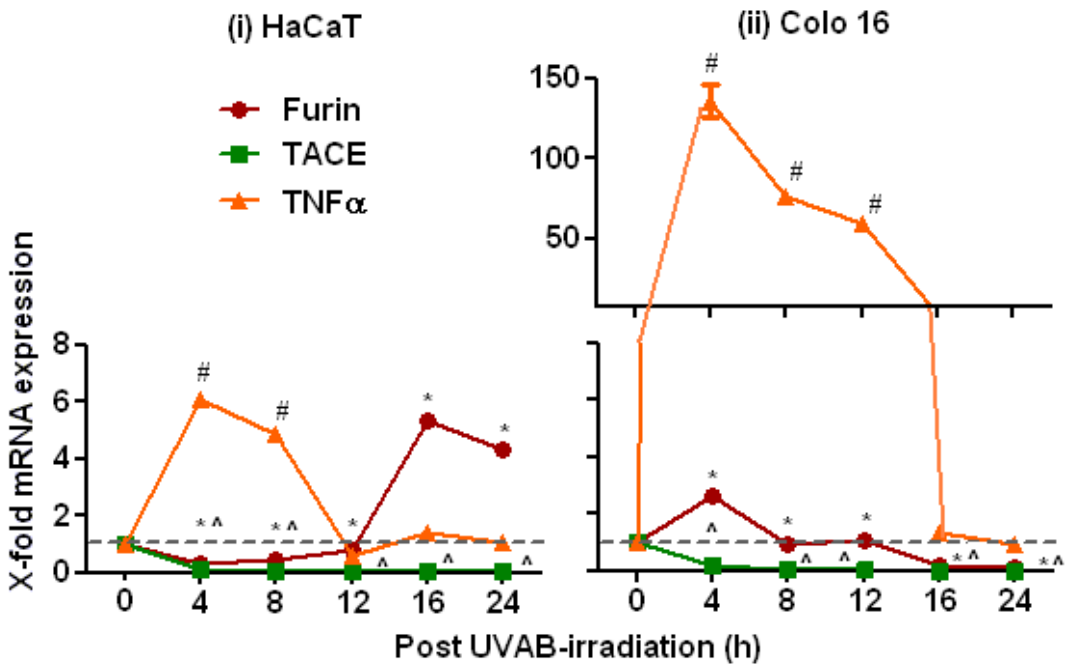

Figure 5.18 Time course of the effect of IL-1α on the expression of furin, TACE and TNFα mRNA induction/expression in UVAB-irradiated HaCaT (i) and Colo 16 cells (ii). Cells were exposed to UVAB radiation and mRNA expression measured over 24 h post-irradiation. Control mRNA levels (=1) were represented as a dotted line. Results expressed are the mean ± SEM for three separate experiments. Statistical significance of the effect of UVAB radiation in the presence of IL-1α on gene expression is shown as $p<0.05$ for furin (*), for TACE (^) and for TNFα (#).

maximal levels between 4 (6-fold) and 8 h (4.3-fold) before falling back to 1.1-fold by 24 h. When plots of furin, TACE and TNFα mRNA levels were constructed, no correlation between the expression of any of the two proteins were observed (results not shown).

In Colo 16 cells, mRNA expression of furin fell following UV exposure in the IL-1α treated cells and remained low over the 24 h period (Figure 5.18ii). A similar result was also seen for TACE mRNA in these cells. The expression of TNFα mRNA, on the other hand rose immediately following irradiation reaching a maximum level at 4 h (136-fold) before falling back to control levels by 24 h. When plots of furin, TACE and TNFα mRNA levels were constructed, no correlation between the expression of any of the two proteins were observed (results not shown).

In conclusion, these results show that IL-1α significantly induces the early expression of TNFα mRNA but not that of furin or TACE in UVAB-irradiated HaCaT and Colo 16 cells. However, the time courses of TACE, TNFα or furin mRNA induction does not appear to be related to each other.

5.2.4 Summary

This study investigated (a) the effect of UVR on furin activation of TACE, and (b) if changes in TACE activity were due to changes in furin expression and/or activity. The effect UVR on the release of TNFα from human keratinocyte-derived cells was also examined. In this study, IL-1α increased TNFα release in sham-irradiated HEK and HaCaT cells but not Colo 16 cells (Figure 5.1). UVAB-irradiated cells treated with IL-1α induced the greatest increase in TNFα release in all cell lines. Therefore, this UV

type was used to investigate further the mechanisms by which IL-1α induces TNFα release by irradiated cells. Results using CHX suggest that the cell does not contain a reservoir of TNFα, and this cytokine is synthesized when required by the cell (Figure 5.2). Results using 1, 10 phe confirmed that TACE is a metalloprotease (341) (Figure 5.3). The drop in TNFα released from Dec RVKR cmk treated UVAB-irradiated cells suggest that furin is involved in TACE activation and maturation (Figure 5.4). TNFα levels were also decreased in the presence of the MMPI which suggests that MMPs may also cleave TNFα in these cells (Figures 5.5 and 5.6).

Following exposure to UVR, mTACE expression was higher than pTACE in all three keratinocyte-derived cell lines (HEK, HaCaT and Colo 16) examined in this study (Figure 5.8). UVR only induced higher levels of total TACE in Colo 16 cells but not in HEK and HaCaT cells, where reduced levels were observed. IL-1α modulated the expression of pTACE and mTACE in the UVAB-irradiated cells, which suggests that its effect on TNFα release is not due to increased TACE expression. CHX experiments show that TACE is not rapidly turned over in these cells (Figures 5.11 and 5.13). UVB-irradiation induced maximum TACE and TNFα mRNA levels compared to UVA and UVAB in these cells 24 h post-irradiation (Figure 5.14). A time course of furin, TACE and TNFα mRNA in UVB-irradiated cells showed that the expression of these genes were not related to each other (Figure 5.15). A similar result was also seen when IL-1α was added to UVAB-irradiated cells (Figure 5.16).

5.3 Discussion

In this chapter I investigated some of the cellular changes elicited by UVR on the activation of TACE and TNFα by furin in cultured keratinocyte-derived cell lines. In most of the experiments used in this study, only HaCaT and Colo 16 cells were used. HEK cells were not available in sufficient quantities and as such future studies should repeat these experiments using cultures of these primary cells.

5.3.1 TNFα release

TNFα has a myriad of pro-inflammatory effects on the skin (77, 276). UVR has been shown to be a potent inducer of TNFα and cytokine gene expression, which mediates signalling by human keratinocytes (30, 135, 136). Kock *et al*. (115) found that there was a significant level of TNFα produced by human keratinocytes following low dose UVB (0.1 kJ/m^2) exposure. We were not able to see a significant increase in TNFα released by UVB-irradiated cells (2 kJ/m^2) in this study (Figure 5.1). Streilein and colleagues (107, 123, 124) suggested that UVB indirectly induces TNFα, which then causes morphologic and functional changes on LC resulting in the impairment of CHS. Bashir *et al*. (77) showed that up-regulation of TNFα mRNA is a key early response to UVB by keratinocytes, and represents an important component of the inflammatory cascade in the skin.

IL-1 is a family of polypeptide cytokines initially found to be produced by activated monocytes and macrophages that mediate a wide variety of cellular responses to injury and infection (236). IL-1α is a major epidermal cytokine that is constitutively synthesized by keratinocytes (273, 274) and fibroblasts (77) and it is released following

injurious stimuli like UV-irradiation (236, 237). Bashir *et al*. (77) showed that IL-1α induces a synergistic induction of TNFα by both UVB-irradiated keratinocytes and fibroblasts. In this study, ELISA was used to quantify TNFα levels in the media of the irradiated cells in the presence and/or absence of IL-1α (Figure 5.1). An increase of TNFα release was observed in the controls that were treated with IL-1α which was in agreement with that seen previously (77). A combination of UV-irradiation (UVA and/or UVB) in the presence of IL-1α, in particular UVAB-irradiation resulted in a significant increase in TNFα shed from HEK, HaCaT and Colo 16 cells. This finding differed to that seen by Bashir *et al*. (77) who showed that only UVB-irradiation induced significant levels of TNFα in the presence of IL-1α. Results from my study showed that UVAB dose has a stronger effect on the cells probably due to the fact that when cells were irradiated with UVA (40 kJ/m^2) followed immediately with 2 kJ/m^2 of UVB; the later dose appeared to be of predominance, dominating the effect of UVA.

The mechanism by which UVR (UVA and/or UVB) and IL-1α induce TNFα in these cells is not known. Cytokines may act in an autocrine manner and thereby regulate their own synthesis. Proinflammatory cytokines like IL-1α in human keratinocytes and vascular endothelial cells and IL-1β in thymic stromal cells exhibit the capacity to induce autocrine up-regulation (240, 347-349). In addition, TNFα is capable of increasing its own expression in ovarian tumour cells (350, 351). The expression of TNFα is regulated at many levels, including transcription, post-transcription, message turnover, protein production, and protein release (352-354). Previous reports showed that TNFα protein synthesis is likely due to an increase of the soluble form of TNFα in response to septic stimuli (77, 276). TNFα also promotes apoptosis, lymphocyte

activation, and hyperproliferative skin disorders (355-357). It is involved not only in the mediation of local inflammatory reactions within the epidermis but it may also enter the circulation and cause systemic effects (107, 115). Thus elevated levels of this cytokine and other skin-derived inflammatory molecules may lead to the induction of inflammation in irradiated skin (77, 276).

In response to UVAB-irradiation, the highest increase of TNFα release was observed in HEK cells (32.9-fold) followed by HaCaT cells (4.2-fold) compared to the respective untreated irradiated cells (Figure 5.1). Colo 16 cells shed less TNFα than did the HEK or HaCaT cells. This difference could be because the keratinocytes in the epidermis are continuously exposed to UV-irradiation (358). HEK cells which are the primary keratinocytes act as a trigger for the release of this cytokine as a result of inflammation. Together with IL-1α, TNFα was one of the first cytokines found to be up-regulated in the skin following UV irradiation (236, 359). There are synergistic interactions between pro-inflammatory cytokines produced in the skin and in synergy with irradiated keratinocytes, leading to later augmentation of TNFα production (77). It can be seen that TNFα plays an important pro-inflammatory role in the skin, both due to (a) the direct effects of UVR and (b) the indirect effects of inflammatory cells that chemotax to the skin. It is clear that UV-and inflammatory cell-derived cytokines further enhance TNFα gene transcription in human skin cells (77), and this can further increase epidermal production of TNFα.

While, TNFα is known to be cytotoxic to some tumour cell lines, it can mediate UV-induced tumorigenesis in others (30, 118). TNFα is involved in all steps of tumourigenesis (tumour initiation, promotion, proliferation and invasiveness) (360). It

has a particularly important role in tumour microenvironment and promotes tumour cell migration and invasion, however, the mechanism by which TNFα facilitates these events remains elusive (361). In my study, Colo 16, being a tumour cell line shed less TNFα than the other cell lines (Figure 5.1). This was probably due to the ability of TNFα to suppress immunity following UV exposure which could be dependent on several factors like the type, dose and mode of UVR, activation of signal pathways and the influence of other cytokines (5). Recently Wu *et al*. (361) emphasized on the contribution of TNFα and the NF-κB pathway on tumour cell invasion and metastasis. Furthermore, the inflammatory nature of the tumour microenvironment can lead to additional genetic changes in cells associated with malignancy. A better understanding of signalling pathways generated by UVR in Colo 16 cells may provide an insight about the regulation of TNFα release from these carcinogenic cells.

In order to investigate further the mechanisms by which IL-1α induces TNFα release from the irradiated cells, various inhibitors were tested. CHX was added to the cells to determine if the cell contains a reservoir of pTNFα or it continuously synthesizes this cytokine. TNFα levels were much lower in UV-irradiated Colo 16 cells compared to that of HaCaT cells irrespective of the different conditions and treatments (Figure 5.2). These results suggest that the cell does not contain a reservoir of proTNFα, and this protein is synthesized when required by the cell in response to external stimuli such as UV-radiation or IL-1α. Next, I added 1, 10 phe which is a broad spectrum metalloprotease inhibitor (304, 305) to the cells. There was a significant drop in TNFα levels shed from treated UVAB-irradiated HaCaT (98% inhibition) and Colo 16 cells (97% inhibition) in the presence and/or absence of IL-1α (Figure 5.3). These results

suggest that TACE is a metalloprotease which agrees with that seen in other studies (113, 125, 126, 145, 220).

TNFα is released from the cells by proteolytic cleavage of its membrane-anchored precursor (341). TACE is the main protease responsible for the ectodomain shedding of TNFα (341). TACE is cleaved from its proform to its catalytically active form by furin (144, 151, 154, 158). Srour *et al*. (158) showed that Dec RVKR cmk blocked TNFα release from the cell by inhibiting PC-mediated TACE maturation in MonoMac-1 and THP-1 cells. In order to determine the effect of furin on TACE, the furin inhibitor (Dec RVKR cmk) was used in this study (154, 156, 266). As shown in Figure 5.4, in the treated UVAB-irradiated HaCaT cells low levels (95% inhibition) of this cytokine were observed. A similar finding was also seen in the Colo 16 cells. This result suggests that furin in involved in the activation and maturation of TACE, which agrees with that seen in previous studies (154, 156, 266).

Previous studies have indicated that TACE and MMPs can process pTNFα to generate bioactive TNFα (126, 147, 345). There have also been reports that certain MMPs like gelatinases (MMP-2 and-9) can process precursor TNFα (343-345). Haro *et al*. (345) observed that MMP-7 is involved in the release of sTNFα from macrophages. Mohan *et al*. (138) showed that the specificity constants (k_{cat}/K_m) for TNFα cleavage by the MMPs were approximately 100-1000-fold lower compared to that of TACE. While TACE cleaved TNFα between Ala^{76} and Gln^{77}, MMP-9 cleaved TNFα only between Ala^{74} and Gln^{75} (138). In keeping with this finding, we added MMPI to UVAB-irradiated HaCaT and Colo 16 cells in order to confirm if MMPs (-2 and -9) also cleave TNFα (Figures 5.5). Results from this study suggested that MMPI gradually

inhibited the release of TNFα over a period of 24 h in HaCaT cells and in Colo 16 cells, 50% of TNFα release was inhibited after 7.8 h (Figure 5.6). In conclusion, these results suggest that apart from TACE, MMPs may also be involved in processing TNFα in these cells. Future work should be undertaken to see if the TNFα processed by MMP-2 and -9 in these cells is biologically active. Gearing *et al*. (343) confirmed that biologically relevant processing of proTNFα is achieved by MMPs and that, *in vitro*, production of mature, secreted TNFα can be blocked by specific inhibitors of these enzymes. If this processing takes place on the cell surface, blocking it could theoretically lead to an accumulation of membrane-anchored proTNFα, which is less biologically active than sTNFα (110). Like that of TACE, MMPs are activated by UVR and play a crucial role in skin tumour cell development and metastasis (187). Their mechanism may not only be directly related to the ability of these enzymes to degrade the ECM, but may also involve processing of bioactive molecules such as TNFα.

5.3.2 TACE expression and/or activity

TACE is the main protease responsible for the ectodomain shedding of TNFα (341). Therefore, the effect of UVR on TACE expression was investigated. Cell lysates were assessed by immunoblotting for pro and mature TACE using ADAM-17 antibody directed against the cytoplasmic domain of the enzyme, so both forms can be detected. Results from this study showed that the expression of pTACE fell in HEK and HaCaT cells following exposure to UVR (Figure 5.8). mTACE expression was higher than that of pTACE in the three keratinocyte-derived cell lines examined in this study. UVR induced expression of pTACE and mTACE was higher in Colo 16 cells when compared

to HEK and HaCaT cells, where reduced levels were observed. This agreed with studies by Ge *et al*. (362) who showed that head and neck cancer cell lines and tissues contained remarkably higher quantities of TACE activity and TACE protein than seen in normal keratinocytes or oral mucosa. These authors suggested that increased TACE expression could be biologically and clinically relevant, and could be used as a biomarker of cancer prognosis (362).

TACE has been shown to be synthesized as a zymogen, which is constitutively processed in the secretory pathway. Removal of the prodomain occurs after the protein exits the medial golgi, but before its arrival on the cell surface (363). TACE possesses the putative proprotein-convertase recognition sequence (RVKR) (126, 147), which is processed to the catalytically active form by the action of furin (144, 151, 154, 158). In order to confirm that furin was involved in cleaving TACE we used Dec RVKR cmk to see if furin inhibition has any effect on both TACE expression and activity. This inhibitor (Dec RVKR cmk) prevents the proteolytic activity of furin by covalently binding at its catalytic site (364). Endres *et al.* (154) confirmed that PC's are involved in prodomain removal of TACE in HEK293 cells. In this study, Dec RVKR cmk was shown to inhibit the conversion of pTACE to mTACE expression in both HaCaT and Colo 16 cells (Figure 5.10).

mTACE levels was expressed as a percentage of the total (mTACE and pTACE) observed in untreated un-irradiated (control) cells. The effect of Dec RVKR cmk treatment on the level of mTACE found in the irradiated cells can be seen in Table 5.1. The effect of Dec RVKR cmk treatment resulted in a 90% drop in mTACE levels in

UV type	Dec RVKR cmk	HaCaT cells mTACE	HaCaT cells Ratio (treated vs untreated)	Colo 16 cells mTACE	Colo 16 cells Ratio (treated vs untreated)
C	–	46.6	0.10	63.1	0.10
	+	4.5		6.1	
A	–	67.7	0.09	143.5	0.06
	+	6.1		8.3	
B	–	32.4	0.31	75.9	0.11
	+	10.2		8.5	
AB	–	42.3	0.32	108.7	0.08
	+	13.4		8.4	

Table 5.1 Effect of Dec RVKR cmk on the expression of mTACE in HaCaT and Colo 16 cells exposed to sham-irradiation or controls (C) and UV-irradiation (UVA, UVB and UVAB). mTACE is expressed as a percentage of the total (mTACE and pTACE) observed in the untreated control cells at 24 h post-irradiation. An average of the level of mTACE and the ratio of Dec RVKR cmk treated vs untreated cultures for three separate experiments is shown.

control and UVA-irradiated HaCaT cells, but only a 70% drop in UVB- and UVAB-irradiated cells. The difference seen in the irradiated HaCaT cells is related to UVB exposure, the reason for which is unclear. However in the Colo 16 cells, it can be seen that Dec RVKR cmk treatment caused a 90% reduction in mTACE levels in irradiated cells irrespective of the UV type used. This reduction in mTACE levels (70-90%) confirms the role furin plays in its processing in these cells. The study was similar to reports published by Srour *et al*. (158) who suggested that the TACE enzyme is completely processed in furin-positive cell lines.

In my study, results using Dec RVKR cmk confirmed that a furin-like cleavage site is located on TACE which agrees with that seen previously (151). In future experiments, to determine if PC's cleave TACE (and/or MMPs) at the RVKR recognition site directly or act via an intermediate, *in vitro* cleavage assays like HPLC and/or mass spectrometry (MS) analysis can be used (158). This will help to determine the furin-recognition site present between the proregion and the active enzyme sequence. As part of future experiments, PDX (365) and ppfurin (227) or siRNA approaches can be used to inhibit furin activation of TACE and/or MMPs following UV-irradiation in HEK, HaCaT and Colo 16 cell lines. Therefore, inhibition of these biologically active molecules (TACE and/or MMPs) should result in the impairment of cancer cell growth, survival, and invasion and in turn reduce the release of TNFα which should decrease the incidence of skin cancer.

Since CHX inhibits *de novo* protein synthesis (230, 269), it was added to the cells to prevent the synthesis of TACE. UVAB radiation was used as it was shown to induce high levels of TNFα release in irradiated cells (Figure 5.1). Based on the changes in the

level of total TACE in the cell, the approximate half-life was estimated to be ~24 h and ~46 h in HaCaT and Colo 16 cells, respectively (Figure 5.11). This estimated half-life is greater than that of furin and it is present in the cell for a longer period of time. Even though only two time points were investigated in this study, the results suggest that CHX treatment reduced TACE protein levels in these cells. However, in order to determine the half-life of TACE in these cells, further time points would need to be investigated.

As IL-1α has been shown to increase the levels of TNFα shed from irradiated keratinocytes (Figure 5.1), it was not known whether this is related to increased TACE levels in the cell. Therefore changes in the level of TACE protein were quantified following exposure to UVR either, in the presence and/or absence of IL-1α. The results obtained suggest that IL-1α reduced the levels of pTACE and mTACE in UVA- and UVB-irradiated HEK, HaCaT and Colo 16 cells (Figure 5.12). On the other hand, IL-1α increased TACE (pTACE and mTACE) levels in UVAB-irradiated HEK and HaCaT cells but not in Colo 16 cells. The reason for which is not clear. The effect of IL-1α treatment on total TACE (pTACE and mTACE) levels in the irradiated cells and the ratio of IL-1α treated cultures to that of untreated cultures are shown in Table 5.2. It can be seen from the table that the addition of IL-1α to the UVA- and UVB-irradiated cells (HEK, HaCaT and Colo 16 cells) caused a similar reduction in total TACE levels compared to that seen in the treated un-irradiated cells. In most cases this level of reduction was between 60-80%. However when IL-1α was added to UVAB-irradiated cells there was a significant increase in TACE levels in HEK and HaCaT cells compared to that seen to untreated UVAB-irradiated cells. These results

UVR	IL-1α	HEK Total	HEK Ratio (treated vs untreated)	HaCaT Total	HaCaT Ratio (treated vs untreated)	Colo 16 Total	Colo 16 Ratio (treated vs untreated)
C	-	100	0.25	100	0.24	100	0.64
	+	25		24		64	
A	-	53	0.46	120	0.21	184	0.3
	+	24		26		55	
B	-	57	0.28	56	0.29	138	0.37
	+	16		17		51	
AB	-	32	4.59	56	2.75	172	0.91
	+	149		155		156	

Table 5.2 Effect of IL-1α on the expression of TACE in HaCaT and Colo 16 cells exposed to sham-irradiation or controls (C) and UV-irradiation (UVA, UVB and UVAB). The amount of TACE in control (un-irradiated) cells was given a value of 100 (pTACE + mTACE) and the changes in pTACE and mTACE levels were expressed as a ratio of this value. An average of the level of total TACE (pTACE and mTACE) and the ratio of IL-1α treated vs untreated cultures for three separate experiments is shown.

suggest that if a person did not apply a sunscreen that there would be an increase in TACE levels in the skin which would result in increased levels of TNFα being released. Support for this can be seen in Figure 5.1 where IL-1α maximally increased the level of TNFα secreted from UVAB-irradiated HEK and HaCaT cells. However if a person used a sunscreen before they were exposed to sunlight, the levels of TACE present in the epidermis would not be increased and the corresponding levels of TNFα released from these cells would also be reduced. This concept is supported by the results seen in Figure 5.1, the level of TNFα released from HEK cells was much lower when the cells were exposed to either UVA or UVB when compared to cells exposed to UVAB-radiation.

Results from Table 5.2 also show that the ratio of total TACE levels in IL-1α treated cultures were highest in UVAB-irradiated HEK cells followed by HaCaT cells and Colo 16 cells. This result is in line with the level of TNFα released from each of these cell lines (Figure 5.1). Therefore, these results suggest that maximum TACE and TNFα increase was observed in the primary keratinocytes (HEK), being the normal skin and the Colo 16 cell, being the tumour cell has the least expression of TACE. This may in turn have a decreased effect on TNFα release thereby not stimulating inflammation. Previous results (Figure 3.9) showed that the addition of IL-1α had a suppressive effect on furin protein expression in all three cell lines. Therefore, results from these two studies (Figures 3.9 and 5.12 and Table 5.2) suggest that according to the proposed pathway (Figure 1.14), the effect of IL-1α on furin or TACE protein expression does not consequently up-regulate TNFα levels. Hence, these results suggest that the increase

in TNFα release in the presence of IL-1α could be either due to transcriptional regulation or other factors in the inflammatory cascade (77).

IL-1α was shown to stimulate the expression of TACE in UVAB-irradiated cells (Figure 5.12). The effect CHX had on TACE expression in cells treated with IL-1α was investigated. Total TACE (pTACE and mTACE) levels in the presence of CHX and IL-1α decreased 14% and 9% in UVAB-irradiated HaCaT and Colo 16 cells, respectively compared to cells treated with IL-1α alone (Figure 5.13). Therefore, these results suggest that IL-1α has no significant effect on the synthesis of TACE protein in CHX treated UV-irradiated HaCaT or Colo 16 cells compared to that seen in the untreated irradiated cells in the presence of IL-1α.

The UVAB dose used in this study (Figures 5.11 and 5.13) is a combination of the respective UVA and UVB components present in one MED of UV light. It would be of interest in future to observe the effect higher single UV dose (e.g. ≥ 2 MED) has on TACE expression and the effect this may have on the release of TNFα from the cell. At this stage it is not known if higher UV doses increase or decrease TACE expression. Since most people would be exposed to a cumulative daily exposure of UVR when they are outdoors, the effect multiple doses of ≤ 1 MED radiation 24 h apart on TACE protein expression and in turn its effects on other downstream events in keratinocyte-derived cells would also warrant investigation. It is unknown if multiple exposures to low UV doses have on the expression of TACE in irradiated skin cells.

5.3.3 TNFα and TACE mRNA expression

Some metalloproteases have been reported to be activated in epidermal cells after UVR (342). However, it is unknown whether UV-irradiation regulates TACE expression in skin cells. Kawaguchi *et al*. (139) showed a significant rise in the level of TACE mRNA expression in lesional psoriatic skin compared with non-lesional skin. In this study, there was an increase (30%) in TACE mRNA levels seen 24 h post-irradiation in UVB-irradiated HaCaT cells. In UV-irradiated Colo 16 cells, there was a decrease in TACE mRNA levels seen 24 h post-irradiation. In the UVA-, UVB- and UVAB-irradiated cells, TACE mRNA expression fell 66% 39% and 97%, respectively compared to the un-irradiated controls. (Figure 5.14). This result differed to that of Skiba *et al*. (136) who showed that TACE mRNA was induced by UVA-irradiation (8 kJ/m^2).

UVR has been shown to induce TNFα gene expression in human keratinocytes (115). Bashir *et al*. (77) showed that TNFα expression and secretion in keratinocytes was induced by UVB (0.3 kJ/m^2) but not by UVA irradiation and this induction was mediated through increased TNFα gene transcription (77) (126). Brink *et al*. (346) and Leverkus *et al*. (347) have shown a rapid and strong induction of TNFα mRNA post-exposure to UVB (0.15 kJ/m^2) in both human skin and SCC12F cells. Clingen *et al*. (366) also showed that irradiation of keratinocytes by UVB induces TNFα mRNA and protein production. The results from my study showed that maximal TNFα mRNA levels were induced by UVB-irradiation compared to UVA- and UVAB-irradiation in both HaCaT and Colo 16 cells (Figure 5.14). These results suggest that UVB significantly induces maximum mRNA expression of TACE and TNFα in these cells.

UV-irradiation has been reported to induce and activate the transcription factors AP-1 and NF-κB (367, 368), and the promoter of the TNFα gene contains consensus binding sites for AP-1 and NF-κB (369). Bazzoni *et al*. (370) suggested that after UV-irradiation TNFα gene is transcriptionally activated. Recent studies suggest that AP-1 plays a critical role in increasing TNFα transcription in UVB-irradiated keratinocytes (77, 276). AP-1 inhibitor suppresses the expression of TNF-α mRNA in endogenous cells (77, 276) and cells transfected with the TNF-α promoter which confirms the mechanism of UVB and IL-1α induction of TNF-α mRNA is through AP-1-mediated transcriptional up-regulation.

In order to investigate the relationship between TACE, TNFα and furin mRNA levels, a time course TNFα gene induction in response to UVB-irradiation was undertaken in HaCaT and Colo 16 cells (Figure 5.15). Distinct time courses for mRNA induction were generated for each gene of interest, which provided a valuable insight into the expression of these proteases at the molecular level in keratinocytes following exposure to UVB-irradiation. Skiba *et al*. (136) showed that maximum induction of furin mRNA in HaCaT cells was detected immediately (0 h) post UVB-irradiation (~5-fold) after which the levels subsequently declined. On the contrary, results from my study showed that in UVB-irradiated HaCaT cells, furin mRNA levels slowly increased with time to a maximal level (90-fold) at 24 h before falling back to 3.3-fold at 32 h (Figure 5.15).

Skiba *et al*. (136) showed that in HaCaT cells exposed to 2 kJ/m^2 UVB, maximum TACE gene expression was observed immediately 0 h post-exposure. In this study, in UVB-irradiated HaCaT cells, TACE mRNA expression was relatively constant throughout the 24 h time course and was detected in very low amounts. Though the

dose of UVB used in my study and the one by Skiba *et al*. (136) were the same, the difference in results may be attributed to two main reasons; the different methods (SYBR® Green ER™ qRT-PCR in this study vs TaqMan™ RT-PCR in Skiba *et al*. (136)) and/or analysis (Pfaffl correction method in my study vs $\Delta\Delta C_T$ method Skiba *et al*. (136)). TNFα gene expression was detected in HaCaT cells 4-24 h post UVB-irradiation. TNFα levels were maximal at 16 h (59-fold) post UVB-irradiation. This was similar to results by Skiba *et al*. (136) who showed that TNFα mRNA induction appeared to be significantly modulated in a dose-dependent manner at 16 and 24 h post UVB-irradiation.

There are no reports in the literature about the effect of UVR on mRNA expression in Colo 16 cells. The results from my study suggest that the expression of the furin gene in UVB-irradiated Colo 16 cells was higher than controls with a maximum induction at 12 h (1.6-fold) (Figure 5.15). The expression of TACE mRNA in UVB-irradiated Colo 16 cells remained fairly constant throughout the same period. However, TNFα mRNA levels were rapidly induced being maximal at 8 h (12.1-fold) after which it fell back to 6.7-fold at 24 h post-irradiation. This study differed to the one by Leverkus *et al*. (347) who showed that TNFα mRNA in the epidermis was rapidly up-regulated after UVB (300 J/m^2) radiation with maximal induction within 4-12 h post-irradiation and post-transcriptional mechanisms play a major role in UV-induced TNFα mRNA induction. Therefore, these results suggest that increased mRNA induction of furin, TACE or TNFα was not associated with increased protein expression. Correlation analysis were done in HaCaT (Figure 5.16) and Colo 16 (Figure 5.17) cells in order to confirm if mRNA levels of these genes of interest had any association to one another.

These results show that in UVB-irradiated HaCaT cells, a weak correlation was observed between furin and TACE and TNFα mRNA but no correlation was observed between furin and TNFα. In the UVB-irradiated Colo16 cells, a weak correlation was observed between furin and TNFα and TACE and TNFα mRNA but no correlation was observed between furin and TACE mRNA. In future studies, DNA gene microarrays can be used to verify the mRNA induction of furin, TACE and TNFα to UVB-irradiation in a time course experiment (0-32 h). This dose needs to be chosen as it induced highest mRNA induction in a time course experiment (Figure 5.15).

There is evidence that TNFα and IL-1α can induce the expression of TNFα mRNA in keratinocytes (371). IL-1α further augments TNFα transcription through mechanisms independent of AP-1(77, 276). The effect of IL-1α on the mRNA expression was investigated post UVAB-irradiation in this study (Figure 5.18). For this purpose, the UVAB dose was chosen as it synergistically increases TNFα release (Figure 5.1). A time course gene induction of furin, TACE and TNFα mRNA levels in response to UVAB in the presence of IL-1α was undertaken (Figure 5.18). In HaCaT cells, furin mRNA reached a maximum at 16 h (5.3-fold) after which it fell at 24 h. The expression of the TACE gene in these cells was reduced throughout the 24 h period following exposure to UVAB in the presence of IL-1α. TNFα mRNA levels increased following exposure reaching maximal levels between 4 and 8 h before falling back at 24 h. In Colo 16 cells, mRNA expression of furin fell following UV exposure and remained low over the 24 h period (Figure 5.16 ii). A similar result was also seen for TACE mRNA in these irradiated cells. The expression of TNFα mRNA rose immediately following irradiation reaching a maximum at 4 h before it fell back to control levels by 24 h.

The result seen above differs to studies by Imaizumi *et al*. (372) who showed that in human unbilical vein endothelial cells (HUVEC), stimulated with IL-1α, expression of TNFα mRNA reached maximal levels 8 h after stimulation and decreased between 16 to 24 h. Though this study has been used as a comparison, it should be noted that HUVEC was not exposed to UVR and the significance of the results from my study is the effect of IL-1α on TNFα mRNA in UV-irradiated skin cells. Therefore, these results show that addition of IL-1α induces TNFα mRNA expression from UVAB-irradiated HaCaT and Colo 16 cells. However, the time course of furin, TACE and TNFα mRNA induction in UVAB-irradiated cells in the presence of IL-1α does not appear to be related and no direct association was evident between the time course of TACE and furin mRNA induction. These results show that while effect of IL-1α up-regulates TNFα mRNA induction, it has no effect on the induction of furin and/or TACE mRNA. Therefore, while induction of TNFα mRNA is due to the effect of IL-1α, increase in the release of TNFα protein is not due to the increased effect of IL-1α on furin (Section 3.2.2.2.1) or TACE (Section 5.2.2.4) as discussed earlier. In conclusion the key finding from this study was that the effects of IL-1α were on TNFα and not on furin and TACE.

5.3.4 Conclusion

5.3.4.1 Effect of UVR on furin activation of TACE

In conclusion, results from this study highlights on some key areas of interest. If IL-1α is added to UV-irradiated cells there is an increase in TNFα release and TNFα mRNA induction which suggests that many of the immediate biological responses to excessive sun exposure could be mediated by this cytokine. Together with IL-1α, TNFα was one of the first cytokines found to be up-regulated in the skin following UV irradiation (236,

359). It was subsequently discovered that keratinocytes and mast cells were the sources of TNFα (115, 373). Once expressed, TNFα has a myriad of different effects on a variety of cell types. It increases MHC class I expression on endothelial cells and dermal fibroblasts (374); induces the production of IL-1α (375); increases the expression of adhesion molecules, including ICAM-1, VCAM-1 and E-selectin (376); and it promotes formation of sunburn cells (89). By up-regulating adhesion molecules on endothelial cells, TNFα helps support the migration of neutrophils and macrophages to UV-exposed skin. Thus, if their local inflammatory milieu changes, they can become more pathogenic, capable of participating in an autoreactive immune response. Therefore, the role of TNFα in inflammation and immunologic reaction have been shown to be either beneficial protective or pathologic, depending on target cells, and magnitude of the inflammatory reaction (107).

It seems likely that the large increase in TNFα secretion after UVAB-irradiation results from changes at various levels, including mRNA transcript stabilization and enhanced release of mature protein from the cell surface. Because UVR is also known to induce keratinocyte apoptosis, perhaps through autocrine stimulation (89), it would be interesting to observe if TNFα mRNA is preferentially up-regulated in pre-apoptotic cells. The addition of IL-1α did not increase either TACE protein or mRNA expression which suggests that it does not exert its effects on this enzyme. Dec RVKR cmk inhibits TNFα release *in vitro* and may have potential to be used in reducing tumour metastasis *in vivo*. Bassi *et al*. (268) showed that inhibition of furin activity by Dec RVKR cmk caused a significant decrease in both substrate processing and *in vitro* invasiveness. Dec RVKR cmk inhibited release of TNFα because it has been shown to inhibit TACE

processing and activation. This study suggests that furin is a key factor in the maturation of TACE and in the conversion of pTACE to mTACE. Therefore, inhibition of furin reduced TACE activation which in turn decreases release of TNFα. This study also confirmed that TACE is the main enzyme involved in the processing of TNFα and MMPs may also play a part. Therefore, future development of specific furin inhibitors or siRNA techniques targeting furin and/or TACE would find use in not only reducing the inflammatory effect seen in UV-irradiated skin cells but also that of SCC being able to metastasise and spread to other sites in the body.

5.3.4.2 Comparing cell types

The three keratinocyte cell lines (HEK, HaCaT and Colo 16) respond differently when exposed to UVR. Based on previous findings (228, 229), we used HaCaT cells as a model cell to study the effects of UV-irradiation in keratinocytes. However, results from this study show that there are differences between the effect of UV types and doses on cell function in the keratinocyte-derived cell lines examined in this study (Table 5.3). These are described below.

5.3.4.2.1 HEK vs HaCaT and Colo 16 cells

TNFα release was highest in UV-irradiated HEK cells in the presence of IL-1α compared to that of HaCaT cells. On the other hand, expression of TACE levels was the lowest in these cells unlike that seen in HaCaT cells where moderate levels were observed. There is a possibility of the HaCaT cells being a precancerous cell and the difference in TACE and TNFα levels could have occurred as part of the immortalization

	Experiments	HEK	HaCaT	Colo 16
1	TNFα release	XXX	XX	X
2	Effect of CHX on TNFα release	-	XX	XX
3	Effect of 1, 10 phe on TNFα release	-	XX	XX
4	Effect of Dec RVKR cmk on TNFα release	-	XX	XX
5	Effect of MMPI on TNFα release	-	XX (over 24 h)	XX (7.8 h)
6	TACE protein expression	X	XX	XXX
7	Effect of Dec RVKR cmk on TACE protein expression	-	XXX	XXX
8	Effect of CHX on TACE protein expression	-	XX	XX
9	Effects of IL-1α on TACE protein expression	-	XX	XX
10	TACE mRNA expression	-	XX (low 0-24 h)	XX (low 0-24 h)
11	TNFα mRNA expression	-	XX (16 h)	XXX (8 h)

Table 5.3 Effect of UVR on the function of keratinocyte-derived cells. Effect of the response is represented by X, XX, XXX and (-) where (-) represents no response and the number of X's represent the intensity of the response with XXX being the highest.

of these cells. While comparisons have been made based on these two studies, results obtained suggest that these immortalized cell lines may not be a suitable model for studying HEK cells which are primary keratinocytes.

Comparing HEK to Colo 16 cells, opposite effects were observed. While little TNFα was shed from the Colo 16 cells, maximal levels of TACE expression were observed in these cells. When the level of TACE in sham-irradiated (control) cell lines were compared (results not shown), it can be seen that Colo 16 cells expressed the highest amounts followed by HaCaT cells with HEK having the lowest levels. TACE is a protease over-expressed in tumours and is implicated in carcinogenesis and tumour growth. This could be the reason why highest TACE levels were observed in the SCC (Colo 16 cells) (Figure 5.8). This indicates that TACE could be a potentially important cancer biomarker (362). Future studies on TACE activity in a range of cancer cell lines (HNSCC) and comparing them to HEK cells might help understand the biology and expression of this protein.

5.3.4.2.2 HaCaT vs Colo 16 cells

While TNFα levels were moderate in UV-irradiated HaCaT cells in the presence of IL-1α, minimal amounts of this cytokine was released from UV-irradiated Colo 16 cells. The mechanisms by which IL-1α induces TNFα release from HaCaT and Colo 16 cells in the presence of various inhibitors (CHX, 1, 10 phe and Dec RVKR cmk) were similar. While MMPI gradually inhibited the release of TNFα over a period of 24 h in HaCaT cells, in Colo 16 cells, 50% of TNFα release was inhibited after 7.8 h. In HaCaT and Colo 16 cells, furin played an important role in the processing and activation of

mTACE and exposure to UV-irradiation had no effect on this process. On the addition of CHX, TACE was not rapidly turned over in these cells and it did not have a significant effect on the ratio of pTACE to mTACE in the cell, under the conditions examined. IL-1α had no significant effect on the synthesis of TACE protein in CHX treated UVAB-irradiated HaCaT or Colo 16 cells compared to that seen in the untreated irradiated cells in the presence of IL-1α. While TACE mRNA levels were low throughout the time period tested in both these cell lines, TNFα mRNA was maximal at 16 h in HaCaT cells and 8 h in Colo 16 cells.

Based on the studies done, results suggest that the behavior of HaCaT cells in response to UVR under different treatments and conditions is similar to that of Colo 16 cells. This could be because the HaCaT cells possess a mutated form of p53 and it is known that constant repeated UV exposure does reduce p53 levels in epidermal keratinocytes (377) which may act as a trigger for these cells to become carcinogenic *in situ*. Disturbance to the cells due to the effects of UVR could lead to malfunction of the cell, disruption of homeostasis, altered gene expression, regulation of cytokines and loss of cell cycle control, all of which can cause the cell to become carcinogenic (29). On the other hand, the profile of Colo16 cells reflects the carcinogenic nature of these cells. In Colo 16 cells maximum mTACE expression was seen which may result in enhanced downstream effects by having higher levels of protease activity in the cell. These cells secrete a broad spectrum of cytokines (378). It is unknown if p53 in these cells are functional. The cancerous nature of these cells probably arises from a possible cross talk of different cytokines, a wide array of chemical reactions and signalling interactions of the cells in response to sun exposure.

Chapter Six:

Conclusions and future directions

6 Conclusion

It is well recognized that exposure to high doses of UVR causes physical, cellular and molecular damage, resulting in erythema, immunosuppression and carcinogenesis, among other biological aberrations (42, 379, 380).

6.1 Furin

This study focused on the effect of UVR on furin expression and/or activity and its subsequent activation on MMPs and TACE. Furin is a PC which is known to process many metalloproteases, including MMPs and TACE, which in turn, when activated, process a wide range of biological molecules crucial for cell function and growth (151, 169, 266, 267).

6.1.1 Effects of UVR

Results from this study suggest that UVR up-regulates furin mRNA and protein expression in these keratinocyte-derived cells. The levels of furin protein and mRNA were much higher in HaCaT cells than in Colo 16 cells which suggest that following exposure to UVB-irradiation (24 h post exposure), increased furin protein levels may be a result of its increased mRNA levels. Colo 16 cells harbor furin protein for much longer than HaCaT cells, which may contribute to their increasing metastatic potential (174). This is because one of the proteases furin processes, MMP, is known to cleave the ECM, allowing for metastasis to occur (265). Of interest is that this, if occurring under *in vivo* conditions, may contribute to the metastasis of SCC in a skin cancer patient. Expression of PCs correlates with rapid growth, invasiveness, or metastatic potential of malignant

cell lines (268, 293, 381-383). These correlative studies provided evidence indicating a paramount role for PCs in cancer development and progression. Studies using furin inhibitors have been shown to inhibit the growth of tumour cell lines *in vitro* (168, 227) and as such may have the potential to be used as anti-tumour agents.

6.1.2 Furin activation of MMPs

In this thesis, higher levels of furin activity were observed in Colo 16 cells than in HaCaT cells. This agrees with that seen in other studies, where furin levels were higher in tumour cells compared with their non-tumorous counterparts (144, 227). Increased furin expression is associated with enhancement of metastatic spread due to elevated expression and activation of MMPs. The specific furin inhibitor Dec RVKR cmk was used in this study in order to determine the role of furin in the expression and activity of MMPs. From the results obtained, it was evident that furin plays a key role in the maturation of MMPs in these keratinocyte-derived cell lines.

6.1.3 Furin activation of TACE

This study confirmed that the changes in TACE activity are due to the conversion of pTACE to mTACE mediated by furin. An elevation in TACE activity would see an increase in TNFα being released from the cells. TACE was shown to be the main enzyme involved in the release of TNFα from these keratinocyte-derived cells but MMPs may also be involved. Once TACE is activated it can cleave a number of important molecules such as TNFα, TNFRI, TNFRII and TGFα (125). Thus, the development of specific furin inhibitors would find use in not only reducing the

inflammatory effect seen in UV-irradiated skin cells but also that of SCC being able to metastasise and spread to other sites in the body. This may in turn help to reduce the incidence of skin cancer among the general population.

Therefore, from the results obtained from this study, a model on the role furin plays in the UV-irradiated keratinocyte cells is shown in Figure 6.1. It highlights the role furin plays in the activation of MMPs and TACE in skin cells. In this model furin cleaves and activates TACE, which in turn can process TNFα from its preproform. Keratinocytes secrete TNFα following exposure to UVB radiation, and this is enhanced if IL-1α is present (Figure 5.1) (77). Furin also cleaves MMPs from their respective proforms (Figure 4.17), and the expression and activity of these proteases are elevated when the cells have been exposed to UVB radiation, and they are enhanced if either IL-1α (MMP-9) or TNFα (MMP-2) is present.

6.2 Keratinocyte-derived cells

In order to understand the effects of UVR on different keratinocyte-derived cell lines, HEK (primary keratinocytes), HaCaT cells (immortalized keratinocytes) and Colo 16 cells (squamous cell carcinoma-SCC) were examined. Results from this study show that there are differences between the effect of UV types and doses on cell function on these different keratinocyte-derived cell lines. The differences in the profile of these cells have been summarized at the end of the discussion section in Chapters 3, 4 and 5.

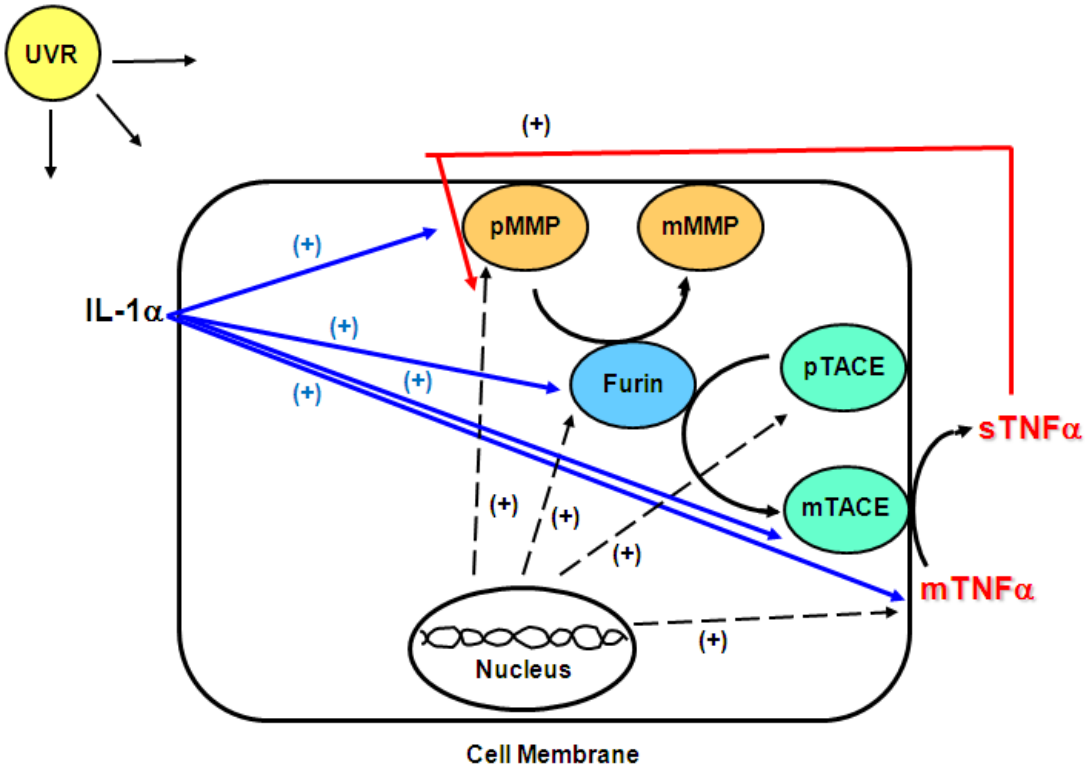

Figure 6.1 The role furin plays in the maturation of TACE and MMPs in skin cells. The effect of UVR on the expression of the enzymes and mTNFα in the cell is represented by dashed lines, if it is enhanced it is represented by (+). The role of IL-1α on MMPs and TNFα is represented by a blue line, if it is enhanced it is represented by (+). The role of IL-1α on TACE in UVAB-irradiated keratinocytes is represented by a blue line, if it is enhanced it is represented by (+).

Previous studies comparing the effect of treatments between HaCaT and primary keratinocyte cultures, and HaCaT and human keratinocytes *in vivo*, reported that the results were comparable and a good correlation existed between the two cell lines (228, 229). Therefore, based on such findings, we chose to use HaCaT cells as a model to study the effects of UV-irradiation in keratinocytes. Some studies could not be completed due to the unavailability of the primary keratinocytes (HEK). The response of HaCaT cells to UVR differs to that of HEK which suggest that these immortalized cell lines may not be a suitable model to study primary keratinocytes. This finding is supported by studies by Muthusamy (RMIT PhD Thesis, 2010) who showed that there were significant differences in UV-induced signalling pathways in the HEK and HaCaT cells. Therefore, in light of these and Muthusamy's findings the use of HaCaT cells as a model for primary keratinocytes is not recommended. On the other hand, Colo 16 cells were chosen to investigate what effect tumorigenesis has on the cellular response to UV exposure in keratinocytes. Colo16 exhibits a different profile to that of HEK cells and shares many similarities to that of HaCaT cells. This finding suggests that maybe HaCaT cells should be considered to be like a precancerous solar keratosis cell line, as it more closely reflects that of a SCC than it does a primary noncancerous cell line.

6.3 Future directions

The results from this study assist our understanding about the effect UVR has on the expression and activity of furin and of the enzymes that it cleaves and activates: MMPs and TACE. These results highlight differences between the effect the different UV types

and doses have on cellular function of the keratinocyte-derived cell lines examined in this study.

6.3.1 Effect of UVR on furin

In the experiments performed in this study, a UV cabinet that housed 6 UV fluorescent lamps (Section 2.3.3) was used. Poon *et al*. (141) used an Oriel 1000 W solar stimulator equipped with twin 240-400 nm dichroic mirrors and an atmospheric attenuation filter to produce an ssUV spectrum. These spectra are compared with standard sunlight as defined by COLIPA (1994). Therefore, as part of our future studies, experiments should be repeated using a solar stimulator (e.g. Vilber Lourmat solar stimulator) so the effect of sunlight (ssUV) on the cells can be examined.

In this study, the UVA dose (40 kJ/m^2) and UVB dose (2 kJ/m^2) used represented the respective UVA and UVB components found in one minimal erythemal dose (MED) (224). The UVAB dose used in this study was a combination of the respective UVA and UVB doses. These doses (Section 2.3.4 and Table 2.1) were chosen because they represent the dose of sunlight most people would be exposed to in a single exposure period when they are outdoors (174).

Huynh *et al.* (174) used low doses UVA (2 kJ/m^2) and/or UVB (0.2 kJ/m^2) radiation to study furin expression on cultured HaCaT and Colo 16 cells. These results suggested that low doses did not have any effect on cell viability but furin expression appeared to be biphasic following irradiation. Skiba *et al*. (136) also used low dose UVA (2 kJ/m^2) and/or low dose UVB (0.2 k J/m^2) in order to study effects of UV on mRNA expression on a variety of genes in HaCaT cells. Therefore, in future studies, it would be interesting

to observe if a single or multiple exposure to low dose UV would also modulate the expression and activity of furin and its subsequent downstream activation of MMPs and TACE if the experiment was conducted over a larger time period (48-72 h). This would help determine the smaller doses over a longer time period will have the same effect on protease activity when compared to that observed when the cells were exposed to a single high dose as used in this study.

6.3.2 Cell culturing

Most of the experiments used in this study have been performed using immortalized keratinocyte (HaCaT) and SCC (Colo16) cells. All the experiments performed in this thesis should be repeated using HEK cells. We have made used of a conventional monolayer (2-dimensional) cell culture system for culturing HEK cells. A better *in vitro* model that mimics an *in vivo* environment can be made use of in future. NanoCulture Plate (NCP) is a novel experimental system developed for the three-dimensional cell culture (384, 385). These NCP cell culture systems have been ideal for 3D culturing of tumour cells as well as primary cells (384, 385). Therefore, it may be more appropriate to use these commercially purchased 3D cell culture systems for culturing primary keratinocytes if possible in future. It would also be worthwhile performing co-culture experiments (keratinocyte-fibroblast) (386) or using skin explants or reconstructed skin models (387) to observe the effect UVR has on the interaction between these skin cells.

6.3.3 Cell viability

Although cell viability determination using trypan blue exclusion is a relatively easy, fast and cost-efficient method, there are limitations to this method. Trypan blue stains dead cells blue as these cells lose their membrane integrity. However, this does not help differentiate between apoptotic and necrotic cells. The trypan blue dye is cytotoxic and can cause cell death if there is a delay in performing viability counts. Similarly, cells in early stage of apoptosis are not stained blue as the plasma membrane is still intact (260). Therefore, this can give rise to inaccurate results. As part of future experiments, cell survival rates can be determined using methods such as MTS assay or flow cytometry. The staining methods which could be used in flow cytometry include acridine orange and EtBr or Hoechst 33342 and propidium iodide (260, 262). These methods might help differentiate and quantify the number of viable, apoptotic, late-stage apoptotic and necrotic cells in treated cell population respectively, by cell sorting and ultrastructural examination of electron micrographs (260). Therefore, the identity of each distinct fluorescent population (whether live, apoptotic, or necrotic) can be determined by sorting and examination of cellular morphology by electron microscopy. Further, it may also be possible to collect viable, apoptotic and necrotic cell populations using flow cytometry and use these in experiments to observe if there are changes in the levels of enzyme activity in these different cell populations.

6.3.4 Furin expression and activity

Furin and other PC family members process inactive precursor proteins to their functional or mature form. These molecules include members of the ADAM family, growth receptors, growth factors, hormones, plasma proteins, MMPs and ECM

components (144, 146, 156, 167). Furin mediates a wide range of processing events, which, in pathological situations, may exacerbate disease states such as tumours (168). In this study, I looked at the effect UVR had on furin expression and its subsequent activation of TACE and MMPs.

Western blots were used to investigate the expression of proteins of interest (furin, MMP-2 and -9 and TACE) in irradiated keratinocyte-derived cell lines. In future, confocal fluorescent microscopy can be used to ascertain the distribution and localization of furin in the irradiated skin cells. Furin staining was detected by immunofluorescent localization within the epidermis by Pearton *et al*. (156) on tissue sections. The antibody to the cytoplasmic domain (c-fur) showed strong staining in the basal and granular layers with less staining in the spinous layers. The same can be repeated in cell culture monolayers for TACE and MMPs using appropriately labelled antibodies. Schlöndorff *et al.* (363) performed confocal immunofluorescence to define the steady state localization of TACE in COS-7 cells using antibodies raised against the extracellular domains of TACE and found that majority of TACE was localized in a perinuclear compartment, with some diffuse localization consistent with surface and ER staining. Onoue *et al*. showed detection of MMP-9 in primary human keratinocytes culture was induced by 3 kJ/m^2 UVB-irradiation using immnufluorescence. Flow cytometry can also be used to observe if membrane localization takes place in the cell.

In future, furin activity can be determined by using the fluorogenic substrate (Pyr-Arg-Thr-Lys-Arg-AMC) and measuring the fluorescene of AMC released at 370 and 450 nm (171). In order to investigate the effect of various treatments on the activity of furin in processing various biological substrates (TACE and/or MMP and other growth factors),

the fluorogenic tetrapeptide boc-Arg-Val-Arg-Arg-MCA (Boc-RVRR-MCA) could also be used (283-286). These experiments will confirm if changes in activity in the irradiated cells are due to changes in furin levels or its kinetic parameters (K_m and V_{max}).

Proprotein convertases such as furin are expressed in many human tumour cell lines and primary tumours (173). Therefore, in order to expand on our current study, it would be ideal to do a comparison of furin, MMP and TACE levels in HEK cells and various other SCC cell lines (e.g. HNSCC, CHO, HT1080 cell lines) to see if the levels of these proteins correlate to the metastatic nature of these cells. Furin has been detected in melanocytes (156) but the effect UVR has on its activity and/or expression and that of the proteases it activates in human melanocyte cell lines is unknown. Therefore, similar studies can be repeated on melanocytic cell lines like malignant melanoma (MM96L) or primary melanocytes and results from this study would give us an improved understanding of the activation of these proteases and their downstream effects and how these may differ as a result of tumorigenesis. Further, CHX can be used to determine the half-life period of furin, MMP and TACE in these cells lines (HEK, HNSCC and/or melanocytes) such that the turn over time of these proteins can be established. This would give us an idea about the turnover time of these proteases in the different cell lines. Further experiments also can be performed to determine if increased cellular expression of furin subsequently activates MMPs and TACE in these cell lines.

6.3.5 MMP activity and expression

Previous studies have reported differences in the effect of UVR on MMP activity on fibroblasts compared to that seen on keratinocytes (179, 209, 217). Interactions between

epidermal-dermal cells via soluble factors provide important signals in regulating the re-epithelialization of wounded skin (388, 389). Witte *et al*. (388) performed keratinocyte-fibroblasts co-culture experiments in order to understand substrates and culture conditions. In keeping with this finding, as part of future studies, performing co-culture experiments with fibroblasts and keratinocytes a might provide a better answer regarding the differences in the effect of UVR on MMP activity and/or expression and how these changes relate to that of furin in irradiated skin cells. This would also help understand the interaction between the cells and the molecules they release and the effect this may have with respect to skin cancer or other skin inflammatory conditions.

6.3.6 Inhibitor studies

Different inhibitors including Dec RVKR cmk (furin convertase inhibitor), 1, 10 phenanthroline (1, 10 phe) (metalloprotease inhibitor), cycloheximide (CHX) (protein synthesis inhibitor) and 2R-2-[(4-Biphenylsulfonyl) amino]-3-phenylpropionic acid (MMPI) inhibitor have been used in some experiments in this study. Dasgupta *et al*. (113) in their review discussed about the development and designs of many potent and selective novel TACE inhibitors. These include succinate-based dual TACE and MMP inhibitors, macrocyclic inhibitors, hydroxamic acid GW 9471 (219), γ-Lactam hydroxamates (151), β-Benzamido TACE inhibitors, PKF-242-484 (390) and PKF-241-466 (391). Therefore, some of these TACE inhibitors could be used in future to inhibit TACE and/or MMPs. In order to achieve inhibition of protein/mRNA expression of target genes (furin, MMP-2 and-9 and TACE), Small interfering RNA

(siRNA) could be used. Tellier *et al*. (171) used siRNAs strategies targeting furin, MT1-MMP and MMP-2 which resulted in inhibition of the activation of their proposed signalling pathway. Such studies could be done using keratinocyte cell lines to confirm the role these proteins play in the cell.

Previous studies have reported the $\alpha_1$anti-trypsin portland (α_1PDX) and PC prosegments to be relevant PC inhibitors (173, 227, 392). α_1PDX has been shown to inhibit the processing of many proteins in the cell such as TGFβ (393), IGF 1R (383), VEGF-C (394) as well as the maturation of the surface glycoproteins of infectious pathogens among others (365). Bassi *et al*. (173) demonstrated that overexpressing α_1PDX in different SCC cell lines effectively reduced the processing of MMP-2 and significantly reduced invasiveness and *in vivo* tumorigenecity.

Although α_1PDX demonstrated to be an exteremely efficient furin inhibitor, PC's own propeptides or prosegments (ppfurin) are the only naturally known PC inhibitors (227). Previous *in vitro* studies have demonstrated that PC prosegments can inhibit intracellularly the processing of some growth factors and growth factor receptors directly involved in cancer development (395, 396). Therefore, as part of future experiments, PDX and ppfurin can be used to inhibit furin activation of MMPs and TACE following UV-irradiation in these keratinocyte-derived cell lines. The results obtained from this study can then be compared to the results obtained in this study using Dec RVKR cmk. This would help determine the specificity of these different furin inhibitors and understand the similarities and/or differences in the way TACE and MMPs are activated in these cells. Also, targeting furin could be a potential additional modality for cancer therapy.

6.3.7 Cell migration studies

The *in vitro* scratch assay used in this study both in the presence and absence of inhibitors was a straightforward, easy, well-developed and economical method to study cell migration *in vitro* (310). The limitations of the *in vitro* scratch assay are that it takes a relatively longer time to perform than some other methods. Two to three days are needed for the formation of cell monolayer and then up to 48 h for cell migration to close the scratch. Last, relatively large amount of cells and chemicals will be required for the assay as it is usually performed in a tissue culture dish. Maquoi *et al*. (175) tested the potential influence of the furin inhibitor (Dec RVKR cmk) on HT1080 cell invasion and migration using cell culture inserts. In the chemoinvasion assays, type IV collagen-coated membranes were used whereas uncoated membranes were employed for chemotaxis assays. Lapierre *et al*. (392) determined cell migration of MDA-MB-231 breast cancer cells using 24-well microchemotaxis chamber alone or precoated with collagen type IV. Another way to expand on this study performed on this thesis would be to use one of the above mentioned methods for chemotaxis or a Boyden chamber assay, as no chemical gradient is established.

6.3.8 TACE activity

Proinflammatory molecules have been shown to have important roles in the pathogenesis of skin cancer, as determined from clinical or experimental animal studies, and the activity or quantities of many of these are affected by UVR (35, 67). It is known that inflammatory mediators such as IL-1α, TNFα and IL-6 are involved in melanoma formation (71). It is not known if TNFα can regulate its expression in the UV-irradiated cells via an autocrine mechanism and if other cytokines are directly or indirectly

involved in this process. Imaizumi *et al*. (372) suggested that sTNFα may be involved in autocrine activation of endothelial cells, and TNFα retained in cell membrane may serve as a juxtacrine system to activate target cells on the endothelial surface. In order to confirm if the increase in TNFα release is due to increased TACE levels in the cell or changes in its kinetic parameters (K_m and V_{max}), the flurogenic substrate MCA-PLAQAV-DPA-rSSSR-NH_2 could be used to determine this information following UV-irradiation of the cells (397). TACE activity will be distinguished from that of the matrix metalloproteases through the use of inhibitors such as TIMP-1, -2 and -3 (398). TIMP-3 at concentrations of 1 μM have been shown to inhibit >90% TACE activity (398) and can be used in similar designed experiments in this study. TAPI-1 (399) and -2 (400) and Batimastat (also known as BB-94) (401) can be used in future studies to differentiate TACE and MMP activity. The effect of UVA and/or UVB on the expression of TACE on the cell surface will be quantified by flow cytometry using TACE antibodies.

6.3.9 TNFα expression

The effect of UVR and that of TNFα on gene expression in the skin cells can also be observed using microarray analysis. DNA microarrays are a powerful tool for studying the molecular basis of interactions on a large scale. It has been shown previously that UVB irradiation of HaCaT cells induced genes involved in cell survival and cell cycle progression (402). However, no information on the change in cytokine gene expression was obtained due to the absence of these genes on the array chip (402). In order to evaluate the role TNFα may play in gene expression, irradiated cells can also be treated

with TACE inhibitors, and/or neutralising TNFα antibodies. Appropriate matched controls can also be used in this study. TNFα can be added to the cells to observe its effect on gene expression. The results of these studies should indicate to what extent does TNFα modulate gene expression in UV-irradiated cells, and it is possible that it plays no role in this process, or has a delayed effect. It is not possible to undertake this comparison if only a single time point is used. Therefore, a time course experiment (0-24 h) will need to be performed to observe changes in the global expression of genes in the cell.

In our study, qRT-PCR was used to determine gene expression. It was a highly sensitive and reproducible method which was used to analyse mRNA levels of proteases and TNFα in these keratinocyte-derived cell lines following exposure to UV-irradiation. This study can be repeated using cultures of skin cells and the results can be used to quantify the results obtained from the cDNA microarray study outlined above. This study should help clarify the roles UV and TNFα play in cytokine gene expression seen in skin cells following UV irradiation.

6.4 Summary

Therefore, future studies could give us a better understanding of the effects of UVR on these proteases and in elucidating their downstream effects. PCs may also serve as a useful marker for cancer as well as a molecular target for cancer therapy (227). Therefore the results from future studies may lead to the development of specific PC or metalloprotease inhibitors capable of reducing TNFα release from UV-irradiated skin cells. This may in turn lead to a decrease in UV-induced immunosuppression and in due

course a reduction in incidence of skin cancer. Future efforts in understanding the mechanisms underlying UV-induced immunosuppression may lead to potential therapeutic targets to reduce TNFα release.

References:

7 References

1. Lynch JM. The histology of the skin. Available from: www.pathology.vcu.edu/education/musculo/MIIlecture06.swf. Date Accessed 20/06/2008.
2. Passeron T, Coelho SG, Miyamura Y, Takahashi K, Hearing VJ. Immunohistochemistry and *in situ* hybridization in the study of human skin melanocytes. Exp Dermatol 2007;16 (3):162-170.
3. Ylä-Outinen H. NF1 tumor suppressor in epidermal differentiation and growth-implications for wound epithelialization and Psoriasis:2.7 Skin 2003: Available from: [http://herkules.oulu.fi/isbn9514271106/html/x426.html]. Date Accessed 28/08/2008.
4. Fuchs E. Beauty is skin deep: the fascinating biology of the epidermis and its appendages. Harvey Lect 1999;94:47-77.
5. Muthusamy V, Piva TJ. The UV response of the skin: a review of the MAPK, NFκB and TNFα signal transduction pathways. Arch Dermatol Res 2010.
6. Amerio P, Toto P, Feliciani C, Suzuki H, Shivji G, Wang B, Sauder DN. Rethinking the role of tumour necrosis factor-α in ultraviolet (UV) B-induced immunosuppression: altered immune response in UV-irradiated TNFR1R2 gene-targeted mutant mice. Br J Dermatol 2001;144 (5):952-957.
7. Matsumura Y, Ananthaswamy HN. Toxic effects of ultraviolet radiation on the skin. Toxicol Appl Pharmacol 2004;195 (3):298-308.
8. Yamaguchi Y, Takahashi K, Zmudzka BZ, Kornhauser A, Miller SA, Tadokoro T, Berens W, Beer JZ, Hearing VJ. Human skin responses to UV radiation:

pigment in the upper epidermis protects against DNA damage in the lower epidermis and facilitates apoptosis. FASEB J 2006;20 (9):1486-1488.

9. Young AR. Tanning devices--fast track to skin cancer? Pigment Cell Res 2004;17 (1):2-9.

10. Reichrath J. The challenge resulting from positive and negative effects of sunlight: how much solar UV exposure is appropriate to balance between risks of vitamin D deficiency and skin cancer? Prog Biophys Mol Biol 2006;92 (1): 9-16.

11. Armstrong BK, Kricker A. The epidemiology of UV induced skin cancer. J Photochem Photobiol B 2001;63 (1-3):8-18.

12. SunSmart Victoria (2006); Skin Cancer Statistics. Available from: (http://www.sunsmart.com.au/browse.asp?ContainerID=1752). Date Accessed 04/08/2009.

13. Eshkoor SA, Ismail P, Rahman SA, Oshkour SA. p16 gene expression in basal cell carcinoma. Arch Med Res 2008;39 (7):668-673.

14. Jhappan C, Noonan FP, Merlino G. Ultraviolet radiation and cutaneous malignant melanoma. Oncogene 2003;22 (20):3099-3112.

15. Katiyar SK. UV-induced immune suppression and photocarcinogenesis: chemoprevention by dietary botanical agents. Cancer Lett 2007;255 (1):1-11.

16. Runger TM. How different wavelengths of the ultraviolet spectrum contribute to skin carcinogenesis: the role of cellular damage responses. J Invest Dermatol 2007;127 (9):2103-2105.

17. Chong AH, Skin Cancer (Non-Melanoma): Common Skin Cancers booklet 2007. Available from: <http://www.cancervic.org.au/about-cancer/cancer_types/skin_cancers_non_melanoma/>. Date Accessed 05/01/2010.

18. The Cancer Council Australia (2007); Facts and Figures, Cancer in Australia . Available from: (http://www.cancer.org.au/content.cfm?randid=101127). Date Accessed 10/10/2007.

19. The Melanoma Foundation, Latest Statistics. Available from: (http://www.melanomafoundation.com.au/MACb.html). Date Accessed 15/05/2007.

20. Staples MP, Elwood M, Burton RC, Williams JL, Marks R, Giles GG. Non-melanoma skin cancer in Australia: the 2002 national survey and trends since 1985. Med J Aust 2006;184 (1):6-10.

21. Fritschi L, Driscoll T. Cancer due to occupation in Australia. Aust N Z J Public Health 2006;30 (3):213-219.

22. Australian Institute of Health and Welfare. Health system expenditures on cancer and other neoplasms in Australia, 2000-01 Health and Welfare Expenditure Series Number 22. Canberra: AIHW 2005.

23. Siskind V, Aitken J, Green A, Martin N. Sun exposure and interaction with family history in risk of melanoma, Queensland, Australia. Int J Cancer 2002;97 (1):90-95.

24. Tran TT, Schulman J, Fisher DE. UV and pigmentation: molecular mechanisms and social controversies. Pigment Cell Melanoma Res 2008;21 (5):509-516.

25. Skin cancers (non-melanoma) 2007. Available from: http://www.cancervic.org.au/about-cancer/cancer_types/skin_cancers_non_melanoma/. Date Accessed 10/03/2009.

26. Medline Plus: Topics on Skin Cancer. Available from: www.nlm.nih.gov/medlineplus/skincancer.html. Date Accessed 02/10/2008.

27. Kelly J, Peter MacCallum Cancer Centre. Melanoma booklet Melbourne, Victoria 2009 Available from: http://www.cancervic.org.au/melanoma. Date Accessed 08/01/2010.

28. Weichenthal M, Godorr M, Altenhoff J, Neuber K, Breitbart EW. Effects of whole-body UVB irradiation on cytokine production by peripheral blood mononuclear cells from stage I melanoma patients. Arch Dermatol Res 2000;292 (7):348-353.

29. de Gruijl FR, van Kranen HJ, Mullenders LH. UV-induced DNA damage, repair, mutations and oncogenic pathways in skin cancer. J Photochem Photobiol B 2001;63 (1-3):19-27.

30. Clydesdale GJ, Dandie GW, Muller HK. Ultraviolet light induced injury: immunological and inflammatory effects. Immunol Cell Biol 2001;79 (6): 547-568.

31. Godar DE. UV doses worldwide. Photochem Photobiol 2005;81 (4):736-749.

32. Qureshi AA, Laden F, Colditz GA, Hunter DJ. Geographic variation and risk of skin cancer in US women. Differences between melanoma, squamous cell carcinoma, and basal cell carcinoma. Arch Intern Med 2008;168 (5):501-507.

33. Agar NS, Halliday GM, Barnetson RS, Ananthaswamy HN, Wheeler M, Jones AM. The basal layer in human squamous tumors harbors more UVA than UVB fingerprint mutations: a role for UVA in human skin carcinogenesis. Proc Natl Acad Sci U S A 2004;101 (14):4954-4959.

34. Kadekaro AL, Kavanagh RJ, Wakamatsu K, Ito S, Pipitone MA, Abdel-Malek ZA. Cutaneous photobiology. The melanocyte vs. the sun: who will win the final round? Pigment Cell Res 2003;16 (5):434-447.

35. Halliday GM. Inflammation, gene mutation and photoimmunosuppression in response to UVR-induced oxidative damage contributes to photocarcinogenesis. Mutat Res 2005;571 (1-2):107-120.

36. Timares L, Katiyar SK, Elmets CA. DNA damage, apoptosis and langerhans cells--Activators of UV-induced immune tolerance. Photochem Photobiol 2008;84 (2):422-436.

37. Fisher MS, Kripke ML. Further studies on the tumor-specific suppressor cells induced by ultraviolet radiation. J Immunol 1978;Sep;121 (3):1139-1144.

38. Kripke ML, Fisher MS. Immunologic aspects of tumor induction by ultraviolet radiation. Natl Cancer Inst Monogr 1978 (50):179-183.

39. Ibuki Y, Allanson M, Dixon KM, Reeve VE. Radiation sources providing increased UVA/UVB ratios attenuate the apoptotic effects of the UVB waveband UVA-dose-dependently in hairless mouse skin. J Invest Dermatol 2007;127 (9):2236-2244.

40. Sander CS, Chang H, Hamm F, Elsner P, Thiele JJ. Role of oxidative stress and the antioxidant network in cutaneous carcinogenesis. Int J Dermatol 2004;43 (5):326-335.

41. Jiang W, Ananthaswamy HN, Muller HK, Kripke ML. p53 protects against skin cancer induction by UV-B radiation. Oncogene 1999;18 (29):4247-4253.

42. Nickoloff BJ, Qin JZ, Chaturvedi V, Bacon P, Panella J, Denning MF. Life and death signaling pathways contributing to skin cancer. J Investig Dermatol Symp Proc 2002;7 (1):27-35.

43. Gallagher RP, Lee TK. Adverse effects of ultraviolet radiation: a brief review. Prog Biophys Mol Biol 2006;92 (1):119-131.

44. He YY, Huang JL, Sik RH, Liu J, Waalkes MP, Chignell CF. Expression profiling of human keratinocyte response to ultraviolet A: implications in apoptosis. J Invest Dermatol 2004;122 (2):533-543.

45. Leccia MT, Richard MJ, Joanny-Crisci F, Beani JC. UV-A1 cytotoxicity and antioxidant defence in keratinocytes and fibroblasts. Eur J Dermatol 1998;8 (7):478-482.

46. Shorrocks J, Paul ND, McMillan TJ. The dose rate of UVA treatment influences the cellular response of HaCaT keratinocytes. J Invest Dermatol 2008;128 (3):685-693.

47. de Gruijl FR, Sterenborg HJ, Forbes PD, Davies RE, Cole C, Kelfkens G, van Weelden H, Slaper H, van der Leun JC. Wavelength dependence of skin cancer induction by ultraviolet irradiation of albino hairless mice. Cancer Res 1993;53 (1):53-60.

48. Halliday GM, Lyons JG. Inflammatory doses of UV may not be necessary for skin carcinogenesis. Photochem Photobiol 2008;84 (2):272-283.

49. Moyal DD, Fourtanier AM. Broad-spectrum sunscreens provide better protection from the suppression of the elicitation phase of delayed-type hypersensitivity response in humans. J Invest Dermatol 2001;117 (5): 1186-1192.

50. Nghiem DX, Kazimi N, Clydesdale G, Ananthaswamy HN, Kripke ML, Ullrich SE. Ultraviolet a radiation suppresses an established immune response: implications for sunscreen design. J Invest Dermatol 2001;117 (5):1193-1199.

51. Peguet-Navarro J, Dalbiez-Gauthier C, Courtellemont P, Schmitt D. *In vitro* determination of sunscreen immune protection factors. Arch Dermatol Res 2000;292 (6):306-311.

52. Sander CS, Hamm F, Elsner P, Thiele JJ. Oxidative stress in malignant melanoma and non-melanoma skin cancer. Br J Dermatol 2003;148 (5):913-922.

53. Aitken GR, Henderson JR, Chang SC, McNeil CJ, Birch-Machin MA. Direct monitoring of UV-induced free radical generation in HaCaT keratinocytes. Clin Exp Dermatol 2007;32 (6):722-727.

54. Sluyter R, Halliday GM. Infiltration by inflammatory cells required for solar-simulated ultraviolet radiation enhancement of skin tumor growth. Cancer Immunol Immunother 2001;50 (3):151-156.

55. Mahns A, Wolber R, Stab F, Klotz LO, Sies H. Contribution of UVB and UVA to UV-dependent stimulation of cyclooxygenase-2 expression in artificial epidermis. Photochem Photobiol Sci 2004;3 (3):257-262.

56. Weller R. Nitric oxide: a key mediator in cutaneous physiology. Clin Exp Dermatol 2003;28 (5):511-514.

57. Valencia A, Kochevar IE. Nox1-based NADPH oxidase is the major source of UVA-induced reactive oxygen species in human keratinocytes. J Invest Dermatol 2008;128 (1):214-222.

58. Fuller BB, Smith DR. Topical anti-inflammatories. In: Draelos ZD, Thaman LA, editors. Cosmetic formulation of skin care products. New York: Informa Healthcare; 2002. p. 351-376.

59. Grether-Beck S, Timmer A, Felsner I, Brenden H, Brammertz D, Krutmann J. Ultraviolet A-induced signaling involves a ceramide-mediated autocrine loop leading to ceramide de novo synthesis. J Invest Dermatol 2005;125 (3):545-553.

60. Beissert S, Ullrich SE, Hosoi J, Granstein RD. Supernatants from UVB radiation-exposed keratinocytes inhibit Langerhans cell presentation of tumor-associated antigens via IL-10 content. J Leukoc Biol 1995;58 (2):234-240.

61. Schwarz T. Photoimmunosuppression. Photodermatol Photoimmunol Photomed 2002;18 (3):141-145.

62. Barr RM, Walker SL, Tsang W, Harrison GI, Ettehadi P, Greaves MW, Young AR. Suppressed alloantigen presentation, increased TNF-α, IL-1, IL-1Ra, IL-10, and modulation of TNF-R in UV-irradiated human skin. J Invest Dermatol 1999;112 (5):692-698.

63. Byrne SN, Limon-Flores AY, Ullrich SE. Mast cell migration from the skin to the draining lymph nodes upon ultraviolet irradiation represents a key step in the induction of immune suppression. J Immunol 2008;180 (7):4648-4655.

64. Khalil Z, Townley SL, Grimbaldeston MA, Finlay-Jones JJ, Hart PH. *cis*-Urocanic acid stimulates neuropeptide release from peripheral sensory nerves. J Invest Dermatol 2001;117 (4):886-891.

65. Li-Weber M, Treiber MK, Giaisi M, Palfi K, Stephan N, Parg S, Krammer PH. Ultraviolet irradiation suppresses T cell activation via blocking TCR-mediated ERK and NF-κB signaling pathways. J Immunol 2005;175 (4):2132-2143.

66. Norval M. Effects of solar radiation on the human immune system. J Photochem Photobiol B 2001;63 (1-3):28-40.

67. Damian DL, Patterson CR, Stapelberg M, Park J, Barnetson RS, Halliday GM. UV radiation-induced immunosuppression is greater in men and prevented by topical nicotinamide. J Invest Dermatol 2008;128 (2):447-454.

68. Coussens LM, Fingleton B, Matrisian LM. Matrix metalloproteinase inhibitors and cancer: trials and tribulations. Science 2002;295 (5564):2387-2392.

69. de Visser KE, Eichten A, Coussens LM. Paradoxical roles of the immune system during cancer development. Nat Rev Cancer 2006;6 (1):24-37.

70. Dinarello CA. The paradox of pro-inflammatory cytokines in cancer. Cancer Metastasis Rev 2006;25 (3):307-313.

71. Morelli JG, Norris DA. Influence of inflammatory mediators and cytokines on human melanocyte function. J Invest Dermatol 1993;100 (2 Suppl):191S-195S.

72. Berhane T, Halliday GM, Cooke B, Barnetson RS. Inflammation is associated with progression of actinic keratoses to squamous cell carcinomas in humans. Br J Dermatol 2002;146 (5):810-815.

73. Meeran SM, Punathil T, Katiyar SK. IL-12 deficiency exacerbates inflammatory responses in UV-irradiated skin and skin tumors. J Invest Dermatol 2008;128 (11):2716-2727.

74. Sluyter R, Halliday GM. Enhanced tumor growth in UV-irradiated skin is associated with an influx of inflammatory cells into the epidermis. Carcinogenesis 2000;21 (10):1801-1807.

75. Thomas-Ahner JM, Wulff BC, Tober KL, Kusewitt DF, Riggenbach JA, Oberyszyn TM. Gender differences in UVB-induced skin carcinogenesis, inflammation, and DNA damage. Cancer Res 2007;67 (7):3468-3474.

76. Yoshizumi M, Nakamura T, Kato M, Ishioka T, Kozawa K, Wakamatsu K, Kimura H. Release of cytokines/chemokines and cell death in UVB-irradiated human keratinocytes, HaCaT. Cell Biol Int 2008;32 (11):1405-1411.

77. Bashir MM, Sharma MR, Werth VP. TNF-α production in the skin. Arch Dermatol Res 2009;301 (1):87-91.

78. Werth VP, Bashir MM, Zhang W. IL-12 completely blocks ultraviolet-induced secretion of tumor necrosis factor α from cultured skin fibroblasts and keratinocytes. J Invest Dermatol 2003;120 (1):116-122.

79. Yarosh D, Both D, Kibitel J, Anderson C, Elmets C, Brash D, Brown D. Regulation of TNFα production and release in human and mouse keratinocytes

and mouse skin after UV-B irradiation. Photodermatol Photoimmunol Photomed 2000;16 (6):263-270.

80. Fisher GJ, Datta SC, Talwar HS, Wang ZQ, Varani J, Kang S, Voorhees JJ. Molecular basis of sun-induced premature skin ageing and retinoid antagonism. Nature 1996;379 (6563):335-339.

81. An KP, Athar M, Tang X, Katiyar SK, Russo J, Beech J, Aszterbaum M, Kopelovich L, Epstein EH, Jr., Mukhtar H, Bickers DR. Cyclooxygenase-2 expression in murine and human nonmelanoma skin cancers: implications for therapeutic approaches. Photochem Photobiol 2002;76 (1):73-80.

82. Patel MJ, Stockfleth E. Does progression from actinic keratosis and Bowen's disease end with treatment: diclofenac 3% gel, an old drug in a new environment? Br J Dermatol 2007;156 Suppl 3:53-56.

83. Butler GJ, Neale R, Green AC, Pandeya N, Whiteman DC. Nonsteroidal anti-inflammatory drugs and the risk of actinic keratoses and squamous cell cancers of the skin. J Am Acad Dermatol 2005;53 (6):966-972.

84. Suschek CV, Mahotka C, Schnorr O, Kolb-Bachofen V. UVB radiation-mediated expression of inducible nitric oxide synthase activity and the augmenting role of co-induced TNF-α in human skin endothelial cells. J Invest Dermatol 2004;123 (5):950-957.

85. Briscoe DM, Cotran RS, Pober JS. Effects of tumor necrosis factor, lipopolysaccharide, and IL-4 on the expression of vascular cell adhesion molecule-1 *in vivo*. Correlation with CD3+ T cell infiltration. J Immunol 1992;149 (9):2954-2960.

86. Ogilvie AL, Luftl M, Antoni C, Schuler G, Kalden JR, Lorenz HM. Leukocyte infiltration and mRNA expression of IL-20, IL-8 and TNF-R P60 in psoriatic skin is driven by TNF-α. Int J Immunopathol Pharmacol 2006;19 (2):271-278.

87. Swerlick RA, Lee KH, Li LJ, Sepp NT, Caughman SW, Lawley TJ. Regulation of vascular cell adhesion molecule 1 on human dermal microvascular endothelial cells. J Immunol 1992;149 (2):698-705.

88. Serwin AB, Sokolowska M, Chodynicka B. Tumour necrosis factor α (TNF-α)-converting enzyme (TACE) and soluble TNF-α receptor type 1 in psoriasis patients treated with narrowband ultraviolet B. Photodermatol Photoimmunol Photomed 2007;23 (4):130-134.

89. Schwarz A, Bhardwaj R, Aragane Y, Mahnke K, Riemann H, Metze D, Luger TA, Schwarz T. Ultraviolet-B-induced apoptosis of keratinocytes: evidence for partial involvement of tumor necrosis factor-α in the formation of sunburn cells. J Invest Dermatol 1995;104 (6):922-927.

90. Rundhaug JE, Fischer SM. Cyclo-oxygenase-2 plays a critical role in UV-induced skin carcinogenesis. Photochem Photobiol 2008;84 (2):322-329.

91. Marrot L, Meunier JR. Skin DNA photodamage and its biological consequences. J Am Acad Dermatol 2008;58 (5 Suppl 2):S139-148.

92. Schwarz A, Maeda A, Kernebeck K, van Steeg H, Beissert S, Schwarz T. Prevention of UV radiation-induced immunosuppression by IL-12 is dependent on DNA repair. J Exp Med 2005;201 (2):173-179.

93. Ullrich SE. The effects of ultraviolet radiation on the immune response. In: Biochemical Modulation of Skin Reaction: Transdermals, Topicals, Cosmetics New York, (Kydonieus AF and Wille JJ. Eds): CRC Press , Boco Raton 2001.

94. Damian DL, Barnetson RS, Halliday GM. Effects of low-dose ultraviolet radiation on *in vivo* human cutaneous recall responses. Australas J Dermatol 2001;42 (3):161-167.

95. De Fabo EC, Noonan FP. Mechanism of immune suppression by ultraviolet irradiation *in vivo*. I. Evidence for the existence of a unique photoreceptor in skin and its role in photoimmunology. J Exp Med 1983;158 (1):84-98.

96. Alard P, Niizeki H, Hanninen L, Streilein JW. Local ultraviolet B irradiation impairs contact hypersensitivity induction by triggering release of tumor necrosis factor-α from mast cells. Involvement of mast cells and Langerhans cells in susceptibility to ultraviolet B. J Invest Dermatol 1999;113 (6):983-990.

97. Laihia JK, Jansen CT. Solar-simulating irradiation of the skin of human subjects *in vivo* produces Langerhans cell responses distinct from irradiation *ex vivo* and *in vitro*. Exp Dermatol 2000;9 (4):240-247.

98. Walterscheid JP, Nghiem DX, Ullrich SE. Determining the role of cytokines in UV-induced immunomodulation. Methods 2002;28 (1):71-78.

99. Shen J, Bao S, Reeve VE. Modulation of IL-10, IL-12, and IFN-γ in the epidermis of hairless mice by UVA (320-400 nm) and UVB (280-320 nm) radiation. J Invest Dermatol 1999;113 (6):1059-1064.

100. Kang K, Hammerberg C, Meunier L, Cooper KD. CD11b+ macrophages that infiltrate human epidermis after *in vivo* ultraviolet exposure potently produce

IL-10 and represent the major secretory source of epidermal IL-10 protein. J Immunol 1994;153 (11):5256-5264.

101. Teunissen MB, Koomen CW, Jansen J, de Waal Malefyt R, Schmitt E, Van den Wijngaard RM, Das PK, Bos JD. In contrast to their murine counterparts, normal human keratinocytes and human epidermoid cell lines A431 and HaCaT fail to express IL-10 mRNA and protein. Clin Exp Immunol 1997;107 (1):213-223.

102. Kaneko K, Smetana-Just U, Matsui M, Young AR, John S, Norval M, Walker SL. *cis*-Urocanic acid initiates gene transcription in primary human keratinocytes. J Immunol 2008;181 (1):217-224.

103. Moodycliffe AM, Bucana CD, Kripke ML, Norval M, Ullrich SE. Differential effects of a monoclonal antibody to *cis*-urocanic acid on the suppression of delayed and contact hypersensitivity following ultraviolet irradiation. J Immunol 1996;157 (7):2891-2899.

104. Simon JC, Edelbaum D, Bergstresser PR, Cruz PD, Jr. Distorted antigen-presenting function of Langerhans cells induced by tumor necrosis factor α via a mechanism that appears different from that induced by ultraviolet B radiation. Photodermatol Photoimmunol Photomed 1991;8 (5):190-194.

105. Skov L, Hansen H, Allen M, Villadsen L, Norval M, Barker JN, Simon J, Baadsgaard O. Contrasting effects of ultraviolet A1 and ultraviolet B exposure on the induction of tumour necrosis factor-α in human skin. Br J Dermatol 1998;138 (2):216-220.

106. Hart PH, Townley SL, Grimbaldeston MA, Khalil Z, Finlay-Jones JJ. Mast cells, neuropeptides, histamine, and prostaglandins in UV-induced systemic immunosuppression. Methods 2002;28 (1):79-89.

107. Kondo S, Wang B, Fujisawa H, Shivji GM, Echtenacher B, Mak TW, Sauder DN. Effect of gene-targeted mutation in TNF receptor (p55) on contact hypersensitivity and ultraviolet B-induced immunosuppression. J Immunol 1995;155 (8):3801-3805.

108. Lewis M, Tartaglia LA, Lee A, Bennett GL, Rice GC, Wong GH, Chen EY, Goeddel DV. Cloning and expression of cDNAs for two distinct murine tumor necrosis factor receptors demonstrate one receptor is species specific. Proc Natl Acad Sci U S A 1991;88 (7):2830-2834.

109. Old LJ. Tumor necrosis factor (TNF). Science 1985;230 (4726):630-632.

110. Goetz FW, Planas JV, MacKenzie S. Tumor necrosis factors. Dev Comp Immunol 2004;28 (5):487-497.

111. Locksley RM, Killeen N, Lenardo MJ. The TNF and TNF receptor superfamilies: integrating mammalian biology. Cell 2001;104 (4):487-501.

112. Mocellin S, Nitti D. TNF and cancer: the two sides of the coin. Front Biosci 2008;13:2774-2783.

113. DasGupta S, Murumkar PR, Giridhar R, Yadav MR. Current perspective of TACE inhibitors: a review. Bioorg Med Chem 2009;17 (2):444-459.

114. Bouwmeester T, Bauch A, Ruffner H, Angrand PO, Bergamini G, Croughton K, Cruciat C, Eberhard D, Gagneur J, Ghidelli S, Hopf C, Huhse B, Mangano R, Michon AM, Schirle M, Schlegl J, Schwab M, Stein MA, Bauer A, Casari G,

Drewes G, Gavin AC, Jackson DB, Joberty G, Neubauer G, Rick J, Kuster B, Superti-Furga G. A physical and functional map of the human TNF-α/NF-κB signal transduction pathway. Nat Cell Biol 2004;6 (2):97-105.

115. Kock A, Schwarz T, Kirnbauer R, Urbanski A, Perry P, Ansel JC, Luger TA. Human keratinocytes are a source for tumor necrosis factor α: evidence for synthesis and release upon stimulation with endotoxin or ultraviolet light. J Exp Med 1990;172 (6):1609-1614.

116. Schreiber S, Kilgus O, Payer E, Kutil R, Elbe A, Mueller C, Stingl G. Cytokine pattern of Langerhans cells isolated from murine epidermal cell cultures. J Immunol 1992;149 (11):3524-3534.

117. Koch F, Heufler C, Kampgen E, Schneeweiss D, Bock G, Schuler G. Tumor necrosis factor α maintains the viability of murine epidermal Langerhans cells in culture, but in contrast to granulocyte/macrophage colony-stimulating factor, without inducing their functional maturation. J Exp Med 1990;171 (1):159-171.

118. Starcher B. Role for tumour necrosis factor-α receptors in ultraviolet-induced skin tumours. Br J Dermatol 2000;142 (6):1140-1147.

119. Sodhi A, Sethi G. Involvement of MAP kinase signal transduction pathway in UVB-induced activation of macrophages *in vitro*. Immunol Lett 2003;90 (2-3):123-130.

120. Yoshida Y, Kang K, Chen G, Gilliam AC, Cooper KD. Cellular fibronectin is induced in ultraviolet-exposed human skin and induces IL-10 production by monocytes/macrophages. J Invest Dermatol 1999;113 (1):49-55.

121. Cumberbatch M, Kimber I. Dermal tumour necrosis factor-α induces dendritic cell migration to draining lymph nodes, and possibly provides one stimulus for Langerhans' cell migration. Immunology 1992;75 (2):257-263.

122. Cumberbatch M, Kimber I. Tumour necrosis factor-α is required for accumulation of dendritic cells in draining lymph nodes and for optimal contact sensitization. Immunology 1995;84 (1):31-35.

123. Kurimoto I, Streilein JW. *cis*-urocanic acid suppression of contact hypersensitivity induction is mediated via tumor necrosis factor-α. J Immunol 1992;148 (10):3072-3078.

124. Streilein JW. Sunlight and skin-associated lymphoid tissues (SALT): if UVB is the trigger and TNF α is its mediator, what is the message? J Invest Dermatol 1993;100 (1):47S-52S.

125. Black RA. Tumor necrosis factor-α converting enzyme. Int J Biochem Cell Biol 2002;34 (1):1-5.

126. Black RA, Rauch CT, Kozlosky CJ, Peschon JJ, Slack JL, Wolfson MF, Castner BJ, Stocking KL, Reddy P, Srinivasan S, Nelson N, Boiani N, Schooley KA, Gerhart M, Davis R, Fitzner JN, Johnson RS, Paxton RJ, March CJ, Cerretti DP. A metalloproteinase disintegrin that releases tumour-necrosis factor-α from cells. Nature 1997;385 (6618):729-733.

127. Tartaglia LA, Goeddel DV. Two TNF receptors. Immunol Today 1992;13 (5):151-153.

128. Zhuang L, Wang B, Shinder GA, Shivji GM, Mak TW, Sauder DN. TNF receptor p55 plays a pivotal role in murine keratinocyte apoptosis induced by ultraviolet B irradiation. J Immunol 1999;162 (3):1440-1447.

129. Bechetoille N, Dezutter-Dambuyant C, Damour O, Andre V, Orly I, Perrier E. Effects of solar ultraviolet radiation on engineered human skin equivalent containing both Langerhans cells and dermal dendritic cells. Tissue Eng 2007;13 (11):2667-2679.

130. Duthie MS, Kimber I, Norval M. The effects of ultraviolet radiation on the human immune system. Br J Dermatol 1999;140 (6):995-1009.

131. Pfeffer K, Matsuyama T, Kundig TM, Wakeham A, Kishihara K, Shahinian A, Wiegmann K, Ohashi PS, Kronke M, Mak TW. Mice deficient for the 55 kd tumor necrosis factor receptor are resistant to endotoxic shock, yet succumb to L. monocytogenes infection. Cell 1993;73 (3):457-467.

132. Rothe J, Lesslauer W, Lotscher H, Lang Y, Koebel P, Kontgen F, Althage A, Zinkernagel R, Steinmetz M, Bluethmann H. Mice lacking the tumour necrosis factor receptor 1 are resistant to TNF-mediated toxicity but highly susceptible to infection by Listeria monocytogenes. Nature 1993;364 (6440):798-802.

133. Erickson SL, de Sauvage FJ, Kikly K, Carver-Moore K, Pitts-Meek S, Gillett N, Sheehan KC, Schreiber RD, Goeddel DV, Moore MW. Decreased sensitivity to tumour-necrosis factor but normal T-cell development in TNF receptor-2-deficient mice. Nature 1994;372 (6506):560-563.

134. Tartaglia LA, Pennica D, Goeddel DV. Ligand passing: the 75-kDa tumor necrosis factor (TNF) receptor recruits TNF for signaling by the 55-kDa TNF receptor. J Biol Chem 1993;268 (25):18542-18548.

135. Jaksic A, Finlay-Jones JJ, Watson CJ, Spencer LK, Santucci I, Hart PH. *Cis*-urocanic acid synergizes with histamine for increased PGE_2 production by human keratinocytes: link to indomethacin-inhibitable UVB-induced immunosuppression. Photochem Photobiol 1995;61 (3):303-309.

136. Skiba B, Neill B, Piva TJ. Gene expression profiles of TNF-α, TACE, furin, IL-1β and matrilysin in UVA- and UVB-irradiated HaCat cells. Photodermatol Photoimmunol Photomed 2005;21 (4):173-182.

137. Tracey KJ, Cerami A. Tumor necrosis factor, other cytokines and disease. Annu Rev Cell Biol 1993;9:317-343.

138. Mohan MJ, Seaton T, Mitchell J, Howe A, Blackburn K, Burkhart W, Moyer M, Patel I, Waitt GM, Becherer JD, Moss ML, Milla ME. The tumor necrosis factor-α converting enzyme (TACE): a unique metalloproteinase with highly defined substrate selectivity. Biochemistry 2002;41 (30):9462-9469.

139. Kawaguchi M, Mitsuhashi Y, Kondo S. Overexpression of tumour necrosis factor-α-converting enzyme in psoriasis. Br J Dermatol 2005;152 (5):915-919.

140. Molife R, Lorigan P, MacNeil S. Gender and survival in malignant tumours. Cancer Treat Rev 2001;27 (4):201-209.

141. Poon TS, Barnetson RS, Halliday GM. Prevention of immunosuppression by sunscreens in humans is unrelated to protection from erythema and dependent

on protection from ultraviolet a in the face of constant ultraviolet B protection. J Invest Dermatol 2003;121 (1):184-190.

142. Shapiro J, Sciaky N, Lee J, Bosshart H, Angeletti RH, Bonifacino JS. Localization of endogenous furin in cultured cell lines. J Histochem Cytochem 1997;45 (1):3-12.

143. Wang P, Tortorella M, England K, Malfait AM, Thomas G, Arner EC, Pei D. Proprotein convertase furin interacts with and cleaves pro-ADAMTS4 (Aggrecanase-1) in the trans-Golgi network. J Biol Chem 2004;279 (15): 15434-15440.

144. Denault J, Bissonnette L, Longpre J, Charest G, Lavigne P, Leduc R. Ectodomain shedding of furin: kinetics and role of the cysteine-rich region. FEBS Lett 2002;527 (1-3):309-314.

145. Black RA, White JM. ADAMs: focus on the protease domain. Curr Opin Cell Biol 1998;10 (5):654-659.

146. Mezyk R, Bzowska M, Bereta J. Structure and functions of tumor necrosis factor-α converting enzyme. Acta Biochim Pol 2003;50 (3):625-645.

147. Moss ML, Jin SL, Milla ME, Bickett DM, Burkhart W, Carter HL, Chen WJ, Clay WC, Didsbury JR, Hassler D, Hoffman CR, Kost TA, Lambert MH, Leesnitzer MA, McCauley P, McGeehan G, Mitchell J, Moyer M, Pahel G, Rocque W, Overton LK, Schoenen F, Seaton T, Su JL, Becherer JD. Cloning of a disintegrin metalloproteinase that processes precursor tumour-necrosis factor-α. Nature 1997;385 (6618):733-736.

148. Milla ME, Leesnitzer MA, Moss ML, Clay WC, Carter HL, Miller AB, Su JL, Lambert MH, Willard DH, Sheeley DM, Kost TA, Burkhart W, Moyer M, Blackburn RK, Pahel GL, Mitchell JL, Hoffman CR, Becherer JD. Specific sequence elements are required for the expression of functional tumor necrosis factor-α-converting enzyme (TACE). J Biol Chem 1999;274 (43):30563-30570.

149. Schlondorff J, Blobel CP. Metalloprotease-disintegrins: modular proteins capable of promoting cell-cell interactions and triggering signals by protein-ectodomain shedding. J Cell Sci 1999;112 (21):3603-3617.

150. Rabinowitz MH, Andrews RC, Becherer JD, Bickett DM, Bubacz DG, Conway JG, Cowan DJ, Gaul M, Glennon K, Lambert MH, Leesnitzer MA, McDougald DL, Moss ML, Musso DL, Rizzolio MC. Design of selective and soluble inhibitors of tumor necrosis factor-α converting enzyme (TACE). J Med Chem 2001;44 (24):4252-4267.

151. Peiretti F, Canault M, Deprez-Beauclair P, Berthet V, Bonardo B, Juhan-Vague I, Nalbone G. Intracellular maturation and transport of tumor necrosis factor α converting enzyme. Exp Cell Res 2003;285 (2):278-285.

152. Anderson ED, VanSlyke JK, Thulin CD, Jean F, Thomas G. Activation of the furin endoprotease is a multiple-step process: requirements for acidification and internal propeptide cleavage. Embo J 1997;16 (7):1508-1518.

153. Molloy SS, Anderson ED, Jean F, Thomas G. Bi-cycling the furin pathway: from TGN localization to pathogen activation and embryogenesis. Trends Cell Biol 1999;9 (1):28-35.

154. Endres K, Anders A, Kojro E, Gilbert S, Fahrenholz F, Postina R. Tumor necrosis factor-α converting enzyme is processed by proprotein-convertases to its mature form which is degraded upon phorbol ester stimulation. Eur J Biochem 2003;270 (11):2386-2393.

155. Enzmann V, Faude F, Kohen L, Wiedemann P. Secretion of cytokines by human choroidal melanoma cells and skin melanoma cell lines *in vitro*. Ophthalmic Res 1998;30 (3):189-194.

156. Pearton DJ, Nirunsuksiri W, Rehemtulla A, Lewis SP, Presland RB, Dale BA. Proprotein convertase expression and localization in epidermis: evidence for multiple roles and substrates. Exp Dermatol 2001;10 (3):193-203.

157. Schwarz A, Grabbe S, Aragane Y, Sandkuhl K, Riemann H, Luger TA, Kubin M, Trinchieri G, Schwarz T. Interleukin-12 prevents ultraviolet B-induced local immunosuppression and overcomes UVB-induced tolerance. J Invest Dermatol 1996;106 (6):1187-1191.

158. Srour N, Lebel A, McMahon S, Fournier I, Fugere M, Day R, Dubois CM. TACE/ADAM-17 maturation and activation of sheddase activity require proprotein convertase activity. FEBS Lett 2003;554 (3):275-283.

159. Itai T, Tanaka M, Nagata S. Processing of tumor necrosis factor by the membrane-bound TNF-α-converting enzyme, but not its truncated soluble form. Eur J Biochem 2001;268 (7):2074-2082.

160. Li X, Perez L, Pan Z, Fan H. The transmembrane domain of TACE regulates protein ectodomain shedding. Cell Res 2007;17 (12):985-998.

161. Sunnarborg SW, Hinkle CL, Stevenson M, Russell WE, Raska CS, Peschon JJ, Castner BJ, Gerhart MJ, Paxton RJ, Black RA, Lee DC. Tumor necrosis factor-α converting enzyme (TACE) regulates epidermal growth factor receptor ligand availability. J Biol Chem 2002;277 (15):12838-12845.

162. Piva TJ, Krause DR, Ellem KO. UVC activation of the HeLa cell membrane "TGFαase," a metalloenzyme. J Cell Biochem 1997;64 (3):353-368.

163. He YY, Council SE, Feng L, Chignell CF. UVA-induced cell cycle progression is mediated by a disintegrin and metalloprotease/epidermal growth factor receptor/AKT/Cyclin D1 pathways in keratinocytes. Cancer Res 2008;68 (10):3752-3758.

164. Singh B, Schneider M, Knyazev P, Ullrich A. UV-induced EGFR signal transactivation is dependent on proligand shedding by activated metalloproteases in skin cancer cell lines. Int J Cancer 2009;124 (3):531-539.

165. Krahn G, Leiter U, Kaskel P, Udart M, Utikal J, Bezold G, Peter RU. Coexpression patterns of EGFR, HER2, HER3 and HER4 in non-melanoma skin cancer. Eur J Cancer 2001;37 (2):251-259.

166. Thomas G. Furin at the cutting edge: from protein traffic to embryogenesis and disease. Nat Rev Mol Cell Biol 2002;3 (10):753-766.

167. Coppola JM, Bhojani MS, Ross BD, Rehemtulla A. A small-molecule furin inhibitor inhibits cancer cell motility and invasiveness. Neoplasia 2008;10 (4):363-370.

168. Bassi DE, Fu J, Lopez de Cicco R, Klein-Szanto AJ. Proprotein convertases: "master switches" in the regulation of tumor growth and progression. Mol Carcinog 2005;44 (3):151-161.

169. Taylor NA, Van De Ven WJ, Creemers JW. Curbing activation: proprotein convertases in homeostasis and pathology. FASEB J 2003;17 (10):1215-1227.

170. McMahon S, Laprise MH, Dubois CM. Alternative pathway for the role of furin in tumor cell invasion process. Enhanced MMP-2 levels through bioactive TGFβ. Exp Cell Res 2003;291 (2):326-339.

171. Tellier E, Negre-Salvayre A, Bocquet B, Itohara S, Hannun YA, Salvayre R, Auge N. Role for furin in tumor necrosis factor α-induced activation of the matrix metalloproteinase/sphingolipid mitogenic pathway. Mol Cell Biol 2007;27 (8):2997-3007.

172. Mahloogi H, Bassi DE, Klein-Szanto AJ. Malignant conversion of non-tumorigenic murine skin keratinocytes overexpressing PACE4. Carcinogenesis 2002;23 (4):565-572.

173. Bassi DE, Lopez De Cicco R, Mahloogi H, Zucker S, Thomas G, Klein-Szanto AJ. Furin inhibition results in absent or decreased invasiveness and tumorigenicity of human cancer cells. Proc Natl Acad Sci U S A 2001;98 (18):10326-10331.

174. Huynh TT, Chan KS, Piva TJ. Effect of ultraviolet radiation on the expression of pp38MAPK and furin in human keratinocyte-derived cell lines. Photodermatol Photoimmunol Photomed 2009;25 (1):20-29.

175. Maquoi E, Noel A, Frankenne F, Angliker H, Murphy G, Foidart JM. Inhibition of matrix metalloproteinase 2 maturation and HT1080 invasiveness by a synthetic furin inhibitor. FEBS Lett 1998;424 (3):262-266.

176. Hussein MR. Ultraviolet radiation and skin cancer: molecular mechanisms. J Cutan Pathol 2005;32 (3):191-205.

177. Jian Cao, Stanley Zucker. Biology and chemistry of matrix metalloproteinases (MMPs). Introduction to the MMP and TIMP families (structures, substrates) and an overview of diseases where MMPs have been incriminated 2009: Available from: www.sapphirebiosciences.com. Date Accessed 24/12/2009.

178. Stocker W, Bode W. Structural features of a superfamily of zinc-endopeptidases: the metzincins. Curr Opin Struct Biol 1995;5 (3):383-390.

179. Onoue S, Kobayashi T, Takemoto Y, Sasaki I, Shinkai H. Induction of matrix metalloproteinase-9 secretion from human keratinocytes in culture by ultraviolet B irradiation. J Dermatol Sci 2003;33 (2):105-111.

180. Suomela S, Kariniemi AL, Impola U, Karvonen SL, Snellman E, Uurasmaa T, Peltonen J, Saarialho-Kere U. Matrix metalloproteinase-19 is expressed by keratinocytes in psoriasis. Acta Derm Venereol 2003;83 (2):108-114.

181. Birkedal-Hansen H. Proteolytic remodeling of extracellular matrix. Curr Opin Cell Biol 1995;7 (5):728-735.

182. Nagase H, Woessner JF, Jr. Matrix metalloproteinases. J Biol Chem 1999;274 (31):21491-21494.

183. Calbiochem, Merck Biosciences. Matrix Metalloproteases (MMPs). Inhibitor Source Book™: Novogen catalogue; FSC mixed sources. 2008/2009. p. 79-82.

184. Overall CM, Lopez-Otin C. Strategies for MMP inhibition in cancer: innovations for the post-trial era. Nat Rev Cancer 2002;2 (9):657-672.

185. Sternlicht MD, Werb Z. How matrix metalloproteinases regulate cell behavior. Annu Rev Cell Dev Biol 2001; 17 (17):463-516.

186. Zucker S, Pei D, Cao J, C L-O. Membrane type-matrix metalloproteinases (MT-MMP). in: Cell Surface Proteases. S. Zucker, Chen W-T, editors: Academic Press.; San Diego, CA, 2003.

187. Murphy G, Nagase H. Progress in matrix metalloproteinase research. Mol Aspects Med 2008;29 (5):290-308.

188. Noel A, Jost M, Maquoi E. Matrix metalloproteinases at cancer tumor-host interface. Semin Cell Dev Biol 2008;19 (1):52-60.

189. Vosseler S, Lederle W, Airola K, Obermueller E, Fusenig NE, Mueller MM. Distinct progression-associated expression of tumor and stromal MMPs in HaCaT skin SCCs correlates with onset of invasion. Int J Cancer 2009;125 (10):2296-2306.

190. Newby AC. Dual role of matrix metalloproteinases (matrixins) in intimal thickening and atherosclerotic plaque rupture. Physiol Rev 2005;85 (1):1-31.

191. Visse R, Nagase H. Matrix metalloproteinases and tissue inhibitors of metalloproteinases: structure, function, and biochemistry. Circ Res 2003;92 (8):827-839.

192. Dumas V, Kanitakis J, Charvat S, Euvrard S, Faure M, Claudy A. Expression of basement membrane antigens and matrix metalloproteinases 2 and 9 in

cutaneous basal and squamous cell carcinomas. Anticancer Res 1999;19 (4B):2929-2938.

193. Chen X, Kanekura T, Zhang GY. [Expression of matrix metalloproteinases in metastatic lesions of cutaneous squamous cell carcinoma]. Hunan Yi Ke Da Xue Xue Bao 2001;26 (4):297-300.

194. Matrisian LM, McDonnell S, Miller DB, Navre M, Seftor EA, Hendrix MJ. The role of the matrix metalloproteinase stromelysin in the progression of squamous cell carcinomas. Am J Med Sci 1991;302 (3):157-162.

195. Meade-Tollin LC, Boukamp P, Fusenig NE, Bowen CP, Tsang TC, Bowden GT. Differential expression of matrix metalloproteinases in activated c-ras-Ha-transfected immortalized human keratinocytes. Br J Cancer 1998;77 (5):724-730.

196. Varani J, Hattori Y, Chi Y, Schmidt T, Perone P, Zeigler ME, Fader DJ, Johnson TM. Collagenolytic and gelatinolytic matrix metalloproteinases and their inhibitors in basal cell carcinoma of skin: comparison with normal skin. Br J Cancer 2000;82 (3):657-665.

197. Hofmann UB, Eggert AA, Blass K, Brocker EB, Becker JC. Expression of matrix metalloproteinases in the microenvironment of spontaneous and experimental melanoma metastases reflects the requirements for tumor formation. Cancer Res 2003;63 (23):8221-8225.

198. Montgomery AM, Mueller BM, Reisfeld RA, Taylor SM, DeClerck YA. Effect of tissue inhibitor of the matrix metalloproteinases-2 expression on the growth

and spontaneous metastasis of a human melanoma cell line. Cancer Res 1994;54 (20):5467-5473.

199. Walker RA, Woolley DE. Immunolocalisation studies of matrix metalloproteinases-1, -2 and -3 in human melanoma. Virchows Arch 1999;435 (6):574-579.

200. McCawley LJ, Matrisian LM. Matrix metalloproteinases: they're not just for matrix anymore! Curr Opin Cell Biol 2001;13 (5):534-540.

201. Shapiro SD. Matrix metalloproteinase degradation of extracellular matrix: biological consequences. Curr Opin Cell Biol 1998;10 (5):602-608.

202. Stahle-Backdahl M, Sudbeck BD, Eisen AZ, Welgus HG, Parks WC. Expression of 92-kDa type IV collagenase mRNA by eosinophils associated with basal cell carcinoma. J Invest Dermatol 1992;99 (4):497-503.

203. Coussens LM, Tinkle CL, Hanahan D, Werb Z. MMP-9 supplied by bone marrow-derived cells contributes to skin carcinogenesis. Cell 2000;103 (3): 481-490.

204. McCawley LJ, Li S, Benavidez M, Halbleib J, Wattenberg EV, Hudson LG. Elevation of intracellular cAMP inhibits growth factor-mediated matrix metalloproteinase-9 induction and keratinocyte migration. Mol Pharmacol 2000;58 (1):145-151.

205. Mohan R, Chintala SK, Jung JC, Villar WV, McCabe F, Russo LA, Lee Y, McCarthy BE, Wollenberg KR, Jester JV, Wang M, Welgus HG, Shipley JM, Senior RM, Fini ME. Matrix metalloproteinase gelatinase B (MMP-9)

coordinates and effects epithelial regeneration. J Biol Chem 2002;277 (3): 2065-2072.

206. Bergers G, Brekken R, McMahon G, Vu TH, Itoh T, Tamaki K, Tanzawa K, Thorpe P, Itohara S, Werb Z, Hanahan D. Matrix metalloproteinase-9 triggers the angiogenic switch during carcinogenesis. Nat Cell Biol 2000;2 (10):737-744.

207. Kobayashi T, Hattori S, Nagai Y, Tajima S, Nishikawa T. Differential regulation of MMP-2 and MMP-9 gelatinases in cultured human keratinocytes. Dermatology 1998;197 (1):1-5.

208. Kobayashi T, Hattori S, H S. Matrix metalloproteinase- 2 and -9 are secreted human fibroblasts. Acta Derm Venereol 2003;83 (2):105-107.

209. Steinbrenner H, Ramos MC, Stuhlmann D, Sies H, Brenneisen P. UVA-mediated downregulation of MMP-2 and MMP-9 in human epidermal keratinocytes. Biochem Biophys Res Commun 2003;308 (3):486-491.

210. Kahari VM, Saarialho-Kere U. Matrix metalloproteinases in skin. Exp Dermatol 1997;6 (5):199-213.

211. Wan Y, Belt A, Wang Z, Voorhees J, Fisher G. Transmodulation of epidermal growth factor receptor mediates IL-1β-induced MMP-1 expression in cultured human keratinocytes. Int J Mol Med 2001;7 (3):329-334.

212. Wan YS, Wang ZQ, Shao Y, Voorhees JJ, Fisher GJ. Ultraviolet irradiation activates PI 3-kinase/AKT survival pathway via EGF receptors in human skin *in vivo*. Int J Oncol 2001;18 (3):461-466.

213. Ramos MC, Steinbrenner H, Stuhlmann D, Sies H, Brenneisen P. Induction of MMP-10 and MMP-1 in a squamous cell carcinoma cell line by ultraviolet radiation. Biol Chem 2004;385 (1):75-86.

214. Dong KK, Damaghi N, Picart SD, Markova NG, Obayashi K, Okano Y, Masaki H, Grether-Beck S, Krutmann J, Smiles KA, Yarosh DB. UV-induced DNA damage initiates release of MMP-1 in human skin. Exp Dermatol 2008;17 (12):1037-1044.

215. Ikeda U, Shimada K. Matrix metalloproteinases and coronary artery diseases. Clin Cardiol 2003;26 (2):55-59.

216. Han YP, Tuan TL, Wu H, Hughes M, Garner WL. TNF-a stimulates activation of pro-MMP2 in human skin through NF-kB mediated induction of MT1-MMP. J Cell Sci 2001;114 (1):131-139.

217. Han YP, Downey S, Garner WL. Interleukin-1α-induced proteolytic activation of metalloproteinase-9 by human skin. Surgery 2005;138 (5):932-939.

218. Sato H, Takino T, Okada Y, Cao J, Shinagawa A, Yamamoto E, Seiki M. A matrix metalloproteinase expressed on the surface of invasive tumour cells. Nature 1994;370 (6484):61-65.

219. Moss ML, Jin SL, Becherer JD, Bickett DM, Burkhart W, Chen WJ, Hassler D, Leesnitzer MT, McGeehan G, Milla M, Moyer M, Rocque W, Seaton T, Schoenen F, Warner J, Willard D. Structural features and biochemical properties of TNF-α converting enzyme (TACE). J Neuroimmunol 1997;72 (2):127-129.

220. Boutet P, Aguera-Gonzalez S, Atkinson S, Pennington CJ, Edwards DR, Murphy G, Reyburn HT, Vales-Gomez M. Cutting edge: the metalloproteinase

ADAM17/TNF-α-converting enzyme regulates proteolytic shedding of the MHC class I-related chain B protein. J Immunol 2009;182 (1):49-53.

221. Boukamp P, Petrussevska RT, Breitkreutz D, Hornung J, Markham A, Fusenig NE. Normal keratinization in a spontaneously immortalized aneuploid human keratinocyte cell line. J Cell Biol 1988;106 (3):761-771.

222. Moore GE, Merrick SB, Woods LK, Arabasz NM. A human squamous cell carcinoma cell line. Cancer Res 1975;35 (10):2684-2688.

223. Laemmli UK. Cleavage of structural proteins during the assembly of the head of bacteriophage T4. Nature 1970;227 (5259):680-685.

224. Kuchel JM, Barnetson RS, Halliday GM. Ultraviolet a augments solar-simulated ultraviolet radiation-induced local suppression of recall responses in humans. J Invest Dermatol 2002;118 (6):1032-1037.

225. Pfaffl MW. A new mathematical model for relative quantification in real-time RT-PCR. Nucleic Acids Res 2001;29 (9):e45.

226. Lissitzky JC, Luis J, Munzer JS, Benjannet S, Parat F, Chretien M, Marvaldi J, Seidah NG. Endoproteolytic processing of integrin pro-α subunits involves the redundant function of furin and proprotein convertase (PC) 5A, but not paired basic amino acid converting enzyme (PACE) 4, PC5B or PC7. Biochem J 2000;346 (1):133-138.

227. de Cicco RL, Bassi DE, Benavides F, Conti CJ, Klein-Szanto AJ. Inhibition of proprotein convertases: approaches to block squamous carcinoma development and progression. Mol Carcinog 2007;46 (8):654-659.

228. Grabbe J, Welker P, Rosenbach T, Nurnberg W, Kruger-Krasagakes S, Artuc M, Fiebiger E, Henz BM. Release of stem cell factor from a human keratinocyte line, HaCaT, is increased in differentiating versus proliferating cells. J Invest Dermatol 1996;107 (2):219-224.

229. Wilhelm KP, Bottjer B, Siegers CP. Quantitative assessment of primary skin irritants *in vitro* in a cytotoxicity model: comparison with *in vivo* human irritation tests. Br J Dermatol 2001;145 (5):709-715.

230. Ennis HL, Lubin M. Cycloheximide: Aspects of Inhibition of Protein Synthesis in Mammalian Cells. Science 1964;146:1474-1476.

231. Fransson LA, Karlsson P, Schmidtchen A. Effects of cycloheximide, brefeldin A, suramin, heparin and primaquine on proteoglycan and glycosaminoglycan biosynthesis in human embryonic skin fibroblasts. Biochim Biophys Acta 1992;1137 (3):287-297.

232. Lobner D, Choi DW. Preincubation with protein synthesis inhibitors protects cortical neurons against oxygen-glucose deprivation-induced death. Neuroscience 1996;72 (2):335-341.

233. Ansel J, Perry P, Brown J, Damm D, Phan T, Hart C, Luger T, Hefeneider S. Cytokine modulation of keratinocyte cytokines. J Invest Dermatol 1990;94 (6 Suppl):101S-107S.

234. Luger TA, Schwarz T. Evidence for an epidermal cytokine network. J Invest Dermatol 1990;95 (6 Suppl):100S-104S.

235. Takashima A, Bergstresser PR. Impact of UVB radiation on the epidermal cytokine network. Photochem Photobiol 1996;63 (4):397-400.

236. Kupper TS, Chua AO, Flood P, McGuire J, Gubler U. Interleukin 1 gene expression in cultured human keratinocytes is augmented by ultraviolet irradiation. J Clin Invest 1987;80 (2):430-436.

237. Gahring L, Baltz M, Pepys MB, Daynes R. Effect of ultraviolet radiation on production of epidermal cell thymocyte-activating factor/interleukin 1 *in vivo* and *in vitro*. Proc Natl Acad Sci U S A 1984;81 (4):1198-1202.

238. Kutsch CL, Norris DA, Arend WP. Tumor necrosis factor-α induces interleukin-1 α and interleukin-1 receptor antagonist production by cultured human keratinocytes. J Invest Dermatol 1993;101 (1):79-85.

239. Kang K, Hammerberg C, Cooper KD. Differential regulation of IL-1 and IL-1 receptor antagonist in HaCaT keratinocytes by tumor necrosis factor-α and transforming growth factor-β 1. Exp Dermatol 1996;5 (4):218-226.

240. Lee SW, Morhenn VB, Ilnicka M, Eugui EM, Allison AC. Autocrine stimulation of interleukin-1 α and transforming growth factor α production in human keratinocytes and its antagonism by glucocorticoids. J Invest Dermatol 1991;97 (1):106-110.

241. Maverakis E, Miyamura Y, Bowen MP, Correa G, Ono Y, Goodarzi H. Light, including ultraviolet. J Autoimmun 2009;34 (3):J247-257.

242. Choi W, Miyamura Y, Wolber R, Smuda C, Reinhold W, Liu H, Kolbe L, Hearing VJ. Regulation of Human Skin Pigmentation *in situ* by Repetitive UV Exposure: Molecular Characterization of Responses to UVA and/or UVB. J Invest Dermatol 2010;130 (6): 1685-1696.

243. Setlow RB. The wavelengths in sunlight effective in producing skin cancer: a theoretical analysis. Proc Natl Acad Sci U S A 1974;71 (9):3363-3366.

244. Halliday GM, Bestak R, Yuen KS, Cavanagh LL, Barnetson RS. UVA-induced immunosuppression. Mutat Res 1998;422 (1):139-145.

245. Rana S, Rogers LJ, Halliday GM. Immunosuppressive ultraviolet-A radiation inhibits the development of skin memory CD8 T cells. Photochem Photobiol Sci;9 (1):25-30.

246. Coelho SG, Hearing VJ. UVA tanning is involved in the increased incidence of skin cancers in fair-skinned young women. Pigment Cell Melanoma Res;23 (1):57-63.

247. de Laat A, van der Leun JC, de Gruijl FR. Carcinogenesis induced by UVA (365-nm) radiation: the dose-time dependence of tumor formation in hairless mice. Carcinogenesis 1997;18 (5):1013-1020.

248. Kelfkens G, de Gruijl FR, van der Leun JC. Ozone depletion and increase in annual carcinogenic ultraviolet dose. Photochem Photobiol 1990;52 (4): 819-823.

249. Kligman LH. The hairless mouse and photoaging. Photochem Photobiol 1991;54 (6):1109-1118.

250. Kelfkens G, de Gruijl FR, van der Leun JC. Tumorigenesis by short-wave ultraviolet A: papillomas versus squamous cell carcinomas. Carcinogenesis 1991;12 (8):1377-1382.

251. Sterenborg HJ, van der Leun JC. Tumorigenesis by a long wavelength UV-A source. Photochem Photobiol 1990;51 (3):325-330.

252. Duvul C, Schmidt R, Regnier M, Facy V, Asselineau D, F. B. The use of reconstructed human skin to evaluate UV-induced modification and sunscreen efficacy. Exp Dermatol 2003;12 (s2):64-70.

253. de Gruijl FR. Skin cancer and solar UV radiation. Eur J Cancer 1999;35 (14):2003-2009.

254. Freshney IR. Basic principles of cell culture: Culture of cells for tissue engineering. R. Ian Freshney, Gordana Vunjak-Novakovic, editors: John Wiley and sons, NY, USA. 2006.

255. Lisby S, Gniadecki R, Wulf HC. UV-induced DNA damage in human keratinocytes: quantitation and correlation with long-term survival. Exp Dermatol 2005;14 (5):349-355.

256. Budai M, Reynaud-Angelin A, Szabo Z, Toth S, Ronto G, Sage E, Grof P. Effect of UVA radiation on membrane fluidity and radical decay in human fibroblasts as detected by spin labeled stearic acids. J Photochem Photobiol B 2004;77 (1-3):27-38.

257. S. Kozmin, G. Slezak, A. Reynaud-Angelin, C. Elie, Y. de Rycke, S. Boiteux, Sage E. UVA radiation is highly mutagenic in cells that are unable to repair 7, 8-dihydro-8-oxoguanine in *Saccharomyces cerevisiae*. Proceedings of the national academy of sciences 2005;102 (38):13538-13543.

258. Latonen L, Laiho M. Cellular UV damage responses--functions of tumor suppressor p53. Biochim Biophys Acta 2005;1755 (2):71-89.

259. Takasawa R, Nakamura H, Mori T, Tanuma S. Differential apoptotic pathways in human keratinocyte HaCaT cells exposed to UVB and UVC. Apoptosis 2005;10 (5):1121-1130.

260. Liegler TJ, Hyun W, Yen TS, Stites DP. Detection and quantification of live, apoptotic, and necrotic human peripheral lymphocytes by single-laser flow cytometry. Clin Diagn Lab Immunol 1995;2 (3):369-376.

261. Armeni T, Damiani E, Battino M, Greci L, Principato G. Lack of *in vitro* protection by a common sunscreen ingredient on UVA-induced cytotoxicity in keratinocytes. Toxicology 2004;203 (1-3):165-178.

262. Piva TJ, Davern CM, Francis KG, Chojnowski GM, Hall PM, Ellem KA. Increased ecto-metallopeptidase activity in cells undergoing apoptosis. J Cell Biochem 2000;76 (4):625-638.

263. Chouinard N, Valerie K, Rouabhia M, Huot J. UVB-mediated activation of p38 mitogen-activated protein kinase enhances resistance of normal human keratinocytes to apoptosis by stabilizing cytoplasmic p53. Biochem J 2002;365 (1):133-145.

264. Bachmeier BE, Nerlich AG, Boukamp P, Lichtinghagen R, Tschesche H, Fritz H, Fink E. Human keratinocyte cell lines differ in the expression of the collagenolytic matrix metalloproteinases-1,-8, and -13 and of TIMP-1. Biol Chem 2000;381 (5-6):509-516.

265. Martin MD, Matrisian LM. The other side of MMPs: protective roles in tumor progression. Cancer Metastasis Rev 2007;26 (3-4):717-724.

266. Khatib AM, Siegfried G, Chretien M, Metrakos P, Seidah NG. Proprotein convertases in tumor progression and malignancy: novel targets in cancer therapy. Am J Pathol 2002;160 (6):1921-1935.

267. Mazzone M, Baldassarre M, Beznoussenko G, Giacchetti G, Cao J, Zucker S, Luini A, Buccione R. Intracellular processing and activation of membrane type 1 matrix metalloprotease depends on its partitioning into lipid domains. J Cell Sci 2004;117 (26):6275-6287.

268. Bassi DE, Mahloogi H, Lopez De Cicco R, Klein-Szanto A. Increased furin activity enhances the malignant phenotype of human head and neck cancer cells. Am J Pathol 2003;162 (2):439-447.

269. Polunovsky VA, Wendt CH, Ingbar DH, Peterson MS, Bitterman PB. Induction of endothelial cell apoptosis by TNF α: modulation by inhibitors of protein synthesis. Exp Cell Res 1994;214 (2):584-594.

270. Yu L, Helms MN, Yue Q, Eaton DC. Single-channel analysis of functional epithelial sodium channel (ENaC) stability at the apical membrane of A6 distal kidney cells. Am J Physiol Renal Physiol 2008;295 (5):F1519-1527.

271. Tracey KJ, Cerami A. Tumor necrosis factor: an updated review of its biology. Crit Care Med 1993;21 (10 Suppl):S415-422.

272. Partridge M, Chantry D, Turner M, Feldmann M. Production of interleukin-1 and interleukin-6 by human keratinocytes and squamous cell carcinoma cell lines. J Invest Dermatol 1991;96 (5):771-776.

273. Sauder DN. Biologic properties of epidermal cell thymocyte-activating factor (ETAF). J Invest Dermatol 1985;85 (1 Suppl):176s-179s.

274. Schmitt A, Hauser C, Jaunin F, Dayer JM, Saurat JH. Normal epidermis contains high amounts of natural tissue IL 1 biochemical analysis by HPLC identifies a MW approximately 17 Kd form with a P1 5.7 and a MW approximately 30 Kd form. Lymphokine Res 1986;5 (2):105-118.

275. Bashir M, Sharma M, Werth VP. UVB-induction of TNF-α gene transcription requires a response element, overlapping the AP-1-binding site, of the proximal promoter. J Invest Dermatol 2006;126:277-282.

276. Bashir MM, Sharma MR, Werth VP. UVB and proinflammatory cytokines synergistically activate TNF-α production in keratinocytes through enhanced gene transcription. J Invest Dermatol 2009;129 (4):994-1001.

277. Brink N, Szamel M, Young AR, Wittern KP, Bergemann J. Comparative quantification of IL-1β, IL-10, IL-10r, TNFα and IL-7 mRNA levels in UV-irradiated human skin *in vivo*. Inflamm Res 2000;49 (6):290-296.

278. Schalken JA, Roebroek AJ, Oomen PP, Wagenaar SS, Debruyne FM, Bloemers HP, Van de Ven WJ. fur gene expression as a discriminating marker for small cell and nonsmall cell lung carcinomas. J Clin Invest 1987;80 (6):1545-1549.

279. Mbikay M, Sirois F, Yao J, Seidah NG, Chretien M. Comparative analysis of expression of the proprotein convertases furin, PACE4, PC1 and PC2 in human lung tumours. Br J Cancer 1997;75 (10):1509-1514.

280. Cheng M, Watson PH, Paterson JA, Seidah N, Chretien M, Shiu RP. Pro-protein convertase gene expression in human breast cancer. Int J Cancer 1997;71 (6):966-971.

281. Spencer JD, Gibbons NC, Bohm M, Schallreuter KU. The Ca2+-binding capacity of epidermal furin is disrupted by H2O2-mediated oxidation in vitiligo. Endocrinology 2008;149 (4):1638-1645.

282. Komiyama T, Coppola JM, Larsen MJ, van Dort ME, Ross BD, Day R, Rehemtulla A, Fuller RS. Inhibition of furin/proprotein convertase-catalyzed surface and intracellular processing by small molecules. J Biol Chem 2009;284 (23):15729-15738.

283. Australian Institute of Health and Welfare. States & territories GRIM (General Record of Incidence of Mortality) Books. Canberra: AIHW, 2005. Date Acessed 13/07/2008.

284. Hatsuzawa K, Murakami K, Nakayama K. Molecular and enzymatic properties of furin, a Kex2-like endoprotease involved in precursor cleavage at Arg-X-Lys/Arg-Arg sites. J Biochem 1992;111 (3):296-301.

285. Hatsuzawa K, Nagahama M, Takahashi S, Takada K, Murakami K, Nakayama K. Purification and characterization of furin, a Kex2-like processing endoprotease, produced in Chinese hamster ovary cells. J Biol Chem 1992;267 (23):16094-16099.

286. Molloy SS, Bresnahan PA, Leppla SH, Klimpel KR, Thomas G. Human furin is a calcium-dependent serine endoprotease that recognizes the sequence Arg-X-X-Arg and efficiently cleaves anthrax toxin protective antigen. J Biol Chem 1992;267 (23):16396-16402.

287. Reagan-Shaw S, Breur J, Ahmad N. Enhancement of UVB radiation-mediated apoptosis by sanguinarine in HaCaT human immortalized keratinocytes. Mol Cancer Ther 2006;5 (2):418-429.

288. Scamuffa N, Calvo F, Chretien M, Seidah NG, Khatib AM. Proprotein convertases: lessons from knockouts. FASEB J 2006;20 (12):1954-1963.

289. Ra HJ, Parks WC. Control of matrix metalloproteinase catalytic activity. Matrix Biol 2007;26 (8):587-596.

290. Watanabe Y, Hirakawa K, Haruyama T, Akaike T. Direct production of an activated matrix metalloproteinase-9 (gelatinase B) from mammalian cells. FEBS Lett 2001;502 (1-2):63-67.

291. Woessner JF, Jr. The family of matrix metalloproteinases. Ann N Y Acad Sci 1994;732:11-21.

292. Sato H, Kinoshita T, Takino T, Nakayama K, Seiki M. Activation of a recombinant membrane type 1-matrix metalloproteinase (MT1-MMP) by furin and its interaction with tissue inhibitor of metalloproteinases (TIMP)-2. FEBS Lett 1996;393 (1):101-104.

293. Mercapide J, Lopez De Cicco R, Bassi DE, Castresana JS, Thomas G, Klein-Szanto AJ. Inhibition of furin-mediated processing results in suppression of astrocytoma cell growth and invasiveness. Clin Cancer Res 2002;8 (6): 1740-1746.

294. Cao J, Rehemtulla A, Pavlaki M, Kozarekar P, Chiarelli C. Furin directly cleaves proMMP-2 in the trans-Golgi network resulting in a nonfunctioning proteinase. J Biol Chem 2005;280 (12):10974-10980.

295. Koo BH, Kim HH, Park MY, Jeon OH, Kim DS. Membrane type-1 matrix metalloprotease-independent activation of pro-matrix metalloprotease-2 by proprotein convertases. FEBS J 2009;276 (21):6271-6284.

296. Illman SA, Keski-Oja J, Parks WC, Lohi J. The mouse matrix metalloproteinase, epilysin (MMP-28), is alternatively spliced and processed by a furin-like proprotein convertase. Biochem J 2003;375 (1):191-197.

297. Kang T, Nagase H, Pei D. Activation of membrane-type matrix metalloproteinase 3 zymogen by the proprotein convertase furin in the trans-Golgi network. Cancer Res 2002;62 (3):675-681.

298. Pei D, Weiss SJ. Furin-dependent intracellular activation of the human stromelysin-3 zymogen. Nature 1995;375 (6528):244-247.

299. Moses MA, Marikovsky M, Harper JW, Vogt P, Eriksson E, Klagsbrun M, Langer R. Temporal study of the activity of matrix metalloproteinases and their endogenous inhibitors during wound healing. J Cell Biochem 1996;60 (3): 379-386.

300. Springman EB, Angleton EL, Birkedal-Hansen H, Van Wart HE. Multiple modes of activation of latent human fibroblast collagenase: evidence for the role of a Cys73 active-site zinc complex in latency and a "cysteine switch" mechanism for activation. Proc Natl Acad Sci U S A 1990;87 (1):364-368.

301. Betsuyaku T, Fukuda Y, Parks EC, Shipley JM, RM. S. Gelatinase b is required for alveolar bronchiolization after intratracheal bleomycin. Am J Pathol 2000;157 (2):524-535.

302. Benassi L, Ottani D, Fantini F, Marconi A, Chiodino C, Giannetti A, Pincelli C. 1,25-dihydroxyvitamin D3, transforming growth factor β1, calcium, and ultraviolet B radiation induce apoptosis in cultured human keratinocytes. J Invest Dermatol 1997;109 (3):276-282.

303. Fisher GJ, Wang ZQ, Datta SC, Varani J, Kang S, Voorhees JJ. Pathophysiology of premature skin aging induced by ultraviolet light. N Engl J Med 1997;337 (20):1419-1428.

304. Krejci-Papa NC, Paus R. A novel in-situ-zymography technique localizes gelatinolytic activity in human skin to mast cells. Exp Dermatol 1998;7 (6): 321-326.

305. Kagatani S, Sasaki Y, Hirota M, Mizuashi M, Suzuki M, Ohtani T, Itagaki H, Aiba S. Oxidation of cell surface thiol groups by contact sensitizers triggers the maturation of dendritic cells. J Invest Dermatol;130 (1):175-183.

306. Ikeda M, Maekawa R, Tanaka H, Matsumoto M, Takeda Y, Tamura Y, Nemori R, Yoshioka T. Inhibition of gelatinolytic activity in tumor tissues by synthetic matrix metalloproteinase inhibitor: application of film *in situ* zymography. Clin Cancer Res 2000;6 (8):3290-3296.

307. Nyormoi O, Mills L, Bar-Eli M. An MMP-2/MMP-9 inhibitor, 5a, enhances apoptosis induced by ligands of the TNF receptor superfamily in cancer cells. Cell Death Differ 2003;10 (5):558-569.

308. Tamura Y, Watanabe F, Nakatani T, Yasui K, Fuji M, Komurasaki T, Tsuzuki H, Maekawa R, Yoshioka T, Kawada K, Sugita K, Ohtani M. Highly selective

and orally active inhibitors of type IV collagenase (MMP-9 and MMP-2): N-sulfonylamino acid derivatives. J Med Chem 1998;41 (4):640-649.

309. Liang CC, Park AY, Guan JL. *In vitro* scratch assay: a convenient and inexpensive method for analysis of cell migration *in vitro*. Nat Protoc 2007;2 (2):329-333.

310. Todaro GJ, Lazar GK, Green H. The initiation of cell division in a contact-inhibited mammalian cell line. J Cell Physiol 1965;66 (3):325-333.

311. Hung WC, Tseng WL, Shiea J, Chang HC. Skp2 overexpression increases the expression of MMP-2 and MMP-9 and invasion of lung cancer cells. Cancer Lett;288 (2):156-161.

312. Saeb-Parsy K, Veerakumarasivam A, Wallard MJ, Thorne N, Kawano Y, Murphy G, Neal DE, Mills IG, Kelly JD. MT1-MMP regulates urothelial cell invasion via transcriptional regulation of Dickkopf-3. Br J Cancer 2008;99 (4):663-669.

313. Brenneisen P, Oh J, Wlaschek M, Wenk J, Briviba K, Hommel C, Herrmann G, Sies H, Scharffetter-Kochanek K. Ultraviolet B wavelength dependence for the regulation of two major matrix-metalloproteinases and their inhibitor TIMP-1 in human dermal fibroblasts. Photochem Photobiol 1996;64 (5):877-885.

314. Brenneisen P, Wlaschek M, Wenk J, Blaudschun R, Hinrichs R, Dissemond J, Krieg T, Scharffetter-Kochanek K. Ultraviolet-B induction of interstitial collagenase and stromelyin-1 occurs in human dermal fibroblasts via an autocrine interleukin-6-dependent loop. FEBS Lett 1999;449 (1):36-40.

315. Kut C, Hornebeck W, Groult N, Redziniack G, Godeau G, Pellat B. Influence of successive and combined ultraviolet A and B irradiations on matrix metalloelastases produced by human dermal fibroblasts in culture. Cell Biol Int 1997;21 (6):347-352.

316. Petersen MJ, Hansen C, Craig S. Ultraviolet A irradiation stimulates collagenase production in cultured human fibroblasts. J Invest Dermatol 1992;99 (4): 440-444.

317. Fagot D, Asselineau D, Bernerd F. Direct role of human dermal fibroblasts and indirect participation of epidermal keratinocytes in MMP-1 production after UV-B irradiation. Arch Dermatol Res 2002;293 (11):576-583.

318. Herrmann G, Wlaschek M, Lange TS, Prenzel K, Goerz G, Scharffetter-Kochanek K. UVA irradiation stimulates the synthesis of various matrix-metalloproteinases (MMPs) in cultured human fibroblasts. Exp Dermatol 1993;2 (2):92-97.

319. Keyse SM, Tyrrell RM. Heme oxygenase is the major 32-kDa stress protein induced in human skin fibroblasts by UVA radiation, hydrogen peroxide, and sodium arsenite. Proc Natl Acad Sci U S A 1989;86 (1):99-103.

320. Applegate LA, Noel A, Vile G, Frenk E, Tyrrell RM. Two genes contribute to different extents to the heme oxygenase enzyme activity measured in cultured human skin fibroblasts and keratinocytes: implications for protection against oxidant stress. Photochem Photobiol 1995;61 (3):285-291.

321. Djavaheri-Mergny M, Gras MP, Mergny JL, Dubertret L. UV-A-induced decrease in nuclear factor-κB activity in human keratinocytes. Biochem J 1999;338 (3):607-613.

322. Klotz LO, Briviba K, Sies H. Singlet oxygen mediates the activation of JNK by UVA radiation in human skin fibroblasts. FEBS Lett 1997;408 (3):289-291.

323. Klotz LO, Pellieux C, Briviba K, Pierlot C, Aubry JM, Sies H. Mitogen-activated protein kinase (p38-, JNK-, ERK-) activation pattern induced by extracellular and intracellular singlet oxygen and UVA. Eur J Biochem 1999;260 (3):917-922.

324. Bredin CG, Liu Z, Klominek J. Growth factor-enhanced expression and activity of matrix metalloproteases in human non-small cell lung cancer cell lines. Anticancer Res 2003;23 (6):4877-4884.

325. Roomi MW, Ivanov V, Netke SP, Niedzwiecki A, M. R, editors. A Novel *In Vitro* Bioassay for Screening Matrix Metalloproteinase Activity in Human Cancer Cell Lines 94th Annual Meeting of AACR (American Association for Cancer Research); Washington DC; July 11-14, 2003.

326. Petra Baumann, Cornelia Mauch, Hans Smola, Nobert E. Fusenig, Nischt R. Induction of MMP-9 in nontumorigenic epidermal HaCaT cell line and two ras-transfected tumorigenic HaCaT clones Journal of Dermatological Science 1998;16 (Supplement 1):s47.

327. Bachmeier BE, Boukamp P, Lichtinghagen R, Fusenig NE, Fink E. Matrix metalloproteinases-2,-3,-7,-9 and-10, but not MMP-11, are differentially

expressed in normal, benign tumorigenic and malignant human keratinocyte cell lines. Biol Chem 2000;381 (5-6):497-507.

328. Schmalfeldt B, Prechtel D, Harting K, Spathe K, Rutke S, Konik E, Fridman R, Berger U, Schmitt M, Kuhn W, Lengyel E. Increased expression of matrix metalloproteinases (MMP)-2, MMP-9, and the urokinase-type plasminogen activator is associated with progression from benign to advanced ovarian cancer. Clin Cancer Res 2001;7 (8):2396-2404.

329. Mira E, Lacalle RA, Buesa JM, de Buitrago GG, Jimenez-Baranda S, Gomez-Mouton C, Martinez AC, Manes S. Secreted MMP9 promotes angiogenesis more efficiently than constitutive active MMP9 bound to the tumor cell surface. J Cell Sci 2004;117 (9):1847-1857.

330. Han YP, Tuan TL, Hughes M, Wu H, Garner WL. Transforming growth factor-β - and tumor necrosis factor-α -mediated induction and proteolytic activation of MMP-9 in human skin. J Biol Chem 2001;276 (25):22341-22350.

331. O'Connell JP, Willenbrock F, Docherty AJ, Eaton D, Murphy G. Analysis of the role of the COOH-terminal domain in the activation, proteolytic activity, and tissue inhibitor of metalloproteinase interactions of gelatinase B. J Biol Chem 1994;269 (21):14967-14973.

332. Han YP, Nien YD, WL. G. Tumor necrosis factor-α-induced proteolytic activation of promatrix metalloprotei-nase-9 by human skin is controlled by down-regulating tissue inhibitor of metalloproteinase-1 and mediated by tissue-associated chymotrypsin-like proteinase. J Biol Chem 2002;277 (30): 27319–27327.

333. Egeblad M, Werb Z. New functions for the matrix metalloproteinases in cancer progression. Nat Rev Cancer 2002;2 (3):161-174.

334. Wagenaar-Miller RA, Gorden L, Matrisian LM. Matrix metalloproteinases in colorectal cancer: is it worth talking about? Cancer Metastasis Rev 2004;23 (1-2):119-135.

335. Zucker S, Lysik RM, DiMassimo BI, Zarrabi HM, Moll UM, Grimson R, Tickle SP, Docherty AJ. Plasma assay of gelatinase B: tissue inhibitor of metalloproteinase complexes in cancer. Cancer 1995;76 (4):700-708.

336. Zeng ZS, Guillem JG. Distinct pattern of matrix metalloproteinase 9 and tissue inhibitor of metalloproteinase 1 mRNA expression in human colorectal cancer and liver metastases. Br J Cancer 1995;72 (3):575-582.

337. Niina Reunanen, Kähäri V. Matrix Metalloproteinases in Cancer Cell Invasion NCBI Bookshelf Available from: http://www.ncbi.nlm.nih.gov. Date Acessed 18/12/2009.

338. Angliker H, Wikstrom P, Shaw E, Brenner C, Fuller RS. The synthesis of inhibitors for processing proteinases and their action on the Kex2 proteinase of yeast. Biochem J 1993;293 (Pt 1):75-81.

339. Van Laethem A, Claerhout S, Garmyn M, Agostinis P. The sunburn cell: regulation of death and survival of the keratinocyte. Int J Biochem Cell Biol 2005;37 (8):1547-1553.

340. Leverkus M, Yaar M, Eller MS, Tang EH, Gilchrest BA. Post-transcriptional regulation of UV induced TNF-α expression. J Invest Dermatol 1998;110 (4):353-357.

341. Hiraoka Y, Yoshida K, Ohno M, Matsuoka T, Kita T, Nishi E. Ectodomain shedding of TNF-α is enhanced by nardilysin via activation of ADAM proteases. Biochem Biophys Res Commun 2008;370 (1):154-158.

342. Fisher GJ, Choi HC, Bata-Csorgo Z, Shao Y, Datta S, Wang ZQ, Kang S, Voorhees JJ. Ultraviolet irradiation increases matrix metalloproteinase-8 protein in human skin *in vivo*. J Invest Dermatol 2001;117 (2):219-226.

343. Gearing AJH, Beckett P, Christodoulou M, Churchill M, Clements J, Davidson AH, Drummond AH, Galloway WA, Gilbert R, Gordon JL, Gordon JL, Leber TM, Mangan M, Miller K, Nayee P, Owen K, Patel S, Thomas W, Wells G, Wood LM, Woolley K. Processing of tumour necrosis factor-α precursor by metalloproteinases. Nature 1994;370 (6490):555-557.

344. Gearing AJ, Beckett P, Christodoulou M, Churchill M, Clements JM, Crimmin M, Davidson AH, Drummond AH, Galloway WA, Gilbert R, Gordon JL, Leber TM, Mangan M, Miller K, Nayee P, Owen K, Patel S, Thomas W, Wells G, Wood LM, Woolley K. Matrix metalloproteinases and processing of pro-TNF-α. J Leukoc Biol 1995;57 (5):774-777.

345. Haro H, Crawford HC, Fingleton B, Shinomiya K, Spengler DM, Matrisian LM. Matrix metalloproteinase-7-dependent release of tumor necrosis factor-α in a model of herniated disc resorption. J Clin Invest 2000;105 (2):143-150.

346. Choo-Kang BS, Hutchison S, Nickdel MB, Bundick RV, Leishman AJ, Brewer JM, McInnes IB, Garside P. TNF-blocking therapies: an alternative mode of action? Trends Immunol 2005;26 (10):518-522.

347. Kameda K, Sato K. Regulation of IL-1 α expression in human keratinocytes: transcriptional activation of the IL-1 α gene by TNF-α, LPS, and IL-1 α. Lymphokine Cytokine Res 1994;13 (1):29-35.

348. Tseng YH, Schuler LA. Transcriptional regulation of interleukin-1β gene by interleukin-1β itself is mediated in part by Oct-1 in thymic stromal cells. J Biol Chem 1998;273 (20):12633-12641.

349. Warner SJ, Auger KR, Libby P. Human interleukin 1 induces interleukin 1 gene expression in human vascular smooth muscle cells. J Exp Med 1987;165 (5):1316-1331.

350. Kulbe H, Thompson R, Wilson JL, Robinson S, Hagemann T, Fatah R, Gould D, Ayhan A, Balkwill F. The inflammatory cytokine tumor necrosis factor-α generates an autocrine tumor-promoting network in epithelial ovarian cancer cells. Cancer Res 2007;67 (2):585-592.

351. Wu S, Boyer CM, Whitaker RS, Berchuck A, Wiener JR, Weinberg JB, Bast RC, Jr. Tumor necrosis factor α as an autocrine and paracrine growth factor for ovarian cancer: monokine induction of tumor cell proliferation and tumor necrosis factor α expression. Cancer Res 1993;53 (8):1939-1944.

352. Huizinga TW, Brinkman BM, Verweij CL. Regulation of tumor necrosis factor-α production: basic aspects and pharmacological modulation. J Rheumatol 1996;23 (3):416-418.

353. Kontoyiannis D, Pasparakis M, Pizarro TT, Cominelli F, Kollias G. Impaired on/off regulation of TNF biosynthesis in mice lacking TNF AU-rich elements:

implications for joint and gut-associated immunopathologies. Immunity 1999;10 (3):387-398.

354. Piecyk M, Wax S, Beck AR, Kedersha N, Gupta M, Maritim B, Chen S, Gueydan C, Kruys V, Streuli M, Anderson P. TIA-1 is a translational silencer that selectively regulates the expression of TNF-α. Embo J 2000;19 (15): 4154-4163.

355. Ashkenazi A, Dixit VM. Death receptors: signaling and modulation. Science 1998;281 (5381):1305-1308.

356. Banno T, Gazel A, Blumenberg M. Effects of tumor necrosis factor-α (TNF α) in epidermal keratinocytes revealed using global transcriptional profiling. J Biol Chem 2004;279 (31):32633-32642.

357. van Hogerlinden M, Rozell BL, Toftgard R, Sundberg JP. Characterization of the progressive skin disease and inflammatory cell infiltrate in mice with inhibited NF-kappaB signaling. J Invest Dermatol 2004;123 (1):101-108.

358. Fusenig NE, Boukamp P. Multiple stages and genetic alterations in immortalization, malignant transformation, and tumor progression of human skin keratinocytes. Mol Carcinog 1998;23 (3):144-158.

359. Oxholm A, Oxholm P, Staberg B, Bendtzen K. Immunohistological detection of interleukin I-like molecules and tumour necrosis factor in human epidermis before and after UVB-irradiation *in vivo*. Br J Dermatol 1988;118 (3):369-376.

360. Balkwill F. Tumour necrosis factor and cancer. Nat Rev Cancer 2009;9 (5): 361-371.

361. Wu Y, Zhou BP. TNF-α/NF-kappaB/Snail pathway in cancer cell migration and invasion. Br J Cancer;102 (4):639-644.

362. Ge L, Baskic D, Basse P, Vujanovic L, Unlu S, Yoneyama T, Vujanovic A, Han J, Bankovic D, Szczepanski MJ, Hunt JL, Herberman RB, Gollin SM, Ferris RL, Whiteside TL, Myers EN, Vujanovic NL. Sheddase activity of tumor necrosis factor-α converting enzyme is increased and prognostically valuable in head and neck cancer. Cancer Epidemiol Biomarkers Prev 2009;18 (11):2913-2922.

363. Schlondorff J, Becherer JD, Blobel CP. Intracellular maturation and localization of the tumour necrosis factor α convertase (TACE). Biochem J 2000;347 (1):131-138.

364. Garten W, Stieneke A, Shaw E, Wikstrom P, Klenk HD. Inhibition of proteolytic activation of influenza virus hemagglutinin by specific peptidyl chloroalkyl ketones. Virology 1989;172 (1):25-31.

365. Jean F, Stella K, Thomas L, Liu G, Xiang Y, Reason AJ, Thomas G. α1-Antitrypsin Portland, a bioengineered serpin highly selective for furin: application as an antipathogenic agent. Proc Natl Acad Sci U S A 1998;95 (13):7293-7298.

366. Clingen PH, Berneburg M, Petit-Frere C, Woollons A, Lowe JE, Arlett CF, Green MH. Contrasting effects of an ultraviolet B and an ultraviolet A tanning lamp on interleukin-6, tumour necrosis factor-α and intercellular adhesion molecule-1 expression. Br J Dermatol 2001;145 (1):54-62.

367. Devary Y, Rosette C, DiDonato JA, Karin M. NF-kappa B activation by ultraviolet light not dependent on a nuclear signal. Science 1993;261 (5127):1442-1445.

368. Simon MM, Aragane Y, Schwarz A, Luger TA, Schwarz T. UVB light induces nuclear factor kappa B (NF kappa B) activity independently from chromosomal DNA damage in cell-free cytosolic extracts. J Invest Dermatol 1994;102 (4):422-427.

369. Spriggs DR, Deutsch S, Kufe DW. Genomic structure, induction, and production of TNF-α. Immunol Ser 1992;56:3-34.

370. Bazzoni F, Kruys V, Shakhov A, Jongeneel CV, Beutler B. Analysis of tumor necrosis factor promoter responses to ultraviolet light. J Clin Invest 1994;93 (1):56-62.

371. Lisby S, Hauser C. Transcriptional regulation of tumor necrosis factor-α in keratinocytes mediated by interleukin-1β and tumor necrosis factor-α. Exp Dermatol 2002;11 (6):592-598.

372. Imaizumi T, Itaya H, Fujita K, Kudoh D, Kudoh S, Mori K, Fujimoto K, Matsumiya T, Yoshida H, Satoh K. Expression of tumor necrosis factor-α in cultured human endothelial cells stimulated with lipopolysaccharide or interleukin-1α. Arterioscler Thromb Vasc Biol 2000;20 (2):410-415.

373. Walsh LJ, Davis MF, Xu LJ, Savage NW. Relationship between mast cell degranulation and inflammation in the oral cavity. J Oral Pathol Med 1995;24 (6):266-272.

374. Collins T, Lapierre LA, Fiers W, Strominger JL, Pober JS. Recombinant human tumor necrosis factor increases mRNA levels and surface expression of HLA-A,B antigens in vascular endothelial cells and dermal fibroblasts *in vitro*. Proc Natl Acad Sci U S A 1986;83 (2):446-450.

375. Dinarello CA, Cannon JG, Wolff SM, Bernheim HA, Beutler B, Cerami A, Figari IS, Palladino MA, Jr., O'Connor JV. Tumor necrosis factor (cachectin) is an endogenous pyrogen and induces production of interleukin 1. J Exp Med 1986;163 (6):1433-1450.

376. Groves RW, Allen MH, Ross EL, Barker JN, MacDonald DM. Tumour necrosis factor α is pro-inflammatory in normal human skin and modulates cutaneous adhesion molecule expression. Br J Dermatol 1995;132 (3):345-352.

377. Ziegler A, Jonason AS, Leffell DJ, Simon JA, Sharma HW, Kimmelman J, Remington L, Jacks T, Brash DE. Sunburn and p53 in the onset of skin cancer. Nature 1994;372 (6508):773-776.

378. Baumann H, Jahreis GP, Sauder DN, Koj A. Human keratinocytes and monocytes release factors which regulate the synthesis of major acute phase plasma proteins in hepatic cells from man, rat, and mouse. J Biol Chem 1984;259 (11):7331-7342.

379. Einspahr JG, Stratton SP, Bowden GT, Alberts DS. Chemoprevention of human skin cancer. Crit Rev Oncol Hematol 2002;41 (3):269-285.

380. Stojic L, Brun R, Jiricny J. Mismatch repair and DNA damage signalling. DNA Repair (Amst) 2004;3 (8-9):1091-1101.

381. Bassi DE, Mahloogi H, Al-Saleem L, Lopez De Cicco R, Ridge JA, Klein-Szanto AJ. Elevated furin expression in aggressive human head and neck tumors and tumor cell lines. Mol Carcinog 2001;31 (4):224-232.

382. Bassi DE, Mahloogi H, Klein-Szanto AJ. The proprotein convertases furin and PACE4 play a significant role in tumor progression. Mol Carcinog 2000;28 (2):63-69.

383. Khatib AM, Siegfried G, Prat A, Luis J, Chretien M, Metrakos P, Seidah NG. Inhibition of proprotein convertases is associated with loss of growth and tumorigenicity of HT-29 human colon carcinoma cells: importance of insulin-like growth factor-1 (IGF-1) receptor processing in IGF-1-mediated functions. J Biol Chem 2001;276 (33):30686-30693.

384. 3D Cell Culture NanoCulture®Plate (NCP) System 2009. Available from: http://www.infinitebio.com Date acessed 22/02/2010.

385. Ana Lazic, Fujiko Ozawa, Manami Shimomura, Yoshio Miyagawa, Masami Hiroyama, Nobutaka Kiyokawa, Akihiro Umezawa, Akito Tanoue, Tetsuya Nakatsura, Tanaka S, editors. A new approach for drug discovery and differentiation study using cutting-edge 3D cell culture system. ASCB; Poster Presentation (B618): Wednesday**,** Dec. 17; San Francisco.

386. Witte RP, Kao WJ. Keratinocyte-fibroblast paracrine interaction: the effects of substrate and culture condition. Biomaterials 2005;26 (17):3673-3682.

387. Guo A, Jahoda CA. An improved method of human keratinocyte culture from skin explants: cell expansion is linked to markers of activated progenitor cells. Exp Dermatol 2009;18 (8):720-726.

388. Richard P. Witte, Weiyuan John Kao. Keratinocyte-fibroblast paracrine interaction: the effects of substrate and culture condition. Biomaterials 2005;26 (17):3673-3682.

389. Bannasch H, Föhn M, Unterberg T, Bach AD, Weyand B, Stark GB. Skin tissue engineering. Clin Plastic Surg 2003;30 (4):573-579.

390. Selmaj K, Raine CS, Cannella B, Brosnan CF. Identification of lymphotoxin and tumor necrosis factor in multiple sclerosis lesions. J Clin Invest 1991;87 (3):949-954.

391. Rus HG, Niculescu F, Vlaicu R. Tumor necrosis factor-α in human arterial wall with atherosclerosis. Atherosclerosis 1991;89 (2-3):247-254.

392. Lapierre M, Siegfried G, Scamuffa N, Bontemps Y, Calvo F, Seidah NG, Khatib AM. Opposing function of the proprotein convertases furin and PACE4 on breast cancer cells' malignant phenotypes: role of tissue inhibitors of metalloproteinase-1. Cancer Res 2007;67 (19):9030-9034.

393. Dubois CM, Blanchette F, Laprise MH, Leduc R, Grondin F, Seidah NG. Evidence that furin is an authentic transforming growth factor-β1-converting enzyme. Am J Pathol 2001;158 (1):305-316.

394. Siegfried G, Basak A, Cromlish JA, Benjannet S, Marcinkiewicz J, Chretien M, Seidah NG, Khatib AM. The secretory proprotein convertases furin, PC5, and PC7 activate VEGF-C to induce tumorigenesis. J Clin Invest 2003;111 (11):1723-1732.

395. Zhong M, Munzer JS, Basak A, Benjannet S, Mowla SJ, Decroly E, Chretien M, Seidah NG. The prosegments of furin and PC7 as potent inhibitors of proprotein

convertases. *In vitro* and *ex vivo* assessment of their efficacy and selectivity. J Biol Chem 1999;274 (48):33913-33920.

396. Nour N, Basak A, Chretien M, Seidah NG. Structure-function analysis of the prosegment of the proprotein convertase PC5A. J Biol Chem 2003;278 (5):2886-2895.

397. Patel IR, Attur MG, Patel RN, Stuchin SA, Abagyan RA, Abramson SB, Amin AR. TNF-α convertase enzyme from human arthritis-affected cartilage: isolation of cDNA by differential display, expression of the active enzyme, and regulation of TNF-α. J Immunol 1998;160 (9):4570-4579.

398. Amour A, Knight CG, Webster A, Slocombe PM, Stephens PE, Knauper V, Docherty AJ, Murphy G. The *in vitro* activity of ADAM-10 is inhibited by TIMP-1 and TIMP-3. FEBS Lett 2000;473 (3):275-279.

399. Slack BE, Ma LK, Seah CC. Constitutive shedding of the amyloid precursor protein ectodomain is up-regulated by tumour necrosis factor-α converting enzyme. Biochem J 2001;357 (3):787-794.

400. Moss ML, Rasmussen FH. Fluorescent substrates for the proteinases ADAM17, ADAM10, ADAM8, and ADAM12 useful for high-throughput inhibitor screening. Anal Biochem 2007;366 (2):144-148.

401. Giavazzi R, Garofalo A, Ferri C, Lucchini V, Bone EA, Chiari S, Brown PD, Nicoletti MI, Taraboletti G. Batimastat, a synthetic inhibitor of matrix metalloproteinases, potentiates the antitumor activity of cisplatin in ovarian carcinoma xenografts. Clin Cancer Res 1998;4 (4):985-992.

402. Peng J, Piva TJ, Jones GL, Boyle G, ParsonsPG, Watson K. Stress response of human cell lines to Ultraviolet B radiation. in Free Radicals & Oxidative Stress: Chemistry, Biochemistry & Pathophysiological Implications. (Galaris, D., ed.) ed. Medimond, Bologna.2003.

Appendix:

A. Appendix

A.1 Appendix 1 - Inhibitor solutions

A.1.1 Furin (Dec RVKR cmk) inhibitor

Amount supplied by the manufacturer = 1 mg

Stock solution = 1 mg/ml = 1 mM solution (dissolved in 1 ml of sterilized H_2O)

Required working concentration = 100 µM

1/10 dilution of 1 mM = 100 µM (0.1 mM)

Therefore, add 100 µl of the stock solution to 900 µl of media to have final concentration of 0.1 mM.

A.1.2 1, 10 phenanthroline (1, 10 phe) inhibitor

Molecular weight: 198.2 g

198.2 g/l = 1 M solution

Stock solution = 0.01982 g/10 ml = 10 mM solution (filter using 0.22 µm filter)

Required working concentration (1/100 dilution of 10 mM) = 100 µM (0.1 mM)

Therefore, add 10 µl of the stock solution to 990 µl of media to have final concentration of 0.1 mM.

A.1.3 Cycloheximide (CHX) inhibitor

Molecular weight = 281.39 g

Stock solution = 10 mg/10 ml (filter using 0.22 µm filter)

Required working concentration = 10 µg/ml (1/100 dilution factor)

Therefore, add 10 µl of the stock solution to 990 µl of media to have final concentration of 0.01 µg/ml.

A.1.4 MMP inhibitor (MMPI)

Stock solution = 5 mM (5 mg dissolved in 2.67 ml DMSO)

Required working concentration needs to be in a range of 10 to 50 fold that of its half maximal inhibitory concentration (IC_{50}) value (5 µM).

MMP-2 = IC_{50} value is 310 nM

MMP-9 = IC_{50} value is 240 nM

Working concentration can be prepared using a two step dilution as shown below:

1 ml of stock into 9 ml of media (1:10)

0.1 ml of the above solution into 9.9 ml of media (1:1000) to have a final concentration of 5 µM.

A.2 Appendix 2 - Output of UV lamps

The UV detector measured the output of the lamps in mW. The example below shows the calculations used to determine the exposure times to achieve the specific UV doses.

Example:

UV output of UVB lamp = 5.68 mW/cm^2

UVB dose required = 2 KJ/m^2

Calculation:

5.68 mW/ cm^2 = 0.00568 W/cm^2

0.00568 W/cm^2 = 56.8 W/m^2 (Note 1 W = 1 J/s)

Therefore, 56.8 W/m^2 = 56.8 $J/s/m^2$

Therefore, 1 sec of UVB exposure gives a dose of 56.8 J/m^2

For 2 kJ/m^2 of UVB dose the exposure time is,

2 kJ/m^2 = 2000 J/m^2

2000 J/m^2 / 56.8 $J/s/m^2$ = 35.2 s ≈ 35 s

A.3 Appendix 3 - Cell viability

$$\text{Cell Viability of Attached Or Detached Cells} = \frac{\text{Viable cells (Attached OR Detached)}}{\text{Attached (Live and Dead) cells + Detached (Live and Dead) cells}} \text{ X } 100\%$$

A.4 Appendix 4 - Cell scratch analysis

An average of the reading of 3 separate experiments was calculated with a ruler as shown in Figure A.1.

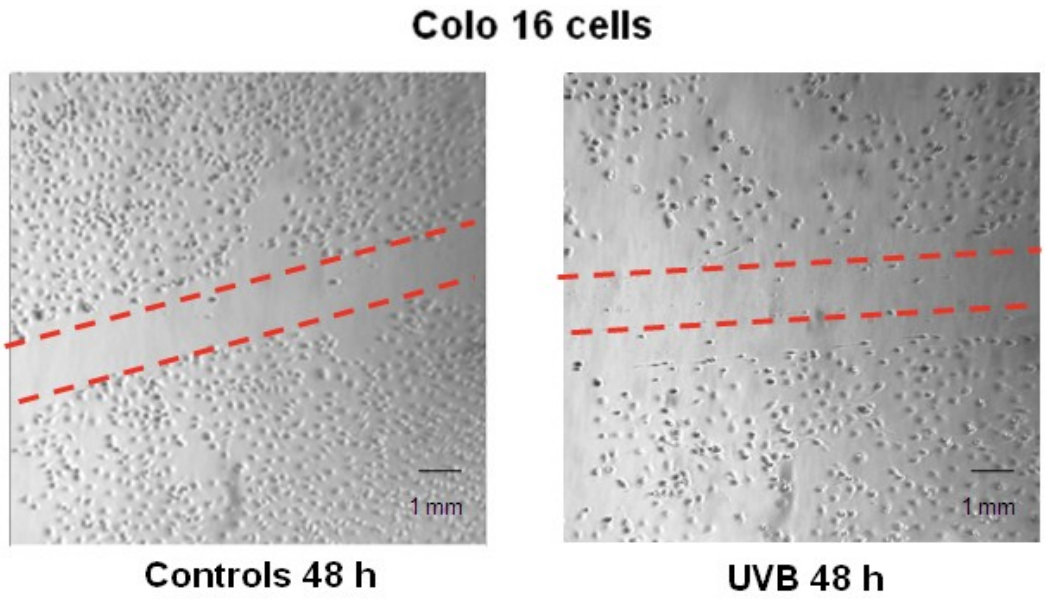

Figure A.1 Time course of recovery of cell scratch experiment in Colo 16 cells.

Sample calculation:

Distance between the scratch in control sample at 48 h = 2.1 mm (Average of 3 readings)

Distance between the scratch in UVB sample at 48 h = 1.9 mm (Average of 3 readings)

Therefore, distance cells migrated (mm) post UVB-irradiation against controls is 0.2 mm (2.1 mm -1.9 mm).

A.5 Appendix 5 - RNA quantification

An absorbance of 1 unit at 260 nm corresponds to 40 µg RNA.

Volume of RNA sample = 200 µl and has been diluted 70x.

It has an absorbance reading of 0.8523.

Then, concentration of RNA in the sample = 40 x A_{260} x dilution factor

= 40 x 0.8523 x 70

= 2386.44 µg/ml

A.6 Appendix 6 - Reconstitution of the primers

From the attached Certificate of Analysis (GeneWorks, Adelaide, Australia), the number of moles for each primer is supplied. These primers were reconstituted in nuclease-free H_2O to make a 100 µM stock solution.

Add (number of nmoles* x 10) µl of nuclease-free H_2O as shown in Table A.1 and dissolve.

To convert µg to µmoles: µmoles primers = µg primers/MW primers

Example:

10 µl of the stock + 190 µl of nuclease-free H_2O = 200 µl (working solution)

Freeze stock and working samples at -20^{o}C

Primers	**nmoles***	**Volume of H_2O to be added (µl)***
β actin forward	25.8 x 10	258
β actin reverse	38.2 x 10	382
Furin forward	51.4 x 10	514
Furin reverse	38.4 x 10	384
TACE forward	38.2 x 10	382
TACE reverse	40.2 x 10	402
MMP-2 forward	54.5 x 10	545
MMP-2 reverse	32.3 x 10	323
MMP-9 forward	34.3 x 10	343
MMP-9 reverse	32.2 x 10	322
TNFα forward	45.6 x 10	456
TNFα reverse	58.4 x 10	584

Table A.1 Reconstitution of primers.

A.7 Appendix 7 - Amplification efficiency (E)

Preparation of samples:

10 µl cDNA sample each from sham, UVA, UVB, UVAB-irradiated cell cultures was pooled into a microfuge tube to give a final volume of 40 µl

This tube contains 50 ng/µl pooled cDNA = 1/4 dilution in nuclease free $H_2O \approx 12.5$ ng

In order to measure amplification efficiency of target genes (Furin, TACE, MMP-2, MMP-9 and TNFα) and reference gene (β actin) 5 point serial dilutions is required as follows:

1st tube: 40 µl of pooled cDNA + 120 µl of nuclease free H_2O = 160 µl ≈ 12.5 ng

2nd tube: 16 µl from the 1st tube + 144 µl of nuclease free H_2O = 1.25 ng/µl

3rd tube: 16 µl from the 2nd tube + 144 µl of nuclease free H_2O = 0.0125 ng/µl

4th tube: 16 µl from the 3rd tube + 144 µl of nuclease free H_2O = 0.00125 ng/µl

5th tube: 16 µl from the 4th tube + 144 µl of nuclease free H_2O = 0.000125 ng/µl

Each one of the diluted samples was then treated as cDNA samples for the PCR run in triplicates with each one the genes.

Example: β actin amplification efficiency

β actin = y = (-3.833) (This equation from the standards is generated by the icycler software).

Then, using the equation below, amplification efficiency of β actin is calculated.

E = POWER (10,(-1/(3.833)) = 1.823443 ≈ 1.82%

Therefore, 1.82% is the amplification efficiency of β actin which is used to calculate mRNA expression as shown in Appendix A.8.

A.8 Appendix 8 - mRNA expression

mRNA expression of the target gene within the unknown sample to be expressed relative to the sham-irradiated control gene expression has been calculated. For each sample, a Threshold cycle (C_T) value was obtained for the target gene and the 18s rRNA controls. The C_T for 18s rRNA was subtracted from the C_T of the target gene to obtain a delta C_T (ΔC_T) value for each sample.

Ref gene: β actin

Target genes: Furin/TACE/MMP-2/MMP-9/TNFα

Controls: sham-irradiated samples

Treated samples: UV-irradiated samples (± CHX) or (± IL-1α)

Three threshold (Ct) values are generated for each sample for each gene under the specified conditions.

Average of these values is calculated and is called Ave Ct

Ref gene - target gene for controls and Ref gene - target gene for treated sample is calculated (Δ Ct)

Formula:

$$\text{Ratio of mRNA expression} = \frac{(E_{target})^{\Delta Ct \text{ target (control-treated)}}}{(E_{ref})^{\Delta Ct \text{ ref (control-treated)}}}$$

Example:

Controls	No of exp	β-actin	Target gene
0 h	Ct 1	15.00	23.40
	Ct 2	14.70	23.30
	Ct 3	14.70	22.90
Average	CT (Ave)	14.80	23.20
	Δ CT	0.00	-8.40

UV-irradiated cells	No of exp	β-actin	Target gene
4 h	Ct 1	15.20	21.50
	Ct 2	15.10	21.90
	Ct 3	15.00	22.00
Average	CT (Ave)	15.10	21.80
	Δ CT	0.00	-6.70

Final Concentration:

Amplification efficiency for β-actin is 1.82

Amplification efficiency for Furin is 1.65 (Note: amplification efficiency for furin is calculated as described in A.7)

Control at 0 h= (POWER(1.82, -8.40))/(POWER(1.82, -8.40))

UV-irradiated cell at 4 h = (POWER(1.65, -6.70))/(POWER(1.82, -8.40))

Therefore, based on the above formula, the final concentration is:

Time point	Target gene
Control (0 h)	1
UV-irradiated cells (4h)	5.34

A.9 Appendix 9 - Protein half-life calculation

Furin protein half-life ($T_{(1/2)}$) (see section 3.2.2.1) was calculated as follows.

Formula:

k = (-LN(24 h value/0 h value)*-1/24)

(Note: 24 h because the half-life in this experiment is calculated over a 24 h time period)

Therefore, $T_{(1/2)}$ = Ln(0.5)/k

Example: CHX + Control

At 24 h: 4.58

At 0 h: 87.48

Therefore, k = (-LN(4.58/87.48))*-1/24 = (-0.12)

$T_{(1/2)}$ = LN(0.5)/(-0.12) = 5.64 h

A.10 Appendix 10 – Publications and conference proceedings

A.10.1 Publications

1) Ravi, R. & Piva, T.J. (2010); The role of furin in inflammation and carcinogenesis. (Resubmitted to J Biomed. Sci) (Appendix A.11).

A.10.2 Conference proceedings

A.10.2.1 Oral presentations

1) Ravi, R. & Piva, T.J. (2007); The effects of UV radiation on TACE activity in human keratinocytes cell lines. 9th MEPSA Meeting, Hobart. Abs 27.

2) Ravi, R. & Piva, T.J. (2008); The effect of UV radiation on furin activity in human keratinocyte cell lines. 4th Australian Health and Medical Research Congress Meeting, Brisbane. Abs 298.

3) Piva, T.J. & Ravi, R. (2009); The effects of UV radiation on furin activation of TACE in human keratinocyte cell lines. Redox Processes in Chemistry, Biology and Medicine Meeting, Sydney (Dec 1-4). Abs 54.

A.10.2.2 Poster presentations

1) Muthusamy, V., Ravi, R. & Piva, T.J. (2009); The role of cell signalling pathways in TNFα release from UV-irradiated keratinocyte-derived cells. 15th International Photobiology Congress, Dusseldorf, Germany. Abs P31.

2) Ravi, R., Muthusamy, V. & Piva, T.J. (2009); The effect of UV radiation on Furin activation of MMPs in human keratinocyte cell lines. 15th International Photobiology Congress, Dusseldorf, Germany. Abs P33.

3) Ravi, R. & Piva, T.J. (2009); The effect of UV radiation on furin activation of matrix metalloproteases in human keratinocyte cell lines. Melbourne Protein Group Meeting, Monash University. Abs 24.

4) Ravi, R. & Piva, T.J. (2009); The effects of UV radiation on furin activation of MMPs in human keratinocyte cell lines. Redox Processes in Chemistry, Biology and Medicine Meeting, Sydney (Dec 1-4). Abs T20.

A.11 Appendix 11-The effect of UV radiation on furin activity in human skin cells

Review

The role of furin in skin inflammation and carcinogensis

Rethika Ravi & Terrence J Piva*[§]

School of Medical Sciences, RMIT University, Bundoora, Vic 3083, Australia

*These authors contributed equally to this work

[§]Corresponding author

Email addresses:

RR: rethika.ravi@rmit.edu.au

TJP: terry.piva@rmit.edu.au

Abstract

It is widely acknowledged that the ultraviolet (UV) component of sunlight is the main carcinogen implicated in the formation of skin cancer. In response to UV radiation, skin cells secrete a range of bioactive molecules including Interleukin-6 and Tumour Necrosis Factor α (TNFα). TNFα it is known to cause inflammation in the skin, and does not appear to be directly related to UV-induced immunosuppression that is observed. Inflammation plays a significant role in creating an environment where cells that have mutated DNA can become carcinogenic. TNFα itself is cleaved from its membrane-bound precursor by the action of the metalloprotease, Tumour Necrosis Factor α Converting Enzyme (TACE). While UVB radiation has been shown to increase the release of TNFα from irradiated skin cells, it is not known whether this increase is due to increased TACE activity and/or expression. However, before TACE is activated it is cleaved from its preproform by the action of a proprotein convertase, furin. Furin also cleaves a number of proteases in the cell including matrix metalloproteases (MMPs). It is known that following exposure to UVB ration that the levels of MMP activity in the skin is increased. While furin is expressed in skin cells, the effect UV radiation has on its expression and/or activity and that of the proteases it activates in keratinocytes is not fully known. The increase in the release of some bioactive molecules from UV-irradiated skin cells, may not be related to their expression but to the activation of furin, which in turn activates many proteases in the cell. In the longer term, elevated furin levels in a mutated cell, may enhance TACE thereby increasing the release of TNFα from the cells which sustains the inflammatory environment allowing for the development of carcinogenic cells. As furin also activates MMP activity, these cells may go onto to become metastatic. Therefore the development of specific furin

inhibitors, thorough reducing the release of inflammatory molecules and MMP activity may offer a new therapy to reduce not only UV-induced inflammation in the skin but that of skin cancer as well.

Background

Skin cancer represents a major, and growing, public health problem [1]. It is the most common type of cancer in fair skinned populations. The three most common forms of skin cancer are basal cell carcinoma (BCC), squamous cell carcinoma (SCC) and malignant melanoma (MM). BCC and SCC are together known as non melanoma skin cancers (NMSC) [2-4]. BCCs and SCCs are derived from keratinocytes, whereas melanoma is derived from melanocytes. SCCs can undergo metastasis, BCCs rarely if ever, while melanomas can be highly metastatic. [3, 4]

It is widely acknowledged that sunlight, or ultraviolet (UV) radiation is the main carcinogen implicated in the formation of skin cancer. UV radiation can be divided into three components: UVC (100-280 nm), UVB (280-320 nm) and UVA (320-400 nm). Ozone depletion, seasonal and weather variations affect the amount of UV radiation reaching the Earth's surface [1, 5]. All of the UVC and most of the UVB radiation emitted from the sun is effectively blocked from reaching the Earth's surface by the stratospheric ozone layer. The component of UV light that reaches the Earth's surface consists of 90-95% UVA and 5-10% UVB [6, 7]. The penetration of shorter-wavelength UVB radiation is predominantly confined to the epidermis while UVA penetrates into the dermis because of its longer wavelength [8].

UVB can cause sunburn, inflammation, cataract formation, DNA mutations and membrane damage as well as skin cancer [6, 9, 10]. It is known that UVB directly damages DNA and can induce Reactive Oxygen Species (ROS) by interactions with chromophores in the skin [11]. The DNA damage seen in epidermal cells caused by UVB irradiation typically results in the formation of cyclobutane pyrimidine dimers (CPD) and pyrimidine (6-4) photoproducts. Mutations of this kind are frequently found in p53, p16, PTCH and INK4α/CDKN2A genes of skin cancer patients [12].

UVA can cause premature skin ageing, wrinkle formation, blotching and induces sunburn cell formation in the epidermis, as well as skin cancer [6, 10]. UVA affects keratinocytes at a transcriptional level by altering the expression of genes involved in apoptosis, cell cycle, DNA repair, signal transduction, RNA processing and translation, cell structure and metabolism [13]. It can cause DNA damage by the generation of ROS [11, 14] that results in a wider range of genomic damage e.g. single-stranded breaks, protein-DNA crosslinks, and oxidative base damage (e.g. 8-oxo-7,8-dihydroxyguanine) [15]. ROS can also cause lipid peroxidation resulting in membrane and protein damage [11, 14]. They can also initiate signal transduction processes leading to rapid synthesis and release of prostaglandin E_2 and isoprostanes [16] as well as induction of new gene products such as cytokines, heme oxygenase-1, cyclooxygenase and intercellular adhesion molecules [17] and inflammatory mediators such as TNFα [18-20]. TNFα is cleaved from its preproform by the action of the metalloprotease Tumour Necrosis Factor α Converting Enzyme (TACE) [21]. TACE along with other enzymes such as matrix metalloproteases (MMP), are must be cleaved from their respective proform by the action of proprotein convertases such as furin [22].

For many years UVB was considered to be the main contributor toward skin cancers, based largely on the DNA action spectrum of UV radiation [19], but UVA has more recently been acknowledged as playing an important role in skin carcinogenesis. This is in keeping with the growing body of evidence that direct molecular targets of UV other than DNA are important to carcinogenesis. UVA, although it does not produce an inflammatory response at doses normally encountered by people, also produces ROS and so, unsurprisingly, activates many of the same signalling pathways as UVB. It is clear that doses of UVB, UVA and solar stimulated UV too low to cause inflammation are able to induce mutations. However, this does not exclude a role for ROS from inflammatory cells contributing to skin carcinogenesis, but it may be important for tumour progression [19]. The inflammation seen in the skin following UV radiation involves the action of many molecules.

UV-induced Inflammation

It has been shown that UV at high doses can induce inflammation which results in the appearance of macrophages and other lecucocytes in the skin [23]. Along with the appearance of these cells, many mediators of inflammation are also seen including prostaglandins [17], nitric oxide (NO) [24] and ROS [11, 14, 16], and cytokines such as interleukin (IL) -1, interferon (IFN) -γ, and TNFα [19, 25–27] (Figure 1). It has been shown that ROS can cause DNA strand breaks as well as lipid peroxidation, membrane and protein damage [11, 14, 15, 28]. A list of immunomodulatory molecules whose expression is upregulated by UV radiation is seen in Table 1 [6, 18, 28-33]. Proinflammatory molecules have been shown to have important roles in the pathogenesis

of skin cancer, as determined from clinical or experimental animal studies, and the activity or quantities of many of these are affected by UV radiation [19, 28].

Even in tumours, which have not been caused by UV radiation, can produce an inflamed environment [26, 34, 35]. It is known that inflammatory mediators such as IL-1, TNFα and IL-6 are involved in melanoma formation [36]. IInflammation has also been shown to play a role in non melanoma skin cancer as well [23, 37-39]. In a recent study, male mice were shown to be more sensitive to UVB-induced skin carcinogenesis than female mice [2], which is consistent with men having a higher incidence of skin cancer than women [19]. In this study, an inflammatory dose of UVB was used to induce the cancers. Damian *et al*. [40] found that while women developed a larger inflammatory response to UVB, men were found to have lower antioxidant protection in the skin resulting in a higher level of oxidative damage to DNA, and are more sensitive to UV immunosuppression than women. This would suggest that UV-induced immunosuppression and DNA damage but not inflammation are associated with the formation of skin cancers in men compared to women [19].

IL-1α and Il-1β are both induced in keratinocytes exposed to UVB radiation [29, 41]. IL1α has also been shown to enhance the expression and release of TNFα from UVB-irradiated keratinocytes [42-44], while IL1β enhances the expression of MMP-9 in these irradiated cells [45]. Apart from IL1β it has been shown that UVB can stimulate MMP9 expression in human skin via the induction of Activator protein-1 and NFκB activities [46].

Apart from inducing cytokines, UVB radiation has been shown to increase cyclooxygenase (COX) -2 expression and activity in keratinocytes [19, 25, 47]. High levels of COX-2 activity have been observed in human epithelial skin cancers which are increased in response to UVB radiation [48]. The addition of nonsteroidal anti-inflammatory drugs (NSAIDs) has been shown to inhibit COX-2 activity and subsequent PGE formation in the skin, and they have been used in the treatment of actinic keratosis (AK) [49], BCC, SCC and melanoma [50], which suggests that COX-2 plays a role in the formation of these tumours. Recent studies using IL-12-deficient mice, have found that they have higher levels of inflammation and increased incidence of skin cancers than wild type controls which suggest that IL-12 may play an important role in modulating the inflammatory response seen in the skin [38].

Upregulation of TNFα is a key early response to UVB by keratinocytes [6, 44, 51, 52] and represents an important component of the inflammatory cascade in skin. UVB irradiation induces TNFα mRNA expression in both keratinocytes and dermal fibroblasts within a few hours following irradiation [44, 51]. IL-1α stimulates TNFα expression [42] and release particularly in skin where there is substantial preformed IL-1α [44]. Recently, Bashir *et al*. [42] found that TNFα expression and secretion in keratinocytes was induced by UVB but not by UVA irradiation. This induction was mediated through increased TNFα gene transcription [42]. The IL1α formed in the epidermis and dermis can in turn induce mast cells to secrete inflammatory cytokines, such as TNFα and IL1α, as well as prostaglandins which can enhance the inflammation caused by direct UV exposure on the epidermal cells [18, 19]. The histamine released from the mast cells can

induce vasodilation of the surrounding blood venules which assists in the leucocytes undergoing diapedesis and entering the region [18, 19]. T

TNFα that has been secreted from the keratinocytes in the epidermis or fibroblasts in the dermins has been shown to induce a myriad of pro-inflammatory effects on the skin. There are synergistic interactions between pro-inflammatory cytokines produced in the skin and in synergy with irradiated keratinocytes, leading to later augmentation of TNFα production in the irradiated tissue. UVB radiation has been shown to induce IL-6 and IL-8 synthesis and release from irradiated keratinocytes and fibroblasts [18, 33, 38, 41]. IL-8 assists in the homing of leucocytes from surrounding blood venules into the inflamed region, while IL-6 is known to trigger the activation of monocytes and other infiltrating leucocytes to secrete cytokines and chemokines [18].

TNFα has been shown to induce adhesion molecules and chemokines in the surrounding epithelial cells, resulting in the recruitment of inflammatory leucocytes from surrounding blood vessels via diapedesis [18, 19, 53-55]. These inflammatory cells secrete additional cytokines that form a positive feedback loop in further upregulating TNFα and downstream TNFα-induced chemokines, cytokines, and other pro-inflammatory pathways in irradiated skin [6, 42, 56]. These effects elicited by the infiltrating inflammatory cells occur some hours after UV irradiation, and this prolongs the observed inflammation. In addition, UVB radiation also induces inducible nitric oxide synthase (iNOS) activity in dermal endothelial cells, which play an important role in UVB-induced inflammation observed in skin, This induction of iNOS has been shown to occur via a TNFα-dependent pathway [42, 52, 57].

It can be seen that TNFα plays an important pro-inflammatory role in the skin, both due to (a) the direct effects of UV radiation and (b) the indirect effects of inflammatory cells that chemotax to the skin. It is clear that UV- and inflammatory cell-derived cytokines further enhance TNFα gene transcription in human skin cells [42, 51], and this can further increase epidermal production of TNFα. However, clustering and internalization of TNF receptors may lessen the response to the TNFα protein over time, and this may account for why persistent TNFα in culture supernatants do not sustain TNFα mRNA upregulation over time [19]. For further information on the complex interplay of cytokines, chemokines and other mediators in UV-induced inflammation please read the following reviews [19, 46, 47].

Tumor Necrosis Factor α

TNFα, which was formerly known as cachexin or cachectin, is a member of the TNF ligand superfamily [56, 58-60]. It is a type II transmembrane glycoprotein of 234 amino acids possessing an extracellular carboxy-terminus and a cytoplasmic amino group [59, 60]. TNFα can exist in two forms; a 26 kDa membrane-bound form (mTNFα) and a 17 kDa soluble form (sTNFα). sTNFα is cleaved from its membrane bound precursor between Ala^{76} - Val^{77} by the action of the metalloprotease TACE [21, 60-62].

TNFα, is mainly produced by macrophages and to a lesser extent by other cells including leucocytes, dendritic cells, keratinocytes, melanocytes and fibroblasts [6, 21, 44, 59, 60]. It plays a crucial role in the pathogenesis of psoriasis, mainly by inducing the expression of ICAM-1 on keratinocytes and other cell adhesion molecules (e.g. vascular adhesion molecules, E-selectin) on dermal microvascular endothelium [56]. TNFα is also

involved in apoptosis, cellular proliferation, differentiation, inflammation, tumorigenesis, apoptosis, viral replication, immune response to extracellular stimuli as well as local and systemic inflammation [21, 43, 51, 59, 63, 64].

Most of the cellular actions described for TNFα correspond to the secreted, soluble form of mature TNFα. There is increasing evidence that mTNFα is also biologically active and that it may be responsible for the localised action of this cytokine [59]. Both forms of TNFα can specifically bind to one of two receptors: a 55-kDa (p55 or CD120a receptor) form designated TNF-Rl; and a 75-kDa (p75 or CD120b receptor) form designated TNF-R2 [21, 64]. These two receptors are transmembrane glycoproteins, which display a high degree of structural homology and are expressed on most cell types [65].

TNFRI is expressed on a wide range of cell types and its signalling mediates cytotoxicity, cell proliferation, antiviral activity and many of the proinflammatory actions of TNFα [58, 59]. TNFRII is expressed on a more limited range of cells, including leukocytes, endothelial cells, LC and epithelial cells but its actions are less clear [58, 59]. Membrane-bound TNFRI and TNFRII can be cleaved by TACE to release the soluble forms of these receptors and this process is activated by IL-10 [59]. The soluble forms of TNFR has been postulated to act as (a) an antagonist to the surface receptors by competing for sTNFα or (b) an agonist by stabilizing the TNF trimer; therefore maintaining saturating concentrations in the extracellular fluids [59, 66].

Studies have shown that when TNFα is bound to the TNFRI receptor it plays a role in UVB-induced apoptosis in keratinocytes, (also known as sunburnt cells) [57, 67]. Transgenic mice deficient for either TNFRI and/or TNFRII have been shown to be less susceptible to UVB-induced skin tumours than the wild type controls [68]. Through the use of TNF-R1 [64, 69, 70] and TNF-R2 [64, 69] gene-targeted mutant mice, it has been shown that TNF-R1 plays a decisive role in the host's defence against microorganisms, while TNF-R2 plays a role in the induction of tissue necrosis. Using agonist and antagonist antibodies specific for each receptor, it has also been indicated that TNFα binding to TNF-R2 does not potentiate the cytotoxicity of TNF-R1, but instead regulates the rate of TNFα association with TNF-RI [64, 71] which suggests that TNF-RI is the main mediator of TNFα action in the cell.

Dermal injection of TNFα results in the accumulation of dendritic cells in draining lymph nodes [64, 72], suggesting that this cytokine may serve as a stimulus for the migration of Langerhans cells (LC) from skin to regional lymph nodes [64, 65]. Streilein and colleagues [64, 73, 74] suggested that UVB indirectly induces TNFα, which then causes morphologic and functional changes on LC resulting in the impairment of contact hypersensitivity (CHS). They also demonstrated that intradermal injection of TNFα immobilizes LC with the epidermis, leading to impaired induction of CHS [64]. Morphologic damage of LC caused by TNFα has also been reported by others [64, 75]. It has been shown that UVB exposure and intradermal TNFα injection have similar morphologic and functional effects on epidermal Langerhans cells [64, 74] suggesting that local UVB-induced impairment of CHS is mediated by TNFα. In studies using TNF-R1(-) mutant mice it has been shown that TNFα is not involved in UVB-induced

immunosuppression [75, 76]. UVB-induced immunosuppression is implicated in the pathogenesis of skin cancers, and is postulated to be mediated in part by *cis*-urocanic acid (*cis*-UCA) [77, 78]. *trans*-Urocanic acid, a deamination product of histidine, is a major chromophore present at a high concentration in the epidermal keratinocytes in the stratum corneum [78].

Upon exposure to UVR, *trans*-UCA undergoes a photoisomerization to its *cis*-isomer until equilibrium is reached with the two isomers being in approximately equal quantities. In humans, this occurs after 1 minimal erythemal dose (MED) of UVR, which is the lowest dose required to induce a just visibly perceptible erythema [77, 78]. *cis*-UCA has been shown that it does not exert its immunosuppressive effects through TNFα, but through other factors such as prostaglandin E_2 [77]. Amerio *et al*. [76] showed that in TNFR1 and TNFR2 (TNFR2; p75) double knockout mice, TNFα plays only a limited part in UVB-induced immunosuppression and that it cannot be considered among the major mediators of *cis*-UCA-induced immunosuppression. While it is now clear that TNFα may not play a major role in UV-induced immunosuppression [64, 65, 76] it does play a significant role in UV-induced immunosuppression [19] as well as in other inflammatory diseases such as rheumatoid arthritis, psoriasis or systemic lupus erythematosus [26, 42].

TACE

TNFα is cleaved from its preproform by the action of the metalloprotease TACE [61]. This enzyme is a member of the disintegrin and metalloprotease (ADAM) family of proteases, and is also known as ADAM 17 or CD156q [61, 62, 79-81]. ADAM proteases

belong to the adamalysin/reprolysin subfamily of the metzincin superfamily, and contain a Zn^{2+}-dependent catalytic domain [61, 81]. Currently the ADAM family comprises more than 30 members, although many are not fully characterized [61, 82, 83].

TACE is a multi-domain type I transmembrane protein of 824 amino acids in length and was first purified, characterized and cloned in 1997 [62, 79, 83]. While the amino acid sequence of TACE shows relatively low homology [62, 84] to other ADAM family members, its structure contains all the domain regions (Figure 2) which are characteristic for this family of metalloproteases [62, 79, 84]. The prodomain of TACE is similar to that of other ADAMs and MMP and, is thought to act as an inhibitor of the protease activity via the cysteine switch mechanism [84]. Before TACE can become biologically active the prodomain region must be removed.

The catalytic domain contains the zinc-binding consensus motif HEXGHXXGXXHD involved in coordinating Zn^{2+} with His residues and creating the active site of the enzyme[84, 85]. The role of the disintegrin domain in TACE is not known. Analysis of the amino acid sequence of TACE also indicates the presence of an EGF-like domain and a unique crambin-like domain, which contains a cysteine switch. However, its roles are not fully understood. The cysteine-rich domain may be important for enzyme maturation or substrate recognition [61, 79]. The cytoplasmic tail of TACE contains a potential phosphorylation site [86] and an SH3-binding site [84].

TACE is synthesized as an inactive zymogen, which is subsequently proteolytically processed to the catalytically active form. In order for TACE to be activated it must first be cleaved from its 120 kDa proform (proTACE) into its 90 kDa mature form by the

removal of its prodomain [81, 87-89]. The cleavage of which occurs at the furin cleavage site RVKR (Arg-Val-Lys-Arg) localized between the pro- and the catalytic domain. The removal of the prodomain is due to the action of a furin-type proprotein convertase [81, 87, 88] and possibly other intracellular proprotein convertases (PC) such as Paired basic amino acid cleaving enzyme (PACE) 4, PC1, PC2, PC5/6 and PC7/8 [22, 84, 88, 90].

In mammalian cells, proTACE is located in the endoplasmic reticulum and the proximal golgi body whereas the mature form is located both intracellularly and on the cell membrane [88, 90]. TACE maturation is closely linked to the transport of proTACE through the medial golgi, where upon exit, prodomain removal occurs before the enzyme reaches the cell's surface [81]. TACE maturation is negatively influenced by the phorbol-12-myristate-13-acetate (PMA), which decreases the amount of mature protein in treated cells [90, 91].

TACE has been shown to cleave a wide range of molecules including TGFα, amphiregulin, neuregulins, growth hormone receptor, both TNFα receptors, L-selectin, amyloid precursor protein and IL-6R [81, 82, 92-94]. TACE-knockout mice are less efficient at processing TNFα on the cell membrane compared to wild type controls [61, 82]. These mice have elevated levels of mTNFα as well as reduced levels of sTNFα compared to wild-type controls, which suggests that TACE is the main protease responsible for its processing. Although some matrix metalloproteases (MMP) can cleave TNFα, the cleaved products are inactive due to hydrolysis occurring at different sites within the molecule [61, 85, 94].

Some metalloproteases are activated in epidermal cells following UV radiation [95-97]. Piva and coworkers found that there were a number of proteases whose activity was upregulated in UVC- or UVB-irradiated HeLa cells [96, 97]. These enzymes included aminopeptidases and a "TGFαase" [96, 97]. On re-evaluation of their data, the TGFαase is most likely TACE, because (a) the later enzyme is known to cleave TGFα among other growth factors [85, 93] and (b) the substrate used in these studies was a nonapeptide based on the N-terminal cleavage site of TGFα [95-97]. In cells undergoing UV-induced apoptosis, the level of cell surface protease activity (aminopeptidase and "TGFαase") was shown to be higher than that seen in viable or necrotic cells [96]. The results of these studies were the first to show that TACE activity was elevated in cells exposed to UV radiation. Recently Skiba *et al*. [27] reported that UVA and UVB irradiation increased TACE mRNA levels in HaCaT cells, with higher induction induced by UVA. The expression patterns for both UVA and UVB radiated cells generally appeared to be constant, although mRNA levels were significantly higher than controls, throughout the 48 h period following exposure [27].

In UV-irradiated HaCaT cells, it has been shown that TACE is responsible for the increased cleavage of EGF family members [98, 99]. Inhibition of TACE activity by metalloprotease inhibitors reduced the release of these growth factors, resulting in an increase in apoptotic cell death [98, 99]. It appears that TACE mediates a EGF receptor/AKT signalling pathway in these cells that is activated as a result of its cleavage of EGF family members. In HaCaT cells exposed to UVA-radiation TACE mediated EGF receptor activation and cell cycle progression, which suggests that UVA, at non lethal doses, has the potential to be a skin cancer promoter [98, 99]. In support of the

role TACE may play in skin cancer development, it was shown to be overexpressed in a large number of skin cancer cells lines compared to non tumour cells [98, 99]. It is also known that members of the EGF family are overexpressed in skin cancers [100], and this could be a mechanism by which skin cancer growth is stimulated by autogenic growth factors. The result of these recent studies suggest that inhibition of the action on TACE following UV radiation may prevent the stimulation of the surviving irradiated cells, which has the potential in reducing the incidence of skin cancer that may arise from prolonged sun exposure. What is not clear is that the increase in TACE activity seen in these irradiated skin cells is due to increased levels or a change in its activity. The proprotein convertase furin is known to activate TACE [88, 90] as well as matrix metalloproteases [22, 101] may play a role in this process.

Furin

Furin, also known as PACE is a 94 kDa, type I transmembrane, Ca^{2+}-dependant serine protease [22, 91, 101]. It is a mosaic protein consisting of a series of multifunctional domains. At its N-terminal region, a signal peptide directs the translocation of the growing peptide chain to the endoplasmic reticulum and the secretory pathway [87, 101, 102]. Next, the pro-region initially folds onto the native protein, thereby keeping the enzyme in a zymogen or inactive state [101, 102]. The pro-region is cleaved early in the endoplasmic reticulum by an intramolecular autocatalytic process, where it then associates with the catalytic domain and helps to guide the protein through the endoplasmic reticulum and golgi apparatus for its enzymatic activation [101, 102].

Furin carries structural information within the cysteine-rich region (CRR) that facilitates shedding of its ectodomain [101, 102]. The CRR could participate in the shedding process by imparting a conformation to furin facilitating recognition and cleavage by its sheddase[101, 102]. The CRR could be considered either as functional regions involved in cell adhesion [82] interacting with specific target proteins or influencing conformation enabling dimerization or shedding of membrane proteins [101, 102]. The CRR is followed by a trans-membrane region that anchors the enzyme in the membrane of the trans golgi network (TGN) or the cell membrane. The cytosolic tail contains the information necessary for furin's sorting to various intracellular compartments [87, 101, 102]. In the epidermis, furin can exist either as: (a) a mature 97 kDa membrane bound enzyme or (b) a smaller 75 kDa form that lacks the transmembrane domain [101]. This suggests that post-translational cleavage at the C-terminus takes place in the cell [22, 101, 102].

Furin is a ubiquitously expressed member of the PC family. This family is related to the bacterial subtisilin[22] and consists of seven distinct members (PC1-PC7) that vary in regards to their tissue and subcellular distribution as well as enzymatic and biochemical properties [101]. Furin and other PC family members functions to process inactive precursor proteins to their functional or mature form. These molecules include growth receptors, growth factors, hormones, plasma proteins, MMP and extracellular matrix components [22, 101, 102]. The PC family members play a crucial role in a variety of physiological processes and are involved in the pathology of diseases such as cancer and viral infection [102-104].

Of these family members, furin, PACE 4, PC5/6 and PC7/8 are widely expressed in the epidermis whereas PC2 and PC1/3 are limited to neuroendocrine tissues and PC4 is restricted to the testis [22]. The PC enzymes recognize basic motifs, cleaving after paired basic residues (PC2 and PC1/3); or after a canonical Rx (R/K) R (Arg-x-(Arg/Lys)-Arg) motif (furin and PACE4) [22, 101, 103]. Both PC7 and furin share an overlapping substrate specificity and therefore the selectivity of substrate proteolysis depends on their cellular localization. As intracellular trafficking is regulated by their cytosolic domains, which contain different sorting motifs, it is likely that the cellular localization of PC7 differs to that for furin [90].

Furin/PC expression and processing can increase the incidence and severity of the cancer phenotype [104, 105]. Overexpression of PACE4 resulted in mouse squamous cell carcinomas acquiring a more aggressive phenotype [105, 106]. Proteolytic degradation of the extracellular matrix (ECM) components is a central event of tumour invasion and metastasis [102-104]. Several classes of proteases, including serine proteinases, cysteine proteinases and matrix metalloproteinases (MMPs), have been implicated in the tumour cell invasive process. Of these, MMPs appear to be primarily responsible for much of the ECM degradation observed during invasive processes [105, 106]. They can contribute to tumour growth not only by degradation of the ECM but by the release of sequestered growth factors or the generation of bioactive fragments VEGF, bFGF or TGF-β, the suppression of tumour cell apoptosis and the destruction of immune-modulating chemokine gradients [106-108].

MMPs are also implicated in cell migration, proliferation, and tissue remodeling and thereby may also play a role in growth and development, angiogenesis, and atherosclerosis [109-111]. Exposure to UV radiation elevates MMP production in human skin, implicating sunlight as a major factor in photoageing [25, 112]. Regulation of MMP activity involves both the control of zymogen activation and the inhibition of the active enzyme by specific inhibitors such as TIMPs [25, 112]. MMPs are synthesized as latent proenzymes which are converted into mature, catalytically active forms by proteolytic cleavage of the N-terminal propeptide mediated by serine proteases, such as furin, or by membrane-type MMPs (MT-MMPs) [105, 110, 113]. TNFα has been shown to induce proMMP-2 in human dermal fibroblasts [114], while IL-1α induced proMMP-9 levels in fibroblasts and keratinocytes [115]. Activation of pro-MMP2 takes place at the cell surface and involves interactions with active MT1-MMP, which is itself activated through rapid trafficking to the cell surface and proteolytic processing [110]. Maquoi *et al*. [116] demonstrated that furin-inhibitor reduces the level of mature MT1-MMP, which is paralleled by a decrease in pro-MMP-2 activation as well as in cell invasiveness, which suggests that furin plays a role in this process.

MMP-2 (also known as gelatinase A or 72-kDa type IV collagenase) and MMP-9 (also known as gelatinase B or 92-kDa type IV collagenase) has been frequently associated with the invasive and metastatic potential of tumour cells [104-106, 112, 117]. MMP-9 [118, 119], has been reported to play important roles in the pathophysiologies of many skin conditions such as wound healing [120], and angiogenesis [92]. On the other hand, the expression of MMP-2, is regulated independently of MMP-9 [118, 119]. The close correlation observed between MMP-2 activation and metastatic progression in various

tumours suggests that MMP-2 is a “master switch” triggering tumour spread [116]. Onoue *et al*. [119] has suggested that MMP-9 secreted from keratinocytes after UVB irradiation might result from apoptotic events. However, the specific roles of the gelatinases, including their expression patterns following UV radiation is not known. MMP-1, which is produced by both dermal fibroblasts and epidermal keratinocytes, cleaves type I collagen into specific fragments. These fragments can then be further hydrolysed by MMP-2 and MMP-9 [117, 120]. Steinbrenner *et al*. [117] found that UVA irradiation dose-dependently decreased the steady-state mRNA levels of MMP-2 and MMP-9 and lowered the gelatinolytic activity of both enzymes in cell culture supernatants.

Apart from MMPs, furin and other PCs are also involved in the maturation of TACE (Figure 3). proTACE is proteolytically processed by both furin and PC7 to its mature form most likely to increase its proteolytic activity [88, 90]. The maturation of TACE occurs during the transit of the protein through the late golgi compartment suggesting that prodomain removal is performed by a furin-type proprotein convertase [81, 90]. As increased amounts of mature TACE are detected in furin over-expressing cells, it would be that proTACE is a better substrate for furin than it is for PC7 [90].

Moss *et al*. [79] showed that when baculovirus-infected insect containing fragments of TACE sequence with its prodomain, it resulted in the production of recombinant active TACE which suggested that pre TACE was cleaved by a furin-like enzyme. Similar results were obtained by using cells overexpressing TACE [59, 88, 91] which confirmed the role furin plays in this process [88, 91]. This finding was conformed as the cell permeable furin inhibitors decanoyl-Arg-Val-Lys-Arg-chloromethylketone

(Dec-RVKR-cmk) and PDX inhibited the formation of mature TACE in Cos7 cells [88] and keratinocytes [22]. It can be concluded from these studies that furin cleaves TACE in many different cells including keratinocytes.

Furin mRNA, protein and enzyme activity has been observed in human epidermal keratinocytes [22, 27, 105, 121, 122]. Skiba *et al*. [27] found that UVA and UVB radiation caused an increase in furin mRNA levels immediately following exposure in HaCaT cells. UVB irradiation was shown to induce higher levels of furin mRNA expression [27]. The time course for furin mRNA levels in cells irradiated with low dose of UVA and high dose of UVB was similar to that for TNFα, whereas maximal TNFα and furin mRNA induction were detected 8 h post-irradiation [27]. Although UV-irradiation does appear to have an effect on furin gene expression, no direct relationship was apparent between TACE and furin mRNA induction. A recent study has shown that following exposure to UVA and UVB, furin levels in HaCaT cells fell with respect to time [122]. It is unknown whether this change in furin levels was that of the immature and/or mature enzyme. Through its effect on stimulating TACE formation and the resultant effect this has on TNFα released by the cell, furin activity has an influence on the inflammation seen in the skin following exposure to UV radiation. If there are cells in the skin which become cancerous as a result of DNA damage, some may go onto become metastatic due to increased MMP activity [105]. This increase in levels of activated MMPs on the surface of the cell could be due to either increased expression of proMMP protein and/or increased furin activity. The role furin plays in the development of skin cancer suggests that it may play a significant role, and as such the development of specific inhibitors may offer a new therapy to treat these tumours.

Conclusion

While it has been shown that UVA and UVB radiation cause different effects on the immune response this could be related to the activity of cell surface metalloproteases found on the skin cells. Although the effect of TNFα in UV-induced inflammation has been well documented, little is known if the changes in TACE activity is due to increased protein levels or a change in enzyme activity. The inflammatory environment, seen in the skin, following exposure to UV radiation is known to stimulate the development of mutated cells which possess DNA damage caused directly by UV radiation or indirectly through the generation of ROS. Apart from increasing the release of TNFα, TACE also cleaves EGF family members, which would stimulate the growth of these mutated cells, which over time may become cancerous. Similar to that of TACE, MMPs are also activated by UV radiation and also play a crucial role in skin tumour cell development and metastasis. Furin and other proprotein convertases have been shown to play an important role in activating both TACE and MMP in skin cells. It is known that UV induces furin mRNA in skin cells, though protein levels do not appear to change with respect to time, which suggests a rapid turnover of the enzyme. Further study is needed on how UV radiation activates these enzymes in the cell. The development of specific furin/PC inhibitors has the potential to reduce the carcinogenic effects of sunlight by preventing the activation of TACE and MMPs and their subsequent downstream effects. Such compounds may have the potential to offer therapies in the treatment of skin cancer.

List of Abbreviations

ADAM, A Disintegrin And Metalloprotease; CRR, Cystine Rich Region; EGF, Epidermal Growth Factor; IL, Interleukin; LC, Langerhans Cell; MMP, Matrix Metalloprotease; NFκB, Nuclear Factor κB; PACE, Paired Basic Amino Acid Cleaving Enzyme; PC, Proprotein Convertase; ROS, Reactive Oxygen Species; TACE, Tumour Necrosis Factor α Converting Enzyme; TGF, Transforming Growth Factor; TNF, Tumour Necrosis Factor; TNF-RI/-RII, TNFα - receptor I/ - receptor II; UV, Ultraviolet.

Competing interests

The authors declare that they have no competing interests.

Author's contributions

RR outlined the topics of the manuscript and contributed to the content under each topic. TJP was involved in the analysis and revision of the review and approved the final manuscript.

Author's information

Rethika Ravi is currently in her final year of PhD with the School of Medical Sciences at RMIT University under the supervision of A/Prof Terry Piva. She has been awarded the School of Medical Sciences scholarship for her project. Prior her current appointment, she worked as a Medical Microbiologist for five years at some of the most reputed pathology laboratories/Hospitals in Melbourne, Australia. She holds a Masters in Applied Microbiology and Biotechnology (2002) from RMIT University, Australia.

A/Prof Terry Piva has been working in the area of Photobiology since 1994. He is currently with the School of Medical Sciences at RMIT. Prior to this current appointment, he was a Research Officer at the Queensland Institute of Medical Research from 1994-1999, a Lecturer/Senior Lecturer in Biomedical Science at CQU from 1999-2003, and Program Coordinator for the Biotechnology and Biomedical Science program at RMIT from 2003-2006. The major research findings from his studies in Photobiology are that (a) "TGFαase" is a metalloprotease which on re-evaluation of the experimental data, is most likely TACE and its activity is upregulated following exposure to UV light, and (b) cells undergoing UV-induced apoptosis have an increased level of cell surface metalloprotease activity compared to viable cells. To date he has published over 30 peer reviewed scientific articles, and over 60 conference abstracts.

Acknowledgements

We would like to that the School of Medical Sciences, RMIT Bundoora, Australia for supporting this study.

Figure legend

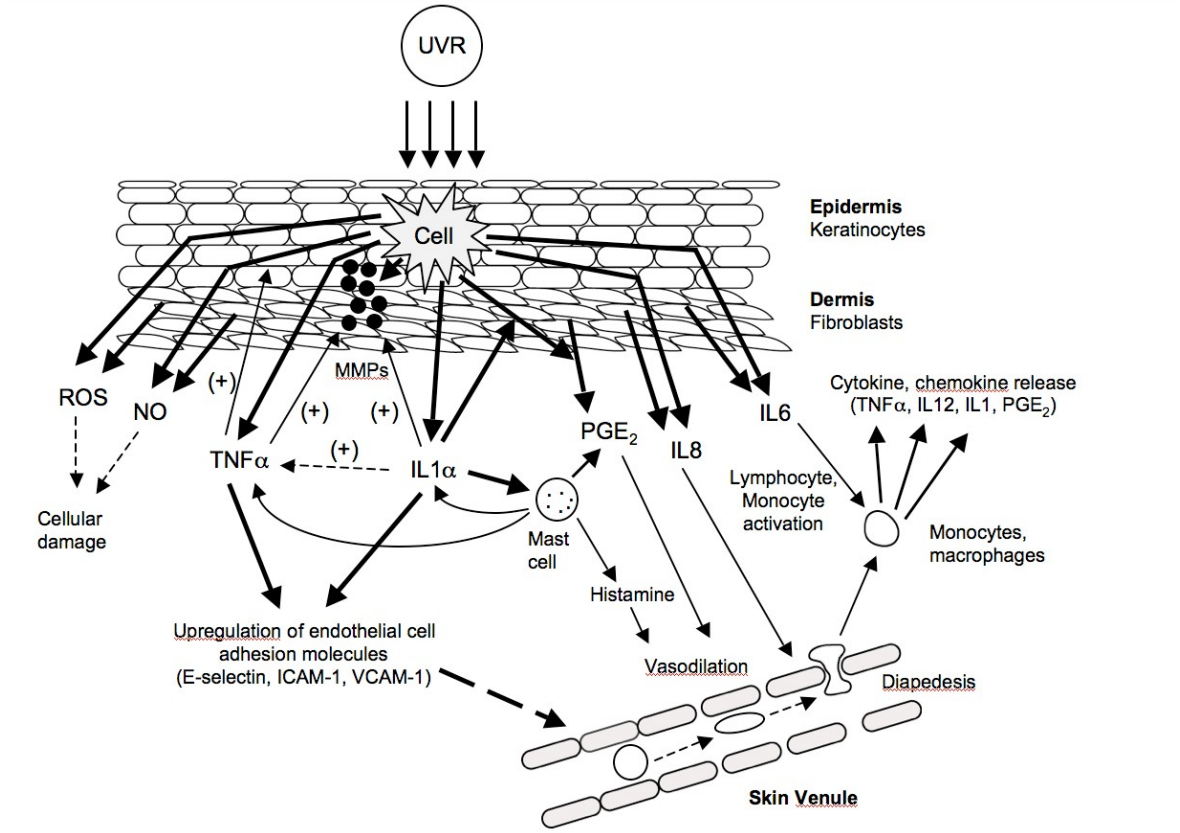

Figure 1: The inflammatory response seen in the skin following exposure to UV radiation, as adapted from [18]. Inflammation can be induced as a direct result of UV exposure on epidermal cells, or due to the release of secreted molecules, which in turn induce the release of inflammatory mediators from the dermis, as well as attracting inflammatory cells from circulation into this region of the skin. The infiltrating monocytes and macrophages, which enter the irradiated skin tissue in turn secrete mediators that prolong the inflammatory response. See text for details and references.

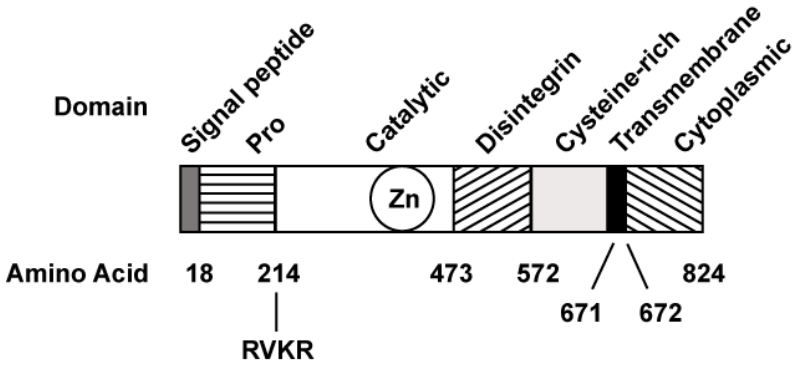

Figure 2: The amino acid and multidomain structure of TACE [85].

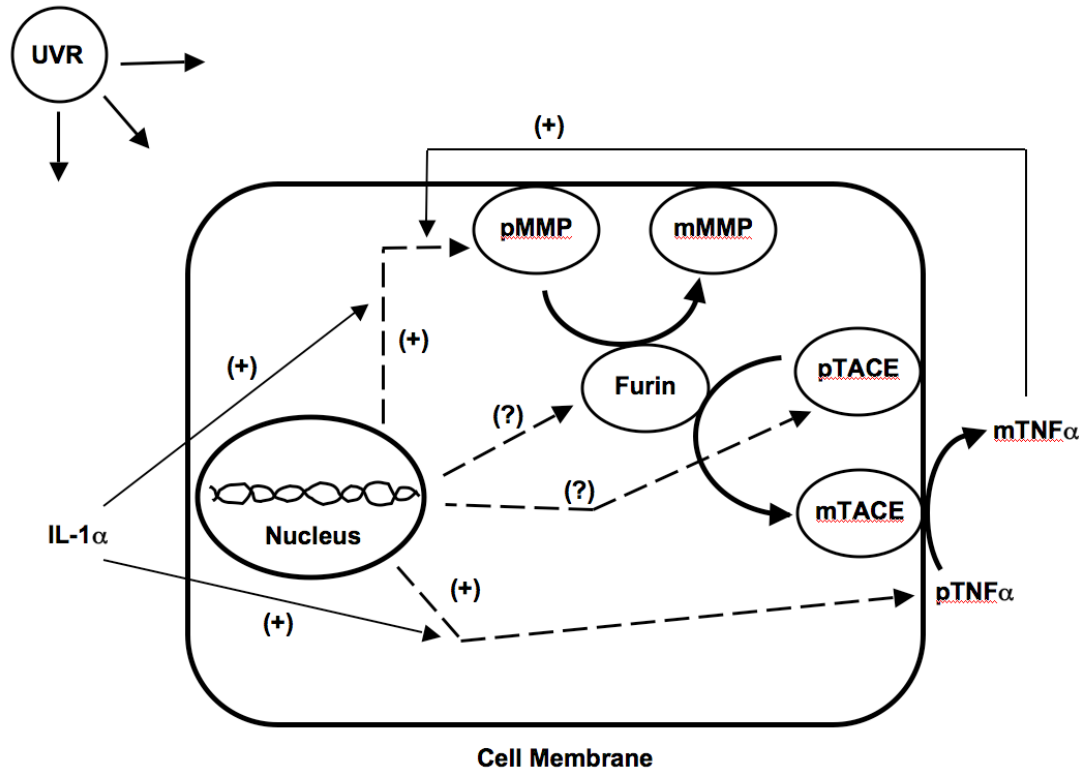

Figure 3: The role furin plays in the maturation of TACE and MMPs in skin cells. Furin cleaves and activates TACE, which in turn can process TNFα from its preproform. Keratinocytes secrete TNFα following exposure to UVB radiation, and this is enhanced if IL-1α is present. Furin also cleaves MMPs from their respective proforms, and the expression and activity of these proteases are elevated when the cells have been exposed to UVB radiation, and they are enhanced if either IL-1α (MMP-9) or TNF α (MMP-2) is present. The effect of UVB radiation on the expression of the enzymes and pTNF α in the cell is represented by dashed lines, if it is enhanced it is represented by (+), and if it is unknown (?). See text for details and references.

Mediator	Produced By	Function	References
TNFα	Keratinocytes Mast cells Dermal fibroblasts Langerhans cells	Langerhans cell migration, sunburn cell information, stimulates prostaglandin (PG) synthesis, changes in adhesion molecule expression	[29, 33]
IL-1α	Keratinocytes Langerhans cells	Simulates PG synthesis, increases TNFα and IL-6, inhibited by IL-1 receptor antagonist	[33]
IL-1β	Keratinocytes Langerhans cells	Langerhans cell migration	[29, 33]
IL-6	Keratinocytes, Langerhans cells	Fever Severe sunburn	[6, 33]
IL-10	Keratinocytes (mouse) Macrophages (human) Melanocytes	Blocks cytokine production by T cells, macrophages and NK cells Decreases antigen presentation, Increases IL-1 receptor antagonist	[33] [6, 30, 33]
IL-I2p40 (not bioactive)	Keratinocytes, Dendritic cell, Langerhans cells	Decreases Th1 response Decreases antigen presentation	[33]
IFNγ	T cells	Triggers apoptosis T-cell mediated tumour cell destruction	[32]
PGE_2	Keratinocytes, Mast cells	Erythema Decreases antigen presentation Increases IL-4, decreases IL-12	[33]
Histamine	Mast Cells	Increases release of PG Inhibit lymphocyte functions like IL-2 and IFNγ	[6, 33]

Table 1: Cutaneous mediators in skin cells whose expression is upregulated by UV radiation.

References

1. Katiyar SK: **UV-induced immune suppression and photocarcinogenesis: chemoprevention by dietary botanical agents.** *Cancer Lett* 2007, **255:**1-11.
2. Thomas-Ahner JM, Wulff BC, Tober KL, Kusewitt DF, Riggenbach JA, Oberyszyn TM: **Gender differences in UVB-induced skin carcinogenesis, inflammation, and DNA damage.** *Cancer Res* 2007, **67:**3468-3474.
3. Erb P, Ji J, Kump E, Mielgo A, Wernli M: **Apoptosis and pathogenesis of melanoma and nonmelanoma skin cancer.** *Adv Exp Med Biol* 2008, **624:**283-295.
4. Rass K, Reichrath J: **UV damage and DNA repair in malignant melanoma and nonmelanoma skin cancer.** *Adv Exp Med Biol* 2008, **624:**162-178.
5. Qureshi AA, Laden F, Colditz GA, Hunter DJ: **Geographic variation and risk of skin cancer in US women. Differences between melanoma, squamous cell carcinoma, and basal cell carcinoma.** *Arch Intern Med* 2008, **168:**501-507.
6. Clydesdale GJ, Dandie GW, Muller HK: **Ultraviolet light induced injury: immunological and inflammatory effects.** *Immunol Cell Biol* 2001, **79:**547-568.
7. Matsumura Y, Ananthaswamy HN: **Toxic effects of ultraviolet radiation on the skin.** *Toxicol Appl Pharmacol* 2004, **195:**298-308.
8. Agar NS, Halliday GM, Barnetson RS, Ananthaswamy HN, Wheeler M, Jones AM: **The basal layer in human squamous tumors harbors more UVA than UVB fingerprint mutations: a role for UVA in human skin carcinogenesis.** *Proc Natl Acad Sci U S A* 2004, **101:**4954-4959.

9. Ibuki Y, Allanson M, Dixon KM, Reeve VE: **Radiation sources providing increased UVA/UVB ratios attenuate the apoptotic effects of the UVB waveband UVA-dose-dependently in hairless mouse skin.** *J Invest Dermatol* 2007, **127:**2236-2244.

10. Tran TT, Schulman J, Fisher DE: **UV and pigmentation: molecular mechanisms and social controversies.** *Pigment Cell Melanoma Res* 2008, **21:**509-516.

11. Sander CS, Chang H, Hamm F, Elsner P, Thiele JJ: **Role of oxidative stress and the antioxidant network in cutaneous carcinogenesis.** *Int J Dermatol* 2004, **43:**326-335.

12. Nickoloff BJ, Qin JZ, Chaturvedi V, Bacon P, Panella J, Denning MF: **Life and death signaling pathways contributing to skin cancer.** *J Investig Dermatol Symp Proc* 2002, **7:**27-35.

13. He YY, Huang JL, Sik RH, Liu J, Waalkes MP, Chignell CF: **Expression profiling of human keratinocyte response to ultraviolet A: implications in apoptosis.** *J Invest Dermatol* 2004, **122:**533-543.

14. Leccia MT, Richard MJ, Joanny-Crisci F, Beani JC: **UV-A1 cytotoxicity and antioxidant defence in keratinocytes and fibroblasts.** *Eur J Dermatol* 1998, **8:**478-482.

15. Shorrocks J, Paul ND, McMillan TJ: **The dose rate of UVA treatment influences the cellular response of HaCaT keratinocytes.** *J Invest Dermatol* 2008, **128:**685-693.

16. Valencia A, Kochevar IE: **Nox1-based NADPH oxidase is the major source of UVA-induced reactive oxygen species in human keratinocytes.** *J Invest Dermatol* 2008, **128:**214-222.

17. Mahns A, Wolber R, Stab F, Klotz LO, Sies H: **Contribution of UVB and UVA to UV-dependent stimulation of cyclooxygenase-2 expression in artificial epidermis.** *Photochem Photobiol Sci* 2004, **3:**257-262.

18. Fuller BB, Smith DR: **Topical anti-inflammatories.** In *Cosmetic formulation of skin care products.* Edited by Draelos ZD, Thaman LA. New York: Informa Healthcare; 2002: 351-376

19. Halliday GM, Lyons JG: **Inflammatory doses of UV may not be necessary for skin carcinogenesis.** *Photochem Photobiol* 2008, **84:**272-283.

20. Schwarz T: **Photoimmunosuppression.** *Photodermatol Photoimmunol Photomed* 2002, **18:**141-145.

21. DasGupta S, Murumkar PR, Giridhar R, Yadav MR: **Current perspective of TACE inhibitors: a review.** *Bioorg Med Chem* 2009, **17:**444-459.

22. Pearton DJ, Nirunsuksiri W, Rehemtulla A, Lewis SP, Presland RB, Dale BA: **Proprotein convertase expression and localization in epidermis: evidence for multiple roles and substrates.** *Exp Dermatol* 2001, **10:**193-203.

23. Sluyter R, Halliday GM: **Infiltration by inflammatory cells required for solar-simulated ultraviolet radiation enhancement of skin tumor growth.** *Cancer Immunol Immunother* 2001, **50:**151-156.

24. Weller R: **Nitric oxide: a key mediator in cutaneous physiology.** *Clin Exp Dermatol* 2003, **28:**511-514.

25. Bennett MF, Robinson MK, Baron ED, Cooper KD: **Skin immune systems and inflammation: protector of the skin or promoter of aging?** *J Investig Dermatol Symp Proc* 2008, **13:**15-19.

26. Dinarello CA: **The paradox of pro-inflammatory cytokines in cancer.** *Cancer Metastasis Rev* 2006, **25:**307-313.

27. Skiba B, Neill B, Piva TJ: **Gene expression profiles of TNF-alpha, TACE, furin, IL-1beta and matrilysin in UVA- and UVB-irradiated HaCat cells.** *Photodermatol Photoimmunol Photomed* 2005, **21:**173-182.

28. Halliday GM: **Inflammation, gene mutation and photoimmunosuppression in response to UVR-induced oxidative damage contributes to photocarcinogenesis.** *Mutat Res* 2005, **571:**107-120.

29. Barr RM, Walker SL, Tsang W, Harrison GI, Ettehadi P, Greaves MW, Young AR: **Suppressed alloantigen presentation, increased TNF-alpha, IL-1, IL-1Ra, IL-10, and modulation of TNF-R in UV-irradiated human skin.** *J Invest Dermatol* 1999, **112:**692-698.

30. Byrne SN, Limon-Flores AY, Ullrich SE: **Mast cell migration from the skin to the draining lymph nodes upon ultraviolet irradiation represents a key step in the induction of immune suppression.** *J Immunol* 2008, **180:**4648-4655.

31. Khalil Z, Townley SL, Grimbaldeston MA, Finlay-Jones JJ, Hart PH: **cis-Urocanic acid stimulates neuropeptide release from peripheral sensory nerves.** *J Invest Dermatol* 2001, **117:**886-891.

32. Li-Weber M, Treiber MK, Giaisi M, Palfi K, Stephan N, Parg S, Krammer PH: **Ultraviolet irradiation suppresses T cell activation via blocking TCR-**

mediated ERK and NF-kappa B signaling pathways. *J Immunol* 2005, **175:**2132-2143.

33. Norval M: **Effects of solar radiation on the human immune system.** *J Photochem Photobiol B* 2001, **63:**28-40.

34. Coussens LM, Werb Z: **Inflammation and cancer.** *Nature* 2002, **420:**860-867.

35. de Visser KE, Eichten A, Coussens LM: **Paradoxical roles of the immune system during cancer development.** *Nat Rev Cancer* 2006, **6:**24-37.

36. Morelli JG, Norris DA: **Influence of inflammatory mediators and cytokines on human melanocyte function.** *J Invest Dermatol* 1993, **100:**191S-195S.

37. Berhane T, Halliday GM, Cooke B, Barnetson RS: **Inflammation is associated with progression of actinic keratoses to squamous cell carcinomas in humans.** *Br J Dermatol* 2002, **146:**810-815.

38. Meeran SM, Punathil T, Katiyar SK: **IL-12 deficiency exacerbates inflammatory responses in UV-irradiated skin and skin tumors.** *J Invest Dermatol* 2008, **128:**2716-2727.

39. Sluyter R, Halliday GM: **Enhanced tumor growth in UV-irradiated skin is associated with an influx of inflammatory cells into the epidermis.** *Carcinogenesis* 2000, **21:**1801-1807.

40. Damian DL, Patterson CR, Stapelberg M, Park J, Barnetson RS, Halliday GM: **UV radiation-induced immunosuppression is greater in men and prevented by topical nicotinamide.** *J Invest Dermatol* 2008, **128:**447-454.

41. Yoshizumi M, Nakamura T, Kato M, Ishioka T, Kozawa K, Wakamatsu K, Kimura H: **Release of cytokines/chemokines and cell death in UVB-irradiated human keratinocytes, HaCaT.** *Cell Biol Int* 2008, **32:**1405-1411.

42. Bashir MM, Sharma MR, Werth VP: **UVB and proinflammatory cytokines synergistically activate TNF-alpha production in keratinocytes through enhanced gene transcription.** *J Invest Dermatol* 2009, **129:**994-1001.

43. Werth VP, Bashir MM, Zhang W: **IL-12 completely blocks ultraviolet-induced secretion of tumor necrosis factor alpha from cultured skin fibroblasts and keratinocytes.** *J Invest Dermatol* 2003, **120:**116-122.

44. Yarosh D, Both D, Kibitel J, Anderson C, Elmets C, Brash D, Brown D: **Regulation of TNFalpha production and release in human and mouse keratinocytes and mouse skin after UV-B irradiation.** *Photodermatol Photoimmunol Photomed* 2000, **16:**263-270.

45. Lyons JG, Birkedal-Hansen B, Pierson MC, Whitelock JM, Birkedal-Hansen H: **Interleukin-1b and transforming growth factor-a/epidermal growth factor induce expression of M(r) 95,000 type IV collagenase/gelatinase and interstitial fibroblast-type collagenase by rat mucosal keratinocytes.** *J Biol Chem* 1993, **268:**19143-19151.

46. Fisher GJ, Datta SC, Talwar HS, Wang ZQ, Varani J, Kang S, Voorhees JJ: **Molecular basis of sun-induced premature skin ageing and retinoid antagonism.** *Nature* 1996, **379:**335-339.

47. Rundhaug JE, Fischer SM: **Cyclo-oxygenase-2 plays a critical role in UV-induced skin carcinogenesis.** *Photochem Photobiol* 2008, **84:**322-329.

48. An KP, Athar M, Tang X, Katiyar SK, Russo J, Beech J, Aszterbaum M, Kopelovich L, Epstein EH, Jr., Mukhtar H, Bickers DR: **Cyclooxygenase-2 expression in murine and human nonmelanoma skin cancers: implications for therapeutic approaches.** *Photochem Photobiol* 2002, **76:**73-80.

49. Patel MJ, Stockfleth E: **Does progression from actinic keratosis and Bowen's disease end with treatment: diclofenac 3% gel, an old drug in a new environment?** *Br J Dermatol* 2007, **156 Suppl 3:**53-56.

50. Butler GJ, Neale R, Green AC, Pandeya N, Whiteman DC: **Nonsteroidal anti-inflammatory drugs and the risk of actinic keratoses and squamous cell cancers of the skin.** *J Am Acad Dermatol* 2005, **53:**966-972.

51. Bashir MM, Sharma MR, Werth VP: **TNF-alpha production in the skin.** *Arch Dermatol Res* 2009, **301:**87-91.

52. Suschek CV, Mahotka C, Schnorr O, Kolb-Bachofen V: **UVB radiation-mediated expression of inducible nitric oxide synthase activity and the augmenting role of co-induced TNF-alpha in human skin endothelial cells.** *J Invest Dermatol* 2004, **123:**950-957.

53. Briscoe DM, Cotran RS, Pober JS: **Effects of tumor necrosis factor, lipopolysaccharide, and IL-4 on the expression of vascular cell adhesion molecule-1 in vivo. Correlation with CD3+ T cell infiltration.** *J Immunol* 1992, **149:**2954-2960.

54. Ogilvie AL, Luftl M, Antoni C, Schuler G, Kalden JR, Lorenz HM: **Leukocyte infiltration and mRNA expression of IL-20, IL-8 and TNF-R P60 in psoriatic skin is driven by TNF-alpha.** *Int J Immunopathol Pharmacol* 2006, **19:**271-278.

55. Swerlick RA, Lee KH, Li LJ, Sepp NT, Caughman SW, Lawley TJ: **Regulation of vascular cell adhesion molecule 1 on human dermal microvascular endothelial cells.** *J Immunol* 1992, **149:**698-705.

56. Serwin AB, Sokolowska M, Chodynicka B: **Tumour necrosis factor alpha (TNF-alpha)-converting enzyme (TACE) and soluble TNF-alpha receptor type 1 in psoriasis patients treated with narrowband ultraviolet B.** *Photodermatol Photoimmunol Photomed* 2007, **23:**130-134.

57. Schwarz A, Bhardwaj R, Aragane Y, Mahnke K, Riemann H, Metze D, Luger TA, Schwarz T: **Ultraviolet-B-induced apoptosis of keratinocytes: evidence for partial involvement of tumor necrosis factor-alpha in the formation of sunburn cells.** *J Invest Dermatol* 1995, **104:**922-927.

58. Choo-Kang BS, Hutchison S, Nickdel MB, Bundick RV, Leishman AJ, Brewer JM, McInnes IB, Garside P: **TNF-blocking therapies: an alternative mode of action?** *Trends Immunol* 2005, **26:**518-522.

59. Goetz FW, Planas JV, MacKenzie S: **Tumor necrosis factors.** *Dev Comp Immunol* 2004, **28:**487-497.

60. Mocellin S, Nitti D: **TNF and cancer: the two sides of the coin.** *Front Biosci* 2008, **13:**2774-2783.

61. Black RA: **Tumor necrosis factor-alpha converting enzyme.** *Int J Biochem Cell Biol* 2002, **34:**1-5.

62. Black RA, Rauch CT, Kozlosky CJ, Peschon JJ, Slack JL, Wolfson MF, Castner BJ, Stocking KL, Reddy P, Srinivasan S, et al: **A metalloproteinase disintegrin that releases tumour-necrosis factor-alpha from cells.** *Nature* 1997, **385:**729-733.

63. Bouwmeester T, Bauch A, Ruffner H, Angrand PO, Bergamini G, Croughton K, Cruciat C, Eberhard D, Gagneur J, Ghidelli S, et al: **A physical and functional**

map of the human TNF-alpha/NF-kappa B signal transduction pathway. *Nat Cell Biol* 2004, **6:**97-105.

64. Kondo S, Wang B, Fujisawa H, Shivji GM, Echtenacher B, Mak TW, Sauder DN: **Effect of gene-targeted mutation in TNF receptor (p55) on contact hypersensitivity and ultraviolet B-induced immunosuppression.** *J Immunol* 1995, **155:**3801-3805.

65. Lewis M, Tartaglia LA, Lee A, Bennett GL, Rice GC, Wong GH, Chen EY, Goeddel DV: **Cloning and expression of cDNAs for two distinct murine tumor necrosis factor receptors demonstrate one receptor is species specific.** *Proc Natl Acad Sci U S A* 1991, **88:**2830-2834.

66. Cumberbatch M, Kimber I: **Tumour necrosis factor-alpha is required for accumulation of dendritic cells in draining lymph nodes and for optimal contact sensitization.** *Immunology* 1995, **84:**31-35.

67. Zhuang L, Wang B, Shinder GA, Shivji GM, Mak TW, Sauder DN: **TNF receptor p55 plays a pivotal role in murine keratinocyte apoptosis induced by ultraviolet B irradiation.** *J Immunol* 1999, **162:**1440-1447.

68. Starcher B: **Role for tumour necrosis factor-alpha receptors in ultraviolet-induced skin tumours.** *Br J Dermatol* 2000, **142:**1140-1147.

69. Erickson SL, de Sauvage FJ, Kikly K, Carver-Moore K, Pitts-Meek S, Gillett N, Sheehan KC, Schreiber RD, Goeddel DV, Moore MW: **Decreased sensitivity to tumour-necrosis factor but normal T-cell development in TNF receptor-2-deficient mice.** *Nature* 1994, **372:**560-563.

70. Rothe J, Lesslauer W, Lotscher H, Lang Y, Koebel P, Kontgen F, Althage A, Zinkernagel R, Steinmetz M, Bluethmann H: **Mice lacking the tumour necrosis**

factor receptor 1 are resistant to TNF-mediated toxicity but highly susceptible to infection by Listeria monocytogenes. *Nature* 1993, **364:**798-802.

71. Tartaglia LA, Pennica D, Goeddel DV: **Ligand passing: the 75-kDa tumor necrosis factor (TNF) receptor recruits TNF for signaling by the 55-kDa TNF receptor.** *J Biol Chem* 1993, **268:**18542-18548.

72. Cumberbatch M, Kimber I: **Dermal tumour necrosis factor-alpha induces dendritic cell migration to draining lymph nodes, and possibly provides one stimulus for Langerhans' cell migration.** *Immunology* 1992, **75:**257-263.

73. Kurimoto I, Streilein JW: **cis-urocanic acid suppression of contact hypersensitivity induction is mediated via tumor necrosis factor-alpha.** *J Immunol* 1992, **148:**3072-3078.

74. Streilein JW: **Sunlight and skin-associated lymphoid tissues (SALT): if UVB is the trigger and TNF alpha is its mediator, what is the message?** *J Invest Dermatol* 1993, **100:**47S-52S.

75. Simon JC, Edelbaum D, Bergstresser PR, Cruz PD, Jr.: **Distorted antigen-presenting function of Langerhans cells induced by tumor necrosis factor alpha via a mechanism that appears different from that induced by ultraviolet B radiation.** *Photodermatol Photoimmunol Photomed* 1991, **8:**190-194.

76. Amerio P, Toto P, Feliciani C, Suzuki H, Shivji G, Wang B, Sauder DN: **Rethinking the role of tumour necrosis factor-alpha in ultraviolet (UV) B-induced immunosuppression: altered immune response in UV-irradiated TNFR1R2 gene-targeted mutant mice.** *Br J Dermatol* 2001, **144:**952-957.

77. Kaneko K, Smetana-Just U, Matsui M, Young AR, John S, Norval M, Walker SL: **cis-Urocanic acid initiates gene transcription in primary human keratinocytes.** *J Immunol* 2008, **181:**217-224.

78. Moodycliffe AM, Bucana CD, Kripke ML, Norval M, Ullrich SE: **Differential effects of a monoclonal antibody to cis-urocanic acid on the suppression of delayed and contact hypersensitivity following ultraviolet irradiation.** *J Immunol* 1996, **157:**2891-2899.

79. Moss ML, Jin SL, Milla ME, Bickett DM, Burkhart W, Carter HL, Chen WJ, Clay WC, Didsbury JR, Hassler D, et al: **Cloning of a disintegrin metalloproteinase that processes precursor tumour-necrosis factor-alpha.** *Nature* 1997, **385:**733-736.

80. Obeid D, Nguyen J, Lesavre P, Bauvois B: **Differential regulation of tumor necrosis factor-alpha-converting enzyme and angiotensin-converting enzyme by type I and II interferons in human normal and leukemic myeloid cells.** *Oncogene* 2007, **26:**102-110.

81. Schlondorff J, Becherer JD, Blobel CP: **Intracellular maturation and localization of the tumour necrosis factor alpha convertase (TACE).** *Biochem J* 2000, **347 Pt 1:**131-138.

82. Li X, Perez L, Pan Z, Fan H: **The transmembrane domain of TACE regulates protein ectodomain shedding.** *Cell Res* 2007, **17:**985-998.

83. Schlondorff J, Blobel CP: **Metalloprotease-disintegrins: modular proteins capable of promoting cell-cell interactions and triggering signals by protein-ectodomain shedding.** *J Cell Sci* 1999, **112 (Pt 21):**3603-3617.

84. Mezyk R, Bzowska M, Bereta J: **Structure and functions of tumor necrosis factor-alpha converting enzyme.** *Acta Biochim Pol* 2003, **50:**625-645.

85. Mohan MJ, Seaton T, Mitchell J, Howe A, Blackburn K, Burkhart W, Moyer M, Patel I, Waitt GM, Becherer JD, et al: **The tumor necrosis factor-alpha converting enzyme (TACE): a unique metalloproteinase with highly defined substrate selectivity.** *Biochemistry* 2002, **41:**9462-9469.

86. Rabinowitz MH, Andrews RC, Becherer JD, Bickett DM, Bubacz DG, Conway JG, Cowan DJ, Gaul M, Glennon K, Lambert MH, et al: **Design of selective and soluble inhibitors of tumor necrosis factor-alpha converting enzyme (TACE).** *J Med Chem* 2001, **44:**4252-4267.

87. Anderson ED, VanSlyke JK, Thulin CD, Jean F, Thomas G: **Activation of the furin endoprotease is a multiple-step process: requirements for acidification and internal propeptide cleavage.** *Embo J* 1997, **16:**1508-1518.

88. Peiretti F, Canault M, Deprez-Beauclair P, Berthet V, Bonardo B, Juhan-Vague I, Nalbone G: **Intracellular maturation and transport of tumor necrosis factor alpha converting enzyme.** *Exp Cell Res* 2003, **285:**278-285.

89. Wang P, Tortorella M, England K, Malfait AM, Thomas G, Arner EC, Pei D: **Proprotein convertase furin interacts with and cleaves pro-ADAMTS4 (Aggrecanase-1) in the trans-Golgi network.** *J Biol Chem* 2004, **279:**15434-15440.

90. Endres K, Anders A, Kojro E, Gilbert S, Fahrenholz F, Postina R: **Tumor necrosis factor-alpha converting enzyme is processed by proprotein-convertases to its mature form which is degraded upon phorbol ester stimulation.** *Eur J Biochem* 2003, **270:**2386-2393.

91. Srour N, Lebel A, McMahon S, Fournier I, Fugere M, Day R, Dubois CM: **TACE/ADAM-17 maturation and activation of sheddase activity require proprotein convertase activity.** *FEBS Lett* 2003, **554:**275-283.

92. Mohan R, Chintala SK, Jung JC, Villar WV, McCabe F, Russo LA, Lee Y, McCarthy BE, Wollenberg KR, Jester JV, et al: **Matrix metalloproteinase gelatinase B (MMP-9) coordinates and effects epithelial regeneration.** *J Biol Chem* 2002, **277:**2065-2072.

93. Peschon JJ, Slack JL, Reddy P, Stocking KL, Sunnarborg SW, Lee DC, Russell WE, Castner BJ, Johnson RS, Fitzner JN, et al: **An essential role for ectodomain shedding in mammalian development.** *Science* 1998, **282:**1281-1284.

94. Sunnarborg SW, Hinkle CL, Stevenson M, Russell WE, Raska CS, Peschon JJ, Castner BJ, Gerhart MJ, Paxton RJ, Black RA, Lee DC: **Tumor necrosis factor-alpha converting enzyme (TACE) regulates epidermal growth factor receptor ligand availability.** *J Biol Chem* 2002, **277:**12838-12845.

95. Brown SB, Krause D, Ellem KA: **Low fluences of ultraviolet irradiation stimulate HeLa cell surface aminopeptidase and candidate "TGF alpha ase" activity.** *J Cell Biochem* 1993, **51:**102-115.

96. Piva TJ, Davern CM, Francis KG, Chojnowski GM, Hall PM, Ellem KA: **Increased ecto-metallopeptidase activity in cells undergoing apoptosis.** *J Cell Biochem* 2000, **76:**625-638.

97. Piva TJ, Krause DR, Ellem KO: **UVC activation of the HeLa cell membrane "TGF alpha ase," a metalloenzyme.** *J Cell Biochem* 1997, **64:**353-368.

98. He YY, Council SE, Feng L, Chignell CF: **UVA-induced cell cycle progression is mediated by a disintegrin and metalloprotease/epidermal growth factor receptor/AKT/Cyclin D1 pathways in keratinocytes.** *Cancer Res* 2008, **68:**3752-3758.

99. Singh B, Schneider M, Knyazev P, Ullrich A: **UV-induced EGFR signal transactivation is dependent on proligand shedding by activated metalloproteases in skin cancer cell lines.** *Int J Cancer* 2009, **124:**531-539.

100. Krahn G, Leiter U, Kaskel P, Udart M, Utikal J, Bezold G, Peter RU: **Coexpression patterns of EGFR, HER2, HER3 and HER4 in non-melanoma skin cancer.** *Eur J Cancer* 2001, **37:**251-259.

101. Denault J, Bissonnette L, Longpre J, Charest G, Lavigne P, Leduc R: **Ectodomain shedding of furin: kinetics and role of the cysteine-rich region.** *FEBS Lett* 2002, **527:**309-314.

102. Thomas G: **Furin at the cutting edge: from protein traffic to embryogenesis and disease.** *Nat Rev Mol Cell Biol* 2002, **3:**753-766.

103. Bassi DE, Fu J, Lopez de Cicco R, Klein-Szanto AJ: **Proprotein convertases: "master switches" in the regulation of tumor growth and progression.** *Mol Carcinog* 2005, **44:**151-161.

104. Coppola JM, Bhojani MS, Ross BD, Rehemtulla A: **A small-molecule furin inhibitor inhibits cancer cell motility and invasiveness.** *Neoplasia* 2008, **10:**363-370.

105. Lopez de Cicco R, Watson JC, Bassi DE, Litwin S, Klein-Szanto AJ: **Simultaneous expression of furin and vascular endothelial growth factor in**

human oral tongue squamous cell carcinoma progression. *Clin Cancer Res* 2004, **10:**4480-4488.

106. Vosseler S, Lederle W, Airola K, Obermueller E, Fusenig NE, Mueller MM: **Distinct progression-associated expression of tumor and stromal MMPs in HaCaT skin SCCs correlates with onset of invasion.** *Int J Cancer* 2009, **125:**2296-2306.

107. Murphy G, Nagase H: **Progress in matrix metalloproteinase research.** *Mol Aspects Med* 2008, **29:**290-308.

108. Noel A, Jost M, Maquoi E: **Matrix metalloproteinases at cancer tumor-host interface.** *Semin Cell Dev Biol* 2008, **19:**52-60.

109. Newby AC: **Dual role of matrix metalloproteinases (matrixins) in intimal thickening and atherosclerotic plaque rupture.** *Physiol Rev* 2005, **85:**1-31.

110. Tellier E, Negre-Salvayre A, Bocquet B, Itohara S, Hannun YA, Salvayre R, Auge N: **Role for furin in tumor necrosis factor alpha-induced activation of the matrix metalloproteinase/sphingolipid mitogenic pathway.** *Mol Cell Biol* 2007, **27:**2997-3007.

111. Visse R, Nagase H: **Matrix metalloproteinases and tissue inhibitors of metalloproteinases: structure, function, and biochemistry.** *Circ Res* 2003, **92:**827-839.

112. Dong KK, Damaghi N, Picart SD, Markova NG, Obayashi K, Okano Y, Masaki H, Grether-Beck S, Krutmann J, Smiles KA, Yarosh DB: **UV-induced DNA damage initiates release of MMP-1 in human skin.** *Exp Dermatol* 2008, **17:**1037-1044.

113. Nagase H, Woessner JF, Jr.: **Matrix metalloproteinases.** *J Biol Chem* 1999, **274:**21491-21494.

114. Han YP, Tuan TL, Wu H, Hughes M, Garner WL: **TNF-a stimulates activation of pro-MMP2 in human skin through NF-kB mediated induction of MT1-MMP.** *J Cell Sci* 2001, **114:**131-139.

115. Han YP, Downey S, Garner WL: **Interleukin-1a-induced proteolytic activation of metalloproteinase-9 by human skin.** *Surgery* 2005, **138:**932-939.

116. Maquoi E, Noel A, Frankenne F, Angliker H, Murphy G, Foidart JM: **Inhibition of matrix metalloproteinase 2 maturation and HT1080 invasiveness by a synthetic furin inhibitor.** *FEBS Lett* 1998, **424:**262-266.

117. Steinbrenner H, Ramos MC, Stuhlmann D, Sies H, Brenneisen P: **UVA-mediated downregulation of MMP-2 and MMP-9 in human epidermal keratinocytes.** *Biochem Biophys Res Commun* 2003, **308:**486-491.

118. McCawley LJ, Matrisian LM: **Matrix metalloproteinases: they're not just for matrix anymore!** *Curr Opin Cell Biol* 2001, **13:**534-540.

119. Onoue S, Kobayashi T, Takemoto Y, Sasaki I, Shinkai H: **Induction of matrix metalloproteinase-9 secretion from human keratinocytes in culture by ultraviolet B irradiation.** *J Dermatol Sci* 2003, **33:**105-111.

120. McCawley LJ, Li S, Benavidez M, Halbleib J, Wattenberg EV, Hudson LG: **Elevation of intracellular cAMP inhibits growth factor-mediated matrix metalloproteinase-9 induction and keratinocyte migration.** *Mol Pharmacol* 2000, **58:**145-151.

121. Bassi DE, Lopez De Cicco R, Mahloogi H, Zucker S, Thomas G, Klein-Szanto AJ: **Furin inhibition results in absent or decreased invasiveness and**

tumorigenicity of human cancer cells. *Proc Natl Acad Sci U S A* 2001, **98:**10326-10331.

122. Huynh TT, Chan KS, Piva TJ: **Effect of ultraviolet radiation on the expression of pp38MAPK and furin in human keratinocyte-derived cell lines.** *Photodermatol Photoimmunol Photomed* 2009, **25:**20-29.